

Charge and Energy Transfer in Multichromophoric Arrays

Inan, Damla

DOI

[10.4233/uuid:3ef5d9cb-915d-4152-a0b4-cedb69eaa62c](https://doi.org/10.4233/uuid:3ef5d9cb-915d-4152-a0b4-cedb69eaa62c)

Publication date

2019

Document Version

Final published version

Citation (APA)

Inan, D. (2019). *Charge and Energy Transfer in Multichromophoric Arrays*. [Dissertation (TU Delft), Delft University of Technology]. <https://doi.org/10.4233/uuid:3ef5d9cb-915d-4152-a0b4-cedb69eaa62c>

Important note

To cite this publication, please use the final published version (if applicable).
Please check the document version above.

Copyright

Other than for strictly personal use, it is not permitted to download, forward or distribute the text or part of it, without the consent of the author(s) and/or copyright holder(s), unless the work is under an open content license such as Creative Commons.

Takedown policy

Please contact us and provide details if you believe this document breaches copyrights.
We will remove access to the work immediately and investigate your claim.



Charge and Energy Transfer in Multichromophoric Arrays

Damla Inan

Charge and Energy Transfer in Multichromophoric Arrays

CHARGE AND ENERGY TRANSFER IN MULTICHROMOPHORIC ARRAYS

Proefschrift

ter verkrijging van de graad van doctor
aan de Technische Universiteit Delft,
op gezag van de Rector Magnificus prof. dr. ir. T.H.J.J. van der Hagen,
voorzitter van het College voor Promoties,
in het openbaar te verdedigen op
maandag 14 januari 2019 om 10:00 uur

door

Damla INAN

Master of Science in Chemistry
Universite Paris XI, Parijs, Frankrijk
geboren te Eskisehir, Turkije.

Dit proefschrift is goedgekeurd door de promotoren

Samenstelling promotiecommissie:

Rector Magnificus,	voorzitter
Dr. F. C. Grozema	Technische Universiteit Delft, promotor
Dr. W. F. Jager	Technische Universiteit Delft, copromotor

Onafhankelijke leden:

Prof.dr. S.J. Picken	Technische Universiteit Delft
Prof.dr. A.M. Brouwer	Universiteit van Amsterdam
Prof. dr. E.J.R. Sudhölter	Technische Universiteit Delft
Dr.ir. T.J. Savenije	Technische Universiteit Delft
Dr. J.M. Huijser	Universiteit Twente



Nederlandse Organisatie
voor Wetenschappelijk Onderzoek

Dit werk maakt deel uit van het onderzoeksprogramma van de Stichting voor Fundamenteel Onderzoek der Materie (FOM), die deel uitmaakt van de Nederlandse Organisatie voor Wetenschappelijk Onderzoek (NWO), in het project "Quantum Interference Effects in Single Molecules"

Printed by: Ridderprint BV, the Netherlands, www.ridderprint.nl

Cover by: Iliana Boshoven-Gkini, AgileColor, Ridderprint BV

Copyright © 2019 by Damla Inan

ISBN 978-94-6375-184-1

An electronic version of this dissertation is available at

<http://repository.tudelft.nl/>.

*If one day, my words are against science,
choose science.*

Mustafa Kemal Atatürk

Contents

1. Introduction.....	9
1.1 Natural to Artificial Systems: Photosynthesis	10
1.2 Organic Photovoltaic	11
1.3 Perylene-based Molecules	12
1.4 Förster Resonance Energy Transfer	14
1.5 Photo-induced Charge Transfer.....	15
1.6 Methodology- Transient Absorption Spectroscopy	16
1.7 Outline of the thesis	18
1.8 References	18
2. How to switch on/ off Charge Transfer with the Substitution of Perylene Derivatives 21	
2.1 Introduction.....	22
2.2 Results and Discussion.....	24
2.3 Conclusions	31
2.4 Experimental and Computational Methodology	31
2.5 References	33
3. How to create artificial light harvesting antennas	35
3.1 Introduction.....	36
3.2 Results and Discussion.....	38
3.3 Discussions.....	45
3.4 Conclusions	47
3.5 Experimental Section.....	48
3.6 References	49
4. Tailoring Photophysical Processes of Perylene-Based Light Harvesting Antenna Systems with Molecular Structure and Solvent Polarity	53
4.1 Introduction.....	54
4.2 Results	56
4.3 Discussion	71
4.4 Conclusions	72
4.5 Experimental Section.....	73
4.6 References	74
5. Inhibition of Intramolecular Charge Transfer in Perylene Imide Light-Harvesting Antenna Molecules by Topological Modifications.....	77
5.1 Introduction	78
5.2 Results and Discussion.....	78
5.3 Conclusions	83
5.4 Experimental Methodology	84
5.5 References	85
A. Appendix for Chapter 2.....	87

B. Appendix for Chapter 3	101
C. Appendix for Chapter 4	119
D. Appendix for Chapter 5.....	139
Summary.....	144
Samenvatting	146
Acknowledgements	149
Curriculum Vitae.....	151

I. Introduction

The current rate of global energy consumption is 18 TW-year, of which the USA and Europe are responsible for 40%.¹ Due to industrialization in underdeveloped and developed countries this consumption will continue to increase. The predicted value for the global energy consumption is 20 TW-year for 2030 and double that in 2050.² This energy demand is mainly supplied by fossil fuels, particularly coal; however, use of fossil fuels has a variety of environmental disadvantages. Even though fossil fuels will be the major source for energy consumption in the short term, alternatives should be developed.³ Among the sources of alternative energy, solar energy is one of the main candidates, especially considering the amount of sunlight falling on earth.² In one hour the earth receives an amount of sunlight equivalent to the total energy consumption by humans in a year.⁴ Therefore, the conversion of solar energy is considered one of main alternatives to fossil fuels.

1.1 Natural to Artificial Systems: Photosynthesis

In nature, solar energy conversion occurs by a process called photosynthesis, where sunlight is captured and the energy is stored in chemical bonds in organic molecules.²⁻³ The estimated maximum energy efficiency of natural photosynthesis is around 4.5 per cent.^{5,6} This low efficiency is due to several energy loss mechanisms during the whole process. (**Figure 1.1**) Firstly, the pigments only absorb a part of the solar spectrum, between 400-700 nm (called as photosynthetic active region). This limits the efficiency of converting incident solar energy by more than half. 4.9% of incident solar energy is lost by reflection. In addition, 6.6% of the incident solar energy is lost as heat when chlorophylls absorb higher-energy photons. This leads to the formation of higher excited states and this excess energy is dissipated as heat. Of the remaining energy, a considerable fraction of the total energy is lost during the catalytic processes (around 28.7%).⁷ In the end, only 4.5% of incident energy from the sun is stored as chemical energy in biomass.

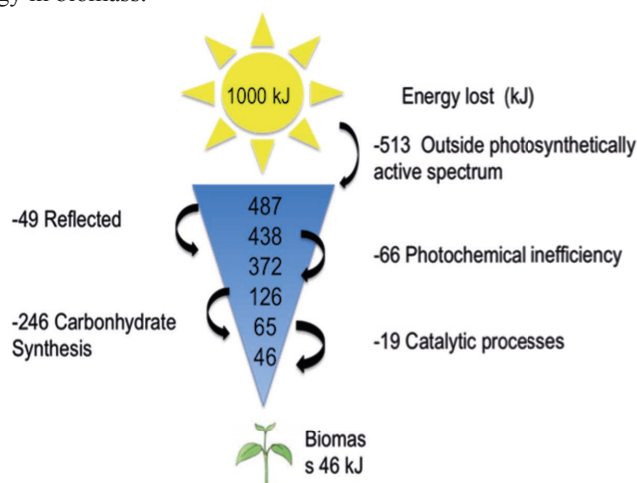


Figure 1.1 Minimum energy losses calculated for 1000 kJ of incident solar radiation at each step of the photosynthetic process from light absorption till the formation of stored chemical energy in biomass (Adapted from reference ⁷).

The natural photosynthetic system can be used as an inspiration to construct efficient artificial energy-converting systems. The key point in natural photosynthesis is the capturing of sunlight in a large number of chromophores, after which the energy is funneled to a central location where chemistry takes place. This process can be mimicked by constructing synthetic multichromophoric systems. These artificial systems should have distinct properties, including the absorption of a large part of the solar spectrum, and should exhibit similar photo physical properties. The main processes that should take place in an artificial photosynthetic system are (1) the absorption of light, (2) transfer of this energy to a central location and (3) separation of the excited state into electrons and holes that can be used in subsequent chemical processes.⁸ In order to optimize such artificial light-harvesting systems, a fundamental understanding of the key photophysical processes that take place is important. This thesis describes a detailed investigation of these photophysical processes in a new series of model systems of artificial light harvesting systems that have been specifically designed for this work.

1.2 Organic Photovoltaic

Organic photovoltaic devices (OPVs) can convert sunlight directly into electricity by using organic semiconductors that will perform light harvesting and charge transport.⁹ Organic photovoltaic devices have several critical advantages over current silicon cells since they potentially are cheaper to produce, have lighter weight and their flexibility can be advantageous in new applications.^{9,10}

The solar energy conversion occurs in several steps that are analogous to natural photosynthesis: light absorption by the active organic material, formation of a bound exciton (electron-hole pair), diffusion of this exciton to a donor-acceptor interface, the dissociation of negative and positive charges and the transport of these charges to corresponding electrodes (Figure 1.2).¹¹

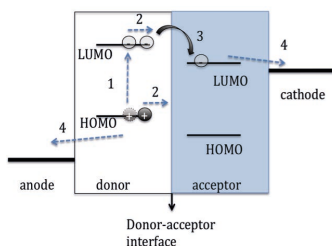


Figure 1.2 Schematic representation of OPV with (1) formation of excitons by absorption of light (2) exciton diffusion to the donor-acceptor interface (3) dissociation into charges, (4) collection of charges by anode and cathode

OPVs can largely be divided in two main architectures. The first one is a so-called bulk hetero-junction (BHJ) where the two active materials (*i.e.* n-type and p-type semiconductors) are blended in one bulk composite.¹² The second is a planar bilayer architecture where donor and acceptor are in distinct layers on top of each other. For each organic photovoltaic system, the active organic material should be selected carefully. Both the donor and the acceptor layer should have a suitable energy band gap and high molar absorption, a sufficiently high charge carrier mobility.^{13,14}

1.3 Perylene-based Molecules

OPVs devices consist of two organic materials, one with a low ionization potential that acts as an electron donor, and other with a high electron affinity acts as the electron acceptor.⁹ The choice of the donor and acceptor materials plays a critical role in constructing efficient OPVs. The optimal choice does not only take into account the electronic properties but depends to a large extent on issues related to the morphology of BHJ layers.

Fullerenes have for a long time been the material of choice due to their advantageous properties to produce highly efficient solar cells. However, fullerenes mostly absorb photons in UV-visible region and their chemical modification is difficult. This limits them to be used in solar cells as acceptor. An elegant approach to focus on the disadvantages of fullerenes is to replace them with smaller electron acceptors. These non-fullerene acceptors (NFAs) should possess matching electron accepting and transport properties. Moreover, compared to fullerene, they should have better optical properties and improved possibilities for chemical modification. Perylene-3,4,9,10-tetracarboxylic derivatives are promising candidates in this respect.¹⁵ The primary perylene-based dye was first described in 1912.¹⁶ Perylene based dyes have attracted a lot of attention as they have a high absorption coefficient in the visible region and they are highly stable.¹⁷⁻²² They have been used in many applications, such as organic field transistors (OFETs)²³⁻²⁶, laser applications^{27,28} as well as organic photovoltaic devices.^{21,29}

Perylene bisimides have a great potential to be used as an acceptor materials in OPVs since they have a high electron affinity (EA~ 3.9 eV for unsubstituted perylene bisimides, similar to fullerene acceptors)^{17,30}, and they exhibit favorable charge transport properties in the solid state. Moreover, they can easily be functionalized at different positions, see **Figure 1.3**.^{31,32} The main optical characteristics of perylene bisimides are a high absorption coefficient between 400-600 nm, a ~ 4 ns singlet excited state lifetime and a fluorescence quantum yield close to unity.³³ They exhibit strong yellow-green fluorescence with pronounced vibronic structure that is a mirror image of the absorption spectrum.^{11,34} (**Figure 1.4**) Functionalized perylene bisimide molecules are also convenient acceptors for use in fundamental spectroscopic studies of charge and energy transfer because their radical anions have distinct absorption features in the near-NIR region. Using time resolved spectroscopy it is easy to determine the rate of formation of the perylene anion by detecting it at these specific IR absorption wavelengths.³⁵

As mentioned above, a particularly attractive feature of perylene bisimides is that the conjugated core can easily be functionalized at different positions. This is especially true in comparison to the more commonly used fullerene-based acceptors.^{33,34} As indicated in **Figure 1.3**, perylene-based molecules can be substituted at the imide or bay/headland position for bisimides. For the monoimides an additional position is available for substitution, the peri position.

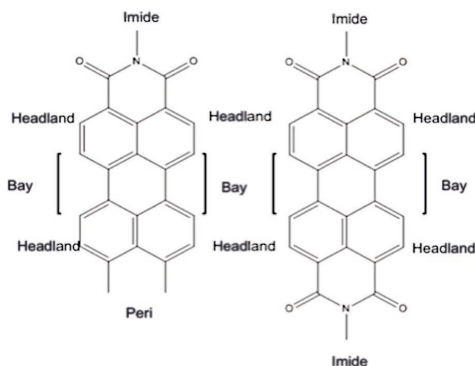


Figure 1.3 Structure of perylene monoimide (left), perylene bisimide (right) and their possible positions to functionalize.

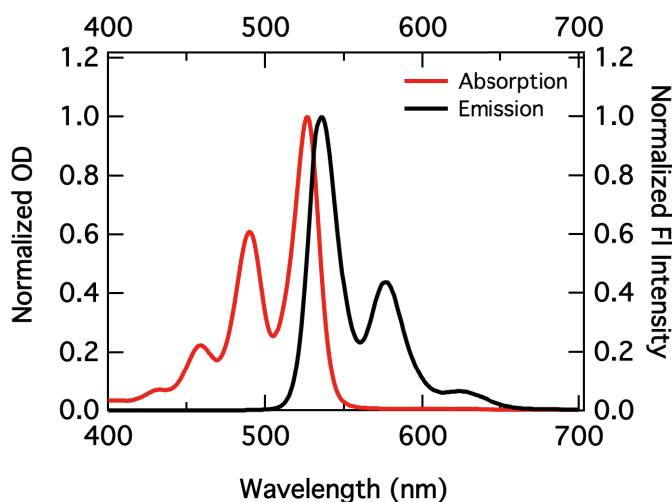


Figure 1.4 Normalized absorption and emission spectra of perylene-3,4,9,10-tetracarboxylic tetrabutylester in toluene.

The effect of substitution on the optical and photophysical properties is described in Chapter 2 of this thesis. Previously, it has been shown that the substitution of various functional groups on imide position can tune the solubility and the organization in the solid state,³⁶ but has a limited effect on the optoelectronic properties of the isolated molecules. On the other hand, functionalizing the perylene core at the bay position can significantly alter these properties.^{28,37-40} Substitution at both positions can be explored to come to optimal perylene bisimide materials for OPV, in terms of their optoelectronic properties, solubility and morphology in the solid state.

The versatility of perylene-based molecules in terms of synthesis also makes it easy to combine them with donor moieties, resulting in donor-acceptor systems (D-A). This approach is of practical interest but is also used to synthesize model systems for fundamental studies of photophysical processes such as energy and charge transfer.

1.4 Förster Resonance Energy Transfer

After the excitation of the donor chromophore in D-A systems, the excited state energy can be transferred to other chromophores by a process called resonance energy transfer, (RET also called as excitation energy transfer-EET). The most widely known examples of energy transfer are found in natural light-harvesting antenna systems where it funnels the energy to the photosynthetic reaction center.⁴¹ A very successful theory for RET was suggested by Theodore Förster in 1948.⁴² Therefore energy transfer for singlet-excited states is often called Förster Resonance Energy Transfer (FRET). According to the Förster Theory, energy transfer occurs between an energy donor and an energy acceptor that are separated by a certain distance.

In the FRET mechanism, energy transfer proceeds by a quantum mechanical coupling between the electronic transitions on different chromophores.⁴³ Photo- excitation of donor (D) will generate an electronically excited state, D*. Subsequently, the energy can transfer to the acceptor, forming A*, while D* will decay to its ground state. The excited acceptor A* can subsequently decay either by fluorescence or by further energy transfer to yet another chromophore. In the approximation of Förster theory, the rate of energy transfer k_{FRET} is given by

$$k_{FRET} = \frac{9\kappa^2 c^4 d\omega}{8\pi\tau_D n^4 R^6} \int F_D(\omega) \sigma_A(\omega) \frac{d\omega}{\omega} \quad (1.1)$$

where n is the refractive index, $F_D(\omega)$ is the normalized emission spectrum of the donor; τ_{D^*} is the associated radiative decay lifetime; $\sigma_A(\omega)$ is the linear absorption cross-section of the acceptor; ω is an optical frequency in radians per second; and c is the speed of light. $F_D(\omega)$ and $\sigma_A(\omega)$ depend on the mutual orientation of the transition dipoles of the donor and acceptor (**Equation 1.2** and **Equation 1.3**). μ_D and μ_A are the magnitudes of the electric transition dipole moments for excitation of the donor decay and acceptor, respectively. These transition dipole moments depend on the electronic state wavefunction of donor and acceptor. (**Equation 1.4**) The indices m, n, p and r are the generic vibrational levels.^{44,45}

$$F_D(\omega) = \frac{\omega^3 \tau_{D^*} \mu_D^2}{3\epsilon_0 \pi c^3} \sum_{n,r} p_{D^*}^{(n)} \left| \left\langle \varphi_D^{(r)} \middle| \varphi_{D^*}^{(n)} \right\rangle \right|^2 \delta(E_{D_n^*} - E_{D_r} - \hbar\omega) \quad (1.2)$$

$$\sigma_A(\omega) = \frac{\omega \pi \mu_A^2}{3\epsilon_0 c} \sum_{m,p} \rho_A^{(m)} \left| \left\langle \varphi_{A^*}^{(p)} \middle| \varphi_A^{(m)} \right\rangle \right|^2 \delta(E_{A_p^*} - E_{A_m} - \hbar\omega) \quad (1.3)$$

$$\mu_D = \langle \psi_D | \mu | \psi_{D^*} \rangle ; \mu_A = \langle \psi_{A^*} | \mu | \psi_A \rangle \quad (1.4)$$

Förster's theory requires two main factors to have this energy transfer between two chromophores.^{41,42,46} First, the emission spectrum of the donor should overlap with the absorption spectrum of acceptor. Second, the chromophores should have an orientation and distance so that the excited state coupling is sufficient. In natural light harvesting systems, the distance and the alignment of the chromophores are close to optimal to maximize energy transfer.⁴⁷ Artificial systems should satisfy these conditions to perform highly efficient FRET.

1.5 Photo-induced Charge Transfer

Perylene-based molecules are often used as the electron acceptor in charge transfer reactions, either in the solid state as an individual molecule or as a component in a covalently linked donor-bridge-acceptor system.¹¹ A schematic representation of photo-induced charge transfer (PICT) in a donor-acceptor system is given in **Figure 1.5**.

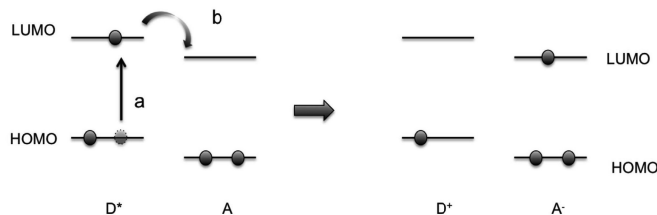


Figure 1.5 Schematic representation of PICT (a) Selectively excitation of the donor chromophore. (b) Electron transfer from the excited donor chromophore to the acceptor chromophore.

The kinetics of PICT can be described by Marcus theory in which k_{CT} is dependent on the driving force, ΔG_{CT} , the reorganization energy, λ , the electronic coupling, V_{DA} , between the initial excited state and the charge-separated state, as seen in **Equations 1.5** and **1.6**.^{48,49} The reorganization energy is the energy required to adjust structures of donor, acceptor (internal reorganization) and reorganize the solvent molecules around them (external reorganization) so that charge transfer can take place iso-energetically. The overall quantum yield of charge transfer depends on the driving force, *i.e.* the energy difference between (D-A)* and (D⁺-A⁻). When the driving force for charge transfer increases, the activation energy barrier is lowered and the rate of electron transfer increases up to the reorganization energy. At some point, ΔG_{CT} becomes equal to the reorganization energy ($\lambda = -\Delta G_{CT}$) resulting the maximum possible rate of charge transfer. After this point, an additional increase in ΔG_{CT} will increase the energy barrier. Therefore, according to Marcus theory, three feasible regions are available: the 'normal' region (**Figure 1.6**), where $-\Delta G_{CT} < \lambda$, the 'optimal' region $-\Delta G_{CT} = \lambda$, and the 'inverted' region $-\Delta G_{CT} > \lambda$.¹¹ The D-A distance is an important parameter in determining the charge transfer rate as the electronic coupling V_{DA} exponentially decreases with the increase in the D-A distance.

$$k_{CS} \approx V_{DA}^2 e^{-\left[\frac{(\Delta G_{CT} + \lambda)^2}{4\lambda k_B T}\right]} \quad (1.5)$$

The driving force (ΔG_{CT}) of charge-transfer reactions for these D-A type molecules depends on many factors, including the effect of solvation. According to Rehm-Weller equation (**Equation 1.6**),⁵⁰ the driving force of charge transfer can be related to the reduction and oxidation potentials of donor and acceptor chromophores ($E_{ox}(D)$ and $E_{red}(A)$). The term $E_{0,0}(A)$ is the energy of relaxed first singlet excited energy. In this equation, the r_{DA} is the donor-acceptor distance and ϵ_s is the dielectric constants of the chosen solvent. When the donor-acceptor distance increases for any given D-A system, coulombic interactions between donor and acceptor will decrease and charge transfer will become less favorable. When the solvent polarity increases (ϵ_s), the charge separation will be more favorable since the charges can stabilize in polar environments and coulombic interaction is more positive ($\Delta G_{CS} < 0$).⁴⁸

$$\Delta G_{CT} = E_{D/D^{+}} - E_{A^{-}/A} - E_{0,0} - \frac{e^2}{r_{DA}\epsilon_s} \quad (1.6)$$

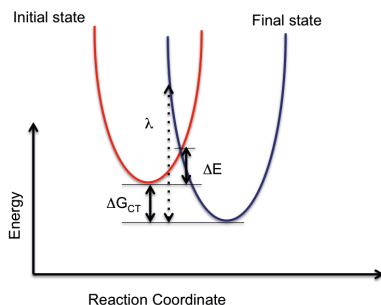


Figure 1.6 Schematic representation of Marcus normal region and the relationship between Gibbs free energy and the reorganization energy.

1.6 Methodology- Transient Absorption Spectroscopy

Transient absorption spectroscopy is a powerful technique to follow the population of different excited states and charged species over time. Briefly, it is a two pulse technique: a high-intensity pump pulse is used to excite ground state molecules to an excited state and subsequently a white light continuum probe pulse to monitor the changes in the optical absorption spectrum over time. A schematic representation of such a system is given in **Figure 1.7**.

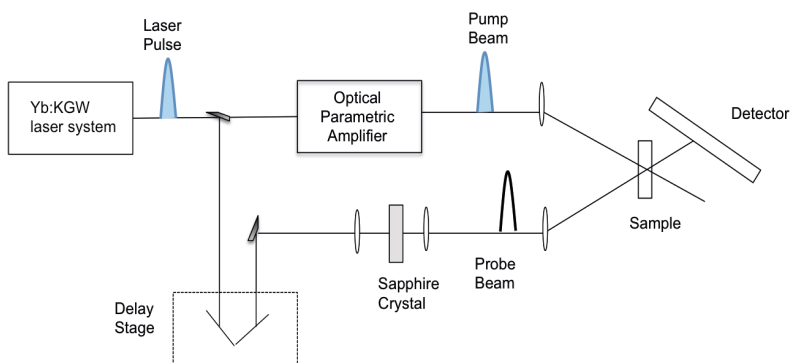


Figure 1.7 Schematic representation of a transient absorption spectroscopy.

Fundamental laser pulses are generated using a Yb:KGW laser (1028 nm) running at 5 kHz with a pulse duration of ~ 180 fs (PHAROS-SP-05-200, Light Conversion). The majority of the beam is used as the pump after passing through an optical parametric amplifier (OPA, ORPHEUS-PO15F5HNP1, Light Conversion), resulting in excitation pulses that are tunable from 350 nm to 1600 nm. A small fraction of initial laser beam is used to generate the probe pulse. It is passed through a delay stage that introduces a temporal delay between the pump and the probe beams. After the delay stage the probe beam is focused on a sapphire crystal resulting in a white light continuum spectrum. The pump and probe polarization can be

controlled with half wave plates. The angle can be set parallel or perpendicular angle and the two obtained spectra are averaged to obtain magic angle ($\approx 54.7^\circ$) to avoid polarization and photoselection effects.⁵¹ Both pump and probe beams are focused on the sample and the transmitted probe light is collected in detector. The collected data is the difference in the absorption ΔOD (Equation 1.8)⁵²

$$\Delta OD = OD_{\text{pumped}} - OD_{\text{unpumped}} \quad (1.8)$$

By varying the delay between the pump and probe pulses, spectra are obtained as a function of the time after the excitation pulse. These spectra represent the difference in the absorption spectrum with and without the pump pulse. An example of a difference spectrum at a particular delay is shown in **Figure 1.8**. Such spectra can contain a number of features at different wavelengths and these evolve in time. The first type of feature is the ground state bleach, which appears as a region where the ΔOD is negative and has the exact same as the ground state absorption spectrum. This bleach is due to the disappearance of ground state molecules, when a fraction of molecules is excited to the excited state, the number of molecules in the ground state is decreased, leading to less ground state absorption. A second contribution that can occur is the stimulated emission. It occurs when a photon from the probe pulse induces emission of another photon from the population of excited molecules. This also appears as a negative ΔOD signal. A third contribution, one that results in a positive ΔOD is called photo-induced absorption. This occurs when photoexcitation leads to a new species that absorbs at wavelengths that are different than the ground state absorption spectrum. These species include radical anions and cations, and excited states of chromophores. An example spectrum of perylene bisimide is given in **Figure 1.8**.

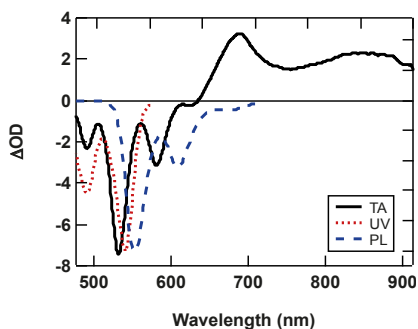


Figure 1.8 Contributions to a ΔOD spectrum: ground state absorption (red line), steady state emission (blue line), sum of these contributions; transient absorption spectra (black line).

After the collection of spectra, valuable information should be subtracted. If there is one straightforward mechanism that is involved, a single wavelength fitting can give information about rates of that mechanism. On the other hand, more complex analysis should be performed for the information on possible mechanisms between species that are products after each photophysical process.

1.7 Outline of the thesis

In this thesis a detailed study is described on the design principles for artificial light harvesting antenna systems based on perylene and naphthalene dyes. A variety of new antenna systems and corresponding model systems are introduced and their photophysical properties are by steady state and time resolved spectroscopy. Together, these studies give a detailed insight in the mechanisms of charge and energy transfer in these systems and result in some design rules for artificial light-harvesting antennas based on perylene dyes.

In **Chapter 2**, charge transfer from appended donor groups to a variety of perylene derivatives is studied. The donor groups are either attached to either the peri- or imide-position. It is shown that by altering the electron donor position and tuning the electron deficiency of the cores can result in control over the yield of charge transfer. From these results, valuable insights were obtained for the design of antenna systems in later chapters.

In **Chapter 3**, five new bi-chromophoric light-harvesting antenna systems are presented. These consist of blue light absorbing naphthalene mono-imide energy donors and green light absorbing perylene-3,4,9,10-tetracarboxylic acid energy acceptors. These antenna systems have a good coverage of solar spectrum between 380-580 nm. The energy transfer characteristics of these systems were investigated in nonpolar solvent (toluene). Efficient excitation energy transfer (EET) by the Förster mechanism was observed in all of them.

In **Chapter 4**, the same antenna systems as described in Chapter 3 are considered but a more detailed photophysical study is carried out, also including polar solvents (chloroform and benzonitrile). The photophysics of these antenna systems depends on both the electron donating strength of the donor and the solvent polarity. In some cases, only energy transfer is obtained, even in polar solvents. In donor-acceptor combinations where the charge transfer state is stabilized more, very fast energy transfer (~1ps) is followed by charge transfer on longer timescales (20-2000 ps) These time scales are similar to natural.

Finally, in **Chapter 5**, two new light harvesting systems were synthesized where the donor is attached to imide position of the acceptor, instead of to the bay area as in Chapters 2 and 3. This gave a control over charge transfer in the sense that it is unfavorable in this case.

1.6 References

- (1) *Key World Energy Statistics* International Energy Agency: Paris, 2017.
- (2) Lewis, N. S.; Nocera, D. G., Powering the planet: Chemical challenges in solar energy utilization. *Proceedings of the National Academy of Sciences* **2006**, *103* (43), 15729-15735.
- (3) Barber, J.; Tran, P. D., From natural to artificial photosynthesis. *Journal of The Royal Society Interface* **2013**, *10* (81).
- (4) Wescott, L. D.; Mattern, D. L., Donor- σ -Acceptor Molecules Incorporating a Nonadecyl-Swallowtailed Perylenediimide Acceptor. *The Journal of Organic Chemistry* **2003**, *68* (26), 10058-10066.
- (5) *Molecular to Global Photosynthesis*. Imperial Collage: London, UK, 2004; Vol. 2.
- (6) Bolton, J. R.; Hall, D. O., THE MAXIMUM EFFICIENCY OF PHOTOSYNTHESIS *. *Photochemistry and Photobiology* **1991**, *53* (4), 545-548.
- (7) Zhu, X.-G.; Long, S. P.; Ort, D. R., What is the maximum efficiency with which photosynthesis can convert solar energy into biomass? *Current Opinion in Biotechnology* **2008**, *19* (2), 153-159.
- (8) Hambourger, M.; Moore, G. F.; Kramer, D. M.; Gust, D.; Moore, A. L.; Moore, T. A., Biology and technology for photochemical fuel production. *Chemical Society Reviews* **2009**, *38* (1), 25-35.
- (9) Kippelen, B.; Bredas, J.-L., Organic photovoltaics. *Energy & Environmental Science* **2009**, *2* (3), 251-261.

- (10) Li, Y., Molecular Design of Photovoltaic Materials for Polymer Solar Cells: Toward Suitable Electronic Energy Levels and Broad Absorption. *Accounts of Chemical Research* **2012**, *45* (5), 723-733.
- (11) Huang, C. Perylene Diimide-based Materials For Organic Electronics and Optical Limiting Applications. Georgia Institute of Technology, USA, 2010.
- (12) Sariciftci, N. S.; Smilowitz, L.; Heeger, A. J.; Wudl, F., Photoinduced Electron Transfer from a Conducting Polymer to Buckminsterfullerene. *Science* **1992**, *258* (5087), 1474-1476.
- (13) Günes, S.; Neugebauer, H.; Sariciftci, N. S., Conjugated Polymer-Based Organic Solar Cells. *Chemical Reviews* **2007**, *107* (4), 1324-1338.
- (14) Thompson, B. C.; Fréchet, J. M. J., Polymer-Fullerene Composite Solar Cells. *Angewandte Chemie International Edition* **2008**, *47* (1), 58-77.
- (15) Wadsworth, A.; Moser, M.; Marks, A.; Little, M. S.; Gasparini, N.; Brabec, C. J.; Baran, D.; McCulloch, I., Critical review of the molecular design progress in non-fullerene electron acceptors towards commercially viable organic solar cells. *Chemical Society Reviews* **2018**.
- (16) Willy Herbst, K. H., *Industrial Organic Pigments*. 2 ed.; Wiley: 1997.
- (17) Li, C.; Wonneberger, H., Perylene Imides for Organic Photovoltaics: Yesterday, Today, and Tomorrow. *Advanced Materials* **2012**, *24* (5), 613-636.
- (18) Huang, C.; Barlow, S.; Marder, S. R., Perylene-3,4,9,10-tetracarboxylic Acid Diimides: Synthesis, Physical Properties, and Use in Organic Electronics. *The Journal of Organic Chemistry* **2011**, *76* (8), 2386-2407.
- (19) Kozma, E.; Catellani, M., Perylene diimides based materials for organic solar cells. *Dyes and Pigments* **2013**, *98* (1), 160-179.
- (20) Yan, Q.; Zhou, Y.; Zheng, Y.-Q.; Pei, J.; Zhao, D., Towards rational design of organic electron acceptors for photovoltaics: a study based on perylenediimide derivatives. *Chemical Science* **2013**, *4* (12), 4389-4394.
- (21) Shivanna, R.; Shoaee, S.; Dimitrov, S.; Kandappa, S. K.; Rajaram, S.; Durrant, J. R.; Narayan, K. S., Charge generation and transport in efficient organic bulk heterojunction solar cells with a perylene acceptor. *Energy & Environmental Science* **2014**, *7* (1), 435-441.
- (22) Guide, M.; Pla, S.; Sharenko, A.; Zalar, P.; Fernandez-Lazaro, F.; Sastre-Santos, A.; Nguyen, T.-Q., A structure-property-performance investigation of perylenediimides as electron accepting materials in organic solar cells. *Physical Chemistry Chemical Physics* **2013**, *15* (43), 18894-18899.
- (23) Jones, B. A.; Ahrens, M. J.; Yoon, M.-H.; Facchetti, A.; Marks, T. J.; Wasielewski, M. R., High-Mobility Air-Stable n-Type Semiconductors with Processing Versatility: Dicyanoperylene-3,4:9,10-bis(dicarboximides). *Angewandte Chemie International Edition* **2004**, *43* (46), 6363-6366.
- (24) Ahrens, M. J.; Fuller, M. J.; Wasielewski, M. R., Cyanated Perylene-3,4-dicarboximides and Perylene-3,4:9,10-bis(dicarboximide): Facile Chromophoric Oxidants for Organic Photonics and Electronics. *Chemistry of Materials* **2003**, *15* (14), 2684-2686.
- (25) Jiménez, Á. J.; Spänig, F.; Rodríguez-Morgade, M. S.; Ohkubo, K.; Fukuzumi, S.; Guldi, D. M.; Torres, T., A Tightly Coupled Bis(zinc(II) phthalocyanine)-Perylenediimide Ensemble To Yield Long-Lived Radical Ion Pair States. *Organic Letters* **2007**, *9* (13), 2481-2484.
- (26) Zhan, X.; Tan, Z. a.; Domercq, B.; An, Z.; Zhang, X.; Barlow, S.; Li, Y.; Zhu, D.; Kippelen, B.; Marder, S. R., A High-Mobility Electron-Transport Polymer with Broad Absorption and Its Use in Field-Effect Transistors and All-Polymer Solar Cells. *Journal of the American Chemical Society* **2007**, *129* (23), 7246-7247.
- (27) Sadrai, M.; Bird, G. R., A new laser dye with potential for high stability and a broad band of lasing action: Perylene-3,4,9,10-tetracarboxylic acid-bis-N,N'(2',6' xylyldyl)diimide. *Optics Communications* **1984**, *51* (1), 62-64.
- (28) Ford, W. E.; Kamat, P. V., Photochemistry of 3,4,9,10-perylenetetracarboxylic dianhydride dyes. 3. Singlet and triplet excited-state properties of the bis(2,5-di-tert-butylphenyl)imide derivative. *The Journal of Physical Chemistry* **1987**, *91* (25), 6373-6380.
- (29) Zhang, X.; Lu, Z.; Ye, L.; Zhan, C.; Hou, J.; Zhang, S.; Jiang, B.; Zhao, Y.; Huang, J.; Zhang, S.; Liu, Y.; Shi, Q.; Liu, Y.; Yao, J., A Potential Perylene Diimide Dimer-Based Acceptor Material for Highly Efficient Solution-Processed Non-Fullerene Organic Solar Cells with 4.03% Efficiency. *Advanced Materials* **2013**, *25* (40), 5791-5797.
- (30) Nielsen, C. B.; Holliday, S.; Chen, H.-Y.; Cryer, S. J.; McCulloch, I., Non-Fullerene Electron Acceptors for Use in Organic Solar Cells. *Accounts of Chemical Research* **2015**, *48* (11), 2803-2812.
- (31) Nakazono, S.; Imazaki, Y.; Yoo, H.; Yang, J.; Sasamori, T.; Tokitoh, N.; Cédric, T.; Kageyama, H.; Kim, D.; Shinokubo, H.; Osuka, A., Regioselective Ru-Catalyzed Direct 2,5,8,11-Alkylation of Perylene Bisimides. *Chemistry – A European Journal* **2009**, *15* (31), 7530-7533.

- (32) Leah E. Shoer, S. W. E., Eric A. Margulies, and Michael R. Wasielewski, Photoinduced Electron Transfer in 2,5,8,11-Tetrakis-Donor-Substituted Perylene-3,4:9,10-bis(dicarboximides). *The Journal of Physical Chemistry B* **2015**, 119 (24), 7635-7643.
- (33) Nagao, Y., Synthesis and properties of perylene pigments. *Progress in Organic Coatings* **1997**, 31 (1), 43-49.
- (34) Wurthner, F., Perylene bisimide dyes as versatile building blocks for functional supramolecular architectures. *Chemical Communications* **2004**, (14), 1564-1579.
- (35) Ford, W. E.; Hiratsuka, H.; Kamat, P. V., Photochemistry of 3,4,9,10-perylene-tetracarboxylic dianhydride dyes. 4. Spectroscopic and redox properties of oxidized and reduced forms of the bis(2,5-di-tert-butylphenyl)imide derivative. *The Journal of Physical Chemistry* **1989**, 93 (18), 6692-6696.
- (36) Langhals, H., Cyclic carboxylic imide structures as structure elements of high stability. Novel developments in perylene dye chemistry. *Heterocycles* **1995**, 40 (1), 477-500.
- (37) Wright, M. E.; Schorzman, D. A.; Feher, F. J.; Jin, R.-Z., Synthesis and Thermal Curing of Aryl-Ethynyl-Terminated coPOSS Imide Oligomers: New Inorganic/Organic Hybrid Resins. *Chemistry of Materials* **2003**, 15 (1), 264-268.
- (38) Zhao, Y.; Wasielewski, M. R., 3,4:9,10-Perylenebis(dicarboximide) chromophores that function as both electron donors and acceptors. *Tetrahedron Letters* **1999**, 40 (39), 7047-7050.
- (39) Lukas, A. S.; Zhao, Y.; Miller, S. E.; Wasielewski, M. R., Biomimetic Electron Transfer Using Low Energy Excited States: A Green Perylene-Based Analogue of Chlorophyll a. *The Journal of Physical Chemistry B* **2002**, 106 (6), 1299-1306.
- (40) Langhals, H.; Karolin, J.; B.-A. Johansson, L., Spectroscopic properties of new and convenient standards for measuring fluorescence quantum yields. *Journal of the Chemical Society, Faraday Transactions* **1998**, 94 (19), 2919-2922.
- (41) Beljonne, D.; Curutchet, C.; Scholes, G. D.; Silbey, R. J., Beyond Förster Resonance Energy Transfer in Biological and Nanoscale Systems. *The Journal of Physical Chemistry B* **2009**, 113 (19), 6583-6599.
- (42) Förster, T., Zwischenmolekulare Energiewanderung und Fluoreszenz. *Annalen der Physik* **1948**, 437 (1-2), 55-75.
- (43) Kallmann, H. a. L., F., Über quantenmechanische Energieübertragung zwischen atomaren Systemen. *Zeitschrift für Physikalische Chemie* **2B**, 207-243.
- (44) Andrews, D.; Bradshaw, D., *Resonance Energy Transfer*. 2009.
- (45) Andrews, D., *Resonance Energy Transfer: Theoretical Foundations and Developing Applications. In Tutorials in Complex Photonic Media*, SPIE: Bellingham, WA, 2009.
- (46) Scholes, G. D., LONG-RANGE RESONANCE ENERGY TRANSFER IN MOLECULAR SYSTEMS. *Annual Review of Physical Chemistry* **2003**, 54 (1), 57-87.
- (47) Scholes, G. D., Quantum-Coherent Electronic Energy Transfer: Did Nature Think of It First? *The Journal of Physical Chemistry Letters* **2010**, 1 (1), 2-8.
- (48) Marcus, R. A., ON THE THEORY OF ELECTROCHEMICAL AND CHEMICAL ELECTRON TRANSFER PROCESSES. *Canadian Journal of Chemistry* **1959**, 37 (1), 155- 163.
- (49) Marcus, R. A., Electron transfer reactions in chemistry theory and experiment. *Journal of Electroanalytical Chemistry* **1997**, 438 (1), 251-259.
- (50) Rehm, D.; Weller, A., Kinetics of Fluorescence Quenching by Electron and H-Atom Transfer. *Israel Journal of Chemistry* **1970**, 8 (2), 259-271.
- (51) Sebastian Schott, A. S., Johannes Buback, Patrick Nuernberger and Tobias Brixner, Generalized magic angle for time-resolved spectroscopy with laser pulses of arbitrary ellipticity. *Journal of Physics B: Atomic, Molecular and Optical Physics* **2014**, 47 (124014).
- (52) Berera, R.; van Grondelle, R.; Kennis, J. T. M., Ultrafast transient absorption spectroscopy: principles and application to photosynthetic systems. *Photosynthesis Research* **2009**, 101 (2- 3), 105-118.

2 ● How to Switch On/Off Charge Transfer With The Substitution of Perylene Derivatives

This chapter describes a photophysical study of a series of electron donor–acceptor molecules, in which electron-donating 4-methoxyphenoxy groups are attached to the 1,7-bay positions of four different perylene tetracarboxylic acid derivatives, namely, perylene tetraesters **1**, perylene monoimide diesters **2**, perylene bisimides **3**, and perylene monobenzimidazole monoimides **4**. The motivation for this study is to achieve control over the photoinduced charge-transfer (CT) process in perylene-based systems by altering the position of electron donor and tuning the electron deficiency of the perylene core.

2.1 Introduction

A good control over photoinduced charge and energy transfer between donor and acceptor moieties is essential for the development of artificial photosynthesis.²⁻⁵ Important variables, which dictate the yields and kinetics of these interactions, are excited state and redox properties of the donor and acceptor components, their relative distance, mutual orientation, and electronic coupling.⁶⁻¹¹ During the past three decades, molecular assemblies consisting of light harvesting chromophores, charge-separators, and catalysts have been designed and studied to gain a better understanding of the photochemistry and photophysics involved in these systems.¹²⁻¹⁴ Such assemblies are of prime importance because of their ability to mimic the natural photosynthetic process and to convert sunlight into fuel.

Several chromophores have been tested as integrative building blocks for light harvesting and charge-separation. Perylene tetracarboxylic acid derivatives, of which perylene bisimides (PBIs) are the best known representatives, are particularly attractive chromophores due to their exceptional photo-chemical stability, high electron deficiency, strong absorption in the visible region of the solar spectrum, and possibility to further tune their photophysical properties by structural modifications.¹⁵⁻¹⁶ Taking advantage of high photochemical robustness and strong absorption, various light-harvesting antenna systems have been prepared using perylene tetracarboxylic acid derivatives as the active chromophore.^{11,17-19} However, due to the high electron deficiency of the perylene core, charge-separation has been commonly observed when these compounds are covalently coupled even with moderately electron-rich donors.^{19,20}

Perylene tetracarboxylic acid derivatives (mostly PBIs) are also attractive components of charge separators, and for this application, their high electron deficiency is highly beneficial. In the past, many separate studies on perylene based donor-acceptor systems have been carried out.²⁰⁻²⁴ These studies have revealed that the efficiency and kinetics of charge transfer (CT) are highly sensitive to even small structural variations. In a recent study on PBI based isoelectronic donor-bridge-acceptor compounds, we have shown that small changes in the molecular bridge have a large impact on the dynamics of charge separation.²⁵ In another recent study, Shoer *et al.* have observed that the charge separation can be an order of magnitude faster for systems in which donors are connected to the ortho (or headland) positions of the perylene core as compared to the imide position.²⁶

Another recent study by Pagoaga *et al.* reported strong fluorescence quenching ascribed to charge separation, for PBIs bearing 4-methoxybenzene substituents as electron donors at various bay positions.²⁷ Preceding work by Flamigni *et al.* on non-bay substituted PBIs, bearing mono-, di- and trimethoxy-benzene at the imide-position, has revealed that CT rates strongly correlate with the redox properties of the methoxybenzene and the positioning of the methoxy group.²⁸ A comparison between efficiency of CT and the positioning of the electron donors cannot be made from these studies, because 1,7-bay substitution decreases the reduction potential of the perylene acceptor, *i.e.* makes the perylene core less electron deficient.¹⁵ Therefore, there is still a need for a comprehensive study to understand the kinetics of charge transfer towards perylenes as a function of the position at which the electron donating substituents are attached. So that perylene-containing devices can be designed in which the perylene derivatives serve a well-defined role of energy acceptor or donor in a light harvesting antenna and that of electron acceptor in a charge-separating unit.

In this work, we report on the design, the synthesis, and the photo physical properties of a series of perylene-3,4,9,10-tetracarboxylic acid derivatives bearing either 4-methoxyphenoxy or 4-methoxyphenyl groups as electron donors. The choice of these groups as electron donors is based on reports in which facile CT was observed upon photoexcitation of perylene bisimides bearing methoxyphenyl groups as electron donors.^{27,28} In this study, the electrochemical and optical properties of the perylene core were also systematically tuned by the modifications at the peri-positions. For the photophysical characterization of our compounds, steady state and time-resolved spectroscopic studies were carried out in solvents of different polarity. In these compounds, the strong fluorescence of the perylene moiety has been quenched to different extent by electron donating groups attached to the perylene core at different positions. The aim of this work is to establish a relation between molecular structure and the extent of fluorescence quenching observed for these molecules in solvents of different polarity. We ascribe this fluorescence quenching to photoinduced CT, and assume that the positions from which quenching is efficient are the appropriate positions to attach electron donors and achieve efficient charge separation. Finally, the obtained experimental results are rationalized by computational calculations based on time dependent density functional theory. (TD-DFT)

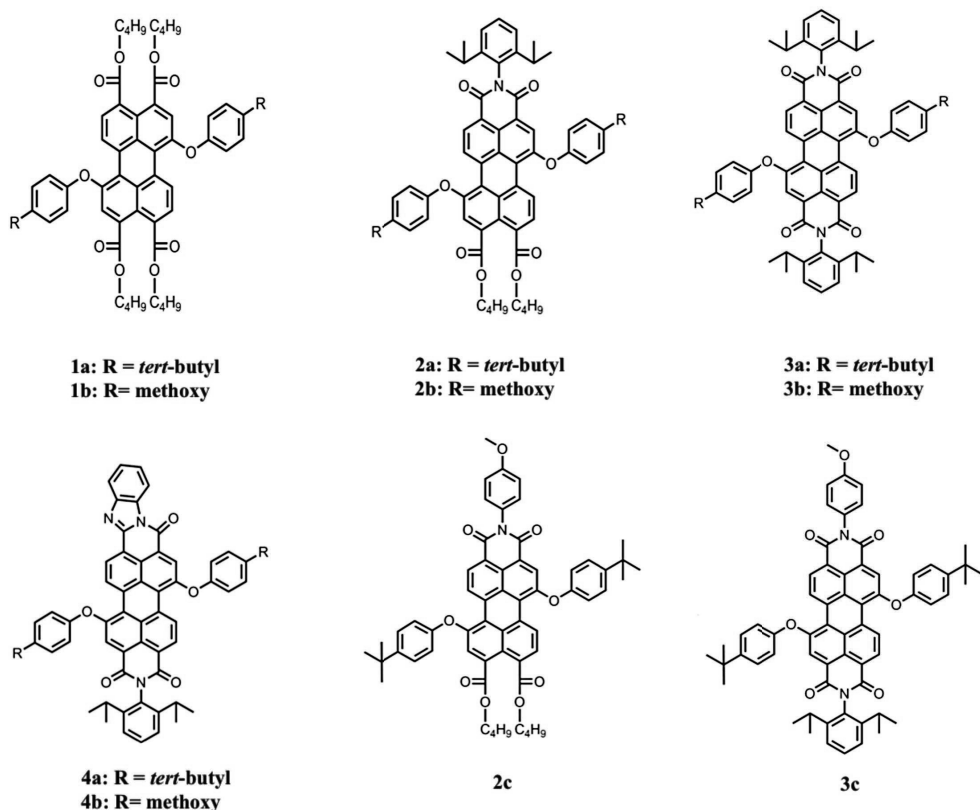


Figure 2.1 Structures of compounds used in this study

2.2 Results and Discussion

2.2.1 Electrochemical Studies

The redox properties of compounds **1-4** were investigated by cyclic voltammetry in dichloromethane. The obtained redox potentials (V vs Fc/Fc⁺) for these molecules are summarized in **Table 2.1**.

As shown in **Table 2.1**, the redox properties of the molecules change significantly if the substitution at the peri-positions is altered. When the groups attached to peri positions become more electron withdrawing (e.g., from tetraester to monoimide), the redox potentials of the compounds become more positive.^{29,30} This clearly shows that molecules have higher electron affinities going from compound **1** to **2** to **3**, which makes them better electron acceptors. From the data in **Table 2.1**, it is clearly seen that the perylene tetracarboxylic derivatives **3** and **4** are rather similar as far as their electronic properties are concerned. This implies that the imide and benzimidazole groups are electrochemically equivalent.²⁹ Finally, it is apparent that attaching different phenoxy groups at the bay positions does not result in notably different redox potentials. This indicates the absence of significant interaction between these groups in the ground state.

Table 2.1 First redox potentials of perylene derivatives (V vs. Fc/Fc⁺) obtained by cyclic voltammetry in CH₂Cl₂.

Compound	<i>E</i> _{1/2 ox}	<i>E</i> _{1/2 red}
1	–	–1.55
1a	+0.84	– ^a
1b	+0.82	– ^a
2a	+0.95	–1.38 ^b
2b	+0.94	–1.38
2c	+0.97	–1.33
3a	+1.05	–1.11
3b	+1.04	–1.10
3c	+1.06	–1.09
4a	+1.01	–1.06
4b	+1.02	– ^c

^aNo reduction potential was observed. ^bIrreversible. ^cNot detectable.

2.2.2 Steady State Absorption Studies

The absorption spectra of compounds **1-4**, in chloroform, are shown in **Figure 2.2** and the relevant data, in toluene, chloroform, and acetonitrile (or benzonitrile), are given in **Table 2.2**. All compounds are readily soluble in toluene and chloroform. However, the solubility in polar and weakly polarizable acetonitrile was much lower. Especially, the compounds **4a** and **4b** were insoluble in this solvent. At low solubility, perylene derivatives tend to aggregate.³¹ This aggregation alters the optical properties and optoelectronic performances. In general, spectral

broadening and shifts in absorption and emission spectra, along with fluorescence quenching, are the common signatures of this aggregation.^{32,33} Therefore, in order to preclude spectral changes caused by aggregation, benzonitrile was used as a polar solvent for compounds **3** and **4**.

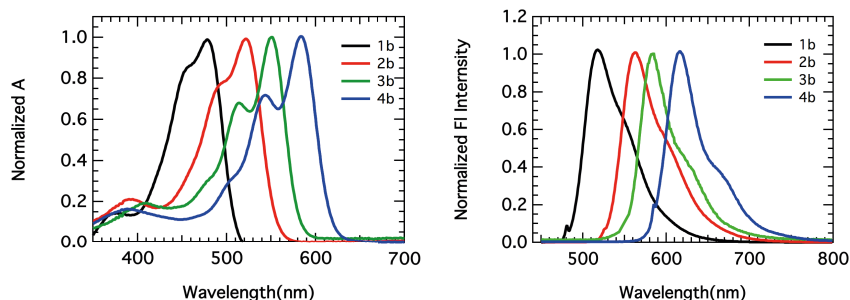


Figure 2.2 The normalized UV/Vis absorption (Left) and emission spectra (Right) of the compounds **1–4b** in chloroform.

The absorption spectra of all donor-substituted compounds (**1b–4b**) are characterized by a strong absorption band at longer wavelengths (425–625 nm), and a weaker absorption band at shorter wavelengths (**Figure 2.2**). As shown previously in literature, bay substitution leads to a disappearance of the pronounced vibronic structure observed for perylenes without bay substitution. This is accompanied by a bathochromic shift of the absorption bands.^{34,35} When the size of the π -system increased, that is going from compounds **1** to **2** to **3** and **4**, the molar extinction coefficient increases gradually and the absorption maxima shift to longer wavelengths. When the bay substituent attached to the perylene core from *tert*-butylphenoxy to 4-methoxyphenoxy is changed, small 5 nm red shifts are observed. The influence of solvent polarity on the absorption maxima is rather modest. Positive solvatochromism, a red shift in absorption upon increasing the solvent polarity, was observed, in particular for compounds with more electron deficient perylene cores, but these spectral shifts do not exceed 15 nm.

2.2.3 Steady State and Time Resolved Emission Studies

The emission spectra of compounds **1–4** roughly resemble the mirror images of the corresponding absorption spectra (**Figure 2.2**). The positions of the emission wavelengths exhibit the same trend as those of the absorption maxima (**Table 2.2**). While the effects of changing the bay-substituents and solvent polarity on the emission wavelengths of these perylene compounds are modest, the emission intensities, quantified by their fluorescence quantum yields (Φ_F), are extremely sensitive to these parameters. Fluorescence quantum yields close to unity with fluorescence lifetimes (τ_F) in the 4–5 ns range are observed for compounds bearing the non-electron donating *tert*-butylphenoxy substituents at the bay positions (compounds **1a–4a**, **Table 2.2**).³⁴ These fluorescent properties are similar to those of non-bay substituted perylenes, *i.e.* no significant fluorescence quenching occurs from the 4-*tert*-butylphenoxy substituents. It should be noted that the high fluorescence of compound **4a** in toluene is remarkable, because fluorescence quantum yields of perylene benzimidazoles are, in general, substantially lower as compared to perylene bisimides.²⁹

For the compounds bearing the electron donating 4-methoxyphenoxy substituents at the bay positions (compounds **1b–4b**), fluorescence quantum yields gradually decreased with the increase in solvent polarity and electron deficiency of the perylene core. The effect of solvent polarity is clearly illustrated by compound **2b** that has strong fluorescence in toluene ($\Phi_F = 0.75$), but shows negligible fluorescence in acetonitrile ($\Phi_F = 0.03$). The effect of the increased electron deficiency of the perylene core is clearly illustrated by the weak fluorescence found for compound **3b** in all solvents. These observations suggest that quenching of perylene fluorescence in these compounds is induced by photoinduced CT, although other quenching mechanisms cannot be excluded.³⁶

Table 2.2 Optical properties of compounds in toluene, chloroform, acetonitrile/benzonitrile.

Compound	Solvent	$\lambda_{\text{abs}}(\text{nm})$	$\lambda_{\text{em}}(\text{nm})$	$\mathcal{E}(\text{M}^{-1}\text{cm}^{-1})$	$\Phi_F^{[a]}$	$\tau_F(\text{ns})^{[b]}$
1a	toluene	475	515	31500	0.91	4.26
	chloroform	475	515	25600	0.84	4.40
	acetonitrile	471	512	24800	0.90	4.73
1b	toluene	479	515	24000	0.88	4.25
	chloroform	478	517	29300	0.81	4.38
	acetonitrile	479	517	33200	0.02	$\sim 0.21^{[c]}$
2a	toluene	515	552	38900	0.85	4.52
	chloroform	517	557	36700	0.87	4.82
	acetonitrile	512	563	31700	0.90	5.23
2b	toluene	520	555	34300	0.85	4.34
	chloroform	522	561	36000	0.32	3.21
	acetonitrile	517	566	34100	0.03	$\sim 0.08^{[c]}$
2c	toluene	513	549	35900	0.93	4.36
	chloroform	519	563	36900	0.87	4.73
	acetonitrile	511	558	34700	0.92	4.69
3a	toluene	543	572	57800	0.94	4.44
	chloroform	547	578	54200	0.91	4.64
	benzonitrile	552	586	54600	0.86	4.47
3b	toluene	549	575	53300	0.19	$\sim 0.71^{[c]}$
	chloroform	551	580	53100	0.04	$\sim 0.43^{[c]}$
	benzonitrile	561	583	51400	0.01	$\sim 0.12^{[c]}$
3c	toluene	542	572	52500	1.00	3.80
	chloroform	548	577	51000	0.87	3.89
	benzonitrile	555	582	50900	0.63	3.30
4a	toluene	578	607	63600	0.71	4.42
	chloroform	581	614	63700	0.66	4.31
	benzonitrile	584	619	61350	0.70	4.22
4b	toluene	582	609	63300	0.75	4.22
	chloroform	584	616	67600	0.23	2.45
	benzonitrile	591	621	69500	0.04	$\sim 0.43^{[c]}$

^[a]Fluorescence quantum yield. ^[b]Fluorescence life-time. ^[c]Non mono-exponential decay.

To establish whether the quenching depends on the position at which the electron donating substituent is attached to the perylene core, the optical properties of the bay-substituted compounds **2b** and **3b** are compared to the corresponding imide-substituted compounds **2c** and **3c**. The fluorescence of the bay-substituted compounds **2b** and **3b** is much weaker compared to the compounds **2c** and **3c**. This is clearly seen by comparing the fluorescence of compound **2b** with that of compound **2c**. While the fluorescence of **2b** strongly decreases upon increasing the solvent polarity, compound **2c** remains strongly fluorescent in all solvents. A similar observation is made by comparing the fluorescence of compounds **3b** and **3c**. Note that ascribing the differences in photo physical properties between **2b** and **2c**, and **3b** and **3c** solely to the positioning of the electron donor is not entirely valid. This is mainly due to the fact that the number of electron donating substituents is different in both cases and the oxidation potential of the 4-methoxyphenoxy bay substituent is ca. 0.30 V lower than that of the methoxyphenyl imide substituent.³⁷ However, since it has been previously shown that 4-methoxyphenyl substituents at all bay-positions strongly quench the fluorescence of PBIs,²⁷ it can still be concluded that fluorescence quenching from bay-position is substantially faster than from imide-position. This conclusion is further supported by a previous report,³⁸ in which we have observed that the fluorescence quenching of perylene tetraester by an aniline electron donor is substantially faster from the bay-position as compared to the peri-position.

Time-resolved fluorescence spectroscopy reveals that the fluorescence of the strongly emitting compounds, ($\Phi_F > 0.2$), decays mono exponentially. Additionally, the emission of these compounds is not significantly influenced by the presence of oxygen. Using the fluorescence quantum yields and the fluorescence lifetimes, the rates of fluorescence and of non-radiative decay (quenching by CT) were calculated and summarized in **Table A.1**. (Appendix A). From this table it is evident that upon increasing the solvent polarity, lifetimes and rates of fluorescence decrease for all compounds. Rates of fluorescence between 2.5 and $1 \times 10^8 \text{ s}^{-1}$ have been determined for all compounds and these rates do not appear to be influenced by the bay substituents. Quenching rates are in the order of $1 \times 10^7 \text{ s}^{-1}$ for the non-quenched compounds. For the strongly quenched compounds, rates of quenching (and fluorescence) cannot be determined accurately because fluorescence decay is no longer mono-exponential. Nevertheless, CT rates are estimated to be in the order of 1×10^9 to $1 \times 10^{10} \text{ s}^{-1}$.

2.2.3 Transient Absorption Studies

To investigate the time resolved photophysics in more detail, we have selected two series of compounds (**2a-c** and **3a-c**) for which femtosecond pump-probe transient absorption spectroscopy measurements were performed. In these series, the molecules have different substitution patterns, near identical absorption spectra and markedly different rates of fluorescence quenching in polar solvents. The transient absorption spectra were measured in either acetonitrile (**2a-2c**) or benzonitrile (**3a-3c**) using pump wavelengths between 510 and 550 nm. The transient absorption spectra, for compounds **2a** and **2b**, and **3a** and **3b**, immediately after excitation are shown in the inset in **Figures 2.3** and **2.4**, respectively. These transient spectra are very similar to previously reported spectra with pronounced excited state absorption features.^{11,23,25,39} For the monoimide compounds (**2a,b,c**) ground state bleaching below 520 nm, stimulated emission between 520 and 620 nm, and a broad excited state-

absorption with two maxima near 685 nm and 800 nm are observed. For the bisimide compounds (**3a,b,c**) similar induced emission and absorption features are observed but now the excited state absorptions are shifted to longer wavelengths (710 nm and >900 nm). The spectra of **2c** and **3c** are depicted in **Figure A.6** in the Appendix A. It is interesting that the spectra for compounds **2a** and **2b** and those of **3a** and **3b** are indistinguishable, even though very large differences in the radiative lifetime and fluorescence quantum yields were observed.

The identical photoinduced absorption spectra immediately after excitation (at 1 ps) indicate that the nature of the excited states is the same in both cases. However, the lifetimes of the excited states are much shorter for **2b** and **3b** than they are for **2a** and **3a**, respectively. To determine the lifetime of the singlet-excited state of **2a-2c** and **3a-3c** we performed a global analysis. When we compared the lifetime of the singlet excited state with the fluorescence lifetime for all compounds in polar solvent, we see that these lifetimes are very close to the fluorescence lifetimes for all the compounds (**Table 2.3**).

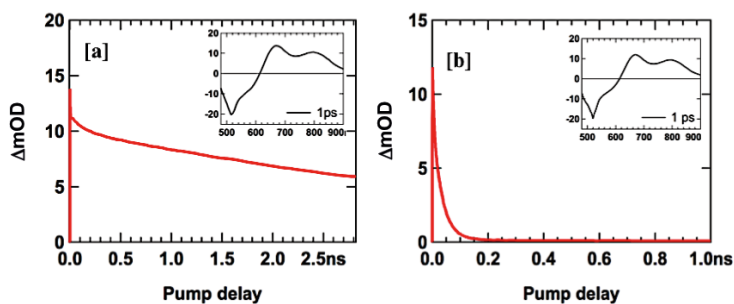


Figure 2.3 The kinetic traces at photo-induced absorption (685 nm) of molecules **2a** [a] and **2b** [b] in acetonitrile. The transient absorption spectrum immediately after excitation is shown in the inset.

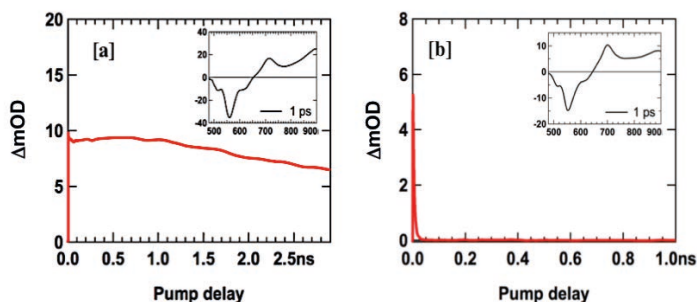


Figure 2.4 The kinetic traces at photo-induced absorption (775 nm) of molecules **3a** [a] and **3b** [b] in benzonitrile. The transient absorption spectrum immediately after excitation is shown in the inset.

Table 2.3 Comparison of the lifetimes of S1 state obtained from the global analysis of transient spectrum (τ_{TA}) and fluorescence lifetimes (τ_F) obtained from time-resolved emission measurements in acetonitrile or benzonitrile.

Compound	τ_{TA} (ns)	τ_F (ns)
2a	5.23	5.23
2b	0.04	0.08
2c	4.53	4.69
3a	4.51	4.47
3b	0.04	0.12
3c	4.81	3.30

The data presented so far are in accordance to the expected photo physical behavior of **2a–2c** and **3a–3c**. For **2a** and **2c**, a very slow decay of the singlet-excited state is observed on a nanosecond time scale. Similar lifetimes have been observed by transient absorption and emission spectroscopy. However, for compound **2b**, a 100-fold increased decay rate of the S₁ state is observed. Similarly, for **3b**, a significantly increased decay rate of the S₁ state is observed, which is indicative of the occurrence of a substantially faster decay process. An explanation that is often invoked for such observations is the formation of a charge-separated state that is stabilized in polar solvents. The proposed scheme for such a photo physical behavior is depicted in **Figure 2.5**.

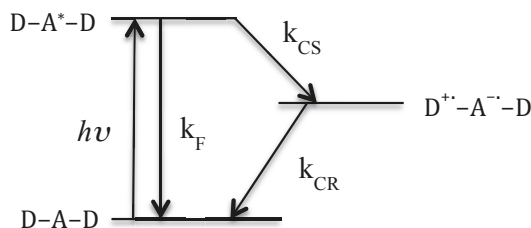


Figure 2.5 Schematic representation of photoinduced processes after photo illumination

Although the initial excited state disappears, it is remarkable that we do not observe the characteristic absorption spectrum of the perylene radical anion of the CS state D^+-A^--D . For related compounds, CS states have been observed upon excitation,²⁸ but on some occasions spectroscopic evidence of charge separation is illusive.^{19,38} The absence of a CS absorption can be explained in a straightforward manner by assuming that charge recombination is faster than charge separation, which prevents accumulation of the CS state. For compounds **2b** and **3b** this implies that charge recombination rates are at least 1×10^9 to $1 \times 10^{10} \text{ s}^{-1}$, respectively (**Table A.1**.)

2.2.4 Molecular Simulations

To gain more insight of the nature of the initial excited state in the studied compounds, we have performed density functional theory (DFT) calculations. The excitations of compounds **2a** and **2b** were calculated by TD-DFT using a DZP basis set consisting of Slater-type function and a M06-2X exchange-correlation function. All calculations were performed using the Amsterdam Density Functional (ADF) theory package. The calculated absorption spectra of compounds **2a** and **2b** show a strong absorption feature with oscillator strength close to 0.8 at 480 nm (**Figure 2.6**). In both cases, these absorptions mainly consist of the transition from highest occupied molecular orbital of perylene (HOMO_{perylene}) to lowest unoccupied molecular orbital (LUMO_{perylene}). The computational transition energies are somewhat higher than those observed experimentally. This is attributed to the absence of solvent effects in the calculations that generally shift the absorption bands to lower energy.

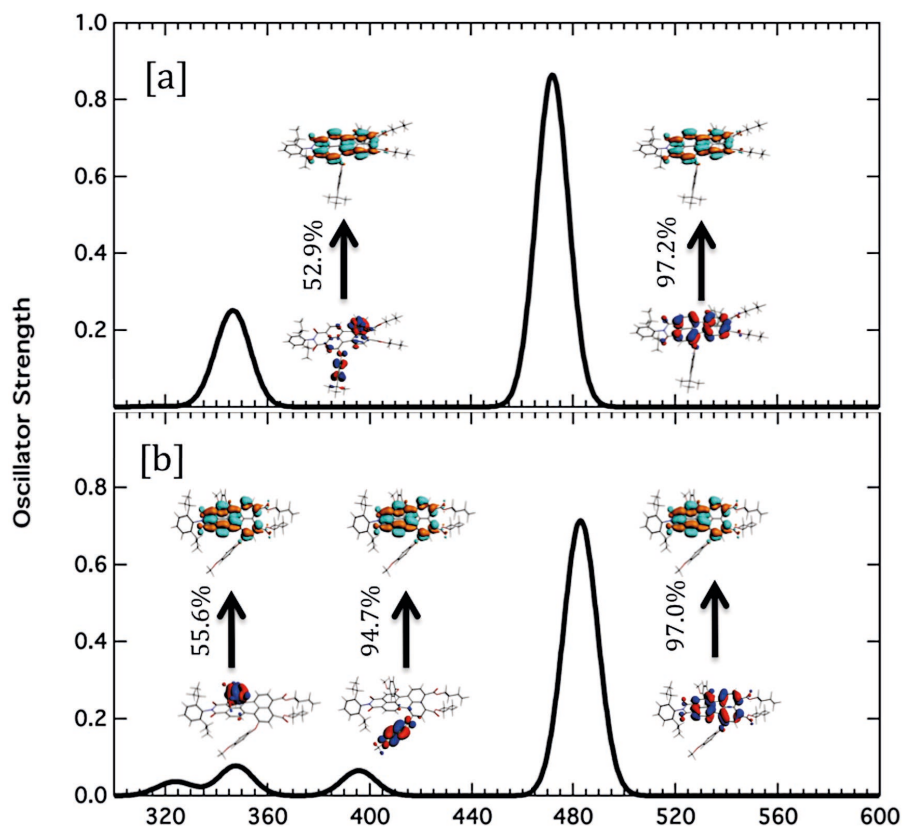


Figure 2.6 Optical excitation of **2a** (top) and **2b** (bottom) calculated using TD-DFT with DZP/M06-2X.

In the calculated spectrum of **2a**, there is an additional absorption near 345 nm, which has transition from the HOMO of bay-substituents to the LUMO of perylene core. For **2b**, multiple higher-lying bands are observed between 300–420 nm. All of these bands contain substantial contributions from the CT transitions from occupied orbitals of the substituents to the LUMO of the perylene core. These calculations show that for both compounds there is no

clear low-energy CT state present in vacuum. However, it should be noted that the nature of the excited states is not necessarily the same in solution. First of all, the excited states with (partial) charge transfer character will be stabilized considerably in highly polar solvents such as acetonitrile and benzonitrile and, therefore, arise much closer to the local excited state localized on the perylene core. From the calculations presented here, it can be seen that for **2b** the excited charge separated states are lower in energy than for **2a**, which can be understood in terms of the stronger electron donating character of the substituents in **2b**. Second, the presence of a polar solvent can also change the nature of the excited state considerably after excitation. This can result in the formation of a CT state that is not present in vacuum.

The results from the molecular simulations are in line with the experimental data obtained by TA and fluorescence spectroscopy. These experimental data reveal the formation of identical “locally excited states” for all compounds of the same class, irrespective of the electron donating substituent attached. Subsequently, fluorescence takes place for compounds bearing weak donors in all solvents, while strong fluorescence quenching takes place for compounds bearing strong donors in polar solvents. The fluorescence quenching takes place by electron transfer from the electron donor to the perylene core. This process is thermodynamically favored and, from bay-attached electron donors, kinetically allowed. This charge separation process occurs *after* the primary excitation process and is therefore not described by the molecular simulations based on DFT calculations.

2.3 Conclusions

We have synthesized a series of perylene tetracarboxylic acid derivatives, bearing electron donating 4-methoxyphenoxy groups at 1,7-bay positions and, in two cases, also a 4-methoxypenyl group at the imide position. Subsequent photophysical characterization of these compounds revealed the various variables that dictate the charge transfer process in perylene-based systems; electronic nature of the perylene core, the position of electron donor, and the solvent polarity. For the perylene tetraester based compound, which has the least electron deficient perylene core, charge transfer was observed only in polar acetonitrile. Upon moving to perylene monoimide diester, which has an increased electron deficiency due to presence of a more electron withdrawing imide group, significant CT is observed already in chloroform. An efficient charge transfer occurred in both polar and non-polar solvents for the most electron deficient perylene bisimide based compounds. From transient absorption spectroscopy and DFT calculations, it has been concluded that charge separation takes place after local excitation of the perylene core. The kinetics of CT is strongly influenced by the positioning of the electron-donor on the perylene scaffold. Changing position from “bay” to “imide” exerted a significantly negative impact on the charge transfer rates. In this way, this study has revealed that the photoinduced charge transfer process can be precisely tuned in perylene-based systems by altering the electronic nature of the perylene core, the positioning of the electron donor, and the solvent polarity.

2.4 Experimental and Computational Methodology

Materials All the reagents utilized in the synthesis were purchased from commercial suppliers, unless otherwise stated. The DMF used in the synthesis was of anhydrous grade. Toluene was dried over sodium under an argon atmosphere prior to use. All other solvents

used in the syntheses were of reagent grade and were used as received from suppliers. The purification of the products was performed by column chromatography (silica gel 60, mesh size 0.063–0.200 mm). For all the spectroscopic measurements, spectroscopy grade solvents were purchased from commercial suppliers and were used as received.

Instrumentation and Characterization The NMR spectra were recorded with 400 MHz pulsed Fourier transform NMR spectrometer in CDCl_3 at room temperature. The chemical shifts are quoted relative to TMS. δ values are given in parts per million and J values in Hertz. Electrochemical behavior of the compounds was studied by cyclic voltammetry in a three-electrode single-compartment cell consisting of a platinum sheet as the working electrode, Ag wire as the reference electrode, and a Pt wire as the counter electrode (Scan-rate = 0.5 V/s). Pre-dried CH_2Cl_2 containing 0.1 M tetrabutylammonium hexafluorophosphate was used as solvent. The measurements were done under continuous flow of nitrogen. The concentration of the prepared samples was ca. 0.5 mM. Under these conditions, the ferrocene oxidation was observed at 0.52 V.

Absorption measurements were carried out in Perkin Elmer Lambda 40 UV-Vis spectrophotometer. Photoluminescence studies were done in SPEX Fluorimeter. Fluorescence lifetimes were performed with LifeSpec-ps Fluorescence spectrometer with fixed excitation wavelength of 400 nm. For quantum yield measurements, the formula for optically dilute solutions was used.⁴⁰ Fluorescence quantum yields of compounds **1–2** were determined by using perylene-3,4,9,10-tetracarboxylic tetrabutylester ($\phi_F = 0.98$ in CH_2Cl_2) as a reference. Whereas, for compounds **3–4**, *N,N'*-bis(1-hexylheptyl)-perylene bisimide ($\phi_F = 0.99$ in CH_2Cl_2) was used.⁴¹

Pump-probe transient-absorption measurements were performed by using tunable Yb:KGW laser system consisting of a YB:KGW laser (1028 nm) which operates at 5 kHz with a pulse duration of <180 fs (PHAROS-SP-06-200 Light Conversion) and an optical parametric amplifier (ORPHEUS-PO15F5HNP1, Light Conversion). A white light continuum probe pulse was generated by focusing part of the fundamental 1028 nm from Pharos into a sapphire crystal. Transient absorption data were collected using a commercial pump-probe spectrometer, HELIOS (Ultrafast Systems) in the wavelength range 490–910 nm. The maximum time-delay between the pump and the probe pulse was 3.3 ns. The compounds were dissolved in spectroscopic grade toluene, chloroform and acetonitrile/benzonitrile and placed in quartz cuvettes with a 2 mm path length. In order to prevent aggregation and photo bleaching, the samples were stirred with a magnetic stirrer.

The geometrical and optical properties of the chromophores were investigated by density functional theory calculations using the Amsterdam Density Functional (ADF) software package. The geometry of the molecules was optimized using the PBE functional together with a double-zeta plus polarization (DZP) type basis set consisting of Slater functions. The optical absorption spectra were calculated by time dependent density functional (TD-DFT) theory calculations using the M06-2X meta-GGA functional with a DZP basis set.

2.5 References

- (1) Inan, D.; Dubey, R. K.; Westerveld, N.; Bleeker, J.; Jager, W. F.; Grozema, F. C., Substitution Effects on the Photoinduced Charge-Transfer Properties of Novel Perylene-3,4,9,10-tetracarboxylic Acid Derivatives. *The Journal of Physical Chemistry A* **2017**, *121* (24), 4633-4644.
- (2) Alstrum-Acevedo, J. H.; Brennaman, M. K.; Meyer, T. J., Chemical Approaches to Artificial Photosynthesis. 2. *Inorganic Chemistry* **2005**, *44* (20), 6802-6827.
- (3) Gust, D.; Moore, T. A.; Moore, A. L., Solar Fuels via Artificial Photosynthesis. *Accounts of Chemical Research* **2009**, *42* (12), 1890-1898.
- (4) Frischmann, P. D.; Mahata, K.; Würthner, F., Powering the future of molecular artificial photosynthesis with light-harvesting metallosupramolecular dye assemblies. *Chemical Society Reviews* **2013**, *42* (4), 1847-1870.
- (5) Wasielewski, M. R., Photoinduced electron transfer in supramolecular systems for artificial photosynthesis. *Chemical Reviews* **1992**, *92* (3), 435-461.
- (6) Gust, D.; Moore, T. A.; Moore, A. L., Molecular mimicry of photosynthetic energy and electron transfer. *Accounts of Chemical Research* **1993**, *26* (4), 198-205.
- (7) Paddon-Row, M. N., Investigating long-range electron-transfer processes with rigid, covalently linked donor-(norbornylogous bridge)-acceptor systems. *Accounts of Chemical Research* **1994**, *27* (1), 18-25.
- (8) Lewis, F. D.; Letsinger, R. L.; Wasielewski, M. R., Dynamics of Photoinduced Charge Transfer and Hole Transport in Synthetic DNA Hairpins. *Accounts of Chemical Research* **2001**, *34* (2), 159-170.
- (9) Wenger, O. S., How Donor–Bridge–Acceptor Energetics Influence Electron Tunneling Dynamics and Their Distance Dependences. *Accounts of Chemical Research* **2011**, *44* (1), 25-35.
- (10) Guldi, D. M.; Hirsch, A.; Scheloske, M.; Dietel, E.; Troisi, A.; Zerbetto, F.; Prato, M., Modulating Charge-Transfer Interactions in Topologically Different Porphyrin–C60 Dyads. *Chemistry – A European Journal* **2003**, *9* (20), 4968-4979.
- (11) Dubey, R. K.; Inan, D.; Sengupta, S.; Sudholter, E. J. R.; Grozema, F. C.; Jager, W. F., Tunable and highly efficient light-harvesting antenna systems based on 1,7-perylene-3,4,9,10-tetracarboxylic acid derivatives. *Chemical Science* **2016**, *7* (6), 3517-3532.
- (12) Wasielewski, M. R., Self-Assembly Strategies for Integrating Light Harvesting and Charge Separation in Artificial Photosynthetic Systems. *Accounts of Chemical Research* **2009**, *42* (12), 1910-1921.
- (13) Youngblood, W. J.; Lee, S.-H. A.; Maeda, K.; Mallouk, T. E., Visible Light Water Splitting Using Dye-Sensitized Oxide Semiconductors. *Accounts of Chemical Research* **2009**, *42* (12), 1966-1973.
- (14) Kärkäs, M. D.; Verho, O.; Johnston, E. V.; Åkermark, B., Artificial Photosynthesis: Molecular Systems for Catalytic Water Oxidation. *Chemical Reviews* **2014**, *114* (24), 11863-12001.
- (15) Würthner, F., Perylene bisimide dyes as versatile building blocks for functional supramolecular architectures. *Chemical Communications* **2004**, (14), 1564-1579.
- (16) Huang, C.; Barlow, S.; Marder, S. R., Perylene-3,4,9,10-tetracarboxylic Acid Diimides: Synthesis, Physical Properties, and Use in Organic Electronics. *The Journal of Organic Chemistry* **2011**, *76* (8), 2386-2407.
- (17) Langhals, H.; Saulich, S., Bichromophoric Perylene Derivatives: Energy Transfer from Non-Fluorescent Chromophores. *Chemistry – A European Journal* **2002**, *8* (24), 5630-5643.
- (18) Hippius, C.; Schlosser, F.; Vysotsky, M. O.; Böhrer, V.; Würthner, F., Energy Transfer in Calixarene-Based Cofacial-Positioned Perylene Bisimide Arrays. *Journal of the American Chemical Society* **2006**, *128* (12), 3870-3871.
- (19) Flamigni, L.; Ventura, B.; You, C.-C.; Hippius, C.; Würthner, F., Photophysical Characterization of a Light-Harvesting Tetra Naphthalene Imide/Perylene Bisimide Array. *The Journal of Physical Chemistry C* **2007**, *111* (2), 622-630.
- (20) Dubey, R. K.; Niemi, M.; Kaunisto, K.; Stranius, K.; Efimov, A.; Tkachenko, N. V.; Lemmetyinen, H., Excited-State Interaction of Red and Green Perylene Diimides with Luminescent Ru(II) Polypyridine Complex. *Inorganic Chemistry* **2013**, *52* (17), 9761-9773.
- (21) Blas-Ferrando, V. M.; Ortiz, J.; Ohkubo, K.; Fukuzumi, S.; Fernandez-Lazaro, F.; Sastre-Santos, A., Submillisecond-lived photoinduced charge separation in a fully conjugated phthalocyanine-perylenebenzimidazole dyad. *Chemical Science* **2014**, *5* (12), 4785-4793.
- (22) Wasielewski, M. R., Energy, Charge, and Spin Transport in Molecules and Self-Assembled Nanostructures Inspired by Photosynthesis. *The Journal of Organic Chemistry* **2006**, *71* (14), 5051-5066.

- (23) Dubey, R. K.; Niemi, M.; Kaunisto, K.; Efimov, A.; Tkachenko, N. V.; Lemmetyinen, H., Direct Evidence of Significantly Different Chemical Behavior and Excited-State Dynamics of 1,7- and 1,6-Regioisomers of Pyrrolidinyl-Substituted Perylene Diimide. *Chemistry – A European Journal* **2013**, *19* (21), 6791-6806.
- (24) Shibano, Y.; Umeyama, T.; Matano, Y.; Tkachenko, N. V.; Lemmetyinen, H.; Araki, Y.; Ito, O.; Imahori, H., Large Reorganization Energy of Pyrrolidine-Substituted Perylenediimide in Electron Transfer. *The Journal of Physical Chemistry C* **2007**, *111* (16), 6133-6142.
- (25) Gorczak, N.; Renaud, N.; Tarkuc, S.; Houtepen, A. J.; Elkekema, R.; Siebbeles, L. D. A.; Grozema, F. C., Charge transfer versus molecular conductance: molecular orbital symmetry turns quantum interference rules upside down. *Chemical Science* **2015**, *6* (7), 4196-4206.
- (26) Shoer, L. E.; Eaton, S. W.; Margulies, E. A.; Wasielewski, M. R., Photoinduced Electron Transfer in 2,5,8,11-Tetrakis-Donor-Substituted Perylene-3,4,9,10-bis(dicarboximides). *The Journal of Physical Chemistry B* **2015**, *119* (24), 7635-7643.
- (27) Pagoaga, B.; Mongin, O.; Caselli, M.; Vanossi, D.; Momicchioli, F.; Blanchard-Desce, M.; Lemercier, G.; Hoffmann, N.; Ponterini, G., Optical and photophysical properties of anisole- and cyanobenzene-substituted perylene diimides. *Physical Chemistry Chemical Physics* **2016**, *18* (6), 4924-4941.
- (28) Flamigni, L.; Ventura, B.; Barbieri, A.; Langhals, H.; Wetzel, F.; Fuchs, K.; Walter, A., On/Off Switching of Perylene Tetracarboxylic Bisimide Luminescence by Means of Substitution at the N-Position by Electron-Rich Mono-, Di-, and Trimethoxybenzenes. *Chemistry – A European Journal* **2010**, *16* (45), 13406-13416.
- (29) Dubey, R. K.; Westerveld, N.; Sudholter, E. J. R.; Grozema, F. C.; Jager, W. F., Novel derivatives of 1,6,7,12-tetrachloroperylene-3,4,9,10-tetracarboxylic acid: synthesis, electrochemical and optical properties. *Organic Chemistry Frontiers* **2016**, *3* (11), 1481-1492.
- (30) Xue, C.; Sun, R.; Annab, R.; Abadi, D.; Jin, S., Perylene monoanhydride diester: a versatile intermediate for the synthesis of unsymmetrically substituted perylene tetracarboxylic derivatives. *Tetrahedron Letters* **2009**, *50* (8), 853-856.
- (31) Würthner, F.; Saha-Möller, C. R.; Fimmel, B.; Ogi, S.; Leowanawat, P.; Schmidt, D., Perylene Bisimide Dye Assemblies as Archetype Functional Supramolecular Materials. *Chemical Reviews* **2016**, *116* (3), 962-1052.
- (32) Echue, G.; Lloyd-Jones, G. C.; Faul, C. F. J., Chiral Perylene Diimides: Building Blocks for Ionic Self-Assembly. *Chemistry – A European Journal* **2015**, *21* (13), 5118-5128.
- (33) Würthner, F.; Thalacker, C.; Diele, S.; Tschierske, C., Fluorescent J-type Aggregates and Thermotropic Columnar Mesophases of Perylene Bisimide Dyes. *Chemistry – A European Journal* **2001**, *7* (10), 2245-2253.
- (34) Dubey, R. K.; Efimov, A.; Lemmetyinen, H., 1,7- And 1,6-Regioisomers of Diphenoxy and Dipyrrolidinyl Substituted Perylene Diimides: Synthesis, Separation, Characterization, and Comparison of Electrochemical and Optical Properties. *Chemistry of Materials* **2011**, *23* (3), 778-788.
- (35) Vajiravelu, S.; Ramunas, L.; Juozas Vidas, G.; Valentas, G.; Vygintas, J.; Valiyaveetil, S., Effect of substituents on the electron transport properties of bay substituted perylene diimide derivatives. *Journal of Materials Chemistry* **2009**, *19* (24), 4268-4275.
- (36) Escudero, D., Revising Intramolecular Photoinduced Electron Transfer (PET) from First- Principles. *Accounts of Chemical Research* **2016**, *49* (9), 1816-1824.
- (37) Zweig, A.; Hodgson, W. G.; Jura, W. H., The Oxidation of Methoxybenzenes. *Journal of the American Chemical Society* **1964**, *86* (19), 4124-4129.
- (38) Dubey, R. K.; Knorr, G.; Westerveld, N.; Jager, W. F., Fluorescent PET probes based on perylene-3,4,9,10-tetracarboxylic tetraesters. *Organic & Biomolecular Chemistry* **2016**, *14* (5), 1564-1568.
- (39) Fron, E.; Pilot, R.; Schweitzer, G.; Qu, J.; Herrmann, A.; Mullen, K.; Hofkens, J.; Van der Auwerer, M.; De Schryver, F. C., Photoinduced electron-transfer in perylenediimide triphenylamine-based dendrimers: single photon timing and femtosecond transient absorption spectroscopy. *Photochemical & Photobiological Sciences* **2008**, *7* (5), 597-604.
- (40) Crosby, G. A.; Demas, J. N., Measurement of photoluminescence quantum yields. Review. *The Journal of Physical Chemistry* **1971**, *75* (8), 991-1024.
- (41) Langhals, H.; Karolin, J.; B-A. Johansson, L., Spectroscopic properties of new and convenient standards for measuring fluorescence quantum yields. *Journal of the Chemical Society, Faraday Transactions* **1998**, *94* (19), 2919-2922.

3 • How To Create Artificial Light Harvesting Antennas

This chapter gives the synthesis and excited-state dynamics of a series of five bichromophoric light-harvesting antenna systems, which are capable of efficient harvesting of solar energy in the spectral range of 350-580 nm. These antenna systems have been synthesized in a modular fashion by the covalent attachment of blue light absorbing naphthalene monoimide energy donors to green light absorbing perylene-3,4,9,10-tetracarboxylic acid derived energy acceptors. The energy donors have been linked at the 1,7-bay-positions of the perylene derivatives, thus leaving the peri positions free for further functionalization and device construction. The selection of donor naphthalene derivatives for attachment with perylene derivatives was based on the effective matching of their respective optical properties to achieve efficient excitation energy transfer (EET) by the Förster mechanism. A comprehensive study of the excited-state dynamics, in toluene, revealed quantitative and ultrafast (ca. 1 ps) intramolecular EET from donor naphthalene chromophores to the acceptor perylenes in all the studied systems. Electron transfer from the donor naphthalene chromophores to the acceptor perylenes has not been observed, not even for antenna systems in which this process is thermodynamically allowed. Due to the combination of an efficient and fast energy transfer along with broad absorption in the visible region, these antenna systems are promising materials for solar-to-electric and solar-to-fuel devices.

3.1 Introduction

Conversion of sunlight into more useful forms of energy is the most sustainable and promising endeavor to tackle the growing global concerns on energy supply and environmental issues. Solar energy can either be turned directly into electricity using solar cells or converted to high-energy compounds that can be used as fuel. The latter approach is reminiscent of natural photosynthesis, which is often used as a source of inspiration to achieve the so-called artificial photosynthesis.^{2,3} The success of both approaches heavily relies on the ability of artificial devices to harvest the maximum amount of incident light energy. Therefore, current research efforts largely focus on the efficient harvesting of solar irradiation, especially between 400 to 920 nm.⁴⁻⁷

In the past, a wide range of organic and organometallic chromophores have been employed as sensitizers in solar-to electric and solar-to-fuel devices, owing to their high molar absorptivities in the visible region.⁸⁻¹⁴ However, the intense transitions of individual chromophores are often narrow, which results in poor overlap of their absorption with the incident solar spectrum. Light-harvesting antenna systems, utilized in natural photosynthesis, contain large numbers of nearly identical chromophores, which are precisely positioned in a protein matrix. This approach ensures a high optical density, even for thin layers, but the spectral coverage from essentially one chromophore is generally poor.¹⁵ Energy transfer between the individual dye molecules in these systems is extremely fast, in the order of 0.1 ps, and the energy transfer mechanism is generally referred to as quantum coherence.³

Synthetic light-harvesting antenna systems generally consist of multiple chromophores with distinct chemical structures and complementary absorption spectra. These chromophores absorb light below a threshold wavelength and funnel the excitation energy unidirectionally towards a single chromophore within the array. In these systems, the excitation energy transfer is generally accomplished by dipole–dipole interactions, commonly referred to as Förster Resonance Energy Transfer (FRET).¹⁶ This approach ensures a large coverage of the visible spectrum using a less demanding and more straightforward molecular design.¹⁷ Obtaining large optical densities on relatively thin layers is an issue that is generally tackled by absorbing dye molecules on a structured interface like TiO₂, as is the case for well-known dye-sensitized solar cells (DSCs).^{18,19}

Artificial light-harvesting (LH) antenna systems are thus an essential building block for the realization of efficient solar energy conversion.^{4,5,20,21} In addition to the careful tuning of the optical properties of the individual chromophores to accomplish fast and efficient energy transfer, a simple and robust antenna design, synthetic accessibility of the components, and elimination of competing photo-induced processes are essential elements for the development of suitable light-harvesting antenna systems that can ultimately be incorporated into devices.

The choice of the acceptor chromophore in light-harvesting antenna systems determines the properties of the antenna to a large extent for several reasons. First of all, the excitation energy of the acceptor determines the upper limit of the spectral range of the antenna system and thereby the energy content of the photons that are harvested. Secondly, the stability of the excited state of the acceptor determines, to a large extent, the stability of the antenna system itself. That is because the energy transfer between the chromophores is generally faster than the electron transfer that follows, and because of that the excitation

energy resides at the acceptor chromophore for most of the time.²² Antenna systems based on various energy acceptor chromophores, which are often attached to dendritic scaffolds, have been reported.^{23–33} Recently, the use of bio-based binding platforms,²⁰ like DNA³⁴ and sugars,³⁵ and the use of hybrid organic–inorganic materials,³⁶ like metal organic frameworks (MOFs) and periodic mesoporous organosilicas (PMOs), for the construction of light-harvesting assemblies has been demonstrated. A wide variety of organic chromophores, such as BODIPY dyes,^{6,29} perylene bisimides,^{37–48} and aromatic hydrocarbons, have been employed for constructing light-harvesting antenna molecules. A particularly attractive chromophore for the design of such light-harvesting arrays is perylene bisimide (PBI), a molecule that is well-known for its exceptional photochemical stability, strong and broad absorption in the visible region, and synthetic versatility.^{49,50} Perylene-based antenna molecules carrying various donors have been reported,^{37–44} along with larger antenna systems in which perylene bisimides are intermediate energy donors.^{45–48} In addition, the strong absorption of PBIs has been successfully utilized to improve the spectral coverage of C₆₀.^{43,51–55} An unfavorable feature of PBI dyes is their high electron deficiency,⁴⁹ and therefore PBI assemblies tend to undergo facile charge-separation when PBIs are coupled with even moderately electron-rich chromophores.⁵⁶ In addition, the strong tendency of PBIs to form π - π aggregates is a severe limitation that needs to be accounted for in the design of molecular PBI based arrays.^{57,58} As a result, the construction of PBI based light-harvesting arrays requires careful design, with regard to matching the electrochemical properties of the donor and acceptor chromophores, the selection of the spacers that connect these units, and the prevention of undesirable aggregation. Otherwise, electron-transfer processes, which are undesirable within the antenna system, will compete with the energy transfer.^{41,44}

In this work, we report on the design, synthesis and characterization of a series of functional, robust, and highly efficient light-harvesting antenna molecules based on perylene-3,4,9,10-tetracarboxylic acid derivatives. In the design of these molecules we have used a modular synthetic approach, employing three naphthalene monoimide-derived energy donor molecules, **D1–D3**, along with three perylene-3,4,9,10-tetracarboxylic acid derived energy acceptors; perylene-3,4,9,10-tetrabutylester (**A1**), perylene-3,4,9,10-monoimide dibutylester (**A2**),⁵⁹ and perylene-3,4,9,10-bisimide **A3**, see **Figure 3.1**. The recently developed acceptors **A1** and **A2** have significantly reduced electron deficiencies and increased solubility compared to PBI (**A3**). The donor fragments 4-(isopentylthio) naphthalene monoimide (**D1**), 4-(n-butylamino) naphthalene monoimide (**D2**), and 4-(dimethylamino) naphthalene monoimide (**D3**) were selected because these molecules are stable, readily accessible, and have appropriate redox properties to limit electron transfer.^{49,60,61} Also, these compounds are highly fluorescent, with emission spectra that strongly overlap with the absorption spectra of the perylene derivatives, which facilitates efficient excitation energy transfer by the Förster mechanism. From the nine possible donor–acceptor combinations depicted in the matrix in **Figure 3.1**, we have synthesized the antenna molecules **D1A1**, **D1A2**, **D2A2**, **D2A3** and **D3A3**. In particular, for the “diagonal compounds” **D1A1**, **D2A2** and **D3A3**, the donor and acceptor absorptions are expected to be complementary and a broad continuous absorption is anticipated for these compounds. Also, the best overlap between donor emission and acceptor absorption, the main prerequisite for efficient Förster energy transfer, is expected for these “diagonal” compounds. For the other compounds, **D1A2** and **D2A3**, donor absorptions are

blue-shifted and a “hole” in the absorption spectrum is anticipated. For the remaining compounds, the donor and acceptor chromophores absorb more or less in the same wavelength region, and for that reason these compounds have not been synthesized.

For the covalent attachment of donors, we have chosen the phenoxy substitution approach to achieve a high chemical stability and a rigid well-defined conformation of the antenna molecules. Also, the phenoxy coupling approach ensured that the donor and acceptor chromophores are electronically decoupled, which implies that the absorption spectra and the electrochemical properties of the donor and acceptor fragments are unaffected by the coupling. This makes the physical properties of these compounds highly predictable and enables the developments of these antenna molecules by a truly modular approach. A detailed photophysical characterization of all the antenna systems was carried out using steady-state and time-resolved spectroscopy, along with cyclic voltammetry, in order to gain a good understanding of the energy transfer process and the effect of perylene structure modification on the excited-state dynamics.

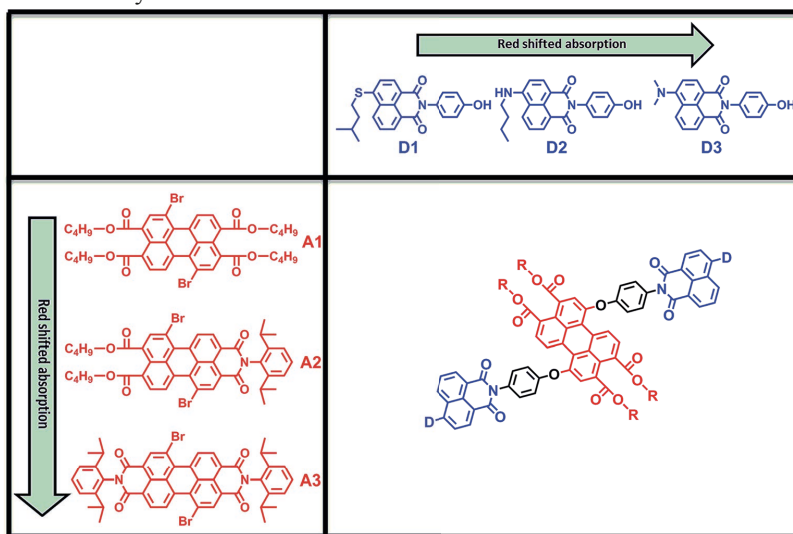


Figure 3.1 The modular design of the light-harvesting antennae based on perylene tetracarboxylic acid derivatives (**A1**, **A2**, and **A3**) and naphthalene monoimides (**D1**, **D2**, **D3**).

3.2 Results and Discussion

3.2.1 Electrochemical Studies

The redox properties of the antenna systems and model compounds were investigated using cyclic voltammetry in dichloromethane. The obtained redox potentials (V vs. Fc/Fc^+) for the antenna systems are reported in **Table 3.1**. For the reference donors **ref-D2** and **ref-D3**, first oxidation potentials were measured at 0.81 and 0.75 V, respectively (**Table B1**, **Appendix B**). For **ref-D1**, no oxidation was observed in the measured potential window. The oxidation potential of **ref-D1** is expected to be higher than that of **ref-D2**, based on the weaker electron donating nature of the isopentylthio group compared to the butylamino group.⁶² For all antenna molecules, the obtained values for the oxidation of **D2** and **D3** units were similar to

those of the reference compounds **ref-D2** and **ref-D3** (Table 3.1). Once more, this indicates the lack of conjugation between the two types of chromophores in the antenna molecules. For the perylene moieties in the antenna molecules (**A1**, **A2**, and **A3**), first reduction potentials were obtained at ca. -1.55, -1.33, and -1.08 V, respectively. These values, which are virtually identical to those measured for the reference compounds **ref-A1**, **ref-A2** and **ref-A3**, shown in Table B1, indicate that the electron deficiency significantly increases upon moving from **A1** to **A3**.

For the antenna molecules, the energies of the charge-separated (CS) states, in DCM, were estimated by calculating the difference between the first oxidation potential of the donor and the first reduction potential of the acceptor [$E_{CS} = E_{1ox}(D) - E_{1red}(A)$]. The energies of the charge-separated states ($D^+ - A^-$) for antenna systems **D2A2**, **D2A3**, and **D3A3** are estimated at ca. 2.13, 1.88, and 1.81 eV, respectively. Among these three systems, **D2A2** has the highest energy of the CS states, which is due to the higher reduction potential of **A2** compared to **A3**. The energies of the CS states could not be estimated for systems **D1A1** and **D1A2** because no redox activity for **D1** has been observed. However, in view of the weaker electron-donating capability of **D1**, the CS states of **D1A1** and **D1A2** should have values that are significantly higher than the 2.13 eV estimated for **D2A2**. The data in Table 3.1 clearly indicate that the energies of the charge-separated states of **D2A2**, **D2A3** and **D3A3** are below those of the singlet excited acceptor state. Therefore photo-induced electron transfer is a thermodynamically allowed process for these compounds in dichloromethane. In apolar toluene, the CS states of all antenna systems should be around 0.20–0.30 eV higher than the corresponding values estimated for DCM.^{41,63} This implies that in toluene, the CS states in most of the antenna systems will be of approximately the same value (or even higher) than that of the first singlet excited state of the respective perylene component, and no photoinduced electron transfer is expected to occur. However, for antenna molecules containing **A3**, in particular antenna molecule **D3A3**, photoinduced electron transfer from the singlet acceptor excited state of the acceptor is an energetically favorable process.

Table 3. 1 Electrochemical properties of the antenna systems (V vs. Fc/Fc⁺) obtained using cyclic voltammetry in CH₂Cl₂^a

Compound	Naphthalimide		Perylene		$E_{CS}(D^+-A^-)^d$ ΔG_{CS}^e	
	$E_{1/2ox}$	E_{S1}^b (eV)	$E_{1/2red}$	E_{S1}^c (eV)	In DCM (eV)	In DCM (eV)
D1A1	— ^f	2.80	-1.55 ^g	2.41	>2.13	-
D1A2	— ^f	2.80	-1.34	2.37	>2.13	-
D2A2	+0.80	2.60	-1.33	2.35	2.13	0.22
D2A3	+0.79	2.58	-1.09	2.15	1.88	0.27
D3A3	+0.74	2.58	-1.07	2.15	1.81	0.34

^a Scan rate 0.10 V s⁻¹. ^b Energy of the first singlet excited state of the naphthalimide unit calculated from the absorption and emission measurements. ^c Energy of the first singlet excited state of the perylene moiety obtained electrochemically. ^d Energy of the lowest charge-separated state. ^e Driving force for charge separation with respect to perylene singlet excited state, $E_{S1} - E_{CS}(D^+-A^-)$. ^f No oxidation signal was detected in the measured potential window. ^g Value taken from compound 15.

3.2.2 Steady-state Absorption Studies

The absorption spectra of all the reference compounds and antenna systems in toluene are shown in **Figure 3.2**.

The absorption spectra of the reference acceptors (**ref-A1**, **ref-A2**, and **ref-A3**) exhibit strong absorptions at wavelengths longer than ca. 430 nm. The absorption band shifts to longer wavelengths by 30–40 nm and the molar absorptivity increases upon going from **ref-A1** to **ref-A2** to **ref-A3** (**Table 3.2**). The reference donors (**ref-D1**, **ref-D2**, and **ref-D3**) exhibit absorption at shorter wavelengths in the range of 350–450 nm. Among them, **ref-D1** has the most blue-shifted absorption with λ_{max} at 383 nm. The absorption of compounds **ref-D2** and **ref-D3** are red-shifted by 20–40 nm relative to **ref-D1**. Surprisingly, the absorption of **D3** is not red-shifted compared to that of **D2**.^{62,64,65} The molar absorptivity of donor molecules is significantly lower compared to those of the acceptors. For that reason, the antenna systems are designed with two donors linked to a single acceptor.

The absorption spectra of the antenna systems clearly revealed the characteristic features of both donor and acceptor moieties (**Figure 3.2**). At shorter wavelengths, absorption is dominated by the naphthalene chromophores, whereas the absorption at longer wavelengths originates exclusively from the perylene chromophores. Moreover, the spectra of all the antenna systems correspond very closely to the sum of the spectra of constituent chromophores, as can be seen in **Figure 3.2.d**. These results reflect the absence of any ground-state interaction between the two chromophores, which can be explained by the absence of conjugation between them. Notable is the excellent spectral coverage of most antenna molecules. Most antenna molecules have a high and uninterrupted absorption over a 200 nm wavelength span. Only in the case of compound **D1A2**, a distinct hole in the absorption spectrum around 430 nm is observed.

Table 3. 2 Photo-physical properties of the model compounds and antenna systems in toluene

Compound	$\lambda_{\text{abs}}(\text{nm})$	$\epsilon (\text{M}^{-1} \text{cm}^{-1})$	$\lambda_{\text{em}}(\text{nm})$	$\phi_{\text{f}}^{\text{a}}$	$\tau_{\text{f}}^{\text{b}} (\text{ns})$	$\tau_{\text{EET}}^{\text{b}} (\text{ps})$
Ref-D1	383	20 000	447	0.77	5.50	-
Ref-D2	420	15 500	489	0.81	8.84	-
Ref-D3	402	12 600	494	0.82	7.86	-
Ref-A1	474	35 900	515	0.92	4.56	-
Ref-A2	515	40 800	554	0.95	4.67	-
Ref-A3	543	54 500	576	0.96	4.52	-
D1A1	382	43 400	512	0.93 ^d	4.50 ^c	0.99
	473	36 300		0.92 ^c		
D1A2	386	41 200	551	0.94 ^d	4.65 ^c	1.31
	512	39 000		0.92 ^c		
D2A2	421	38 000	553	0.92 ^d	4.60 ^c	1.16
	514	41 100		0.95 ^c		
D2A3	421	38 300	572	0.96 ^d	4.54 ^c	0.92
	539	50 300		0.97 ^c		
D3A3	402	35 100	571	0.96 ^d	4.51 ^c	0.87
	538	50 900		0.94 ^c		

^a Fluorescence quantum yield. ^b Fluorescence lifetime ($\lambda_{\text{ex}} = 400 \text{ nm}$). ^c Lifetime data for energy transfer obtained from femtosecond transient absorption experiments. ^d Obtained after selective excitation of the perylene moiety. ^e Obtained after predominant excitation of the naphthalene moiety.

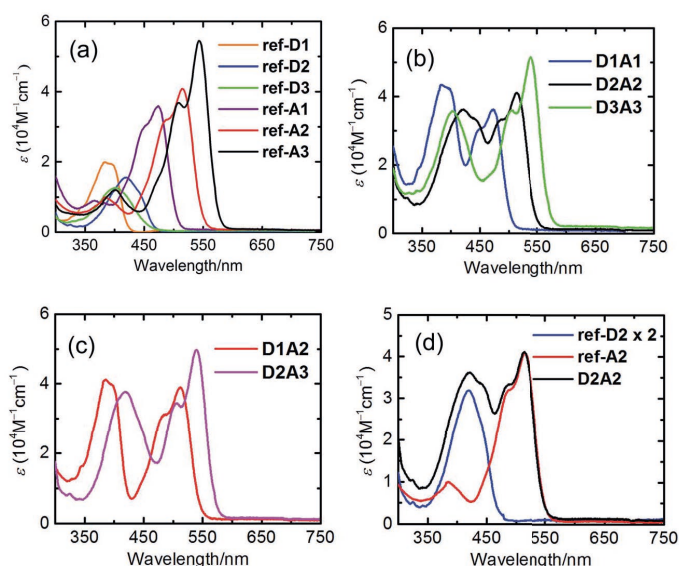


Figure 3.2 UV/Vis absorption spectra in toluene: (a) reference donor and acceptor compounds; (b) antenna systems **D1A1**, **D2A2** and **D3A3**; (c) antenna systems **D1A2** and **D2A3**; (d) antenna system **D2A2** with **ref-D2** and **ref-A2** (note: the spectrum of **ref-D2** is multiplied by two).

3.2.3 Steady-state and Time Resolved Emission Studies

Efficient transfer of excitation energy from the outer naphthalene chromophores to the inner perylene moiety is a prerequisite for a good light-harvesting antenna system. Therefore, we first examined the overlap between the donor's emission and acceptor's absorption, which is an important condition for efficient fluorescence resonance based energy transfer. In all antenna systems, the donor's emission overlapped strongly with the absorption of perylene derivatives. For example, the donor compound **ref-D2** emits strongly in the range of 450–575 nm and **ref-A2** absorbs strongly in the same range as is shown in **Figure 3.3**.

All the reference acceptor compounds are highly emissive with fluorescence quantum yields of *ca.* 0.95 and singlet-state lifetimes around 4.6 ns (**Table 3.2**). Their emission bands are red shifted compared to the reference donors as depicted in **Figure 3.4.a**. The reference donors also exhibit strong emissions ($\Phi_f > 0.75$) with singlet lifetimes in the range of 5.5–8.8 ns.

The fluorescence emission studies of the antenna molecules were performed at two separate wavelengths to achieve selective excitation of only one chromophore. First, the perylene moieties were selectively excited at wavelengths higher than 460 nm and their emission, in terms of intensity and lifetime, was found to be identical to those of reference acceptors (**Figure 3.4.c** and **Table 3.2**). This indicates that the perylene excited state decays to the ground state exclusively via emission in all antenna molecules.

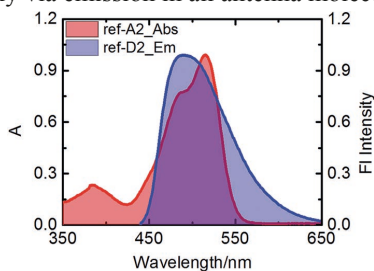


Figure 3.3 Overlap of the emission of **ref-D2** with the absorption of **ref-A2** in toluene.

Subsequently, the antenna molecules were excited at the absorption maxima of the naphthalene chromophores in the range of 380–420 nm, to achieve predominant excitation of the donor chromophores. In these measurements, the emission of the naphthalene chromophores was found to be completely quenched in all the antennae (**Figure 3.4.b**). At the same time, all the antenna molecules produced the characteristic sensitized emission of perylene moieties with fluorescence quantum yields and lifetimes identical to those of the reference acceptors (**Figure 3.4.d** and **Table 3.2**). These results not only indicate a quantitative photo-induced energy transfer from the naphthalene moieties to the perylene chromophores, but also show an absence of other photo-induced processes in these antenna systems, such as photo-induced electron transfer from the naphthalene to the perylene unit. This conclusion was further verified by the excitation spectra of the antenna molecules measured at 600 nm (*i.e.* at the emission band of the perylene component), which resemble their absorption spectra within experimental error (**Figure 3.5**).

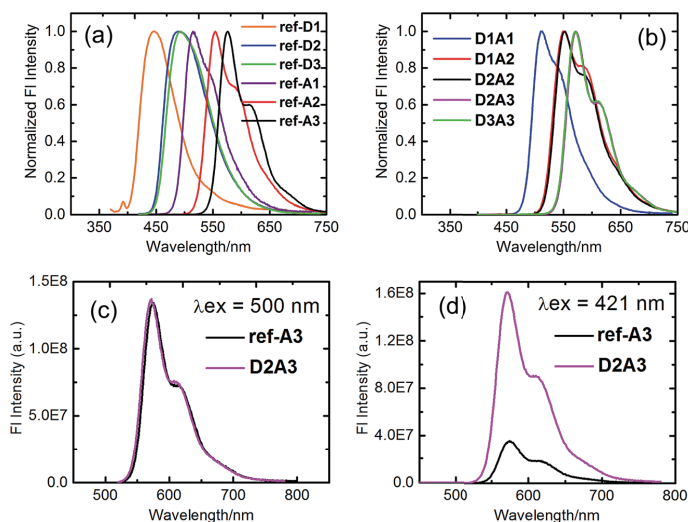


Figure 3.4 Normalized steady-state emission spectra in toluene: (a) the reference compounds; (b) the antenna systems obtained after excitation at the absorption maxima of the naphthalene moieties. (c) Excitation at 500 nm; **ref-A3** ($A = 0.16$) and **D2A3** ($A = 0.16$). (d) Excitation at 421 nm; **ref-A3** ($A = 0.04$) and **D2A3** ($A = 0.18$).

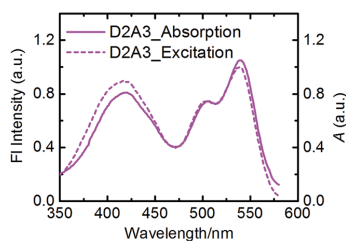


Figure 3.5 Excitation spectrum of **D2A3** (dashed-line) measured at $\lambda_{em} = 600$ nm along with the absorption spectrum (solid-line) in toluene.

3.2.4 Transient Absorption Studies

Finally, the excited state dynamics of all antenna molecules in toluene was examined on the femtosecond time-scale to gain insight into the kinetics of the intramolecular photo-induced energy transfer process. For these measurements, the antenna systems were excited at two different excitation wavelengths. First, at the absorption maxima of the perylene chromophores is to achieve an exclusive excitation of the perylene component. And secondly, at 400 nm, which resulted in the predominant excitation of the donor naphthalene moieties.

Excitation of all the antenna molecules at the perylene absorption maximum resulted in the instant formation of the first singlet excited state of the perylene acceptor, as illustrated for antenna **D1A2** in **Figure 3.6**. These perylene singlet excited states are characterized by their typical features, *i.e.* strong absorption between 650–850 nm and a bleach of the ground state absorption at ca. 500 nm,^{41,44,54} as has been reported for perylene bisimides. The absorption spectra of the singlet excited state of the perylene tetraester **A1** and the perylene monoimide diester **A2**, which have not been reported previously, are slightly blue shifted compared to the excited state absorption spectrum of **A3** (**Figure B.7, Appendix B**). No

changes in the absorption spectra of the perylene excited state at picosecond delay times were observed. At nanosecond delay times, the magnitude of the time resolved absorption spectra gradually decreases. This leads to the conclusion that for all antenna molecules, the perylene excited state decays directly to the ground state *via* emission from the singlet excited state.

Excitation of the antenna molecules at the donor absorption maxima is illustrated for antenna **D1A2** in **Figure 3.6**. Immediately after the laser excitation of antenna **D1A2** at 400 nm, absorption due to the singlet-excited state of the perylene unit was observed. The immediate appearance of the perylene singlet excited state can be rationalized based on the fact that the perylene chromophore also has a limited absorption at the excitation wavelength (*i.e.* 400 nm). With the increase in delay times in the range of 0–10 ps, the perylene singlet excited state absorption increases drastically. At nanosecond delay times the magnitude of the time resolved absorption spectra gradually decreases, due to stimulated emission from the acceptor. Similar results were observed for the other antenna systems as well (**Figure B.7**, **Appendix B**).

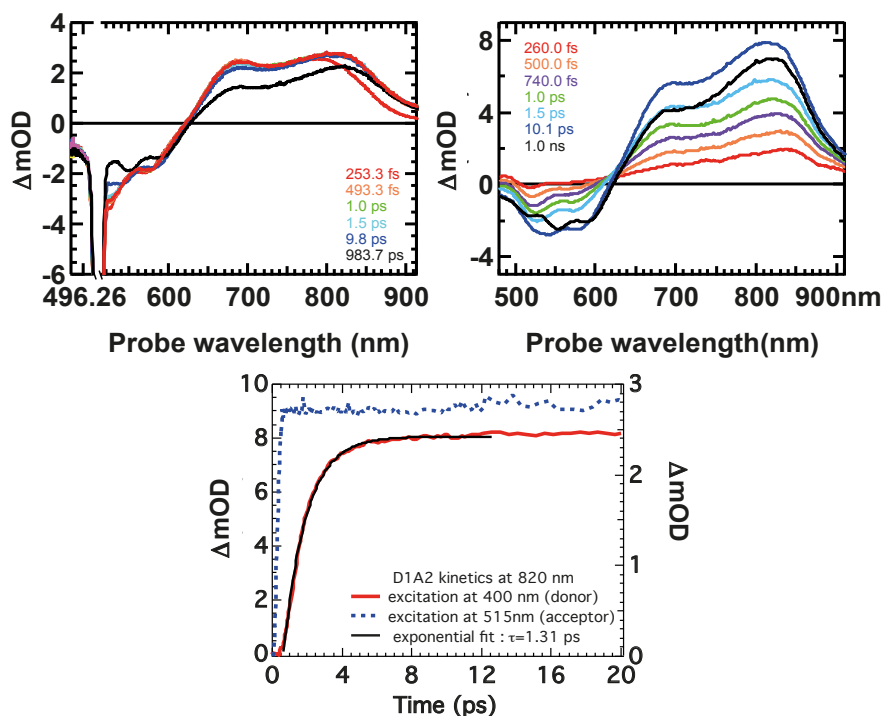


Figure 3.6 Time evolution of the femtosecond transient absorption spectra of the antenna system **D1A2** after selective excitation of the perylene chromophore at 515 nm (top left) and after predominant excitation of the naphthalene chromophore at 400 nm (top right). Kinetics of **D1A2** at 820 nm obtained after excitation at 400 and 515 nm (bottom).

The kinetics of the formation of the perylene singlet excited state absorption that was obtained after the excitation of the antenna molecules at 400 nm, was compared with the one obtained after the selective excitation of the perylene chromophore at 515 nm, and is represented in **Figure 3.6**. These kinetic profiles are consistent with a fast excitation energy

transfer from the naphthalene chromophore to the perylene component and subsequent slow decay of the perylene singlet excited state to the ground state *via* emission (or non-radiative decay). The time constants τ_{EET} (as shown in **Figure 3.7**) for the energy transfer processes were determined by fitting the curves in **Figure 3.6** and **B.6** and are compiled in **Table 3.2**. All antenna molecules show ultrafast energy transfer with time constants ranging from 0.9 to 1.3 ps. This ultrafast energy transfer is explained by the large values of the overlap integrals of donor emission and acceptor absorption, and the short distances between the donor and acceptor moieties in the antenna molecules. For synthetic light-harvesting antenna molecules containing perylene energy acceptors, energy transfer with significantly longer time constants, typically in the order of 5–50 ps, have been reported.^{23–32,37–44} This is most likely due to the larger D–A distances along with a decreased overlap between the donor emission and acceptor absorption spectra in these systems. The modest increase in energy transfer rates, upon going from antenna molecules based on **A2** to **A3**, may be explained by a gradual increase of the acceptor extinction coefficients in this series.

As far as the occurrence of electron transfer processes are concerned, no spectral evidence for the formation of the perylene radical anions, which in the case of perylene bisimides can be easily recognized by their characteristic strong and relatively narrow absorption at ca. 725 nm,^{44,54,66,67} has been detected. This observation as such does not fully exclude the occurrence of photo-induced electron transfer within the antenna molecules. This is because very small quantities of CT species (<1%) may not be detected by transient absorption. Also, accumulation of CT states will not occur if the back electron transfer (BET) to the ground state is faster than the forward photo-induced electron transfer. Nevertheless, the lack of spectral evidence for photoinduced charge transfer is fully in line with the results obtained by steady state fluorescence, notably the unaltered lifetimes and fluorescence quantum yields of the singlet states of the perylene acceptors moieties upon incorporation in light-harvesting antenna molecules.

3.3 Discussions

We have designed and synthesized a series of five light-harvesting antenna molecules that exhibit 150 to 200 nm wide strong absorptions in the 350–580 nm wavelength region. For these compounds the absorption wavelength region is tunable in steps of 30–40 nm. The high absorption throughout a large part of the visible wavelength region is in contrast to most other light-harvesting molecules that generally exhibit large differences in the extinction coefficient within their absorption range. All antenna molecules exhibit the desired photo-physics for light-harvesting antenna systems, depicted in **Figure 3.7**; quantitative and ultrafast energy transfer from the donor excited state towards the acceptor, $D^* \rightarrow A$ to $D \rightarrow A^*$, no charge transfer from the acceptor excited state ($D \rightarrow A^*$ to $D^+ \cdot - A^- \cdot$), and a long lifetime of the acceptor excited state.

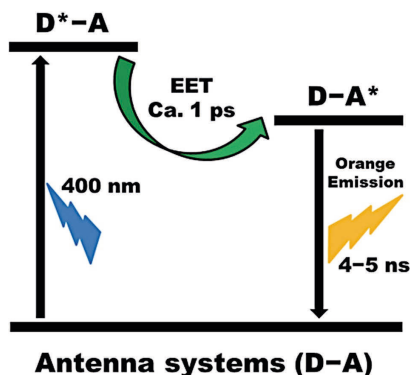


Figure 3.7 Summary of processes that take place in our antenna systems upon excitation of the naphthalene chromophore in toluene.

The absence of electron transfer in all antenna molecules that we report here is remarkable. For example, a structurally similar antenna molecule, in which four 4-dimethylaminonaphthalimide moieties (similar to **D3**) were covalently linked to the bay positions of perylene bisimide using a long and flexible linker, was earlier reported by Flamigni *et al.*⁴¹ The photophysics of this molecule were investigated in toluene. Energy transfer from the peripheral naphthalimide donors to the PBI acceptor is relatively slow with $\tau_{ET}=54$ ps and 90% efficient due to competitive electron transfer from the excited naphthalene unit to the perylene, a process with $\tau_{CT} = 0.6$ ns. From the perylene excited state, charge-transfer to the naphthalene moieties is slower ($\tau_{CT} = 2.1$ ns) and in competition with perylene fluorescence ($\tau_F = 6.0$ ns). Interestingly, we did not observe any charge-separation in our PBI based antenna **D3A3**, which has the same donor and a slightly more electronegative acceptor chromophore compared to the above-mentioned system. This difference in photoinduced behavior can only be explained by the different design of the linkers. In our antenna systems, the rigid structure of the spacer keeps the two acting moieties away from each other, which reduces the rate of electron transfer. This finding underlines the importance of employing rigid linkers in the construction of perylene based antenna systems.

Finally, it is worthwhile to evaluate the utility of the reported light-harvesting antenna molecules for constructing practical devices for photovoltaics or solar fuel generation. In such devices, fast and efficient energy transfer towards the acceptor should be followed by an efficient electron transfer from the acceptor excited state towards other components in the device, to produce either a potential difference for photovoltaics or charged catalysts that produce a solar fuel. Thus, the basic device requirements for such devices are that the energy transfer from the donor to the acceptor within the antenna molecule outcompetes other photo-physical processes from the donor excited state, notably electron transfer from the donor to the acceptor within the antenna system. In addition, the desired electron transfer processes starting from the acceptor excited state must outcompete other photo physical processes, notably electron transfer from the donor towards the acceptor and acceptor fluorescence. In this perspective it is important to realize that electron transfer processes are strongly enhanced in polar media, whereas energy transfer for rigid molecules does not depend on solvent polarity. For our antenna molecules, the energy transfer process from the naphthalene donor

to the perylene acceptor, D^*-A to $D-A^*$, occurs in approximately 1 ps, which is relatively fast for a synthetic antenna system, and will be fast enough to outcompete electron transfer processes. From the acceptor-excited state thus obtained, electron transfer should be the dominant process. Time constants for the electron transfer from perylene excited states to good electron donors,^{56,68,69,70,71} are typically 2 orders of magnitude below the 4–5 ns fluorescence lifetimes of our perylene acceptors. In solvents of high polarity, electron transfer from the naphthalene donor towards the perylene excited state will be thermodynamically allowed, in particular from the antenna systems based on the electron deficient PDI acceptor A3. However, it should be a rather straightforward exercise to design the antenna systems, such that the desired electron transfer process outcompetes electron transfer within the antenna molecules. Choosing appropriate linkers to limit electron transfer within the antenna molecules, like the phenoxy linker described herein, and applying acceptors with a decreased electron affinity, like **D1** or **D2**, are the most obvious design criteria for limiting intermolecular energy transfer within the antenna.

3.4 Conclusions

A series of light-harvesting antenna molecules have been synthesized in a modular fashion, by a highly efficient covalent attachment of two identical naphthalene chromophores to the 1,7-bay positions of perylene-3,4,9,10-tetracarboxy derivatives. All the antenna molecules showed an efficient light absorption over a 200 nm wavelength span that is tunable in the 350–580 nm wavelength region. All antenna molecules exhibit good overlap between the donor's emission and the acceptor's absorption, which is a prerequisite for an efficient excited energy transfer (EET) by the Förster mechanism. In toluene, the light harvested by the naphthalene unit is transferred quantitatively to the perylene chromophore in picosecond time-scale in all antenna systems. Subsequently, the perylene singlet excited state decays to the ground state by the exclusive emission of light on a nanosecond time-scale (**Figure 3.7**).

No signs of photoinduced electron transfer were observed in our antenna molecules, despite the fact that the estimated energies of the charge-separated states obtained by cyclic voltammetry indicate that excited state deactivation by electron transfer is thermodynamically allowed and may already compete with the energy transfer process in apolar solvents like toluene. Therefore, we conclude that the rigid phenol linker group that is used in our antenna molecule systems prevents electron transfer in toluene.

In solvents of higher polarity, electron transfer from the energy donor to the energy acceptor gets increasingly favorable. Therefore, the antenna molecules containing the less electron deficient energy acceptors **A1** and **A2**, are the most promising candidates for the construction of efficient light harvesting components in light-driven devices. That is the case because the lowest electron transfer rates within the antenna molecules is expected for these antenna molecules. Further photophysical characterization of antenna systems in more polar solvents and their functionalization for the attachment to solid surfaces and molecular catalysts are currently undertaken in our research group.

3.5 Experimental Section

Materials All the reagents utilized in the synthesis were purchased from commercial suppliers and used as received unless otherwise stated. Toluene was dried over sodium under an argon atmosphere prior to use. NMP used for the reaction was of anhydrous grade. Purification of the products was performed using column chromatography (silica gel 60, mesh size 0.063–0.200 mm). TLC plates and the sorbent for the column chromatography were purchased from commercial suppliers.

Instrumentation and characterization The NMR spectra were recorded with a 400 MHz pulsed Fourier transform NMR spectrometer in either CDCl_3 or DMSO-d_6 at room temperature. The chemical shift values are given in ppm and J values in Hz. High-resolution mass spectra were collected on an AccuTOF GCv 4G JMS-T100GCV Mass Spectrometer (JEOL, Japan). The FD/FI probe (FD/FI) was equipped with an FD Emitter, Carbotec (Germany), and FD 10 μm . Typical measurement conditions were as follows: current rate 51.2 mA min^{-1} over 1.2 min; counter electrode -10 kV ; ion source 37 V . The samples were prepared in dichloromethane.

Electrochemical behavior of the compounds was studied using cyclic voltammetry (CHI 600D electrochemical analyzer) in a three-electrode single-compartment cell consisting of a platinum sheet as the working electrode, Ag wire as the reference electrode, and a Pt wire as the counter electrode (scan rate = 0.10 V s^{-1}). The cell was connected to a computer-controlled potentiostat (CH Instruments Inc. 600D). Pre-dried CH_2Cl_2 containing 0.1 M tetrabutylammonium hexa-fluorophosphate was used as the solvent. The measurements were done under continuous flow of nitrogen. The concentration of the prepared samples was *ca.* 0.5 mM . Under these experimental conditions, the ferrocene oxidation was observed at 0.52 V .

All the spectroscopic measurements were carried out at room temperature. The emission spectra were corrected for the wavelength response of the detection system. Fluorescence quantum yields were determined by the comparative method, using perylene-3,4,9,10-tetracarboxylic tetramethyl ester ($\phi_{\text{F}} = 0.95$ in CH_2Cl_2) as a reference.⁷² Optical densities at the excitation wavelengths were maintained at around 0.1 to avoid reabsorption.

Fluorescence lifetime measurements were performed on a Lifespec-ps Fluorescence spectrometer from Edinburgh Instruments. Samples were placed in 1 cm quartz cuvettes and their time correlated fluorescence was analyzed by exponential tail fit with F900 Lifespec software. Transient absorption measurements were performed in a Pharos SP YKGBW Light Conversion laser, which is sent from 180 fs pulses at 1028 nm and amplified. This main beam is divided into a highly energetic pump beam and a white light probe beam, which is generated in a sapphire. The delay between the pump and probe beam can be adjusted up to 3 ns by using a time delay stage consisting of moveable mirrors. The desired wavelength of the pump beam can be changed by using an optical parametric amplifier (OPA) and an Orpheus second harmonics module from Light Conversion. The light after the sample (probe beam) was collected by a Helios detector from Ultrafast Systems. The samples were placed in 2 mm quartz cuvettes and were stirred with a magnetic stirrer to prevent aggregation.

3.6 References

- (1) Dubey, R. K.; Inan, D.; Sengupta, S.; Sudholter, E. J. R.; Grozema, F. C.; Jager, W. F., Tunable and highly efficient light-harvesting antenna systems based on 1,7-perylene-3,4,9,10-tetracarboxylic acid derivatives. *Chemical Science* **2016**, 7 (6), 3517-3532.
- (2) van Grondelle, R.; Dekker, J. P.; Gillbro, T.; Sundstrom, V., Energy transfer and trapping in photosynthesis. *Biochimica et Biophysica Acta (BBA) - Bioenergetics* **1994**, 1187 (1), 1-65.
- (3) Scholes, G. D.; Fleming, G. R.; Olaya-Castro, A.; van Grondelle, R., Lessons from nature about solar light harvesting. *Nature Chemistry* **2011**, 3, 763.
- (4) Harriman, A., Artificial light-harvesting arrays for solar energy conversion. *Chemical Communications* **2015**, 51 (59), 11745-11756.
- (5) Frischmann, P. D.; Mahata, K.; Wurthner, F., Powering the future of molecular artificial photosynthesis with light-harvesting metallosupramolecular dye assemblies. *Chemical Society Reviews* **2013**, 42 (4), 1847-1870.
- (6) Ziessel, R.; Ulrich, G.; Haefele, A.; Harriman, A., An Artificial Light-Harvesting Array Constructed from Multiple Bodipy Dyes. *Journal of the American Chemical Society* **2013**, 135 (30), 11330-11344.
- (7) Fermi, A.; Ceroni, P.; Roy, M.; Gingras, M.; Bergamini, G., Synthesis, Characterization, and Metal Ion Coordination of a Multichromophoric Highly Luminescent Polysulfurated Pyrene. *Chemistry – A European Journal* **2014**, 20 (34), 10661-10668.
- (8) Grätzel, M., Solar Energy Conversion by Dye-Sensitized Photovoltaic Cells. *Inorganic Chemistry* **2005**, 44 (20), 6841-6851.
- (9) Mishra, A.; Fischer, M. K. R.; Bäuerle, P., Metal-Free Organic Dyes for Dye-Sensitized Solar Cells: From Structure: Property Relationships to Design Rules. *Angewandte Chemie International Edition* **2009**, 48 (14), 2474-2499.
- (10) Mathew, S.; Yella, A.; Gao, P.; Humphry-Baker, R.; Curchod, B. F. E.; Ashari-Astani, N.; Tavernelli, I.; Rothlisberger, U.; Nazeeruddin, M. K.; Grätzel, M., Dye-sensitized solar cells with 13% efficiency achieved through the molecular engineering of porphyrin sensitizers. *Nature Chemistry* **2014**, 6, 242.
- (11) Youngblood, W. J.; Lee, S.-H. A.; Maeda, K.; Mallouk, T. E., Visible Light Water Splitting Using Dye-Sensitized Oxide Semiconductors. *Accounts of Chemical Research* **2009**, 42 (12), 1966-1973.
- (12) Gust, D.; Moore, T. A.; Moore, A. L., Solar Fuels via Artificial Photosynthesis. *Accounts of Chemical Research* **2009**, 42 (12), 1890-1898.
- (13) Andreiadis, E. S.; Chavarot-Kerlidou, M.; Fontecave, M.; Artero, V., Artificial Photosynthesis: From Molecular Catalysts for Light-driven Water Splitting to Photoelectrochemical Cells. *Photochemistry and Photobiology* **2011**, 87 (5), 946-964.
- (14) Jradi, F. M.; O'Neil, D.; Kang, X.; Wong, J.; Szymanski, P.; Parker, T. C.; Anderson, H. L.; El-Sayed, M. A.; Marder, S. R., A Step Toward Efficient Panchromatic Multi-Chromophoric Sensitizers for Dye Sensitized Solar Cells. *Chemistry of Materials* **2015**, 27 (18), 6305-6313.
- (15) Cinque, G.; Croce, R.; Bassi, R., Absorption spectra of chlorophyll a and b in Lhcb protein environment. *Photosynthesis Research* **2000**, 64 (2), 233-242.
- (16) Lakowicz, J. P., In *Principles of Fluorescence Spectroscopy*, Kluwer Academic and Plenum Publishers: New York, 1999.
- (17) In case donor and acceptor units exhibit through bond interaction (conjugation), which is generally achieved by using acetylene linkers, energy transfer can take place by an electron exchange mechanism, that is generally referred to as the Dexter mechanism, see ref. 5.
- (18) Takuro N. Murakami, S. I., Qing Wang, Md. Khaja Nazeeruddin, Takeru Bessho, Ilkay Cesar, Paul Liska, Robin Humphry-Baker, Pascal Comte, P  ter P  chy and Michael Gr  tzel, Highly Efficient Dye-Sensitized Solar Cells Based on Carbon Black Counter Electrodes. *J. Electrochem. Soc.* **2006**, 153, A2255-A2261.
- (19) Gr  tzel, M., Recent Advances in Sensitized Mesoscopic Solar Cells. *Accounts of Chemical Research* **2009**, 42 (11), 1788-1798.
- (20) Peng, H.-Q.; Niu, L.-Y.; Chen, Y.-Z.; Wu, L.-Z.; Tung, C.-H.; Yang, Q.-Z., Biological Applications of Supramolecular Assemblies Designed for Excitation Energy Transfer. *Chemical Reviews* **2015**, 115 (15), 7502-7542.

- (21) Wasielewski, M. R., Self-Assembly Strategies for Integrating Light Harvesting and Charge Separation in Artificial Photosynthetic Systems. *Accounts of Chemical Research* **2009**, *42* (12), 1910-1921.
- (22) Alamiry, M. A. H.; Harriman, A.; Haefele, A.; Ziessel, R., Photochemical Bleaching of an Elaborate Artificial Light-Harvesting Antenna. *ChemPhysChem* **2015**, *16* (9), 1867-1872.
- (23) Devadoss, C.; Bharathi, P.; Moore, J. S., Energy Transfer in Dendritic Macromolecules: Molecular Size Effects and the Role of an Energy Gradient. *Journal of the American Chemical Society* **1996**, *118* (40), 9635-9644.
- (24) Gilat, S. L.; Adronov, A.; Fréchet, J. M. J., Light Harvesting and Energy Transfer in Novel Convergent Constructed Dendrimers. *Angewandte Chemie International Edition* **1999**, *38* (10), 1422-1427.
- (25) Adronov, A.; Gilat, S. L.; Fréchet, J. M. J.; Ohta, K.; Neuwahl, F. V. R.; Fleming, G. R., Light Harvesting and Energy Transfer in Laser-Dye-Labeled Poly(aryl ether) Dendrimers. *Journal of the American Chemical Society* **2000**, *122* (6), 1175-1185.
- (26) Weil, T.; Reuther, E.; Müllen, K., Shape-Persistent, Fluorescent Polyphenylene Dyads and a Triad for Efficient Vectorial Transduction of Excitation Energy. *Angewandte Chemie International Edition* **2002**, *41* (11), 1900-1904.
- (27) De Schryver, F. C.; Vosch, T.; Cotlet, M.; Van der Auweraer, M.; Müllen, K.; Hofkens, J., Energy Dissipation in Multichromophoric Single Dendrimers. *Accounts of Chemical Research* **2005**, *38* (7), 514-522.
- (28) Cotlet, M.; Vosch, T.; Habuchi, S.; Weil, T.; Müllen, K.; Hofkens, J.; De Schryver, F., Probing Intramolecular Förster Resonance Energy Transfer in a Naphthaleneimide-Peryleneimide-Terryleneimide-Based Dendrimer by Ensemble and Single-Molecule Fluorescence Spectroscopy. *Journal of the American Chemical Society* **2005**, *127* (27), 9760-9768.
- (29) Dichtel, W. R.; Hecht, S.; Fréchet, J. M. J., Functionally Layered Dendrimers: A New Building Block and Its Application to the Synthesis of Multichromophoric Light-Harvesting Systems. *Organic Letters* **2005**, *7* (20), 4451-4454.
- (30) Zhang, X.; Xiao, Y.; Qian, X., Highly Efficient Energy Transfer in the Light Harvesting System Composed of Three Kinds of Boron-Dipyrromethene Derivatives. *Organic Letters* **2008**, *10* (1), 29-32.
- (31) Harriman, A.; Mallon, L.; Ziessel, R., Energy Flow in a Purpose-Built Cascade Molecule Bearing Three Distinct Chromophores Attached to the Terminal Acceptor. *Chemistry – A European Journal* **2008**, *14* (36), 11461-11473.
- (32) Fron, E.; Puhl, L.; Oesterling, I.; Li, C.; Müllen, K.; De Schryver Frans, C.; Hofkens, J.; Vosch, T., Energy Transfer Pathways in a Rylene-Based Triad. *ChemPhysChem* **2010**, *12* (3), 595-608.
- (33) Fischer, M. K. R.; Kaiser, T. E.; Würthner, F.; Bauerle, P., Dendritic oligothiophene-perylene bisimide hybrids: synthesis, optical and electrochemical properties. *Journal of Materials Chemistry* **2009**, *19* (8), 1129-1141.
- (34) Ensslen, P.; Wagenknecht, H.-A., One-Dimensional Multichromophor Arrays Based on DNA: From Self-Assembly to Light-Harvesting. *Accounts of Chemical Research* **2015**, *48* (10), 2724-2733.
- (35) Bonaccorsi, P.; Aversa, M. C.; Barattucci, A.; Papalia, T.; Puntoriero, F.; Campagna, S., Artificial light-harvesting antenna systems grafted on a carbohydrate platform. *Chemical Communications* **2012**, *48* (85), 10550-10552.
- (36) Rao, K. V.; Datta, K. K. R.; Eswaramoorthy, M.; George, S. J., Light-Harvesting Hybrid Assemblies. *Chemistry – A European Journal* **2012**, *18* (8), 2184-2194.
- (37) Langhals, H.; Saulich, S., Bichromophoric Perylene Derivatives: Energy Transfer from Non-Fluorescent Chromophores. *Chemistry – A European Journal* **2002**, *8* (24), 5630-5643.
- (38) Serin, J. M.; Brousmiche, D. W.; Fréchet, J. M. J., A FRET-Based Ultraviolet to Near-Infrared Frequency Converter. *Journal of the American Chemical Society* **2002**, *124* (40), 11848-11849.
- (39) Hippus, C.; Schlosser, F.; Vysotsky, M. O.; Böhrer, V.; Würthner, F., Energy Transfer in Calixarene-Based Cofacial-Positioned Perylene Bisimide Arrays. *Journal of the American Chemical Society* **2006**, *128* (12), 3870-3871.
- (40) Yilmaz, M. D.; Bozdemir, O. A.; Akkaya, E. U., Light Harvesting and Efficient Energy Transfer in a Boron-dipyrin (BODIPY) Functionalized Perylenediimide Derivative. *Organic Letters* **2006**, *8* (13), 2871-2873.
- (41) Flamigni, L.; Ventura, B.; You, C.-C.; Hippus, C.; Würthner, F., Photophysical Characterization of a Light-Harvesting Tetra Naphthalene Imide/Perylene Bisimide Array. *The Journal of Physical Chemistry C* **2007**, *111* (2), 622-630.

- (42) Hurenkamp, J. H.; Browne, W. R.; Augulis, R.; Pugzlys, A.; van Loosdrecht, P. H. M.; van Esch, J. H.; Feringa, B. L., Intramolecular energy transfer in a tetra-coumarinperylene system: influence of solvent and bridging unit on electronic properties. *Organic & Biomolecular Chemistry* **2007**, *5* (20), 3354-3362.
- (43) Konemann, M. 2008.
- (44) Fujitsuka, M.; Harada, K.; Sugimoto, A.; Majima, T., Excitation Energy Dependence of Photoinduced Processes in Pentathiophene–Perylene Bisimide Dyads with a Flexible Linker. *The Journal of Physical Chemistry A* **2008**, *112* (41), 10193-10199.
- (45) Wagner, R. W.; Johnson, T. E.; Lindsey, J. S., Soluble Synthetic Multiporphyrin Arrays. 1. Modular Design and Synthesis. *Journal of the American Chemical Society* **1996**, *118* (45), 11166-11180.
- (46) Kelley, R. F.; Shin, W. S.; Rybtchinski, B.; Sinks, L. E.; Wasielewski, M. R., Photoinitiated Charge Transport in Supramolecular Assemblies of a 1,7,N,N'-Tetrakis(zinc porphyrin)-perylene-3,4,9,10-bis(dicarboximide). *Journal of the American Chemical Society* **2007**, *129* (11), 3173-3181.
- (47) Jiménez, Á. J.; Spänig, F.; Rodríguez-Morgade, M. S.; Ohkubo, K.; Fukuzumi, S.; Guldi, D. M.; Torres, T., A Tightly Coupled Bis(zinc(II) phthalocyanine)–Perylenediimide Ensemble To Yield Long-Lived Radical Ion Pair States. *Organic Letters* **2007**, *9* (13), 2481-2484.
- (48) Blas-Ferrando, V. M.; Ortiz, J.; Bouissane, L.; Ohkubo, K.; Fukuzumi, S.; Fernandez-Lazaro, F.; Sastre-Santos, A., Rational design of a phthalocyanine-perylenediimide dyad with a long-lived charge-separated state. *Chemical Communications* **2012**, *48* (50), 6241-6243.
- (49) Huang, C.; Barlow, S.; Marder, S. R., Perylene-3,4,9,10-tetracarboxylic Acid Diimides: Synthesis, Physical Properties, and Use in Organic Electronics. *The Journal of Organic Chemistry* **2011**, *76* (8), 2386-2407.
- (50) Würthner, F., Perylene bisimide dyes as versatile building blocks for functional supramolecular architectures. *Chemical Communications* **2004**, (14), 1564-1579.
- (51) Gómez, R.; Segura, J. L.; Martín, N., Highly Efficient Light-Harvesting Organofullerenes. *Organic Letters* **2005**, *7* (4), 717-720.
- (52) Jérôme, B.; Stéphanie, L.-L.; Nguyễn, V. A.; M., W. R.; Piétrick, H., Fullerene C60–Perylene-3,4,9,10-bis(dicarboximide) Light-Harvesting Dyads: Spacer-Length and Bay-Substituent Effects on Intramolecular Singlet and Triplet Energy Transfer. *Chemistry – A European Journal* **2008**, *14* (16), 4974-4992.
- (53) Hofmann, C. C.; Lindner, S. M.; Ruppert, M.; Hirsch, A.; Haque, S. A.; Thelakkat, M.; Köhler, J., Mutual Interplay of Light Harvesting and Triplet Sensitizing in a Perylene Bisimide Antenna–Fullerene Dyad. *The Journal of Physical Chemistry B* **2010**, *114* (28), 9148-9156.
- (54) Dubey Rajeev, K.; Niemi, M.; Kaunisto, K.; Efimov, A.; Tkachenko Nikolai, V.; Lemmetyinen, H., Direct Evidence of Significantly Different Chemical Behavior and Excited-State Dynamics of 1,7- and 1,6-Regioisomers of Pyrrolidinyl-Substituted Perylene Diimide. *Chemistry : A European Journal* **2013**, *19* (21), 6791-6806.
- (55) Sara, P.; Luis, M.-G.; Kei, O.; Shunichi, F.; Fernando, F.-L.; Ángela, S.-S., Macrocyclic Dyads Based on C60 and Perylenediimides Connected by Click Chemistry. *Asian Journal of Organic Chemistry* **2014**, *3* (2), 185-197.
- (56) Kirmaier, C.; Hindin, E.; Schwartz, J. K.; Sazanovich, I. V.; Diers, J. R.; Muthukumar, K.; Taniguchi, M.; Bocian, D. F.; Lindsey, J. S.; Holten, D., Synthesis and Excited-State Photodynamics of Perylene-Bis(Imide)-Oxochlorin Dyads. A Charge-Separation Motif. *The Journal of Physical Chemistry B* **2003**, *107* (15), 3443-3454.
- (57) Chen, Z.; Baumeister, U.; Tschierske, C.; Würthner, F., Effect of Core Twisting on Self-Assembly and Optical Properties of Perylene Bisimide Dyes in Solution and Columnar Liquid Crystalline Phases. *Chemistry A European Journal* **2007**, *13* (2), 450-465.
- (58) Würthner, F.; Saha-Möller, C. R.; Fimmel, B.; Ogi, S.; Leowanawat, P.; Schmidt, D., Perylene Bisimide Dye Assemblies as Archetype Functional Supramolecular Materials. *Chemical Reviews* **2016**, *116* (3), 962-1052.
- (59) Sengupta, S.; Dubey, R. K.; Hoek, R. W. M.; van Eeden, S. P. P.; Gunbaş, D. D.; Grozema, F. C.; Sudhölter, E. J. R.; Jäger, W. F., Synthesis of Regioisomerically Pure 1,7-Dibromoperylene-3,4,9,10-tetracarboxylic Acid Derivatives. *The Journal of Organic Chemistry* **2014**, *79* (14), 6655-6662.
- (60) Kucheryavy, P.; Li, G.; Vyas, S.; Hadad, C.; Glusac, K. D., Electronic Properties of 4-Substituted Naphthalimides. *The Journal of Physical Chemistry A* **2009**, *113* (23), 6453-6461.
- (61) Collado, D.; Remón, P.; Vida, Y.; Najera, F.; Sen, P.; Pischel, U.; Perez-Inestrosa, E., Energy Transfer in Aminonaphthalimide-Boron-Dipyrromethene (BODIPY) Dyads upon One- and

- Two-Photon Excitation: Applications for Cellular Imaging. *Chemistry : An Asian Journal* **2014**, *9* (3), 797-804.
- (62) Hansch, C.; Leo, A.; Taft, R. W., A survey of Hammett substituent constants and resonance and field parameters. *Chemical Reviews* **1991**, *91* (2), 165-195.
- (63) Weller, A., Photoinduced Electron Transfer in Solution: Exciplex and Radical Ion Pair Formation Free Enthalpies and their Solvent Dependence. In *Zeitschrift für Physikalische Chemie*, 1982; Vol. 133, p 93.
- (64) E. Lippert, *Z. Electrochem* **1957**, *61*, 962-975.
- (65) Jager, W. F.; Berg, O. v. d.; Picken, S. J., Novel Color-Shifting Mobility Sensitive Fluorescent Probes for Polymer Characterization. *Macromolecular Symposia* **2005**, *230* (1), 11-19.
- (66) Ford, W. E.; Hiratsuka, H.; Kamat, P. V., Photochemistry of 3,4,9,10-perylenetetracarboxylic dianhydride dyes. 4. Spectroscopic and redox properties of oxidized and reduced forms of the bis(2,5-di-tert-butylphenyl)imide derivative. *The Journal of Physical Chemistry* **1989**, *93* (18), 6692-6696.
- (67) Rodríguez-Morgade, M. S.; Torres, T.; Atienza-Castellanos, C.; Guldi, D. M., Supramolecular Bis(rutheniumphthalocyanine)-Perylenediimide Ensembles: Simple Complexation as a Powerful Tool toward Long-Lived Radical Ion Pair States. *Journal of the American Chemical Society* **2006**, *128* (47), 15145-15154.
- (68) Prodi, A.; Chiorboli, C.; Scandola, F.; Iengo, E.; Alessio, E.; Dobrawa, R.; Würthner, F., Wavelength-Dependent Electron and Energy Transfer Pathways in a Side-to-Face Ruthenium Porphyrin/Perylene Bisimide Assembly. *Journal of the American Chemical Society* **2005**, *127* (5), 1454-1462.
- (69) Flamigni, L.; Ventura, B.; Tasior, M.; Becherer, T.; Langhals, H.; Gryko Daniel, T., New and Efficient Arrays for Photoinduced Charge Separation Based on Perylene Bisimide and Corroles. *Chemistry – A European Journal* **2007**, *14* (1), 169-183.
- (70) Flamigni, L.; Ventura, B.; Barbieri, A.; Langhals, H.; Wetzel, F.; Fuchs, K.; Walter, A., On/Off Switching of Perylene Tetracarboxylic Bisimide Luminescence by Means of Substitution at the N-Position by Electron-Rich Mono-, Di-, and Trimethoxybenzenes. *Chemistry – A European Journal* **2010**, *16* (45), 13406-13416.
- (71) Dubey, R. K.; Knorr, G.; Westerveld, N.; Jager, W. F., Fluorescent PET probes based on perylene-3,4,9,10-tetracarboxylic tetraesters. *Organic & Biomolecular Chemistry* **2016**, *14* (5), 1564-1568.
- (72) Langhals, H.; Karolin, J.; B-A. Johansson, L., Spectroscopic properties of new and convenient standards for measuring fluorescence quantum yields. *Journal of the Chemical Society, Faraday Transactions* **1998**, *94* (19), 2919-2922.

4 . Tailoring Photophysical Processes of Perylene-Based Light Harvesting Antenna Systems with Molecular Structure and Solvent Polarity

The excited state dynamics of perylene based bichromophoric light harvesting antenna systems has been systematically tailored by modification of the molecular structure and by using the solvents of increasing polarity in the series toluene, chloroform and benzonitrile. The antenna systems consist of blue-light absorbing naphthalene monoimide (NMI) based energy-donors (**D1**, **D2**, and **D3**) and perylene derived green-light absorbing energy acceptor moieties, 1,7-perylene-3,4,9,10-tetracarboxylic tetrabutylester (**A1**), 1,7-perylene-3,4,9,10-tetracarboxylic monoimide dibutylester (**A2**), and 1,7-perylene-3,4,9,10-tetracarboxylic bisimide (**A3**). The design of these antenna systems is such that they exhibit ultrafast excitation energy transfer (EET), due to the effective matching of optical properties of the constituent chromophores. At the same time, electron transfer has been minimized by the use of a rigid and non-conjugated phenoxy bridge to link the donor and acceptor components. As a result, all the antenna systems exhibit a quantitative and ultrafast excited energy transfer ($\tau_{\text{EET}} \sim 1$ ps) from the donor naphthalene moieties to the acceptor perylenes in all solvents. The three systems (**D1A1**, **D1A2**, and **D1A3**), which have least electron-rich energy donor (isopentylthio-substituted NMI, **D1**), exhibited EET as the only photophysical process and, resultantly, emit a strong yellow-orange fluorescence upon excitation of the donor. However, in the other three systems (**D2A2**, **D2A3**, and **D3A3**) with relatively electron-rich energy donors (amino-substituted NMIs; **D2** and **D3**), a quantitative and ultrafast energy transfer is followed by a slower (ca. 20-2000 ps) and less efficient charge transfer as the secondary process. In this way, these antenna systems mimic the primary events occurring in the natural photosynthesis, *i.e.* energy capture, efficient energy funneling towards the central chromophore and finally, charge separation. Since the energy transfer and charge transfer proceed in a sequential manner in these systems, they do not compete with each other. These antenna systems are suitable for artificial photosynthesis, especially for photocatalytic water splitting, because of their robustness and favorable photophysical processes.

4.1 Introduction

Artificial light-harvesting antenna systems are key elements for an efficient solar energy conversion because of their ability to harvest a substantial part of the incident light.¹⁻⁵ Their structural and functional designs are often inspired by nature, most specifically from natural photosynthesis, in which efficient energy capture, efficient energy funneling to the reaction center, and charge separation occur in a sequential manner as primary events.⁶⁻¹⁰ Artificial antenna systems are generally composed of an organized group of chromophores with distinct chemical structures and complementary absorption spectra to maximize the absorption of visible light.^{5,11-13} An idealized light-harvesting antenna must enable efficient energy capture and efficient transfer of excitation energy among the constituent chromophores, so that the absorbed energy can be efficiently funneled to the reactive site.^{13,14} In order to perform efficiently, the antenna systems also require a perfect match of electronic properties between constituent chromophores, so that competing photoinduced processes will be eliminated.

Photoinduced charge transfer is the major process that competes with energy transfer process.^{12,15-17} Therefore, limiting the rate of charge transfer is an important challenge in designing efficient artificial light harvesting antenna systems. Whether or not charge transfer processes take place primarily depends on the energy of the charge-separated state relative to the energies of singlet-excited states of constituent chromophores. Since the energy of charge-separated state is lower in polar environments, this process becomes more feasible in polar solvents.^{18,19} However, rates of charge transfer, apart from the thermodynamic driving force, also depend on the attachment of the donor chromophores to the acceptor. Consequently, the major challenges in designing such artificial antenna systems are to keep a good balance of spectral and electronic properties of the constituting chromophores, and to choose an appropriate linking strategy with respect to the position and the identity of the linker units between the donors and the acceptor.

Among suitable chromophores as building blocks for light-harvesting antennae, perylene bisimides (PBIs) are particularly attractive, due to their high photo-chemical and thermal stability, ease of functionalization, and strong absorption in the visible region of the solar spectrum.^{20,21} Taking advantage of these favorable properties, PBIs have been widely used as the constituent chromophore in light-harvesting antenna systems.^{12,15,22-25} However, due to the high electron deficiency of the perylene core, competing charge transfer has often been observed among constituent chromophores within these antenna systems, even if PBIs are covalently coupled with moderately electron-rich energy donors.^{12,15-17,26}

Recently, we reported the modular design, synthesis and photo-physical characterization of five bichromophoric light-harvesting antennae, which were constructed by the covalent attachment of blue light absorbing naphthalene monoimide energy-donors to green light absorbing perylene tetracarboxylic acid derived energy acceptors.²⁷ In addition to the highly electron deficient PBIs, we introduced the less electron deficient perylene tetraesters PTEs and perylene monoimide diester PMIDEs as energy acceptors. We successfully demonstrated that these donor and acceptor molecules possess an excellent spectral overlap between donor's emission and acceptor's absorption spectra, which facilitates an efficient and ultrafast ($\tau_{\text{EET}} \sim 1$ ps) energy transfer *via* the FRET mechanism in the antenna molecules.²⁷ Simultaneously, intramolecular charge transfer was not observed, not even for PBIs based antenna systems where this process is thermodynamically allowed. All the

reported results, however, were obtained in the apolar solvent toluene, which suppresses charge transfer processes.²⁸ In artificial photosynthesis, however, charge separation processes in the reaction center are a prerequisite for performing chemical reactions and therefore it is of paramount importance to characterize the performance of the antenna systems in polar solvents as well.

Herein, we report on the effect of solvent polarity on the excited-state dynamics of six antenna systems composed of naphthylimide donors and perylene 3,4,9,10-tetracarboxylic acid derived energy donors, named as **D1A1**, **D1A2**, **D2A2**, **D1A3**, **D2A3** and **D3A3** (**Figure 4.1**). We have selected the polar solvents chloroform and benzonitrile, which have dielectric constants of 4.81 and 25.90, respectively, to complement the results obtained previously in toluene, which has a dielectric constant of 2.38.²⁸ Steady-state absorption and emission spectroscopies, time-dependent fluorescence measurements, and femtosecond pump-probe spectroscopy have been employed to investigate in detail the photo-physical behavior of these antenna systems. Model donor (**D1**, **D2**, **D3**) and model acceptor (**A1**, **A2**, **A3**) compounds were also studied under the same experimental setup to characterize the excited states of the constituent chromophores (**Figure C.1**, **Appendix C**). Electrochemical measurements were performed in order to correlate the rates of photoinduced charge transfer with the energetics of this process. Finally, the structure property relationships of the antenna molecules, their molecular design are discussed and evaluated in the framework of their application within artificial photosynthesis.

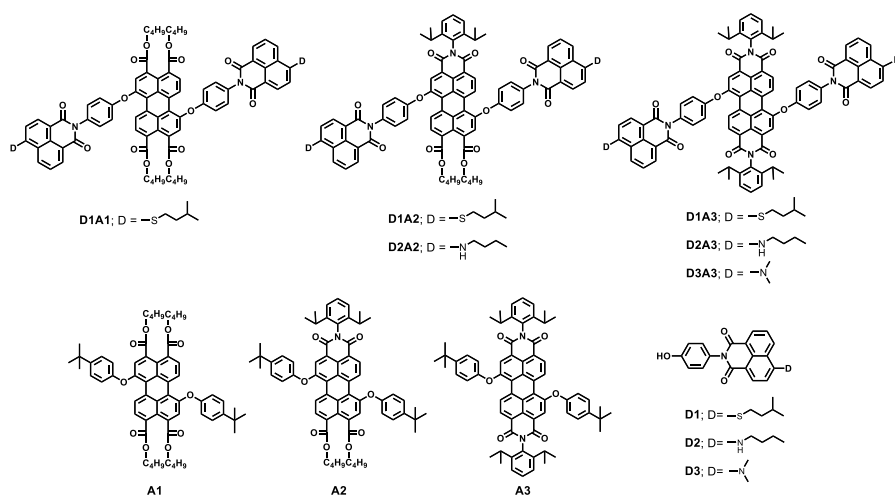


Figure 4.1 The chemical structures of studied light-harvesting antennae based on perylene tetracarboxylic acid derivatives (**A1**, **A2**, and **A3**) and naphthalene monoimides (**D1**, **D2**, **D3**).

4.2 Results

4.2.1 Synthesis

The modular synthesis of the antenna molecules **D1A1**, **D1A2**, **D2A2**, **D2A3** and **D3A3** and the synthesis of the model compounds **D1-D3** and **A1-A3** have been reported previously.²⁷ The synthesis of antenna molecule **D1A3**, is given in **Appendix C**.

4.2.2 Electrochemical Studies

The redox potentials of the antenna systems and model compounds (V vs. Fc/Fc⁺) have been determined by cyclic voltammetry in anhydrous dichloromethane ($\epsilon_s = 8.93$).²⁷ For the antenna containing acceptors **A1**, **A2** and **A3**, reduction potentials E_{red} increase, i.e. become less negative, from -1.55 to -1.33 to -1.08 V, as the acceptor gets less electron deficient. For the antenna containing donors **D2** and **D3**, oxidation potentials E_{ox} decrease from 0.80 to 0.75 V, as the donor gets more electron rich. The oxidation potential of antenna containing **D1** could not be determined experimentally, as it is outside the measured potential window. We have calculated the ionization energy of the donors, using DFT calculations and obtained values of 7.83, 7.42 and 7.37 eV for **D1**, **D2** and **D3**, respectively. Based on the differences between these values, we estimate the oxidation potential of **D1** in DCM to be 1.2 eV, and will use this value in the coming discussion.

Table 4. 1 Energies of charge separation from the excited acceptor, calculated using **Eq 4.1**.

Comp	ΔG_{CS}^0 (eV)			
	In TOL	In CHL	In DCM	In BZN
D1A1	0.43	0.20	0.09	0.05
D1A2	0.26	0.02	-0.08	-0.17
D1A3	0.22	-0.02	-0.12	-0.21
D2A2	-0.14	-0.38	-0.48	-0.57
D2A3	-0.18	-0.42	-0.52	-0.61
D3A3	-0.23	-0.47	-0.57	-0.66

For the antenna systems, the energies of photoinduced charge separation ΔG_{CS}^0 , can be calculated using the Rehm-Weller expression based on the Born dielectric continuum model, **Equation 4.1**:²⁹

$$\Delta G_{CS}^0 = [E_{ox}(D) - E_{red}(A)] - E_{00}(A) - \frac{e^2}{r_{DA}\epsilon_s} + e^2 \left(\frac{1}{2r_D} + \frac{1}{2r_A} \right) \left(\frac{1}{\epsilon_s} - \frac{1}{\epsilon_{ref}} \right) \quad (4.1)$$

In **Equation 4.1**, $E_{ox}(D)$ and $E_{red}(A)$ are the oxidation potential of the donor and the reduction potential of the acceptor, measured in dichloromethane, while $E_{00}(A)$ is the spectroscopic excited state energy of the acceptor. In this equation r_D and r_A are the ionic radii of the donor and acceptor radical ions, r_{DA} is the donor-acceptor distance, while ϵ_{ref} and ϵ_s are

the dielectric constants of the reference solvent dichloromethane and the chosen solvent, respectively. Using the Rehm-Weller equation is a rather crude approximation, as it assumes the formation of spherical ions and fixed distances for the charges in the charge separated state. For the ionic radii, r_D and r_A , values were taken from the literature,³⁰ and for charge separation distance, r_{DA} , the minimum distance of 6.4 Å was used.

Using **Equation 4.1**, photoinduced charge separation energies ΔG_{CS}^0 for all antenna molecules in DCM were calculated. The obtained values indicate that for **D1A1**, **D1A2** and **D1A3** the driving force for charge transfer is negligible, whereas for **D2A2**, **D2A3** and **D3A3** the driving force for charge separation is around -0.5 eV (**Table 4.1**). Therefore, photoinduced charge separation at appreciable rates is expected for the latter molecules. In dichloromethane a value of -0.25 eV was calculated for the energy gained by bringing the charges in close proximity, $-e^2/r_{DA}\epsilon_s$, using the lowest possible separation distance r_{DA} of 6.4 Å. Taking the center to center separation distances of 12 Å instead, decreases the value of $-e^2/r_{DA}\epsilon_s$, to -0.13 eV, and thus increases the energy of charge transfer ΔG_{CS}^0 by 0.12 eV. In toluene, chloroform and benzonitrile the corresponding increase in ΔG_{CS}^0 are 0.45, 0.22 and 0.04 eV, respectively.

In apolar toluene, the charge separation energies ΔG_{CS}^0 are ~0.3 eV higher than the corresponding values estimated for dichloromethane. This means that only for **D2A2**, **D2A3** and **D3A3** charge separation from the perylene excited-state is an energetically favorable process. Spectroscopic studies of these antenna compounds in toluene showed that none of the antenna molecules exhibited charge transfer from the excited acceptor state. This observation suggests that calculated values of the driving force for charge separation should exceed 0.2 eV for obtaining electron transfer at observable rates. In chloroform, charge separation energies are approximately 0.2 eV lower than in less polar toluene. The values compiled in **Table 4.1** indicate that the energy of charge transfer is strongly negative, around -0.4 eV, only for **D2A2**, **D2A3** and **D3A3**. This suggests that charge transfer may be observed for these antenna molecules. In benzonitrile, charge transfer energies are ~0.2 eV lower than in chloroform. Negative charge transfer energies have been calculated for all antenna molecules, but strongly negative values, around -0.6 eV, have been calculated for **D2A2**, **D2A3** and **D3A3** only. Taking charge transfer energy of -0.2 eV as the threshold for observing electron transfer, fast charge transfer is expected for these compounds.

Energies of charge transfer from the excited donor have been calculated as well, and are compiled in **Table C1 in Appendix C**. From this table, it is clear that for compounds **D1A3**, **D2A2**, **D2A3** and **D3A3**, these energies are below -0.4 eV in all solvents. Based on these values, one would expect charge transfer at observable rates from these compounds in all solvents.

4.2.3 Steady-state Absorption Studies

The absorption spectra of all the reference compounds and antenna systems in benzonitrile are shown in **Figure 4.2**. Results obtained in chloroform are presented in **Figure C.2**.

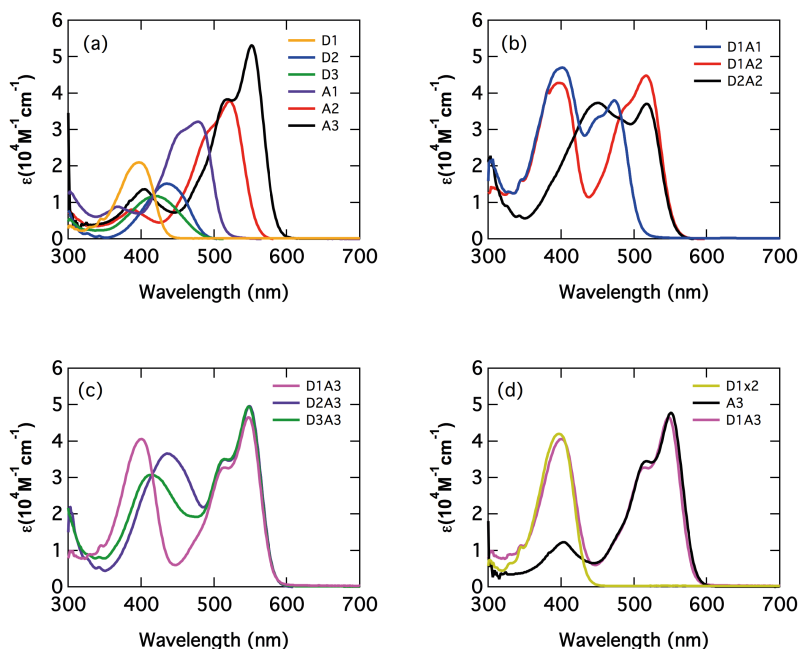


Figure 4.2 UV/Vis absorption spectra in benzonitrile (a) reference donor and acceptor compounds (b) antenna systems **D1A1**, **D1A2**, **D2A2** (c) antenna systems **D1A3**, **D2A3**, **D3A3** (d) comparison of absorption spectrum of antenna **D1A3** with reference compounds.

The donors **D1**–**D3** absorb in the visible region at 380–460 nm. Among them, **D1** has the bluest shifted absorption. The absorption maxima are shifted to higher wavelengths by ca. 15–20 nm upon moving from **D1** to **D3** to **D2** (Table 4.2). In view of the stronger electron-donating nature of dimethyl-amino group compared to the butylamino group, **D3** was expected to exhibit the most red-shifted absorption, not **D2**. The absorption spectra of the acceptors **A1**–**A3** are dominated by the characteristic strong π – π^* transitions of the perylene-3,4,9,10-tetracarboxylic moieties in the region between 430–600 nm.^{31,32} This absorption band shifts to longer wavelengths by ca. 40 nm while the molar extinction coefficient increases strongly, upon moving from **A1** to **A2** to **A3** (Table 4.2).^{32,33} Upon changing the solvent from benzonitrile to chloroform, only small blue shifts (5–10 nm) in the absorption maxima have been observed for both model acceptors and model donors (Table 4.2). This shows that the solvent polarity does not have a strong influence on the absorption properties of these molecules.

Most antenna systems exhibit good to excellent spectral coverage between 350–600 nm due to the complementary absorption of energy donor and acceptor chromophores (Figures 4.2b and c). The contributions from donor and acceptor moieties can be easily seen in the absorption of antenna systems, i.e. the absorption at shorter wavelength is mainly from the naphthalene moieties, whereas the longer wavelength absorption is from perylene part. The absorption spectra of all the antenna systems are found to be almost equivalent to the sum of the absorption spectra of constituent chromophores (Figure 4.2d). This indicates the absence of ground state interaction between the energy donor and acceptor components,

which is indeed expected because these chromophores are connected by non-conjugating rigid aminophenol linkers.

Table 4. 2 Optical properties of reference compounds and antenna systems in chloroform and benzonitrile.

Compound	Solvent	$\lambda_{\text{abs}}(\text{nm})$	$\epsilon (\text{M}^{-1}\text{cm}^{-1})$	$\lambda_{\text{em}}(\text{nm})$	$\Phi_{\text{f}}^{\text{[a]}}$	$\tau_{\text{f}}(\text{ns})^{\text{[b]}}$
D1	Chloroform	396	20400	449	0.83	5.52
	Benzonitrile	400	20600	461	0.66	5.40
D2	Chloroform	427	15800	500	0.98	8.65
	Benzonitrile	437	15200	514	0.87	8.29
D3	Chloroform	411	11900	504	0.91	7.78
	Benzonitrile	422	11700	516	0.40	4.90
A1	Chloroform	477	35800	520	0.90	4.47
	Benzonitrile	481	32100	523	0.85	4.25
A2	Chloroform	516	40900	562	0.82	4.73
	Benzonitrile	522	37800	573	0.79	4.73
A3	Chloroform	546	55600	580	0.91	4.48
	Benzonitrile	553	52900	590	0.86	4.47
D1A1	Chloroform	405	48700	510	0.73 ^[c]	4.27
		477	37900		0.76 ^[d]	
	Benzonitrile	402	47100	516	0.73 ^[c]	4.23
		474	36300		0.75 ^[d]	
D1A2	Chloroform	395	46500	558	0.83 ^[c]	4.42
		504	44400		0.85 ^[d]	
	Benzonitrile	400	42700	565	0.78 ^[c]	4.35
		520	44200		0.77 ^[d]	
D2A2	Chloroform	441	38000	554	0.83 ^[c]	4.62
		505	37800		0.80 ^[d]	
	Benzonitrile	448	37600	560	0.03 ^[c]	0.49(40%); 4.25(60%)
		520	36900		0.05 ^[d]	
D1A3	Chloroform	397	42700	568	0.84 ^[c]	3.71
		526	49400		0.83 ^[d]	
	Benzonitrile	398	42600	576	0.70 ^[c]	3.05
		549	48500		0.68 ^[d]	
D2A3	Chloroform	427	39300	572	0.28 ^[c]	1.36(81%); 3.84 (19%)
		526	50500		0.26 ^[d]	
	Benzonitrile	437	36500	578	0.003 ^[c]	0.17(83%); 3.95 (17%)
		550	49400		0.005 ^[d]	
D3A3	Chloroform	418	32500	569	0.26 ^[c]	0.98(76%); 7.93(24%)
		526	50100		0.26 ^[d]	
	Benzonitrile	418	30800	582	0.002 ^[c]	0.21(83%); 4.12(17%)
		550	49000		0.001 ^[d]	

^a Fluorescence quantum yield ^b Fluorescence lifetime ($\lambda_{\text{exc}} = 400\text{nm}$) ^c Obtained after selective excitation of the naphthalene moiety. ^d Obtained after predominant excitation of the perylene moiety.

4.2.4 Steady-state and Time Resolved Emission Studies

Preliminary information regarding the excited-state interaction between naphthalene monoimide and perylene chromophores was obtained by the steady state and time-resolved fluorescence spectroscopy. In general, both the naphthalene monoimide and the perylene model compounds are highly emissive with fluorescence quantum yields ranging from 0.80 to unity. The fluorescence decay is mono exponential and life-times are usually observed between 5–8 ns for naphthalene monoimide derivatives and 4–5 ns for perylene based compounds.^{27,33}

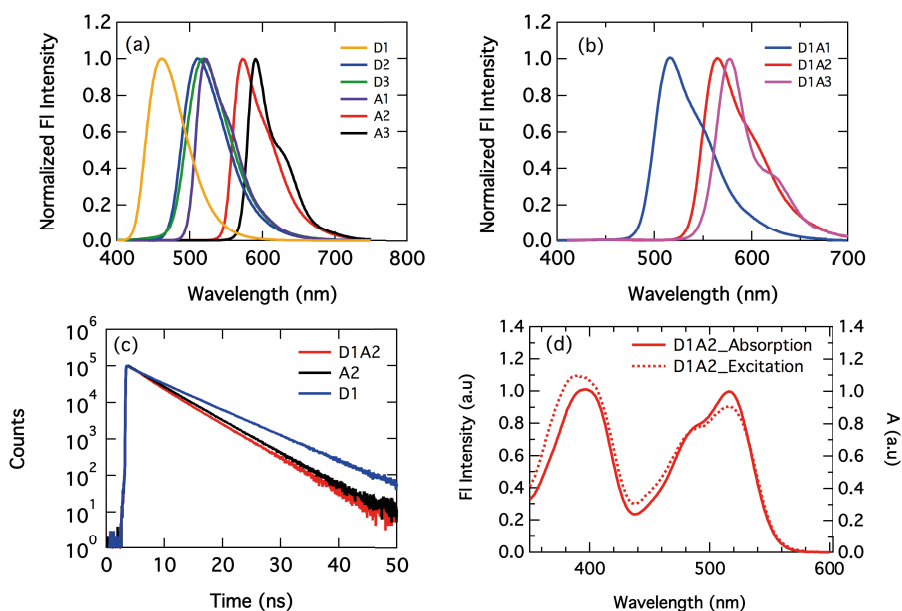


Figure 4.3 Normalized steady state fluorescence spectra in benzonitrile of (a) model donor and acceptors (b) Antenna systems **D1A1**, **D1A2**, **D1A3** after excitation of the naphthalene moiety. (c) Fluorescence decay time profiles of **D1A2** and its model compounds **D1** and **A2** in benzonitrile ($\lambda_{\text{ex}} = 400$ nm). (d) Excitation spectrum (dashed-line) of **D1A2** measured at $\lambda_{\text{em}} = 650$ nm along with the absorption spectrum (solid-line) in benzonitrile.

The normalized fluorescence spectra of model donor and acceptor compounds in benzonitrile are given in **Figure 4.3a** and the fluorescence quantum yields and lifetimes are summarized in **Table 4.2**. Model donor compound **D1** has the most blue-shifted emission with a maximum at ca. 460 nm, whereas **D3** exhibits the most red-shifted emission spectrum ($\lambda_{\text{max}} = 516$ nm). The emission of **D2** is very similar to that of **D3**, slightly blue shifted by a few nanometers. A blue shift of 10–15 nm occurred for all the model donors upon changing the solvent to chloroform. All the model donors are highly emissive in chloroform with fluorescence quantum yields higher than 0.80 and lifetimes between 5.52–8.65 ns. Benzonitrile slightly reduces the quantum yields and lifetimes of **D1** and **D2**. However, for **D3**, the fluorescence quantum yield and lifetime significantly decrease to 0.40 and 4.90 ns, respectively in benzonitrile.

The emission bands of reference acceptor compounds **A1–A3** are red shifted compared to those of the reference donors (**Figure 4.3a**). Their fluorescence spectra exhibit a similar

trend as in the case of absorption, *i.e.* a red shift is observed upon going from **A1** to **A2** to **A3**. These compounds are highly emissive with fluorescence quantum yields greater than 0.80 and lifetimes around 4.50 ns. Fluorescence quantum yields are hardly affected by the solvent polarity for all the model acceptors.

The antenna systems were excited at two different wavelengths in order to perform emission studies after separate excitation of each chromophore. At first, antenna molecules were excited at the absorption maxima of the naphthalene chromophores at wavelengths around 410 nm. The characteristic emission of naphthalene moieties was found to be completely quenched for all the antenna systems in both solvents (**Figure 4.3b**). This implies that the “slow” 5.0–8.5 ns fluorescence of the donor is completely outcompeted by other photoinduced processes. Energy transfer, which is known to be ultrafast in toluene, is the most obvious process, but electron transfer from the excited donor to the acceptor cannot be excluded at this stage.

For the antennae **D1A1**, **D1A2**, and **D1A3** that contain the electron poor donor **D1**, the characteristic sensitized emission of perylene moieties was observed with fluorescence quantum yields and lifetimes identical to those observed when the antennae are excited at the acceptor chromophore (*ca* 510 nm) (**Figures 4.3b** and **4.3c**, and **Table 4.2**). The fluorescence quantum yields and lifetimes of these antennae were also identical to those of the corresponding model acceptors **A1–A3**. These observations can be explained by assuming quantitative exciton energy transfer (EET) from the donor part, followed by an undisturbed fluorescence of the acceptor part. This implies that other photoinduced processes, notably charge transfer processes from the excited donor or the excited acceptor chromophore, do not take place at competing rates.²⁷ This is fully in line with the behavior of all antenna systems in toluene that we reported upon previously. The excitation spectra of **D1A1**, **D1A2**, and **D1A3**, measured at the perylene emission wavelength of *ca.* 650 nm, are identical to the absorption spectra of these compounds within the margin of error (**Figure 4.3d**). This finding is indicative of highly efficient energy transfer from the donor to the acceptor.

Different results were obtained for the antenna systems **D2A3** and **D3A3**, which contain the amino functionalized electron rich donors **D2** and **D3** along with the electron deficient PBI acceptor **A3**. Again, the emission of the naphthalene part was completely quenched for these antenna systems both in chloroform and benzonitrile (**Figure 4.4a**). However, for these compounds the fluorescence of the perylene chromophore was strongly quenched (**Figures 4.4a**), not only when the donor was excited but also, and to the same extent, when the acceptor was excited. These findings indicate that fluorescence of the excited donor is fully outcompeted by other photoinduced processes, notably exciton energy transfer from the excited donor to the acceptor. The diminished emission from the excited acceptor chromophore implies that other quenching processes, most likely electron transfer towards the excited acceptor (from the donor), take place at competitive rates. And finally, the identical quantum yields observed upon exciting either the donor or the acceptor chromophore in the antenna systems, implies that energy transfer from the donor to the acceptor chromophore is quantitative. This conclusion is confirmed by excitation spectra of **D2A3**, and **D3A3** that closely resemble the absorption spectra of these compounds (**Figure 4.4d**).

The quenching of perylene fluorescence was significantly increased upon moving from chloroform to benzonitrile, for both compounds. For example, the fluorescence quantum

yields of the perylene part in antenna system **D2A3** in chloroform and benzonitrile were obtained as 0.26 and 0.005, respectively, (Table 4.2). Since increasing solvent polarity makes the charge-separated state thermodynamically more feasible, photoinduced charge transfer from the excited acceptor is the most likely quenching process.

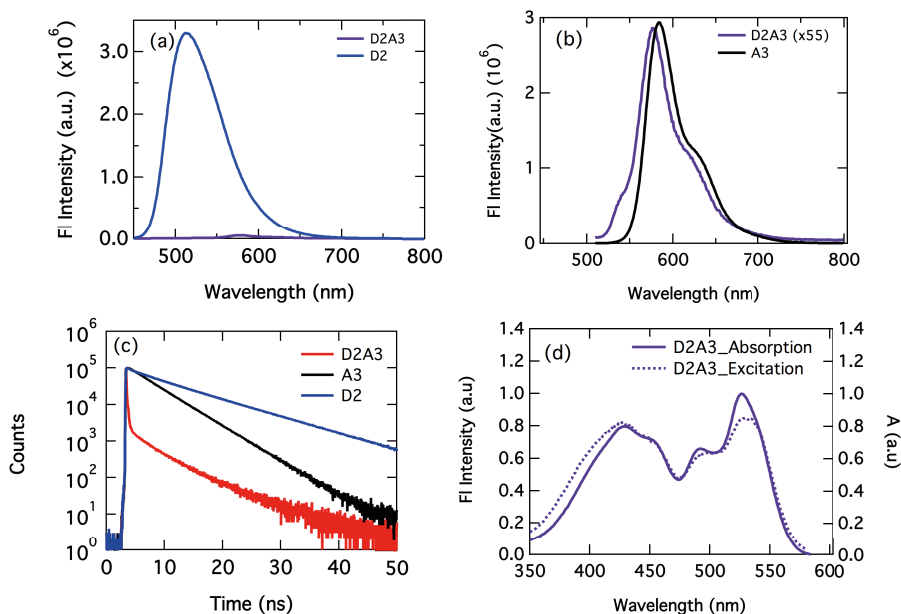


Figure 4.4 (a) Comparison between the steady-state emission of **D2A3** ($A=0.21$) and **D2** ($A=0.21$) in benzonitrile after predominant excitation of donor part at 420 nm (b) Comparison between the steady-state emission of **D2A3** (multiplied with 55 times, $A=0.18$) and **A3** ($A=0.18$) in benzonitrile after selective excitation of perylene part at 500 nm (c) Fluorescence decay curves of **D2A3** and its model molecules **D2** and **A3** in benzonitrile (d) Excitation spectrum in benzonitrile (dashed-line) of **D2A3** measured at $\lambda_{em} = 650$ nm along with the absorption spectrum (solid-line) in chloroform.

The photophysical behavior of antenna system **D2A2** undergoes large changes upon altering the solvent. In chloroform, the photophysics of **D2A2** was found to be very similar to that of **D1A1** and **D1A2**, i.e. upon excitation of the donor efficient excitation energy transfer was observed, followed by an efficient acceptor emission. In contrast, in polar benzonitrile, fluorescence of the perylene acceptor was found to be severely quenched, which is indicative of an efficient non-radiative deactivation of the excited acceptor chromophore, as was seen in the case of antenna systems **D2A3** and **D3A3**. Clearly this polarity effect points towards the involvement of charge transfer processes.

From the steady state and time-resolved fluorescence experiments rates of fluorescence quenching can be determined, using Equation C.1 in Appendix C.³⁴ For **D2A3** and **D3A3** in chloroform, rates of fluorescence quenching of $5\text{--}6 \times 10^8 \text{ s}^{-1}$ have been calculated, which is in the same order as the rates of fluorescence. For **D2A2**, **D2A3** in benzonitrile, quenching rates k_Q of $8 \times 10^9 \text{ s}^{-1}$ and $4 \times 10^{10} \text{ s}^{-1}$, have been obtained. These quenching rates have not been obtained with high accuracy, as they were calculated based on very low and inaccurate fluorescence quantum yields, but nevertheless, correlate well with the rates obtained by transient absorption spectroscopy, *vide infra*.

4.2.5 Transient Absorption Studies

In the steady-state fluorescence studies, quantitative quenching of donor emission was observed for all the antenna systems. For all **D1** containing antenna systems (**D1A1**, **D1A2**, and **D1A3**), sensitized emission of the perylene chromophore was observed due to an efficient EET from the naphthalene chromophore to the perylene. The perylene fluorescence was as intense as for the corresponding model acceptors **A1-A3**, and thus the excited acceptor was not quenching by any process. In the case of systems **D2A3** and **D3A3**, quenching of perylene emission was observed, which was significantly stronger in benzonitrile as compared to chloroform. For molecule **D2A2**, the intermediate case, perylene quenching was observed in benzonitrile, but not in chloroform. These observations are indicative of intramolecular photoinduced charge transfer from the excited acceptor chromophore. Therefore, femtosecond transient absorption studies were carried out to gain further insight in the excited state dynamics in these systems. For these studies, all antenna systems along with model compounds were investigated in chloroform and benzonitrile. Measurements were conducted at two different excitation wavelengths to excite the donor and acceptor components separately. The excitation wavelengths corresponding to the absorption maxima of perylene were used for selective excitation of the perylene component. Selective excitation of the naphthalene chromophore, however, was not possible because perylene derivatives also absorb at ca. 410 nm, i.e. the absorption maximum of the naphthalene donor. Therefore, the predominant excitation of the donor part was achieved by selecting the excitation wavelengths with the highest ratio of donor versus acceptor absorption. The extent of acceptor absorption at short wavelengths was taken into account with the data analysis.

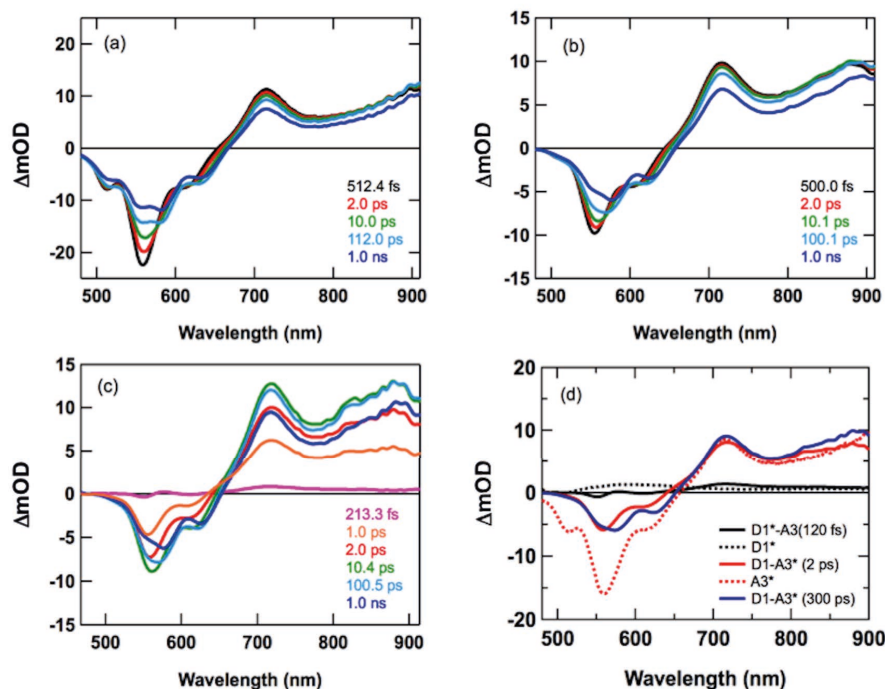


Figure 4.5 Transient absorption spectra in benzonitrile (a) A3 (b) D1A3 after selective excitation of perylene chromophore at 540 nm (c) D1A3 after predominant excitation of naphthalene part at 400 nm (d) D1A3 spectra along with that of D1 and A3.

Transient absorption measurements were carried out on the reference acceptor compounds (A1–A3). As an example, the excitation of A3 in benzonitrile is shown in **Figure 4.5a**. Excitation of A3 resulted in an immediate formation of the first singlet excited state of the perylene chromophore that is characterized by its typical strong photoinduced absorption between 650–900 nm and a bleach of the ground state absorption at ca. 550 nm.^{12,26,27,35} Furthermore, a negative band corresponding to the stimulated emission of the perylene chromophore was seen at ca. 600 nm. With the increase in delay times, the characteristic absorption of perylene singlet excited state remains at the same wavelength (ca. 700 nm) and slowly decays with a time constant corresponding to the fluorescence of the perylene chromophore (~4.5 ns). Small spectral changes were observed in the bleach region between 525–650 nm, including a significant loss of amplitude, which were most pronounced at ca. 100 ps delay. These spectral changes are attributed to the relaxation of the initially excited perylene chromophore.³⁶ Similar results were obtained for all the reference acceptor compounds in both chloroform and benzonitrile.

Subsequently, transient absorption measurements were carried out on the antenna systems D1A1, D1A2, and D1A3. The antennae were first selectively excited at their perylene absorption maxima, which resulted in the transient absorption spectra similar to those of the respective reference acceptor compounds, as is illustrated for antenna D1A3 in **Figure 5b**. In the bleach region, small changes were observed in the picosecond time scale due to the relaxation of the excited perylene. The positive absorption bands between 700–900 nm

remain unchanged at picosecond delay times and, eventually, start to decrease at nanosecond delay times. This leads to the conclusion that for these antenna systems, the perylene excited state decays to the ground state in the same manner as in the model acceptor, *via* emission from the singlet excited state. So, for this compound, even in the polar solvent benzonitrile, charge transfer processes have not been detected.

Upon excitation of these antenna molecules at ca. 400 nm, immediate formation of the donor's excited state, along with excited acceptor, was observed at femtosecond delay times, (**Figures 4.5c and d**). Subsequently, the perylene excited state absorption increases with further increase in delay times in the range of 0–10 ps. At nanosecond delay times, the magnitude of the perylene absorption gradually decreases. The swift increase in absorption at picosecond delay times is consistent with a fast excitation energy transfer from the naphthalene donor to the perylene acceptor, and the decrease at nanosecond delay times with the subsequent slow decay of perylene excited state to the ground state via emission. No signs of charge separation, i.e. the characteristic sharp absorption of the perylene radical anion at ca. 700 nm,^{36,26} were observed in these antenna systems despite the use of polar solvent (**Figures C.9 and C.10, Appendix C**). The photophysical pathways taking place in these antenna systems (**D1A1**, **D1A2**, and **D1A3**) after donor excitation are summarized in **Figure 4.6**.

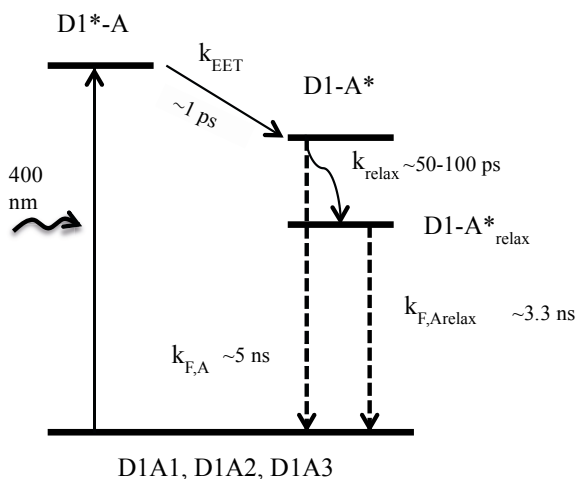


Figure 4.6 Kinetic scheme describing the photophysical processes occurring upon excitation of donor part in antenna systems **D1A1**, **D1A2**, and **D1A3** in chloroform and benzonitrile.

Similar measurements were carried out for the antenna systems **D2A2**, **D2A3**, and **D3A3**, which contain relatively electron rich energy donors (**D2** and **D3**) and the moderately and highly electron deficient acceptors **A2** and **A3**. At first, measurements were performed in polar benzonitrile in which the perylene emission of the antenna systems was almost entirely quenched. In **Figure 4.7a**, the time resolved absorption of **D2A3** after selective irradiation of the perylene chromophore at 540 nm is shown. Immediate formation of the perylene-excited state, characterized by the positive absorption between 700–900 nm with a maximum at 705 nm, was observed. This absorption remained practically the same (apart from a red shift of maxima) with further increase in evolution time in the range 1–10 ps. At longer delay times

(ca. 100 ps), two noticeable changes appeared in the transient absorption spectra. The positive absorption between 700–900 nm significantly sharpened with the maxima at 730 nm, which is a characteristic signature of the perylene bisimide radical anion.^{37,26} Secondly, the stimulated emission at 610 nm completely vanished, indicating the formation of a non-emissive excited state. These spectral changes strongly suggest the formation of a new excited state. Since the driving force for photoinduced charge separation significantly increases in highly polar solvents like benzonitrile, these spectral changes can be attributed to the formation of a charge-separated state. This conclusion is in line with the strong fluorescence quenching that was observed for **D2A3** upon moving from chloroform to benzonitrile.

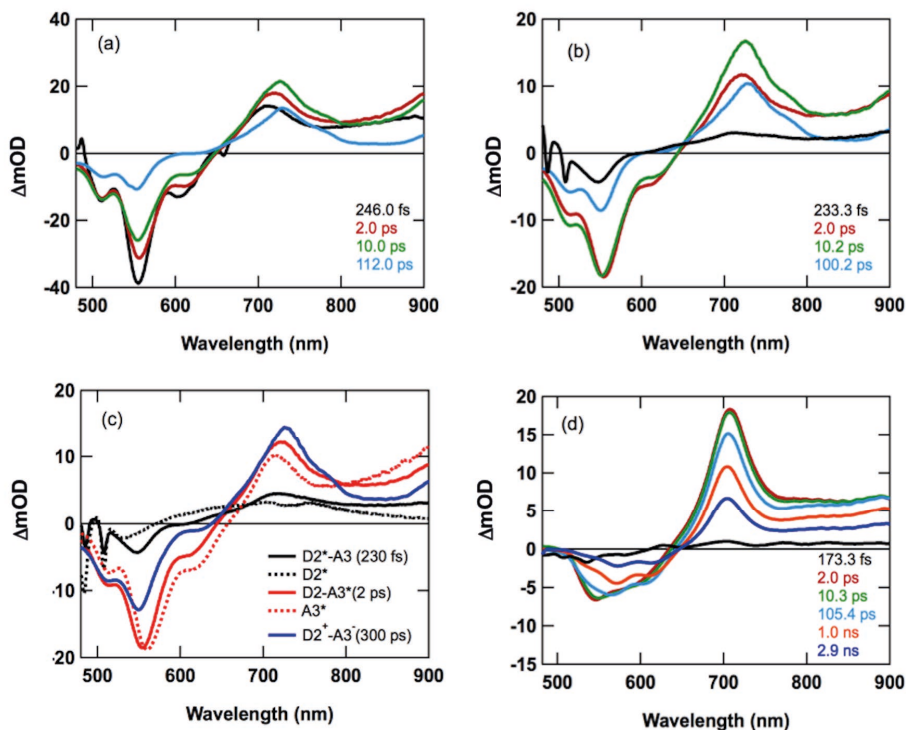


Figure 4. 7 Transient absorption spectra of antenna **D2A3** in benzonitrile (a) after selective excitation of **A3** at 540 nm (b) after excitation of **D2** at 440 nm (c) comparison with **D2** and **A3** (d) **D2A3** after excitation at 440 nm in chloroform.

When the naphthalene chromophore of antennae **D2A2**, **D2A3**, and **D3A3** was excited using 440 nm laser light, the spectroscopic signature of the singlet excited state of the donor, along with that of the acceptor, appeared in femtosecond time scale, as is illustrated for compound **D2A3** in **Figure 4.7b**. Subsequently, the perylene singlet excited state absorption increased at delay times in the range of 0–10 ps. At ca. 100 ps delay, the spectrum significantly changed, with the sharpening of the positive absorption at ~730 nm and the disappearance of the stimulated emission band at ca. 610 nm. These features are exactly same as obtained after the selective excitation of the perylene bisimide at 540 nm (**Figure 4.7a**). To summarize, on illumination of antennae **D2A2**, **D2A3** and **D3A3**, **D*A** is formed instantaneously. Subsequently, the donor transfers its energy to the acceptor within a few

picoseconds, forming DA^* . Eventually, charge transfer occurs to form the charge-separated state, D^+A^- , which recombines to the ground state at the nanosecond time scale. It is important to mention that we did not observe any signature of the perylene excited state relaxation process in the transient absorption spectra of **D2A3** and **D3A3** in benzonitrile. However, in the case of **D2A2**, where the charge transfer process is considerably slower, the perylene excited state relaxation process precedes charge transfer. The photophysical pathways taking place in **D2A2**, **D2A3** and **D3A3**, in benzonitrile, after donor excitation is summarized in **Figure 4.8**.

In less polar chloroform, as illustrated for compound **D2A3** in **Figure 4.7d**, no spectral evidence for the formation of a charge transfer state was detected, *i.e.* by the characteristic absorption of perylene radical anion and loss of stimulated emission. The perylene excited state was clearly seen, even after 2 ns delay times in the transient absorption spectra. This suggests that the perylene singlet excited state decays to the ground state by fluorescence. However, from the steady state measurements it is known that the fluorescence of the acceptor fluorescence in **D2A3** ($\Phi_F \sim 0.25$) is severely quenched compared to that of **A3** ($\Phi_F \sim 0.9$). The fact that the charge-separated state is invisible in this case may be due to a fast charge recombination, which prevents build-up of this species. In addition, the fact that the rate of fluorescence and the rate of charge transfer are comparable impedes detection of a charge-separated state. Contrary to the measurements in benzonitrile, we were also able to notice the internal relaxation process for all the antenna systems in chloroform. This is attributed to the fact that charge separation in chloroform is slower than in benzonitrile and therefore is not able to outcompete the internal relaxation of the singlet-excited state.

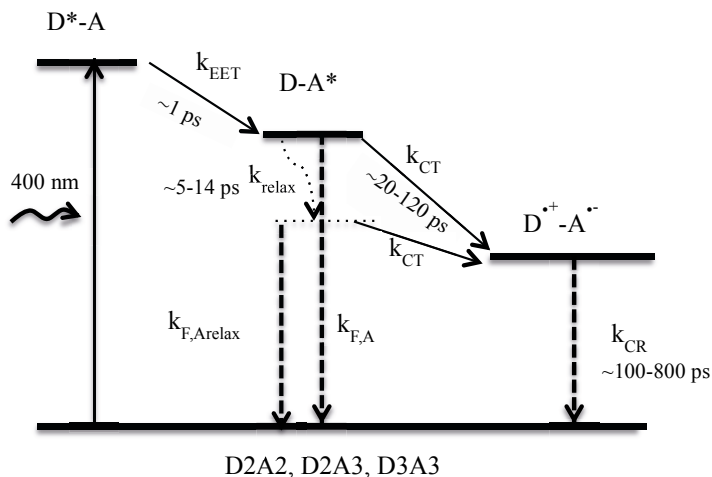


Figure 4. 8 Kinetic scheme describing the photophysical processes upon excitation of donor (at 440nm) for compounds **D2A2**, **D2A3**, and **D3A3** in benzonitrile.

4.2.6 Rates of Energy and Charge Transfer

Since there are several photophysical processes involved after the excitation, the rates of these processes could not be derived from changes in the absorption at a single wavelength. Therefore, global and target analysis were performed by taking into account the rates of individual processes taken from the model compounds along with their optical densities at the

excitation wavelengths. The open software package Glotaran³⁸ was used and further details are provided in the **Appendix C**. Analysis of the TA data by global and target analysis was performed only for the benzonitrile case, because the analysis of TA data obtained in chloroform was severely hampered by the presence of CH Raman peaks in the absorption spectra. In order to find the rates of excited energy transfer k_{EET} , acceptor relaxation k_{relax} , charge separation k_{CS} and charge recombination k_{CR} , the rates of the fluorescence decay of the donor ($k_{F,D}$) and the rate of fluorescence decay of the acceptor ($k_{F,A}$, $k_{F,Arelax}$) are taken from the global analysis of model compounds and kept constant in the target analysis of the antenna, similar to the approach reported by Gorczak *et al.*³⁸ We have previously analyzed the photophysics of the antenna systems in toluene by a single wavelength analysis. In this case single wavelength data analysis was allowed because the photophysics of these antenna molecules in toluene is very straightforward, without the involvement of competing charge transfer processes.

The kinetic scheme of photo-physical processes for **D1A1**, **D1A2**, and **D1A3** in benzonitrile is given in **Figure 4.6** and for **D2A2**, **D2A3**, and **D3A3** in the same solvent is given in **Figure 4.8**. The initially excited donor (D^*) undergoes energy transfer within a couple of picoseconds with a rate characterized by the time constant τ_{EET} . For all antenna molecules, this process is the first photo-physical process that occurs. From the steady state fluorescence measurements, that all show fluorescence quantum yields independent from the excitation wavelength, it is clear that charge transfer from the excited donor is insignificant, *i.e.* outcompeted by the ultrafast energy transfer.

For compounds **D1A1**, **D1A2**, and **D1A3**, the excited acceptor part undergoes a relaxation process. This relaxation has also been seen in the model acceptors, albeit with different rate constants (**Figure C.13**, **Appendix C**). Both the A^* and A^*_{relax} singlet excited states decay to the ground state via emission.

Table 4.3 Time constants of all photophysical processes determined from transient absorption after donor excitation in benzonitrile. Time constants in chloroform are given in Table S1 (supporting info).

	τ_{relax} (ps)	τ_{EET} (ps)	τ_{CS} (ps)	τ_{CR} (ps)
D1A1	57.9	1.16	-	-
D1A2	52.1	1.39	-	-
D1A3	97.8	1.10	-	-
D2A2	14.3	0.91	117.5	345
D2A3	5.58	0.74	32.3	800
D3A3	-	0.79	17.4	106

The time constants of the photophysical processes in benzonitrile, as determined by global analysis, are compiled in **Table 4.3**. From **Table 4.3**, it can be concluded that excited energy transfer is ultrafast for all antenna systems, with time constants τ_{EET} between 740 fs to 1.39 ps. The modest differences in τ_{EET} values may be explained by differences in the overlap integrals and acceptor extinction coefficients, *vide infra*. The charge separation rates reported

in **Table 4.2** are in accordance with the Rehm-Weller behavior, *i.e.*, they increase as the charge separation energy ΔG^0_{CS} increases. Also, charge transfer is not observed if the calculated charge transfer energies ΔG^0_{CS} , depicted in **Table 4.1**, are higher than -0.2 eV. For compounds **D2A2**, **D2A3** and **D3A3** charge recombination rates are lower than the charge separation rates, by a factor of 2-25, which results in build-up and detection of the charge separated states. For these charge recombination rates, no obvious correlation with molecular structure has been observed. For the relaxation of the acceptor singlet excited state, no obvious correlation with the molecular structure is apparent either. Comparison of the relaxation rates in **Table 4.3** with the τ_{relax} values measured for **A1**, **A2** and **A3**, being 10.8, 13.0 and 7.8 ps, respectively, suggests that donor attachment decreases these relaxation rates.

In **Table 4.4**, the energy and charge transfer rates of the six antenna molecules in toluene, chloroform and benzonitrile are compiled. For the energy transfer rates, the values in the different solvents as well as the trends within each solvent are strikingly similar. From this similarity it is concluded that for the rigid antenna molecules studied here, solvent polarity has no significant influence on energy transfer rates. In addition, the influence of molecular structure on energy transfer rates is modest as well, typically $\pm 30\%$ in our case.

The influence of molecular structure on charge separation rates is strong and determined by the excitation energy of the acceptor chromophore and the redox properties of the donor and acceptor chromophores in a straightforward manner. The effect of the solvent is also very pronounced, as an increase in solvent polarity specifically stabilizes the charge-separated state, according to **Equation 4.1**. In apolar toluene no charge separation is observed, while in chloroform charge separation is seen in two cases only, with rates comparable to those of acceptor fluorescence. Only in polar benzonitrile fast charge transfer that is able to outcompete fluorescence has been observed.

Table 4. 4 Time constants of energy and charge transfer processes in our antennae in different solvents.

	$\tau_{EET}(\text{tol})$ (ps)	$\tau_{EET}(\text{Chl})$ (ps)	$\tau_{EET}(\text{Bzn})$ (ps)	$\tau_{CS}(\text{Chl})$ (ps)	$\tau_{CS}(\text{Bzn})$ (ps)
D1A1	0.99	1.02	1.12	-	-
D1A2	1.31	1.38	1.39	-	-
D1A3	1.07	1.10	1.16	-	-
D2A2	1.16	1.10	0.90		118
D2A3	0.92	0.66	0.74	2000	32
D3A3	0.87	0.90	0.79	1700	17

4.3 Discussion

The results obtained by the photophysical measurements in the solvents toluene, chloroform and benzonitrile, provide a clear picture of the photochemical processes that take place upon excitation of the investigated antenna molecules.

In toluene all antenna molecules, upon excitation of the donor, exhibited a fast energy transfer ($\tau_{\text{EET}} \sim 1$ ps), followed by intense acceptor fluorescence ($\tau_{\text{F}} \sim 5$ ns). In this solvent, photoinduced charge transfer is absent for all compounds even after being thermodynamically allowed for some of them. In chloroform, the increased solvent polarity did not change the photophysical behavior of the antenna molecules containing the acceptor units **A1** and **A2**. Fast energy transfer and highly efficient fluorescence was observed after donor excitation. Only for compounds with the strongly electron deficient PBI acceptor **A3**, significant fluorescence quenching was observed due to a relatively slow photoinduced electron transfer process, $\tau_{\text{CS}} \sim 1.7\text{--}2$ ns. Transient absorption measurements in chloroform provided a qualitative description of the photophysics, because accurate rate constants cannot be derived by this technique due to the presence of chloroform CH Raman peaks in the absorption spectra. Charge separated states were not observed in chloroform by TA measurements and this may be due to fast charge recombination. In benzonitrile, the antenna molecules containing the weakest electron donating energy donor **D1** did not undergo photoinduced charge transfer at all. For the remaining antenna molecules **D2A2**, **D2A3** and **D3A3** fluorescence quenching was almost quantitative due to a fast photoinduced charge separation from the excited acceptor. Global analysis of the data obtained by transient absorption spectroscopy, provided the rate constants of the photophysical processes of the antenna molecules in benzonitrile.

The rates of energy transfer in benzonitrile correlate very well with those obtained in toluene and chloroform by single wavelength fitting. The fastest energy transfer is observed for **D2A3** and **D3A3**, followed by **D2A2**, **D1A1** and **D1A3**. In all cases **D1A2** is slower, but the difference is modest, $\pm 30\%$. Assuming that the conformation of the rigid antenna molecules is not solvent dependent, differences in overlap integrals J , more specifically the overlap of normalized donor emission and acceptor absorption spectra, and acceptor extinction coefficients ϵ_{A} , may explain this trend using classical Förster theory. For example, faster energy transfer for **D2A2** than for **D1A2** is explained by a larger overlap of normalized donor emission and acceptor absorption, while the trend in acceptor extinction coefficients, **A3**>**A2**>**A1**, explains the general trend in energy transfer rates for antenna molecules with identical donors.

The rates of charge separation strongly depend on antenna structure and solvent polarity. Rates of charge separation are fastest in benzonitrile, and the order of k_{CS} , **D3A3**>**D2A3**>**D2A2**, is in accordance with the calculated charge separation energies ΔG^0_{CS} for these processes. For the charge recombination rates k_{CR} the order **D2A3**>**D2A2**>**D3A3**, has been observed. For **D2A3** $k_{\text{CS}}/k_{\text{CR}} \sim 25$ and for this compound the charge separated state is best visible in the transient absorption spectra.

The photophysical behavior of our antenna can be accurately tuned by changing the molecular structure and solvent polarity and these changes are predictable and fairly well understood. Excitation energy transfer is always fast, in the 1 ps range, modestly influences by the molecular structure, and unaffected by the solvent. Photoinduced charge transfer from

the excited donor is thermodynamically allowed in most cases, but has not been observed experimentally, as it is outcompeted by ultrafast energy transfer. Photoinduced charge transfer from the excited acceptor takes place when the calculated values of the charge separation energy ΔG_{CS}^0 are below -0.2 eV, a value that appears to be a threshold for this process, and rates of this process scale with ΔG_{CS}^0 . Tuning the thermodynamic potential is achieved by structural modification of the antenna, *i.e.* using different donor-acceptor combinations, and by changing the solvent polarity, which influences the stability of the charge separated state relative to those of the other states. It should be noted that, to the best of our knowledge, **D1A1**, **D1A2** and **D1A3** are the only perylene-based antenna molecules in which photoinduced electron transfer is absent in all tested solvents, including polar benzonitrile. Although this series suggests that incorporating the electron poor energy-donor **D1** in the antenna molecule is the key ingredient, the substitution of the strongly electron deficient PBI acceptor **A3** by its less electron deficient counterparts PMIDE **A2** or the PTE **A1** is also an important modification for diminishing charge transfer from the excited acceptor.

Based on their strong, tunable, absorption in the visible region, ultrafast excited energy transfer, and modest, tunable charge transfer within the antenna systems, the light harvesting antenna molecules presented here are very well suited for the construction of devices for artificial photosynthesis.³ For incorporation into larger antenna systems, that contain an additional red-shifted acceptor, all antenna molecules appear to be well-suited. This is based on the assumption that energy transfer to the additional acceptor should be ultrafast and will outcompete charge transfer within the antenna molecules. Compounds **D1A1**, **D2A1** and **D1A3** are particularly suited for this purpose as these assemblies do not exhibit charge transfer within the antenna assembly under all investigated conditions.

In devices for artificial photosynthesis, charge transfer should take place from an energy acceptor chromophore, referred to as the sensitizer, towards charge separator units. Efficient device operation will take place only if these desired charge transfer processes, which drive the catalytic reactions, outcompete other processes that may occur from the excited acceptor. In the antenna molecules investigated here, energy transfer takes place from donors attached at bay positions, while peri positions are available for attaching charge-separating units. Previous research on the photophysics of perylene tetracarboxylic acid derivatives, however, has shown that rates of photoinduced charge transfer processes from bay positions^{33,34,39} are one order of magnitude faster than from the peri positions. This implies that charge separators should preferably be attached at bay positions, which facilitate faster charge transfer, and therefore, additional bay substituents for attaching charge separators, should be attached to the antenna systems presented here. This can be achieved by starting the antenna synthesis from tetrachloro^{32,40} instead of dibromoperylene, and by implementing the recently developed chemistry for regioselective substitution of bay halogens.⁴¹

4.4 Conclusions

Six artificial light-harvesting antenna systems with tunable optical and electrochemical properties, composed of naphthylimide energy donors attached to the bay positions of perylene 3,4,9,10 tetracarboxylic acid derived acceptor parts, were investigated by cyclic voltammetry, steady state and time resolved spectroscopy in solvents of different polarity. All

the antenna molecules exhibit a strong absorption in a large part of the visible region by complementary absorption of the donor and acceptor constituents. Energy transfer from the excited donor to the acceptor was ultrafast for all antenna molecules in all solvents, with time constants τ_{EET} ranging from 0.7 to 1.4 ps. This process was hardly depending on solvent polarity and only modestly influenced by molecular structure. Other photoinduced processes originating from the excited donor, notable the thermodynamically allowed charge transfer, have not been observed.

Charge transfer, from the excited acceptor was strongly dependent on both the molecular structure and solvent polarity. In toluene this process is absent for all antenna molecules, and after donor excitation and ultrafast excitation energy transfer to the acceptor, only emission from the acceptor is observed. In chloroform only for **D2A3** and **D3A3**, the molecules with the stronger electron donors **D2** and **D3** and the strongest electron acceptor **A3**, charge transfer, from the excited acceptor, was observed. Charge transfer rates were relatively slow, $\tau_{\text{CT}} \sim 1.7\text{--}2$ ns, and comparable with the fluorescence rate of the acceptor. In benzonitrile fast charge transfer was observed for antenna **D2A2**, **D2A3** and **D3A3**. Rates were ranging from 20–120 ps, and correlate with the calculated free energy of the charge transfer process ΔG^0_{CT} . In some cases, the acceptor radical anion was detected in TA. Quite remarkable, the “other” antenna molecules **D1A1**, **D1A2** and **D1A3**, exhibited ideal antenna behavior, *i.e.* fast energy transfer and no charge transfer or other competing processes, even in polar benzonitrile. This makes these molecules extremely suitable for incorporation in devices for artificial photosynthesis.

Our current research is focused on incorporating antenna molecules in larger antenna assemblies and on changing the antenna design by attaching energy donors at peri-positions, while keeping the bay positions available for charge transfer.

4.5 Experimental Section

Materials. All solvents used in the spectroscopic measurements were of reagent grade and were used as received from suppliers.

Instrumentation and Characterization. Absorption measurements were carried out in Perkin Elmer Lambda 40 UV-Vis spectrophotometer. Photoluminescence studies were done in SPEX Fluorimeter. Fluorescence lifetimes were performed with LifeSpec-ps Fluorescence spectrometer with fixed excitation wavelength of 400 nm. For quantum yield measurements, the formula for optically dilute solutions was used.⁴² Fluorescence quantum yields were determined by using perylene-3,4,9,10-tetracarboxylic tetrabutylester ($\phi_{\text{F}} = 0.98$ in CH_2Cl_2) and *N,N'*-bis(1-hexylheptyl)-perylene bisimide ($\phi_{\text{F}} = 0.99$ in CH_2Cl_2) as reference.⁴³

Pump-probe transient-absorption measurements were performed by using tunable Yb:KGW laser system consisting of a YB:KGW laser (1028 nm) which operates at 5 kHz with a pulse duration of <180 fs (PHAROS-SP-06-200 Light Conversion) and an optical parametric amplifier (ORPHEUS-PO15F5HNP1, Light Conversion). A white light continuum probe pulse was generated by focusing part of the fundamental 1028 nm from Pharos into a sapphire crystal. Transient absorption data were collected using a commercial pump-probe spectrometer, HELIOS (Ultrafast Systems) in the wavelength range 490–910 nm. The maximum time-delay between the pump and the probe pulse was 3.3 ns. The compounds

were dissolved in spectroscopic grade toluene, chloroform and benzonitrile and placed in quartz cuvettes with a 2 mm path length. In order to prevent aggregation and photo-bleaching, the samples were stirred with a magnetic stirrer. The transient absorption spectra are taken in both parallel and perpendicular polarization angle between pump and probe light. Later, the data is averaged to a magic angle ($\sim 54.7^\circ$) to eliminate the polarization and photoselective effects.⁴⁴⁻⁴⁵

Transient absorption data was analyzed with global and target analysis using the open source software Glotaran⁴⁶, TIMP is assuming that the time dependent spectra is a linear combination of difference absorption of various species with their respective population.⁴⁷ Gaussian instrument response function, which is the account for dispersion and the coherent artifact, were taken into account while the analysis carried out. The schemes in **Figure 4.6** and **Figure 4.8** were taken into account. The quality of fits and the relevance to correct species were compared with the global analysis of individual model compounds. (see the **Figure C.14-C.19, Appendix C**) Small deviations were observed due to different chemical surroundings, which can introduce slight shifts of transition energies or change in oscillator strength.³⁸

All calculations were performed by using Amsterdam Density Functional software.⁴⁸ The molecular structures in ground-state geometry were obtained by using PBE functional with DZP basis set. The molecules were charged +1 and geometry optimization were performed in same functional and basis set as in neutral molecule. The ionization potentials were obtained by subtracting total bonding energies of neutral and cation.

4.6 References

- (1) Harriman, A., Artificial light-harvesting arrays for solar energy conversion. *Chemical Communications* **2015**, 51 (59), 11745-11756.
- (2) Alstrum-Acevedo, J. H.; Brennaman, M. K.; Meyer, T. J., Chemical Approaches to Artificial Photosynthesis. 2. *Inorganic Chemistry* **2005**, 44 (20), 6802-6827.
- (3) Frischmann, P. D.; Mahata, K.; Wurthner, F., Powering the future of molecular artificial photosynthesis with light-harvesting metallocsupramolecular dye assemblies. *Chemical Society Reviews* **2013**, 42 (4), 1847-1870.
- (4) Swierk, J. R.; Mallouk, T. E., Design and development of photoanodes for water-splitting dye-sensitized photoelectrochemical cells. *Chemical Society Reviews* **2013**, 42 (6), 2357-2387.
- (5) Jradi, F. M.; O'Neil, D.; Kang, X.; Wong, J.; Szymanski, P.; Parker, T. C.; Anderson, H. L.; El-Sayed, M. A.; Marder, S. R., A Step Toward Efficient Panchromatic Multi-Chromophoric Sensitizers for Dye Sensitized Solar Cells. *Chemistry of Materials* **2015**, 27 (18), 6305-6313.
- (6) Gust, D.; Moore, T. A.; Moore, A. L., Mimicking Photosynthetic Solar Energy Transduction. *Accounts of Chemical Research* **2001**, 34 (1), 40-48.
- (7) Meyer, T. J., Chemical approaches to artificial photosynthesis. *Accounts of Chemical Research* **1989**, 22 (5), 163-170.
- (8) Wasielewski, M. R., Photoinduced electron transfer in supramolecular systems for artificial photosynthesis. *Chemical Reviews* **1992**, 92 (3), 435-461.
- (9) Gust, D.; Moore, T. A.; Moore, A. L., Solar Fuels via Artificial Photosynthesis. *Accounts of Chemical Research* **2009**, 42 (12), 1890-1898.
- (10) Scholes, G. D.; Fleming, G. R.; Olaya-Castro, A.; van Grondelle, R., Lessons from nature about solar light harvesting. *Nat Chem* **2011**, 3 (10), 763-774.
- (11) Iehl, J.; Nierengarten, J.-F.; Harriman, A.; Bura, T.; Ziessel, R., Artificial Light-Harvesting Arrays: Electronic Energy Migration and Trapping on a Sphere and between Spheres. *Journal of the American Chemical Society* **2012**, 134 (2), 988-998.
- (12) Flamigni, L.; Ventura, B.; You, C.-C.; Hippus, C.; Würthner, F., Photophysical Characterization of a Light-Harvesting Tetra Naphthalene Imide/Perylene Bisimide Array. *The Journal of Physical Chemistry C* **2007**, 111 (2), 622-630.

- (13) Fron, E.; Puhl, L.; Oesterling, I.; Li, C.; Müllen, K.; De Schryver, F. C.; Hofkens, J.; Vosch, T., Energy Transfer Pathways in a Rylene-Based Triad. *ChemPhysChem* **2011**, *12* (3), 595- 608.
- (14) Ziessel, R.; Ulrich, G.; Haefele, A.; Harriman, A., An Artificial Light-Harvesting Array Constructed from Multiple Bodipy Dyes. *Journal of the American Chemical Society* **2013**, *135* (30), 11330-11344.
- (15) Zhang, J.; Fischer, M. K. R.; Bäuerle, P.; Goodson, T., Energy Migration in Dendritic Oligothiophene-Perylene Bisimides. *The Journal of Physical Chemistry B* **2013**, *117* (16), 4204-4215.
- (16) Fujitsuka, M.; Harada, K.; Sugimoto, A.; Majima, T., Excitation Energy Dependence of Photoinduced Processes in Pentathiophene-Perylene Bisimide Dyads with a Flexible Linker. *The Journal of Physical Chemistry A* **2008**, *112* (41), 10193-10199.
- (17) Dinçalp, H.; Kızılok, Ş.; İçli, S., Fluorescent macromolecular perylene diimides containing pyrene or indole units in bay positions. *Dyes and Pigments* **2010**, *86* (1), 32-41.
- (18) Wang, S.; Cai, J.; Sadygov, R.; Lim, E. C., Intramolecular Charge Transfer and Solvent- Polarity Dependence of Radiative Decay Rate in Photoexcited Dinaphthylamines. *The Journal of Physical Chemistry* **1995**, *99* (19), 7416-7420.
- (19) Davis, K. M. C., Solvent Effects on Charge-transfer Fluorescence Bands. *Nature* **1969**, *223* (5207), 728-728.
- (20) Würthner, F., Perylene bisimide dyes as versatile building blocks for functional supramolecular architectures. *Chemical Communications* **2004**, (14), 1564-1579.
- (21) Huang, C.; Barlow, S.; Marder, S. R., Perylene-3,4,9,10-tetracarboxylic Acid Diimides: Synthesis, Physical Properties, and Use in Organic Electronics. *The Journal of Organic Chemistry* **2011**, *76* (8), 2386-2407.
- (22) Langhals, H.; Saulich, S., Bichromophoric Perylene Derivatives: Energy Transfer from Non-Fluorescent Chromophores. *Chemistry – A European Journal* **2002**, *8* (24), 5630-5643.
- (23) Hippus, C.; Schlosser, F.; Vysotsky, M. O.; Böhmer, V.; Würthner, F., Energy Transfer in Calixarene-Based Cofacial-Positioned Perylene Bisimide Arrays. *Journal of the American Chemical Society* **2006**, *128* (12), 3870-3871.
- (24) Gómez, R.; Segura, J. L.; Martín, N., Highly Efficient Light-Harvesting Organofullerenes. *Organic Letters* **2005**, *7* (4), 717-720.
- (25) Hurenkamp, J. H.; Browne, W. R.; Augulis, R.; Pugzlys, A.; van Loosdrecht, P. H. M.; van Esch, J. H.; Feringa, B. L., Intramolecular energy transfer in a tetra-coumarinperylene system: influence of solvent and bridging unit on electronic properties. *Organic & Biomolecular Chemistry* **2007**, *5* (20), 3354-3362.
- (26) Dubey, R. K.; Niemi, M.; Kaunisto, K.; Stranius, K.; Efimov, A.; Tkachenko, N. V.; Lemmetyinen, H., Excited-State Interaction of Red and Green Perylene Diimides with Luminescent Ru(II) Polypyridine Complex. *Inorganic Chemistry* **2013**, *52* (17), 9761-9773.
- (27) Dubey, R. K.; Inan, D.; Sengupta, S.; Sudholter, E. J. R.; Grozema, F. C.; Jager, W. F., Tunable and highly efficient light-harvesting antenna systems based on 1,7-perylene-3,4,9,10-tetracarboxylic acid derivatives. *Chemical Science* **2016**, *7* (6), 3517-3532.
- (28) Haynes, W. M., CRC handbook of chemistry and physics : a ready-reference book of chemical and physical data. 96 ed.; Boca Raton, Florida: CRC Press: 2015.
- (29) Weller, A., Photoinduced Electron Transfer in Solution: Exciplex and Radical Ion Pair Formation Free Enthalpies and their Solvent Dependence. In *Zeitschrift für Physikalische Chemie*, 1982; Vol. 133, p 93.
- (30) Goldsmith, R. H.; Sinks, L. E.; Kelley, R. F.; Betzen, L. J.; Liu, W.; Weiss, E. A.; Ratner, M. A.; Wasielewski, M. R., Wire-like charge transport at near constant bridge energy through fluorene oligomers. *Proceedings of the National Academy of Sciences of the United States of America* **2005**, *102* (10), 3540-3545.
- (31) Dubey, R. K.; Efimov, A.; Lemmetyinen, H., 1,7- And 1,6-Regioisomers of Diphenoxy and Dipyrrolidinyl Substituted Perylene Diimides: Synthesis, Separation, Characterization, and Comparison of Electrochemical and Optical Properties. *Chemistry of Materials* **2011**, *23* (3), 778-788.
- (32) Dubey, R. K.; Westerveld, N.; Sudholter, E. J. R.; Grozema, F. C.; Jager, W. F., Novel derivatives of 1,6,7,12-tetrachloroperylene-3,4,9,10-tetracarboxylic acid: synthesis, electrochemical and optical properties. *Organic Chemistry Frontiers* **2016**, *3* (11), 1481-1492.
- (33) Inan, D.; Dubey, R. K.; Westerveld, N.; Bleeker, J.; Jager, W. F.; Grozema, F. C., Substitution Effects on the Photoinduced Charge-Transfer Properties of Novel Perylene-3,4,9,10-tetracarboxylic Acid Derivatives. *The Journal of Physical Chemistry A* **2017**, *121* (24), 4633-4644.

- (34) Dubey, R. K.; Knorr, G.; Westerveld, N.; Jager, W. F., Fluorescent PET probes based on perylene-3,4,9,10-tetracarboxylic tetraesters. *Organic & Biomolecular Chemistry* **2016**, *14* (5), 1564-1568.
- (35) Dubey, R. K.; Niemi, M.; Kaunisto, K.; Efimov, A.; Tkachenko, N. V.; Lemmetyinen, H., Direct Evidence of Significantly Different Chemical Behavior and Excited-State Dynamics of 1,7- and 1,6-Regioisomers of Pyrrolidinyl-Substituted Perylene Diimide. *Chemistry – A European Journal* **2013**, *19* (21), 6791-6806.
- (36) Hippus, C.; van Stokkum, I. H. M.; Zangrando, E.; Williams, R. M.; Würthner, F., Excited State Interactions in Calix[4]arene–Perylene Bisimide Dye Conjugates: Global and Target Analysis of Supramolecular Building Blocks. *The Journal of Physical Chemistry C* **2007**, *111* (37), 13988-13996.
- (37) Ford, W. E.; Hiratsuka, H.; Kamat, P. V., Photochemistry of 3,4,9,10-perylenetetracarboxylic dianhydride dyes. 4. Spectroscopic and redox properties of oxidized and reduced forms of the bis(2,5-di-tert-butylphenyl)imide derivative. *The Journal of Physical Chemistry* **1989**, *93* (18), 6692-6696.
- (38) Gorczak, N.; Renaud, N.; Tarkuc, S.; Houtepen, A. J.; Eelkema, R.; Siebbeles, L. D. A.; Grozema, F. C., Charge transfer versus molecular conductance: molecular orbital symmetry turns quantum interference rules upside down. *Chemical Science* **2015**, *6* (7), 4196-4206.
- (39) Pagoaga, B.; Mongin, O.; Caselli, M.; Vanossi, D.; Momicchioli, F.; Blanchard-Desce, M.; Lemercier, G.; Hoffmann, N.; Ponterini, G., Optical and photophysical properties of anisole- and cyanobenzene-substituted perylene diimides. *Physical Chemistry Chemical Physics* **2016**, *18* (6), 4924-4941.
- (40) Dubey, R. K.; Westerveld, N.; Grozema, F. C.; Sudhölter, E. J. R.; Jager, W. F., Facile Synthesis of Pure 1,6,7,12-Tetrachloroperylene-3,4,9,10-tetracarboxy Bisanhydride and Bisimide. *Organic Letters* **2015**, *17* (8), 1882-1885.
- (41) Dubey, R. K.; Westerveld, N.; Eustace, S. J.; Sudhölter, E. J. R.; Grozema, F. C.; Jager, W. F., Synthesis of Perylene-3,4,9,10-tetracarboxylic Acid Derivatives Bearing Four Different Substituents at the Perylene Core. *Organic Letters* **2016**, *18* (21), 5648-5651.
- (42) Crosby, G. A.; Demas, J. N., Measurement of photoluminescence quantum yields. Review. *The Journal of Physical Chemistry* **1971**, *75* (8), 991-1024.
- (43) Langhals, H.; Karolin, J.; B-A. Johansson, L., Spectroscopic properties of new and convenient standards for measuring fluorescence quantum yields. *Journal of the Chemical Society, Faraday Transactions* **1998**, *94* (19), 2919-2922.
- (44) Lakowicz, J. R., *Principles of Fluorescence Spectroscopy*. Springer US: 2006.
- (45) Berera, R.; van Grondelle, R.; Kennis, J. T. M., Ultrafast transient absorption spectroscopy: principles and application to photosynthetic systems. *Photosynthesis Research* **2009**, *101* (2-3), 105-118.
- (46) Snellenburg, J. J.; Liptonok, S.; Seger, R.; Mullen, K. M.; van Stokkum, I. H. M.; Glotaran, A. Java-Based Graphical User Interface for the R Package TIMP. *2012* **2012**, *49* (3), 22.
- (47) van Stokkum, I. H. M.; Larsen, D. S.; van Grondelle, R., Global and target analysis of time-resolved spectra. *Biochimica et Biophysica Acta (BBA) - Bioenergetics* **2004**, *1657* (2-3), 82-104.
- (48) te Velde, G.; Bickelhaupt, F. M.; Baerends, E. J.; Fonseca Guerra, C., van Gisbergen, S. J., Snijders, J. G. and Ziegler, T, Chemistry with ADF. *J. Comput. Chem.* **2001**, *22*, 931-967.

5 • Inhibition of Intramolecular Charge Transfer in Perylene Imide Light-Harvesting Antenna Molecules by Topological Modifications

This chapter is based on D. Inan, R. K. Dubey, W. F. Jager, and F. C. Grozema *in preparation*.

5.1 Introduction

Artificial photosynthesis, in which the essential processes occurring in natural photosynthesis are mimicked by synthetic systems to produce synthetic fuels, is amongst the most promising techniques for generating sustainable energy.¹⁻⁷ In particular when the stability of chemical fuels and the amount of light that falls onto the surface of the earth are considered.⁸⁻⁹ In the molecular approach, light harvesting antenna molecules composed of chromophores that exhibit complementary absorption, are essential components. In ideal light-harvesting antenna molecules, excited energy transfer from the donor to the acceptor is quantitative, and the acceptor-excited state is stable and long-lived. For artificial photosynthesis, charge separators and catalysts are attached to acceptor to efficiently convert the acceptors excited energy into chemical energy.¹⁰

With the development of a series of modular antenna systems composed of naphthalimide donors and exceptionally stable perylene 3,4,9,10-tetracarboxylic acid acceptors, we have proven to meet the abovementioned requirements.¹¹⁻¹⁶ Energy transfer from the donors to the acceptor is in the 1-1.5 ps range and the excited state acceptor is long-lived and decays by a slow fluorescence in the 4-5 ns range only.¹⁷⁻²⁰ However, for the antenna molecules in which electron rich donor and electron deficient acceptors are connected we have observed *intramolecular* charge transfer in polar solvents. This parasitic process seriously reduces the light-harvesting efficiency, and should be excluded. This is particularly important also because polar environments are required to stabilize the charge-separated states that drive the redox reactions that produce synthetic fuels. Herein, we will demonstrate that when antenna molecules are constructed by employing the identical donor and acceptor constituents, *i.e.* by changing the topology of the molecules, the undesired intramolecular charge transfer is fully excluded. This is achieved by transferring the donor attachment from the acceptor bay to the peri positions. An additional advantage of this design is that charge separators are conveniently attached at the acceptor bay positions, from which charge transfer is proven to be a highly efficient process.

5.2 Results and Discussion

The antenna molecules we have designed are the compounds **Im-D2A2** and **Im-D2A4**, which have the naphthalimide donor **D2** attached at the peri positions of the perylene tetracarboxylic acid acceptors **A2** and **A4**, respectively. The synthesis of antenna molecule **Im-D2A2** starts from the readily available monoanhydride diester **1**.²¹ Using the newly developed amino-functionalised naphthalimide donor **2**, (**Appendix D, Scheme D.1**), the monoimide diester **3** was made under standard imidisation conditions. Subsequently, the bromine atoms at the bay positions were substituted by solubilizing 4-(*tert*-butyl) phenol moieties in a 61% yield see **Scheme 5.1**.

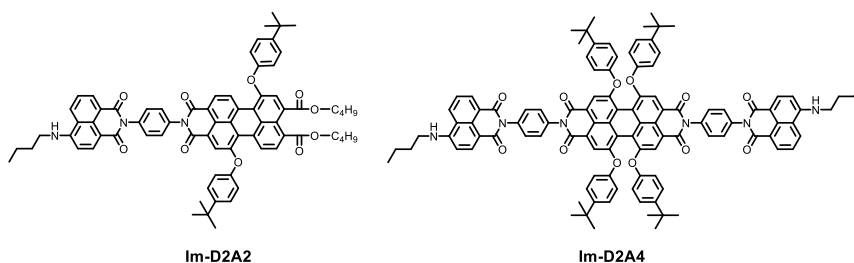
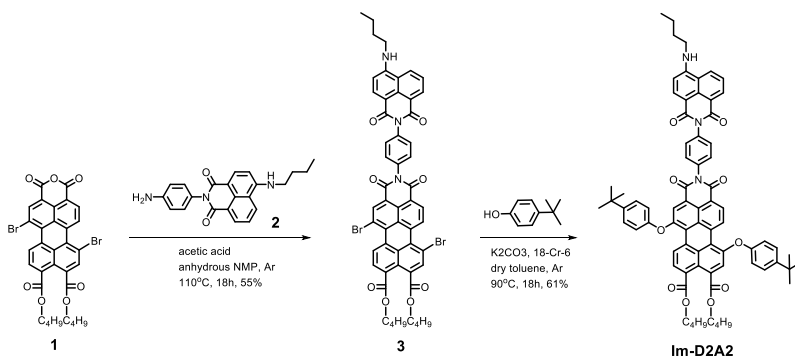
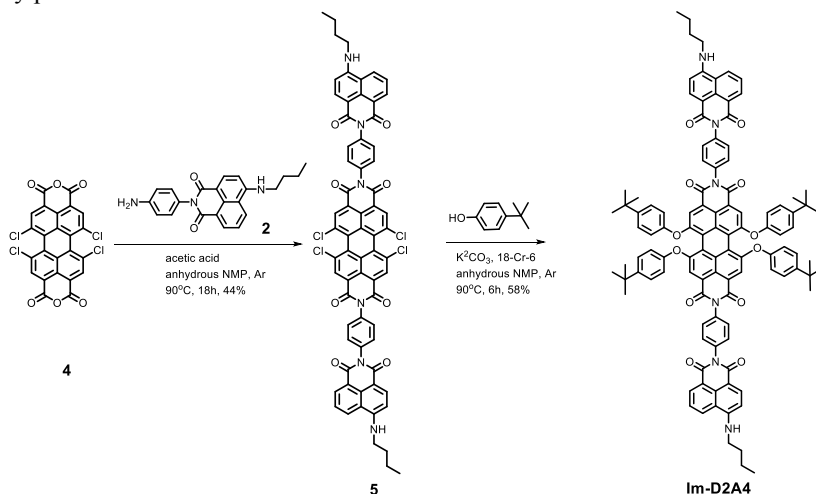


Figure 5. 1 Structures of the two antenna systems **Im-D2A2** and **Im-D2A4**.



Scheme 5. 1 Synthesis of perylene monoimide based antenna system **Im-D2A2**.

For the synthesis of the perylenebisimide antenna compound **Im-D2A4**, we used pure tetrachlorobis(4-ethoxyphenyl)anhydride **4** as our starting material.²²⁻²³ The conversion of the bisanhydride **4** to the bisimide **5**, was achieved using mild imidisation conditions in a 44% yield. Finally, antenna **Im-D2A4** was made by the attachment of four solubilizing 4(*tert*-butyl)phenol units at the bay positions.



Scheme 5. 2 Synthesis of perylene bisimide based antenna system **Im-D2A4**.

The photophysical properties of the antenna molecules **Im-D2A2** and **Im-D2A4** and the reference compounds **D2**, **A2** and **A4**, see **Figure D.1**, have been determined in benzonitrile. We have chosen benzonitrile as the solvent, because in this polar solvent fast charge transfer has been reported for the analogous bay-substituted antenna molecules **D2A2** and **D2A3**, See **Figure D.1**. From steady state spectroscopy, it can be seen that the absorption spectra of the antenna compounds are the sum of the spectra of the constituents, which indicates the absence of ground state interactions between the chromophores. Complementary absorption of the donor and the acceptor constituents is clearly not optimal for these antenna compounds, see **Figure 5.2**. For **Im-D2A2** the absorption is too low at short wavelength, due to the presence of only a single energy donor. For **Im-D2A4**, on the other hand, a hole in the absorption around 500 nm is clearly visible, which is mainly due to the fact that the attachment of four electron donating phenoxy bay substituents has shifted the absorption of the perylene acceptor 35 nm to the red, as compared to the disubstituted PBI acceptor **A3**.

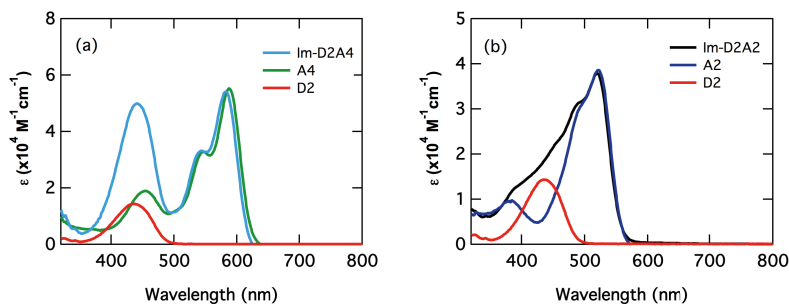


Figure 5. 2 UV/Vis absorption spectra in benzonitrile: (a) **Im-D2A4**, reference acceptor **A4** and reference donor **D2** (b) **Im-D2A2**, reference acceptor **A2** and reference donor **D2**

Upon selective excitation of the donor chromophore in **Im-D2A2** and **Im-D2A4**, acceptor fluorescence was observed exclusively. Also, absorption and excitation spectra of both antenna molecules were identical within the experimental error. Both observations indicate that energy transfer from the excited donor to the acceptor is quantitative, see **Figure 5.3**. However, fluorescence quantum yields of the antenna molecules were about 10% lower than those of the model acceptors **A2** and **A4**. Time-resolved emission of the acceptor molecules **A2** and **A4** were monoexponential with time with time constants of 4.7 and 5.7 ns, respectively, whereas the antenna molecules showed bi-exponential decay, in which the slow decay components were prevalent and had time constants close to those of the model acceptors. These findings reveal that the attachment of the large energy donors at the peripositions, induce slightly enhanced non-radiative relaxation of the acceptor-excited state in the antenna molecules.

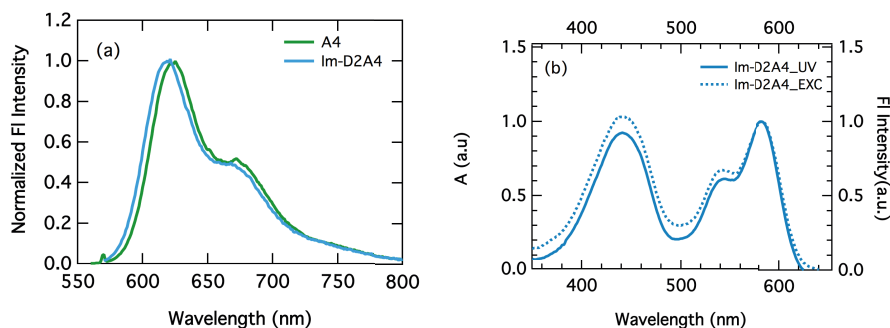


Figure 5. 3. (a) Normalized steady-state emission spectra of **Im-D2A4** compared with reference acceptor **A4** (b) Excitation spectrum of **Im-D2A4** (dashed-line) measured at $\lambda_{em} = 650$ nm along with the absorption spectrum (solid-line) in benzonitrile. (**Im-D2A2** is in **Appendix D**)

Table 5. 1 Photo-physical properties of the reference compounds and donor-acceptor systems in benzonitrile ^a Fluorescence Quantum Yield ^b Fluorescence lifetime ($\lambda_{exc} = 400$ nm) ^c Lifetime data for energy transfer obtained from femtosecond transient absorption spectroscopy

Compounds	$\lambda_{abs}(nm)$	$\epsilon(M^{-1}cm^{-1})$	$\lambda_{ems}(nm)$	ϕ_{FL}^a	$\tau_{FL}(ns)^b$	$\tau_{EET}^c(ps)$
D2	437	15200	514	0.87	8.29	-
A2	522	37800	573	0.79	4.73	-
Im-D2A2	520	37900	571	0.70	1.3(42%)/4.0 (58%)	0.51
A4	588	55300	625	0.92	4.43	-
Im-D2A4	441	50000	621	0.84	1.8(18%)/4.5 (82%)	0.61
	582	54200				

The transient absorption spectra of **Im-D2A2** and **Im-D2A4**, when excited at the donor absorption maximum, are given in **Figures 5.4** and **D.4**. After the laser excitation, first the excited state of the donor along with the excited state spectra of acceptor are observed. This can be explained by partial absorption of acceptor at the donor excitation wavelength. In the picosecond time domain, the excited state of the acceptor completely formed, due to an ultrafast energy transfer process. At nanosecond delay times, the spectra of excited acceptor start decaying in the time frame of the acceptor emission. No further changes in the spectra were observed, apart from changes in the shape of the excited state acceptor absorption around 530 nm. These changes are identical to those seen in the decay of the model acceptor **A2**, and are most likely due to solvent relaxation processes. (see **Chapter 4**). Control experiments on the individual donor and acceptor components **D2**, **A2** and **A4** can be found in **Figure D.5**.

The kinetics of energy transfer has been determined using single wavelength fitting. This method can be used since ultrafast excitation energy transfer is the only process that occurs after donor excitation, apart from slow acceptor emission. The time constants of the energy transfer are 0.51 and 0.61 ps for **Im-D2A2** and **Im-D2A4**, respectively (**Table 5.2**), which is substantially faster than for the antenna molecules where the donor moieties are

substituted at the bay positions. This increased energy transfer rate is presumably due to the parallel alignment of the donor and acceptor transition dipoles. The decay kinetics of the excited acceptors is in the nanosecond time scale and corresponds to the singlet-state lifetimes of the model acceptors **A2** and **A4**. This observation suggests that the excited perylene molecule goes back to ground state via emission, and those additional quenching mechanisms, if present at all, do not contribute significantly to the acceptor decay.

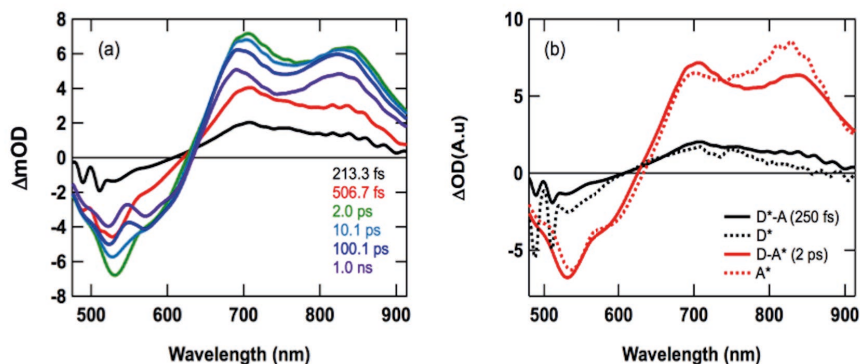


Figure 5. 4 (a) Time evolution of the femtosecond transient absorption spectra of **Im-D2A2** excitation at 430 nm in benzonitrile (b) The spectra of **Im-D2A2** with the dissociation of species after different time delays along with reference donor and reference acceptor

Table 5. 2 The rates, the time constants of the energy transfer in donor-acceptor systems excited at 430 nm

Compound	k_{ET} (ps^{-1})	τ_{ET} (ps)
Imido-D2A4	1.64	0.61
Imido-D2A2	1.96	0.51

The combined results, obtained by steady state and time-resolved spectroscopy, clearly show that donor-acceptor systems **Im-D2A2** and **Im-D2A4** undergo ultrafast energy transfer from the naphthalene-based donor to the perylene-based acceptor. In both compounds, the acceptor excited state decays to the ground state via emission with a fluorescence quantum yield that is 10% lower than that of the acceptor model compounds **A2** and **A4**. Clearly this implies that the antenna performance of **Im-D2A2** and **Im-D2A4** is superior compared to that of the corresponding bay-substituted antenna molecules **D2A2** and **D2A3**, for which a fast charge transfer process was observed. Still the question remains whether or not this slightly enhanced quenching is due to charge- transfer from the excited acceptor.

Based on the Weller equation using the Born continuum approximation (Eq D.1),(see Chapter 4) charge transfer energies ΔG_{CT}^0 for antennae **Im-D2A2** and **Im-D2A4** in benzonitrile of -0.54 and -0.35 eV, respectively, have been calculated by keeping donor-acceptor distance as 9.5 Å and $E_{1/2 \text{ red}} = -1.17$ eV, $E_{SI} = 2.01$ eV for **A4**. The charge transfer energy found for **Im-D2A2** is identical to that calculated for the analogous bay-substituted antenna molecule **D2A2**, for which we found fast charge transfer in benzonitrile. The charge transfer energy calculated for **Im-D2A4** is significantly higher, and this is mainly because the

singlet energy of **A4** is 0.34 eV lower than that of **A2**. Based on these charge transfer energies, charge transfer is possible for **Im-D2A2**, but for **Im-D2A4** this process, if present at all, should be considerably slower. These considerations make charge-transfer as the additional quenching process in both antenna molecules highly unlikely.

We performed additional photophysical measurements on **Im-D2A2** and **Im-D2A4** in toluene, a solvent in which charge transfer processes have not been observed for the bay antenna molecules. These experiments showed that in toluene the fluorescence quantum yields of the antenna compounds were also 10% lower than those of the corresponding model acceptors **A2** and **A4**, **Table D.1**. Photo-induced charge transfer processes for **Im-D2A2** and **Im-D2A4** in toluene have positive charge transfer energies ΔG_{CT}^0 of +0.17 and +0.35 eV, respectively and are therefore thermodynamically forbidden. Thus intramolecular charge-transfer as the cause of this additional quenching of both antenna molecules in toluene and benzonitrile has been excluded. What it is still an open question.

5.3 Conclusions

In conclusion, we have designed, synthesized the light-harvesting antenna molecules **Im-D2A2** and **Im-D2A4** where the donor attachment is at the imide position of the acceptor, with the specific aim of blocking undesired intramolecular charge transfer processes. Detailed spectroscopic analysis by both steady state and time resolved measurements, has proven that intramolecular charge transfer does not take place for these compounds, not even in the highly polar solvent benzonitrile. Energy transfer occurred within 0.5-0.6 ps, which is substantially faster than for corresponding antenna with bay-attached donor moieties. The absence of photo induced charge transfer is in line with our previous findings that charge transfer is at least an order of magnitude slower when the donor is in the imide position. The absence of charge transfer, combined with the opportunity to attach up to four additional substituents at the bay positions from which charge transfer reactions are highly efficient, show that our molecules are ideal light harvesting antenna components for application in artificial photosynthesis. Our current research will focus on the integration of these antenna molecules in devices for artificial photosynthesis.

5.4 Experimental Methodology

Materials The compounds 1,7-dibromoperylene monoanhydride diester (**5**), 1,6,7,12-perylene bisanhydride (**8**), **ref-A2**, and **ref-A4** were synthesized according to the previously described procedures²¹⁻²³. All other reagents utilized in the syntheses were used as received from the manufacturers, unless otherwise stated. The NMP used in the synthesis was of anhydrous grade. Toluene was dried over sodium under an argon atmosphere prior to use. The purification of the products was performed by column chromatography (0.3–0.200 mm).

Instrumentation and Characterization The NMR spectra were recorded with 400 MHz pulsed Fourier transform NMR spectrometer in either CDCl₃ or DMSO-d₆ at room temperature. The chemical shift values are given in ppm and *J* values in Hz. High-resolution mass spectra were collected on an AccuTOF GCv 4G, JMS-T100GCV, Mass spectrometer (JEOL, Japan). The FD/FI probe (FD/FI) was equipped with an FD Emitter, Carbotec (Germany), FD 10 μm. Typical measurement conditions were as follow: Current rate 51.2 mA/min over 1.2 min; Counter electrode –10 kV; Ion source 37 V. The samples were prepared in dichloromethane.

Absorption measurements were performed in PerkinElmer Lambda 40 UV–vis spectro-photometer. Photoluminescence studies were done in SPEX Fluorimeter. Fluorescence lifetimes were performed with LifeSpec-ps Fluorescence spectrometer with fixed excitation wavelength of 400 nm. For quantum yield measurements, the formula for optically dilute solutions was used.²⁴ Fluorescence quantum yields of compounds were determined by using perylene-3,4,9,10-tetracarboxylic tetrabutylester ($\Phi_F = 0.98$ in CH₂Cl₂) as a reference.¹¹

Pump-probe transient-absorption measurements were performed by using tunable Yb:KGW laser system consisting of a YB:KGW laser (1028 nm), which operates at 5 kHz with a pulse duration of less than 180 fs (PHAROS-SP-06– 200 Light Conversion) and an optical parametric amplifier (ORPHEUS- PO15F5HNP1, Light Conversion). A white light continuum probe pulse was generated by focusing part of the fundamental 1028 nm from Pharos into a sapphire crystal. Transient absorption data were collected using a commercial pump-probe spectrometer, HELIOS (Ultrafast Systems) in the wavelength range of 490– 910 nm. The maximum time-delay between the pump and the probe pulse was 3.3 ns. The compounds were dissolved in spectroscopic grade benzonitrile and placed in quartz cuvettes with a 2 mm path length. To prevent aggregation and photobleaching, the samples were stirred with a magnetic stirrer. The data was taken in magic angle to prevent any polarization dependence.

5.5 References

- (1) *Molecular to Global Photosynthesis*. Imperial College: London, UK, 2004; Vol. 2.
- (2) Gust, D.; Moore, T. A.; Moore, A. L., Solar Fuels via Artificial Photosynthesis. *Accounts of Chemical Research* **2009**, *42* (12), 1890-1898.
- (3) Ziessel, R.; Harriman, A., Artificial light-harvesting antennae: electronic energy transfer by way of molecular funnels. *Chemical Communications* **2011**, *47* (2), 611-631.
- (4) Blankenship, R. E., *Molecular Mechanisms of Photosynthesis*. Blackwell Science: Oxford, 2002.
- (5) Wasielewski, M. R., Photoinduced electron transfer in supramolecular systems for artificial photosynthesis. *Chemical Reviews* **1992**, *92* (3), 435-461.
- (6) Wasielewski, M. R., Energy, Charge, and Spin Transport in Molecules and Self-Assembled Nanostructures Inspired by Photosynthesis. *The Journal of Organic Chemistry* **2006**, *71* (14), 5051-5066.
- (7) Fukuzumi, S.; Ohkubo, K., Assemblies of artificial photosynthetic reaction centres. *Journal of Materials Chemistry* **2012**, *22* (11), 4575-4587.
- (8) Lewis, N. S., Toward Cost-Effective Solar Energy Use. *Science* **2007**, *315* (5813), 798-801.
- (9) Lewis, N. S.; Nocera, D. G., Powering the planet: Chemical challenges in solar energy utilization. *Proceedings of the National Academy of Sciences* **2006**, *103* (43), 15729-15735.
- (10) Frischmann, P. D.; Mahata, K.; Würthner, F., Powering the future of molecular artificial photosynthesis with light-harvesting metallosupramolecular dye assemblies. *Chemical Society Reviews* **2013**, *42* (4), 1847-1870.
- (11) Langhals, H.; Karolin, J.; B.-A. Johansson, L., Spectroscopic properties of new and convenient standards for measuring fluorescence quantum yields. *Journal of the Chemical Society, Faraday Transactions* **1998**, *94* (19), 2919-2922.
- (12) Flamigni, L.; Ventura, B.; You, C.-C.; Hippus, C.; Würthner, F., Photophysical Characterization of a Light-Harvesting Tetra Naphthalene Imide/Perylene Bisimide Array. *The Journal of Physical Chemistry C* **2007**, *111* (2), 622-630.
- (13) Echeverry, C. A.; Cotta, R.; Insuasty, A.; Ortiz, A.; Martín, N.; Echegoyen, L.; Insuasty, B., Synthesis of novel light harvesters based on perylene imides linked to triphenylamines for Dyes Sensitized Solar Cells. *Dyes and Pigments* **2018**, *153*, 182-188.
- (14) Dubey, R. K.; Inan, D.; Sengupta, S.; Sudholter, E. J. R.; Grozema, F. C.; Jager, W. F., Tunable and highly efficient light-harvesting antenna systems based on 1,7-perylene-3,4,9,10-tetracarboxylic acid derivatives. *Chemical Science* **2016**, *7* (6), 3517-3532.
- (15) Lefler, K. M.; Kim, C. H.; Wu, Y.-L.; Wasielewski, M. R., Self-Assembly of Supramolecular Light-Harvesting Arrays from Symmetric Perylene-3,4-dicarboximide Trefoils. *The Journal of Physical Chemistry Letters* **2014**, *5* (9), 1608-1615.
- (16) Alamiry Mohammed, A. H.; Harriman, A.; Haefele, A.; Ziessel, R., Photochemical Bleaching of an Elaborate Artificial Light-Harvesting Antenna. *ChemPhysChem* **2015**, *16* (9), 1867-1872.
- (17) Li, C.; Wonneberger, H., Perylene Imides for Organic Photovoltaics: Yesterday, Today, and Tomorrow. *Advanced Materials* **2012**, *24* (5), 613-636.
- (18) Huang, C.; Barlow, S.; Marder, S. R., Perylene-3,4,9,10-tetracarboxylic Acid Diimides: Synthesis, Physical Properties, and Use in Organic Electronics. *The Journal of Organic Chemistry* **2011**, *76* (8), 2386-2407.
- (19) Kozma, E.; Catellani, M., Perylene diimides based materials for organic solar cells. *Dyes and Pigments* **2013**, *98* (1), 160-179.
- (20) Kozma, E.; Kotowski, D.; Catellani, M.; Luzzati, S.; Famulari, A.; Bertini, F., Synthesis and characterization of new electron acceptor perylene diimide molecules for photovoltaic applications. *Dyes and Pigments* **2013**, *99* (2), 329-338.
- (21) Sengupta, S.; Dubey, R. K.; Hoek, R. W. M.; van Eeden, S. P. P.; Gunbaş, D. D.; Grozema, F. C.; Sudhölter, E. J. R.; Jager, W. F., Synthesis of Regioisomerically Pure 1,7-Dibromoperylene-3,4,9,10-tetracarboxylic Acid Derivatives. *The Journal of Organic Chemistry* **2014**, *79* (14), 6655-6662.
- (22) Dubey, R. K.; Westerveld, N.; Sudholter, E. J. R.; Grozema, F. C.; Jager, W. F., Novel derivatives of 1,6,7,12-tetrachloroperylene-3,4,9,10-tetracarboxylic acid: synthesis, electrochemical and optical properties. *Organic Chemistry Frontiers* **2016**, *3* (11), 1481-1492.
- (23) Dubey, R. K.; Westerveld, N.; Grozema, F. C.; Sudhölter, E. J. R.; Jager, W. F., Facile Synthesis of Pure 1,6,7,12-Tetrachloroperylene-3,4,9,10-tetracarboxy Bisanhydride and Bisimide. *Organic Letters* **2015**, *17* (8), 1882-1885.

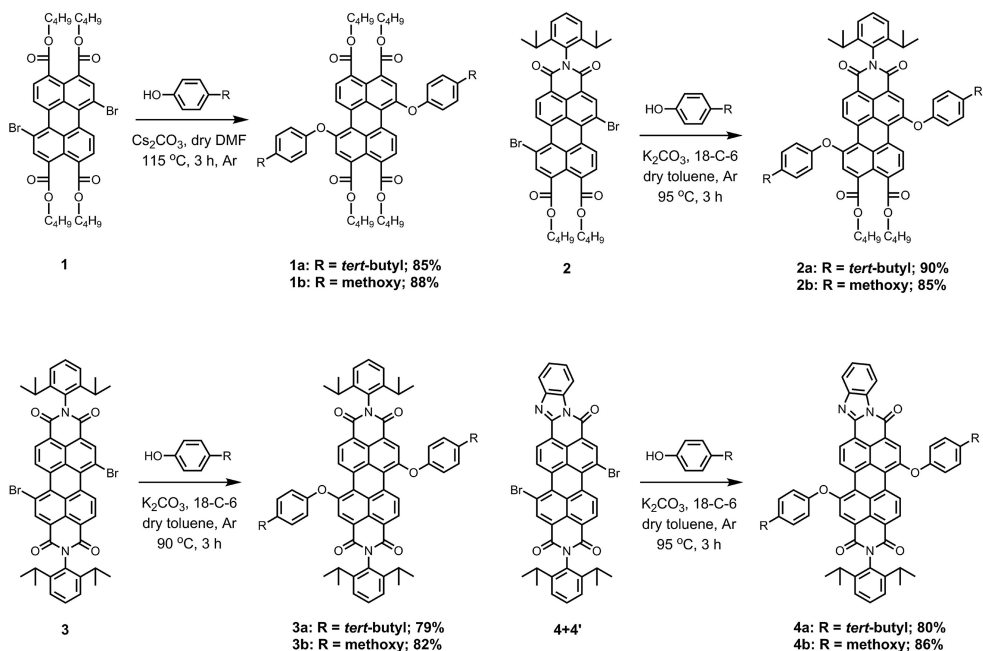
- (24) Crosby, G. A.; Demas, J. N., Measurement of photoluminescence quantum yields. Review. *The Journal of Physical Chemistry* **1971**, 75 (8), 991-1024.

A ● Appendix for Chapter 2

A.1 Synthesis and Characterization

As described in **Scheme A.1**, the reported 1,7-diphenoxy-substituted compounds (**1a–b**, **2a–c**, **3a–c**, and **4a–b**) were synthesized from their corresponding 1,7-dibromoperylene-3,4,9,10-tetracarboxylic acid derivatives, 1,7-dibromoperylene tetrabutylester **1**, *N*-(2,6-diisopropylphenyl)-1,7-dibromoperylene monoimide dibutylester **2**, *N,N'*-bis(2,6-diisopropylphenyl)-1,7-dibromoperylene bisimide **3**, and the *N*-(2,6-diisopropylphenyl)-1,7-dibromoperylene monoimide monobenzimidazoles (**4** and **4'**).

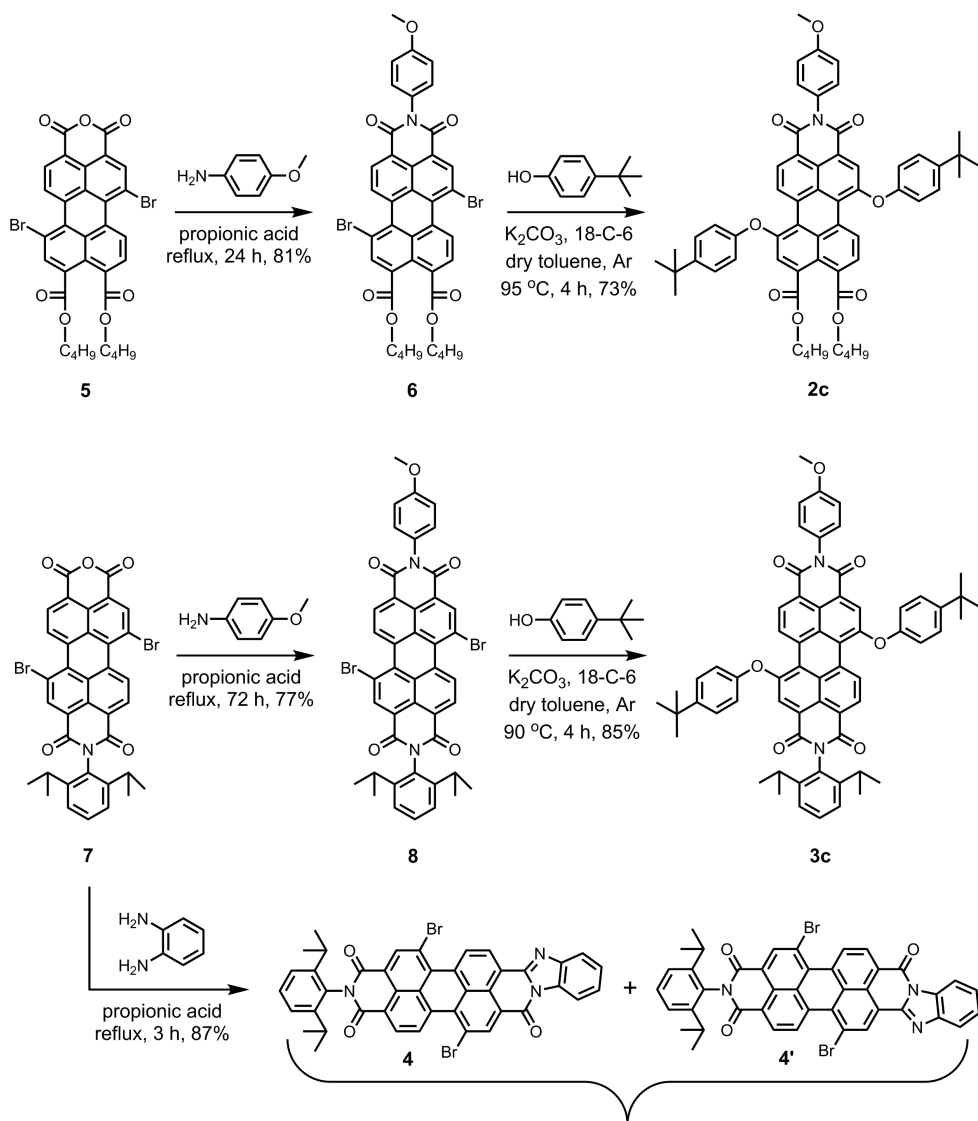
The syntheses of these regioisomerically pure 1,7-dibromo-precursors (**1–4**) was carried out from commercially available perylene-3,4,9,10-tetracarboxylic bisanhydride (PBA) using a previously reported procedure.¹ The subsequent substitution of bromine atoms with 4-*tert*-butylphenoxy and 4-methoxyphenoxy groups was achieved in high yields (80–90%) as shown in **Scheme A.1**. The phenoxy substitution on 1,7-dibromoperylene tetrabutylester **1** was performed in anhydrous DMF at elevated temperature (115 °C) owing to the low reactivity of the 1,7-dibromoperylene tetrabutylester towards nucleophilic substitution reactions.¹ For all other derivatives (**2**, **3**, and **4**), the reaction was carried out under milder reaction conditions in toluene at temperatures around 90 °C.^{2,3}



Scheme A. 1 Synthesis of 1,7-di(4-*tert*-butylphenoxy) and 1,7-di(4-methoxyphenoxy)perylene-3,4,9,10-tetracarboxylic acid derivatives.

An isomeric mixture of 1,7-dibromoperylene monoimide monobenzimidazole compounds (**4** + **4'**) was obtained by the reaction between 1,7-dibromoperylene monoimide monoanhydride **7** and 1,2-diaminobenzene in refluxing propionic acid (**Scheme A.2**).⁴ The TLC analysis of this mixture revealed two slightly separated spots corresponding to **4** and **4'**. Efforts to separate the two region-isomers by column chromatography, however, were not successful. The presence of two isomers was also evident from the ¹H NMR spectrum, in which two sets of signals in the aromatic region are clearly visible (**Figure A.1**). These signals, corresponding to the perylene core protons H⁸, H^{8'} and H¹¹, H^{11'}, were very well resolved. On the basis of the relative intensities of these signals, surprisingly, the two regioisomers (**4** and **4'**) were found in a ratio ca. 2:1. The obtained ratio is rather surprising because we cannot deduct differences in electron density of both anhydride carbonyl in compound **7**, based on resonance structures. Thus the reactivity of both anhydride carbonyl moieties is expected to be identical. For the synthesis of tetrachlorobisimidazoles, both 1:1⁵ and 2:1⁶ isomeric mixtures have been reported. The assignment of the signals (H⁸, H^{8'} and H¹¹, H^{11'}) to the individual regioisomers was done based on ¹H–¹H COSY, and by the direct comparison of ¹H NMR spectrum of (**4**+**4'**) with the spectrum of 1,7-dibromoperylene bisimide **3** (**Figure A.1**). The ring current effect of the additional aromatic benzimidazole moiety was a decisive argument for explaining changes in the chemical shifts.

When comparing the ¹H NMR spectra of compounds **3** and **4**+**4'**, the chemical shifts for the perylene core protons H² and H⁵, in the “left” imide part of these compounds, are expected to be very similar. Indeed, protons H² and H⁵ have identical chemical shifts in compounds **3** and **4**+**4'**. Placement of the imidazole moiety on the “right” part of the molecule should affect the chemical shifts of protons H⁸ and H¹¹, upon going from **3** to **4** or **4'**, but to a different extent. A larger shift is expected for the proton H¹¹ in compound **4**, whereas the imidazole placement in compound **4'** should have a larger effect on the chemical shift of proton H^{8'}. The predicted shifts are clearly visible in the ¹H NMR spectrum depicted in **Figure A.1**, in which the proton assignment is shown.



Scheme A. 2 Synthesis of 4-methoxyphenyl functionalized derivatives **2c** and **3c**.

The two compounds **2c** and **3c**, containing 4-methoxyphenyl moiety at the imide position, were synthesized to investigate photoinduced CT from substituents attached to the imide position of perylene tetracarboxylic acid derivatives **2** and **3**. The synthesis was carried out in two steps from their corresponding monoanhydride precursors **5** and **7**, respectively. In the first step, imidization was carried out with 4-methoxyaniline in refluxing propionic acid to afford corresponding imides **6** and **8**.³ Thereafter, nucleophilic substitution of bromine atoms with 4-*tert*-butylphenol yielded the desired products **2c** and **3c** in good yields.

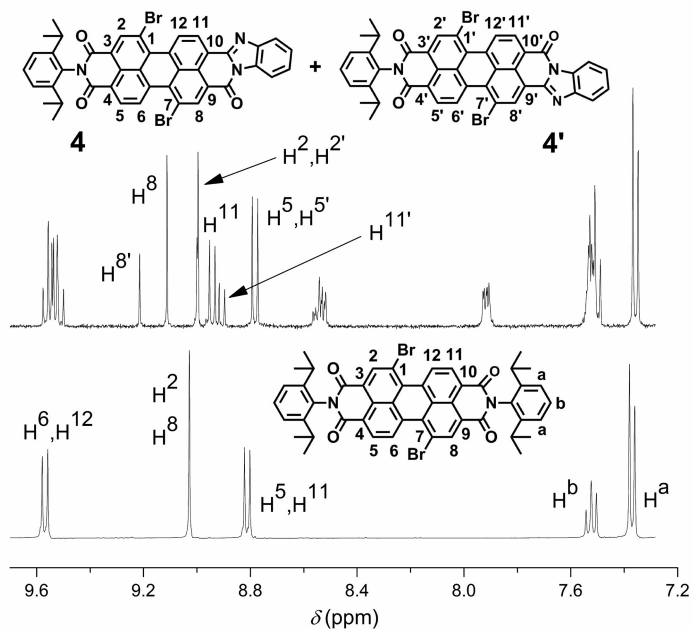


Figure A. 1 Comparison between ^1H NMR spectra of compound 4+4' and 1,7-dibromoperylene bisimide **3**.

A.2 Synthesis Details

Synthesis of 1,7-di(4-*tert*-butylphenoxy)perylene-3,4,9,10-tetracarboxy tetrabutylester (1a**):** In a 25 mL round-bottomed flask, weighed amounts of 1,7-dibromoperylene tetrabutylester **1** (200 mg, 0.25 mmol), 4-*tert*-butylphenol (148 mg, 0.99 mmol), and Cs_2CO_3 (485 mg, 1.49 mmol) were taken. Subsequently, anhydrous DMF (8 mL) was added. The reaction mixture was stirred at 115 $^\circ\text{C}$ for 3 hours under argon atmosphere. After the mixture cooled to room temperature, CH_2Cl_2 (50 mL) was added to the reaction mixture and the resultant solution was washed with water several times. The organic layer was collected and evaporated. The crude product was chromatographed with DCM to afford the desired product **1a** (199 mg, 85%). Later on, it was recrystallized from refluxing EtOH. ^1H NMR (400 MHz, CDCl_3): δ = 9.08 (d, J = 8.0 Hz, 2H), 7.98 (d, J = 8.0 Hz, 2H), 7.73 (s, 2H), 7.39 (d, J = 8.0 Hz, 4H), 7.01 (d, J = 8.0 Hz, 4H), 4.29 (t, J = 6.8 Hz, 4H), 4.23 (t, J = 6.8 Hz, 4H), 1.78–1.70 (m, 4H), 1.69–1.62 (m, 4H), 1.50–1.33 (m, 4H), 1.41–1.30 (m, 4H), 1.33 (s, 18H), 0.96 (t, J = 6.8 Hz, 6H), 0.89 ppm (t, J = 6.8 Hz, 6H). ^{13}C NMR (100 MHz, CDCl_3): δ = 168.5, 167.8, 153.3, 152.2, 147.0, 132.0, 131.2, 129.4, 129.1, 127.1, 127.0, 124.7, 124.3, 122.5, 118.3, 65.3, 65.2, 34.4, 31.4, 30.6, 30.4, 19.2, 19.1, 13.8, 13.7 ppm.

Synthesis of 1,7-di(4-methoxyphenoxy)perylene-3,4,9,10-tetracarboxy tetrabutylester (1b): Prepared from 1,7-dibromoperylene tetrabutylester **1** (100 mg, 0.12 mmol), 4-methoxyphenol (61 mg, 0.49 mmol), and Cs_2CO_3 (240 mg, 0.74 mmol) according to the procedure described for compound **1a**. The crude product was purified using silica-60/ CHCl_3 and, subsequently, recrystallized from refluxing ethanol (97 mg, 88%). ^1H NMR (400 MHz, CDCl_3): δ = 9.10 (d, J = 8.0 Hz, 2H), 7.99 (d, J = 8.0 Hz, 2H), 7.68 (s, 2H), 7.04 (d, J = 8.8 Hz, 4H), 6.92 (d, J = 8.8 Hz, 4H), 4.29 (t, J = 6.8 Hz, 4H), 4.23 (t, J = 6.8 Hz, 4H), 3.82 (s, 6H), 1.78–1.71 (m, 4H), 1.71–1.63 (m, 4H), 1.52–1.41 (m, 4H), 1.40–1.30 (m, 4H), 0.97 (t, J = 7.2 Hz, 6H), 0.90 ppm (t, J = 7.2 Hz, 6H). ^{13}C NMR (100 MHz, CDCl_3): δ = 168.5, 167.8, 156.4, 152.9, 149.0, 131.2, 131.1, 129.2, 129.0, 127.1, 124.4, 123.4, 121.8, 120.5, 115.2, 65.3, 65.2, 55.7, 30.6, 30.4, 19.2, 19.1, 13.8, 13.7 ppm.

Synthesis of N-(2,6-diisopropylphenyl)-1,7-di(4-tert-butylphenoxy)perylene-3,4,9,10-tetracarboxy monoimide dibutylester (2a): A mixture of 4-tert-butylphenol (54 mg, 0.36 mmol), K_2CO_3 (100 mg, 0.72 mmol), and 18-Crown-6 (190 mg; 0.72 mmol) was stirred in anhydrous toluene (20 mL) for 20 minutes at room temperature under argon atmosphere. Subsequently, 1,7-dibromoperylene monoimide dibutylester **2** (100 mg, 0.12 mmol) was added and the reaction mixture was stirred for 3h at 95 °C. After being cooled to room temperature, more toluene (30 mL) was added and the organic solution was extracted with water twice. The solvent was evaporated and the crude product was purified by silica gel column chromatography in DCM to afford compound **2a** (105 mg; 90%). ^1H NMR (400 MHz, CDCl_3): δ = 9.30 (t, J = 8.4 Hz, 2H), 8.61 (d, J = 8.4 Hz, 1H), 8.39 (s, 1H), 8.03 (d, J = 8.4 Hz, 1H), 7.78 (s, 1H), 7.46–7.38 (m, 5H), 7.29 (d, J = 8.0 Hz, 2H), 7.09–7.02 (m, 4H), 4.31 (t, J = 6.8 Hz, 2H), 4.24 (t, J = 6.8 Hz, 2H), 2.75–2.65 (m, 2H), 1.80–1.61 (m, 4H), 1.49–1.33 (m, 4H), 1.34 (s, 9H), 1.33 (s, 9H), 1.16–1.10 (m, 12H), 0.98 (t, J = 7.2 Hz, 3H), 0.91 ppm (t, J = 7.2 Hz, 3H). ^{13}C NMR (100 MHz, CDCl_3): δ = 168.4, 167.6, 163.7, 163.1, 153.9, 153.8, 153.1, 152.8, 147.6, 147.4, 145.6, 134.3, 132.6, 132.1, 130.8, 130.8, 130.70, 130.66, 129.4, 129.1, 128.4, 127.8, 127.2, 127.1, 125.8, 125.7, 125.2, 124.8, 123.9, 123.8, 122.8, 121.3, 121.1, 118.7, 118.3, 65.5, 65.4, 34.5, 34.4, 31.4, 30.6, 30.4, 29.1, 24.0, 23.9, 19.2, 19.1, 13.8, 13.7 ppm.

Synthesis of N-(2,6-diisopropylphenyl)-1,7-di(4-methoxyphenoxy)perylene-3,4,9,10-tetracarboxy monoimide dibutylester (2b): Prepared from 4-methoxyphenol (40 mg, 0.32 mmol), K_2CO_3 (89 mg, 0.64 mmol) and 18-Crown-6 (170 mg, 0.64 mmol), and 1,7-dibromoperylene monoimide dibutylester **2** (90 mg, 0.11 mmol) as per the procedure described for the compound **2a**. The crude product was purified by column chromatography (silica-60/ CHCl_3) and, subsequently, recrystallized from refluxing EtOH to afford the product **2b** (84 mg, 85%). ^1H NMR (400 MHz, CDCl_3): δ = 9.41 (t, J = 8.0 Hz, 2H), 8.64 (d, J = 8.0 Hz, 1H), 8.33 (s, 1H), 8.05 (d, J = 8.0 Hz, 1H), 7.73 (s, 1H), 7.45 (t, J = 7.6 Hz, 1H), 7.30 (d, J = 8.0 Hz, 2H), 7.09 (t, J = 8.8 Hz, 4H), 6.97 (d, J = 9.2 Hz, 2H), 6.94 (d, J = 9.2 Hz, 2H), 4.32 (t, J = 6.8 Hz, 2H), 4.25 (t, J = 6.8 Hz, 2H), 3.85 (s, 3H), 3.82 (s, 3H), 2.73–2.65 (m, 2H), 1.78–1.71 (m, 2H), 1.70–1.62 (m, 2H), 1.49–1.43 (m, 2H), 1.36–1.31 (m, 3H), 1.15–1.12 (m, 12H), 0.98 (t, J = 7.2 Hz, 3H), 0.91 ppm (t, J = 7.2 Hz, 3H). ^{13}C NMR (100 MHz, CDCl_3): δ = 167.9, 167.1, 163.1, 162.6, 156.3, 156.1, 154.1, 154.0, 148.3, 147.9,

145.1, 133.8, 132.0, 131.6, 130.3, 130.2, 130.13, 130.08, 128.91, 128.88, 128.5, 127.9, 127.3, 125.1, 124.6, 124.0, 123.8, 123.4, 122.3, 122.2, 120.5, 120.3, 119.9, 114.9, 114.9, 65.0, 64.9, 55.2, 30.1, 29.9, 28.6, 23.4, 18.7, 18.6, 13.3, 13.2 ppm.

Synthesis of *N,N'*-bis(2,6-diisopropylphenyl)-1,7-di(4-*tert*-butylphenoxy) perylene-3,4,9,10-tetracarboxy bisimide (3a**):** Prepared from 4-*tert*-butylphenol (53 mg, 0.35 mmol), K₂CO₃ (96 mg, 0.70 mmol), 18-Crown-6 (185 mg, 0.70 mmol), and 1,7-dibromoperylene bisimide **3** (100 mg, 0.12 mmol) in dry toluene (30 ml) at 90 °C according to the procedure described for compound **2a**. The crude product was refluxed in MeOH (20 mL) and filtered to remove unreacted phenol. Thereafter, the dried precipitate was chromatographed using silica-60/DCM to afford compound **3a** (91 mg, 79%). ¹H NMR (400 MHz, CDCl₃): δ = 9.67 (d, *J* = 8.0 Hz, 2H), 8.69 (d, *J* = 8.0 Hz, 2H), 8.45 (s, 2H), 7.46 (m, 6H), 7.32 (d, *J* = 7.2 Hz, 4H), 7.11 (d, *J* = 7.2 Hz, 4H), 2.72 (m, 4H), 1.36 (s, 18H), 1.20–1.12 ppm (m, 24H). ¹³C NMR (100 MHz, CDCl₃): δ = 163.5, 162.9, 155.3, 152.6, 148.0, 145.6, 133.8, 130.7, 130.5, 129.7, 129.6, 129.0, 127.4, 125.8, 124.7, 124.5, 124.0, 122.3, 118.7, 31.4, 29.2, 24.0, 23.9 ppm.

Synthesis of *N,N'*-bis(2,6-diisopropylphenyl)-1,7-di(4-methoxyphenoxy) perylene-3,4,9,10-tetracarboxy bisimide (3b**):** Prepared from 4-methoxyphenol (86 mg, 0.69 mmol), K₂CO₃ (191 mg, 1.38 mmol), 18-Crown-6 (365 mg, 1.38 mmol) and 1,7-dibromoperylene bisimide **3** (200 mg, 0.23 mmol) in dry toluene (50 ml) according to the procedure described for compound **2a**. The crude product was refluxed in MeOH (25 mL) and filtered (after cooling) to remove unreacted phenol. Thereafter, the dried precipitate was chromatographed (silica-60/DCM:toluene 1:1) to afford compound **3b** (180 mg, 82%). ¹H NMR (400 MHz, CDCl₃): δ = 9.71 (d, *J* = 8.0 Hz, 2H), 8.73 (d, *J* = 8.0 Hz, 2H), 8.41 (s, 2H), 7.48 (t, *J* = 7.6 Hz, 2H), 7.33 (d, *J* = 7.6 Hz, 4H), 7.16 (d, *J* = 7.6 Hz, 4H), 7.01 (d, *J* = 7.6 Hz, 4H), 3.85 (s, 6H), 2.74 (m, 4H), 1.17 ppm (s, 24H). ¹³C NMR (100 MHz, CDCl₃): δ = 163.5, 162.9, 157.0, 156.0, 148.3, 145.6, 133.8, 130.6, 130.5, 129.6, 129.0, 125.6, 124.0, 123.9, 123.8, 122.2, 120.8, 115.6, 55.7, 29.2, 24.0 ppm.

Synthesis of *N*-(2,6-diisopropylphenyl)-1,7-dibromoperylene-3,4,9,10-tetracarboxy monoimide monobenzimidazole (4+4'**):** 1,7-dibromo perylene monoimide monoanhydride **7** (50 mg, 0.07 mmol) and 1,2-diaminobenzene (10 mg, 0.09 mmol) were taken in propionic acid (10 ml). The mixture was refluxed for 3 h. After the mixture cooled down to room temperature, it was poured into water to precipitate the crude product. The precipitate was filtered off and washed with several portions of water to remove all the propionic acid. The precipitate was dried and chromatographed on silica-60 eluting with DCM to afford the pure product (48 mg, 87%) as the mixture of two regioisomers **4** and **4'** in a ratio ca. 2:1. ¹H NMR (400 MHz, CDCl₃): δ = 9.60–9.50 (m, 2H), 9.22 (s, 0.35H), 9.11 (s, 0.65H), 8.99 (s, 1H), 8.94 (d, *J* = 8.0 Hz, 0.65H), 8.90 (d, *J* = 8.0 Hz, 0.35H), 8.78 (d, *J* = 8.0 Hz, 1H), 8.56–8.51 (m, 1H), 7.95–7.90 (m, 1H), 7.56–7.47 (m, 3H), 7.35 (d, *J* = 8.0 Hz, 2H), 2.79–2.70 (m, *J* = 6.8 Hz, 2H), 1.22–1.16 ppm (m, 12H). ¹³C NMR spectra could not be measured because of its low solubility.

Synthesis of *N*-(2,6-diisopropylphenyl)-1,7-di(4-*tert*-butylphenoxy)perylene-3,4,9,10-tetracarboxy monoimide monobenzimidazole (4a):

Synthesized from 4-*tert*-butylphenol (59 mg, 0.39 mmol), K₂CO₃ (108 mg, 0.78 mmol), 18-Crown-6 (206 mg, 0.78 mmol) and 1,7-dibromoperylene monoimide monobenzimidazole **4** (100 mg, 0.13 mmol) in dry toluene (25 ml) according to the procedure described for compound **2a**. The crude product was chromatographed using silica-60/CHCl₃ to afford compound **4a** (95 mg; 80%) as the mixture of two regioisomers. ¹H NMR (400 MHz, CDCl₃): δ = 9.68–9.52 (m, 2), 8.80–8.74 (m, 1H), 8.64–8.58 (m, 1.45 H), 8.52 (s, 0.55H), 8.49–8.45 (m, 0.60H), 8.42–8.36 (m, 1.50H), 7.83–7.75 (m, 1H), 7.51–7.38 (m, 7H), 7.30 (d, *J* = 7.6 Hz, 2H), 7.17–7.09 (m, 4H), 2.77–2.73 (m, 2H), 1.39–1.34 (m, 18H), 1.17–1.14 ppm (m, 12H). ¹³C NMR spectrum could not be measured because of its low solubility.

Synthesis of *N*-(2,6-diisopropylphenyl)-1,7-di(4-methoxyphenoxy)perylene-3,4,9,10-tetracarboxy monoimide monobenzimidazole (4b):

Synthesized from 4-methoxyphenol (48 mg, 0.39 mmol), K₂CO₃ (108 mg, 0.78 mmol), 18-Crown-6 (206 mg, 0.78 mmol) and 1,7-dibromoperylene monoimide monobenzimidazole **4** (100 mg, 0.13 mmol) in dry toluene (30 ml) according to the procedure described for compound **2a**. The crude product was chromatographed using silica-60/CHCl₃ to afford compound **4b** (96 mg, 86%) as the mixture of two regioisomers. ¹H NMR (400 MHz, CDCl₃): δ = 9.68–9.52 (m, 2H), 8.72 (d, *J* = 8.4 Hz, 1H), 8.65–8.55 (m, 1H), 8.50 (s, 0.55H), 8.41 (s, 0.45H), 8.40–8.29 (m, 2H), 7.77–7.71 (m, 1H), 7.46 (t, *J* = 8.0 Hz, 1H), 7.41–7.35 (m, 2H), 7.31 (d, *J* = 8.0 Hz, 2H), 7.22–7.13 (m, 4H), 7.08–6.94 (m, 4H), 3.89–3.83 (m, 6H), 2.77–2.73 (m, 2H), 1.19–1.13 ppm (m, 12H). ¹³C NMR spectrum could not be measured because of its low solubility.

Synthesis of *N*-(4-methoxyphenyl)-1,7-dibromoperylene-3,4,9,10-tetracarboxy monoimide dibutylester (6): A 25 mL round-bottomed flask was charged with 1,7-dibromoperylene monoanhydride dibutylester **5** (150 mg, 0.22 mmol), 4-methoxyaniline (35 mg, 0.29 mmol), and propionic acid (6 mL). The reaction mixture was refluxed for 24 h. After it cooled down to room temperature, the reaction mixture was poured into the water to precipitate the crude product. The precipitate was filtered off and washed with several portions of water to remove all the propionic acid. The precipitate was dried and chromatographed on silica, eluting with CH₂Cl₂, to afford the desired product **6** (140 mg, 81%). ¹H NMR (400 MHz, CDCl₃): δ = 9.24 (d, *J* = 8.0 Hz, 1H), 9.21 (d, *J* = 8.0 Hz, 1H), 8.89 (s, 1H), 8.68 (d, *J* = 8.0 Hz, 1H), 8.34 (s, 1H), 8.13 (d, *J* = 8.0 Hz, 1H), 7.24 (d, *J* = 8.0 Hz, 2H), 7.08 (d, *J* = 8.0 Hz, 2H), 4.35 (t, *J* = 6.8 Hz, 4H), 3.88 (s, 3H), 1.84–1.75 (m, 4H), 1.53–1.46 (m, 4H), 1.00 ppm (t, *J* = 7.2 Hz, 6H). ¹³C NMR (100 MHz, CDCl₃): δ = 167.7, 166.9, 166.8, 163.5, 162.95, 162.91, 159.7, 138.0, 136.8, 134.2, 133.7, 132.0, 131.9, 131.6, 130.8, 130.5, 130.4, 130.3, 129.6, 129.5, 129.1, 129.0, 128.2, 128.13, 128.11, 127.3, 127.0, 126.9, 122.2, 122.1, 120.3, 119.4, 114.8, 66.0, 65.8, 55.5, 30.6, 30.5, 19.3, 19.2, 19.1, 13.8, 13.7 ppm.

Synthesis of *N*-(4-methoxyphenyl)-1,7-di(4-*tert*-butylphenoxy)perylene-3,4,9,10-tetracarboxy monoimide dibutylester (2c): Synthesized from 4-*tert*-

butylphenol (50 mg, 0.33 mmol), K_2CO_3 (69 mg, 0.50 mmol), 18-Crown-6 (131 mg, 0.50 mmol) and 1,7-dibromoperylene monoimide dibutylester **6** (65 mg, 0.08 mmol) in dry toluene (12 ml) according to the procedure described for compound **2a**. The crude product was chromatographed using silica-60/DCM to afford compound **2c** (56 mg, 73%). 1H NMR (400 MHz, $CDCl_3$): δ = 9.39 (d, J = 8.4 Hz, 2H), 8.58 (d, J = 8.4 Hz, 1H), 8.34 (s, 1H), 8.04 (d, J = 8.4 Hz, 1H), 7.77 (s, 1H), 7.45–7.38 (m, 4H), 7.20 (d, J = 8.8 Hz, 2H), 7.09–7.01 (m, 6H), 4.31 (t, J = 6.8 Hz, 2H), 4.24 (t, J = 6.8 Hz, 2H), 3.85 (s, 3H), 1.78–1.63 (m, 4H), 1.52–1.34 (m, 4H), 1.34 (s, 9H), 1.32 (s, 9H), 0.97 (t, J = 7.6 Hz, 3H), 0.90 ppm (t, J = 7.2 Hz, 3H). ^{13}C NMR (100 MHz, $CDCl_3$): δ = 168.3, 167.6, 163.9, 163.6, 159.5, 153.9, 153.0, 152.7, 147.7, 147.6, 134.3, 132.7, 132.0, 130.8, 130.7, 130.5, 129.5, 129.2, 129.0, 128.4, 127.7, 127.6, 127.2, 127.1, 125.3, 124.73, 124.70, 123.6, 122.7, 121.13, 121.10, 118.8, 118.7, 114.7, 77.3, 77.0, 76.7, 65.5, 65.4, 55.5, 34.5, 34.4, 31.4, 30.6, 30.4, 19.2, 19.1, 13.8, 13.7 ppm.

Synthesis of *N*-(2,6-diisopropylphenyl)-*N'*-(4-methoxyphenyl)-1,7-dibromoperylene-3,4,9,10-tetracarboxy bisimide (8**):** Synthesized as per the procedure described for compound **6** from 1,7-dibromoperylene monoimide monoanhydride **7** (150 mg, 0.21 mmol), 4-methoxyaniline (78 mg, 0.63 mmol), and propionic acid (8 mL). The reaction mixture was refluxed for 24 h. After it cooled down to room temperature, the reaction mixture was poured into the water to precipitate the crude product. The precipitate was filtered off and washed with several portions of water to remove all the propionic acid. The precipitate was dried and chromatographed on silica, eluting with CH_2Cl_2 , to afford the desired product **8** (133 mg, 77%). 1H NMR (400 MHz, $CDCl_3$): δ = 9.56 (d, J = 8.0 Hz, 1H), 9.54 (d, J = 8.0 Hz, 1H), 9.00 (s, 1H), 8.98 (s, 1H), 8.79 (d, J = 8.0 Hz, 1H), 8.77 (d, J = 8.0 Hz, 1H), 7.51 (t, J = 7.6 Hz, 1H), 7.35 (d, J = 7.6 Hz, 2H), 7.24 (d, J = 8.8 Hz, 2H), 7.09 (d, J = 8.8 Hz, 2H), 3.89 (s, 3H), 2.78–2.66 (m, 2H), 1.19 (s, 6H), 1.17 ppm (s, 6H). ^{13}C NMR (100 MHz, $CDCl_3$): δ = 162.7, 162.5, 159.8, 145.6, 138.4, 138.3, 133.2, 133.1, 131.0, 130.6, 130.4, 130.1, 129.9, 129.6, 129.5, 129.4, 129.0, 128.7, 127.6, 127.4, 127.1, 124.2, 123.4, 123.0, 122.8, 120.9, 114.9, 55.5, 29.3, 23.99, 23.97 ppm.

Synthesis of *N*-(2,6-diisopropylphenyl)-*N'*-(4-methoxyphenyl)-1,7-di(4-*tert*-butylphenoxy)perylene-3,4,9,10-tetracarboxy bisimide (3c**):** Synthesized as per the procedure described for compound **2a** from 4-*tert*-butylphenol (50 mg, 0.33 mmol), K_2CO_3 (69 mg, 0.50 mmol), 18-Crown-6 (131 mg, 0.50 mmol) and 1,7-dibromoperylene bisimide **8** (65 mg, 0.08 mmol) in dry toluene (12 ml) according to the procedure described for compound **2a**. The crude product was chromatographed using silica-60/DCM to afford compound **2c** (65 mg, 85%). 1H NMR (400 MHz, $CDCl_3$): δ = 9.67 (d, J = 8.0 Hz, 1H), 9.62 (d, J = 8.0 Hz, 1H), 8.70 (d, J = 8.0 Hz, 1H), 8.62 (d, J = 8.0 Hz, 1H), 8.43 (s, 1H), 8.35 (s, 1H), 7.50–7.42 (m, 5H), 7.31 (d, J = 8.0 Hz, 2H), 7.22 (d, J = 8.8 Hz, 2H), 7.15–7.01 (m, 6H), 3.86 (s, 3H), 2.77–2.67 (m, 2H), 1.35 (s, 9H), 1.34 (s, 9H), 1.25–1.11 ppm (m, 12H). ^{13}C NMR (100 MHz, $CDCl_3$): δ = 163.5, 163.3, 159.6, 155.5, 155.4, 152.5, 152.4, 148.2, 148.1, 145.6, 133.8, 133.7, 130.7, 130.5, 130.4, 129.6, 129.5, 129.4, 129.0, 128.9, 127.4, 127.3, 125.7, 125.3, 124.4, 124.24, 124.20, 124.0, 123.8, 122.3, 122.2, 119.0, 118.9, 114.7, 55.5, 36.8, 34.6, 34.5, 31.4, 29.2, 24.0, 23.9 ppm.

A.3 Extra Experimental Results

Table A. 1 Calculated rate of fluorescence and fluorescence quenching of compounds 1–4 in toluene, chloroform, and acetonitrile/benzonitrile.

Compound	Solvent	k_F ($\times 10^{-8} \text{ s}^{-1}$)	k_{nr} ($\times 10^{-8} \text{ s}^{-1}$)
1a	toluene	2.13	0.21
	chloroform	1.90	0.36
	acetonitrile	1.90	0.21
1b	toluene	2.07	0.28
	chloroform	1.80	0.43
	acetonitrile	~0.95	~46.7
2a	toluene	1.89	0.33
	chloroform	1.72	0.25
	acetonitrile	1.72	0.19
2b	toluene	1.95	0.44
	chloroform	1.00	2.12
	acetonitrile	~0.37	~12.1
2c	toluene	2.13	0.16
	chloroform	1.84	0.27
	acetonitrile	1.96	0.17
3a	toluene	2.12	0.13
	chloroform	1.96	0.19
	benzonitrile	1.92	0.31
3b	toluene	~2.67	~11.4
	chloroform	~0.93	~22.3
	benzonitrile	~0.66	~82.6
3c	toluene	2.63	0.00
	chloroform	2.23	0.33
	benzonitrile	1.81	1.21
4a	toluene	1.60	0.65
	chloroform	1.53	0.78
	benzonitrile	1.66	0.71
4b	toluene	1.78	0.05
	chloroform	0.94	3.14
	benzonitrile	~0.93	~22.3

The rate of fluorescence (k_F) and rate of fluorescence quenching (k_{nr}) were obtained from steady state and time-resolved optical measurements using **Equations 1–4**.

$$\Phi_F = \frac{k_F}{k_F + k_Q} \quad (\text{A.1})$$

$$\tau_F = \frac{1}{k_F + k_Q} \quad (\text{A.2})$$

$$k_F = \frac{\Phi_F}{\tau_F} \quad (\text{A.3})$$

$$k_Q = \frac{k_F}{\Phi_F} - k_F \quad (\text{A.4})$$

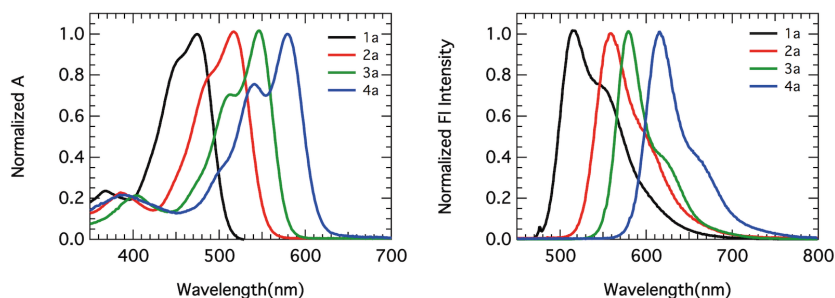


Figure A. 2 The normalized UV/Vis absorption (Left) and emission (Right) spectra of compounds **1–4a** in chloroform.

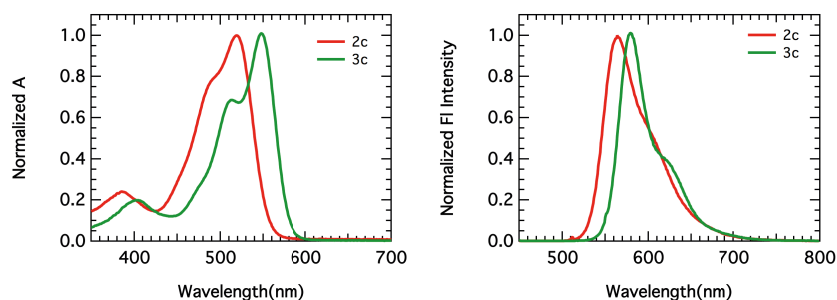
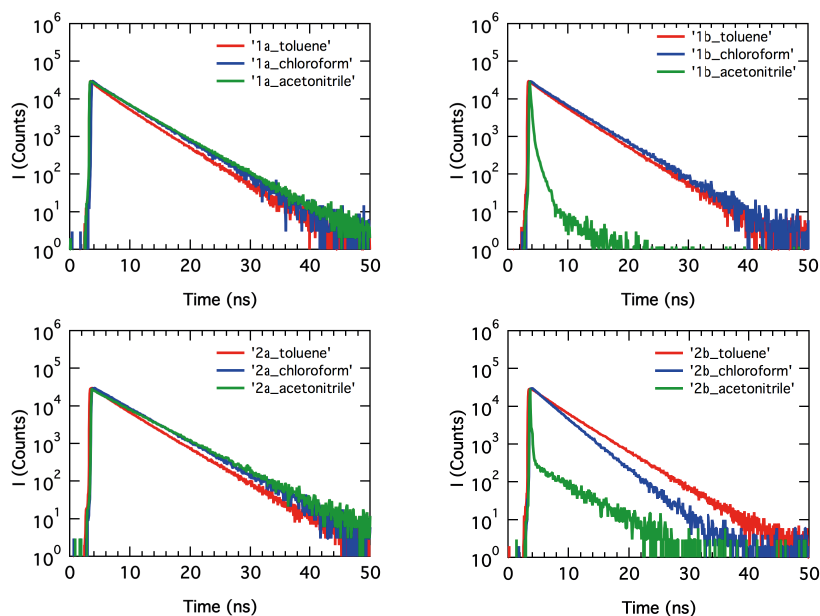


Figure A. 3 The normalized UV/Vis absorption (Left) and emission (Right) spectra of compounds **2c** and **3c** in chloroform.



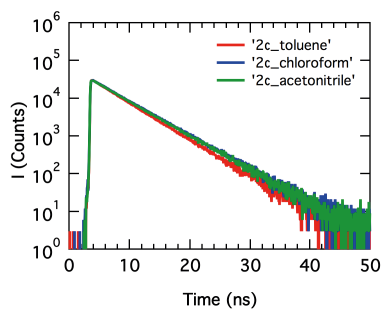


Figure A. 4 Fluorescence decay curves of compounds **1a–b** and **2a–c** in toluene, chloroform, and acetonitrile.

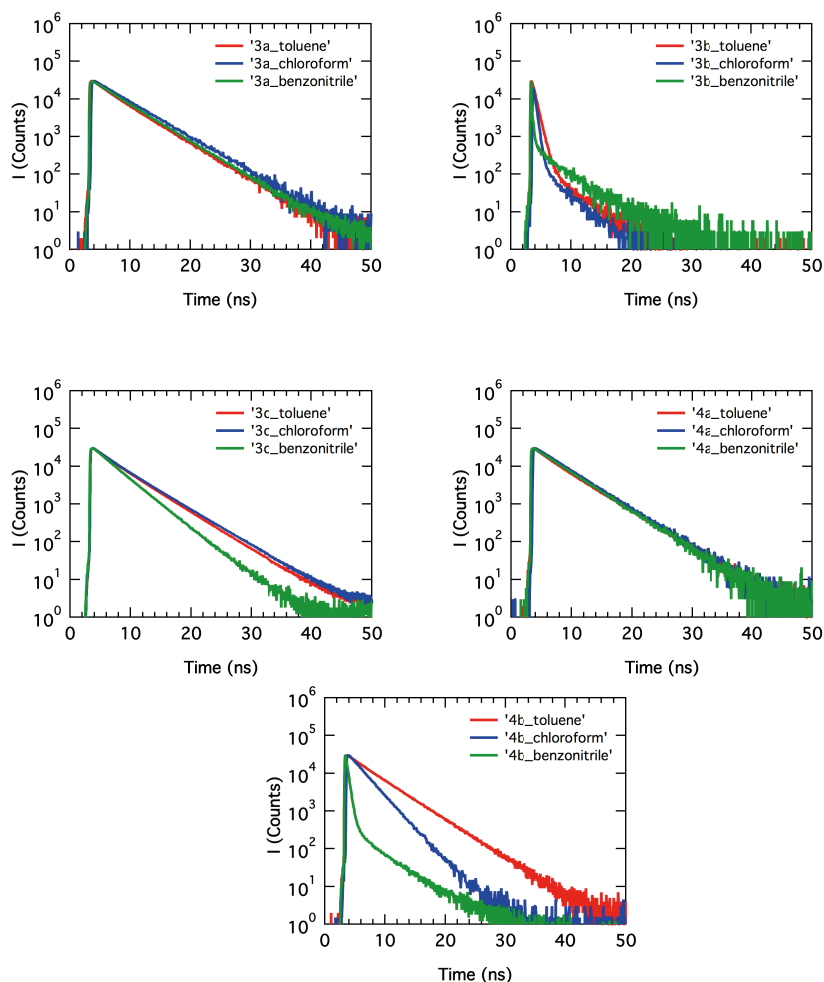


Figure A. 5 Fluorescence decay curves of compounds **3a–c** and **4a–b** in toluene, chloroform, and benzonitrile.

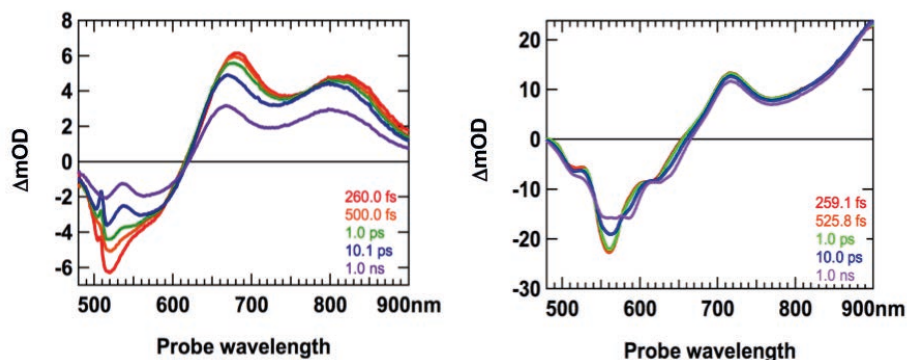


Figure A. 6 Transient absorption spectra of **2c** (left, in acetonitrile) and **3c** (right, in benzonitrile) with respect to different time delays between pump and probe light.

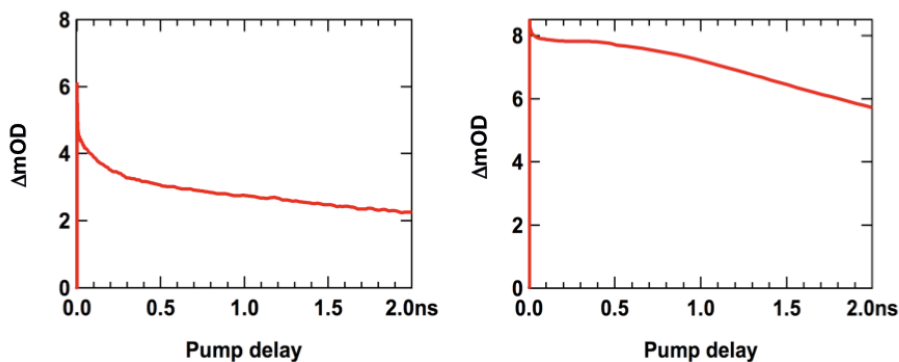


Figure A. 7 Kinetics of **2c** at 685 nm in acetonitrile (left) and of **3c** at 775 nm (right) in benzonitrile

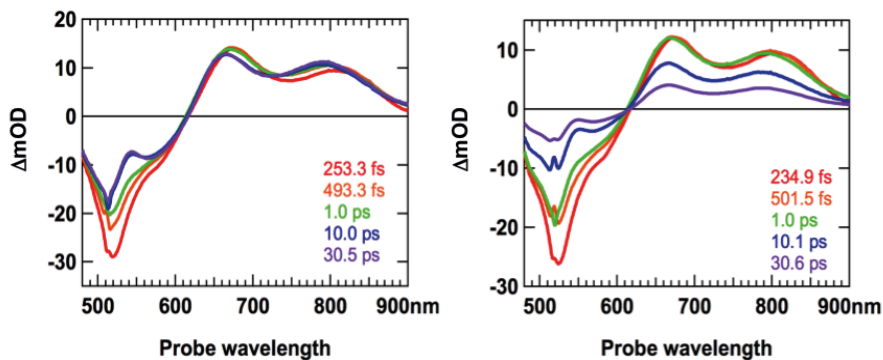


Figure A. 8 Transient absorption spectra of **2a** (left) and **2b** (right) in acetonitrile with respect to different time delays between pump and probe light.

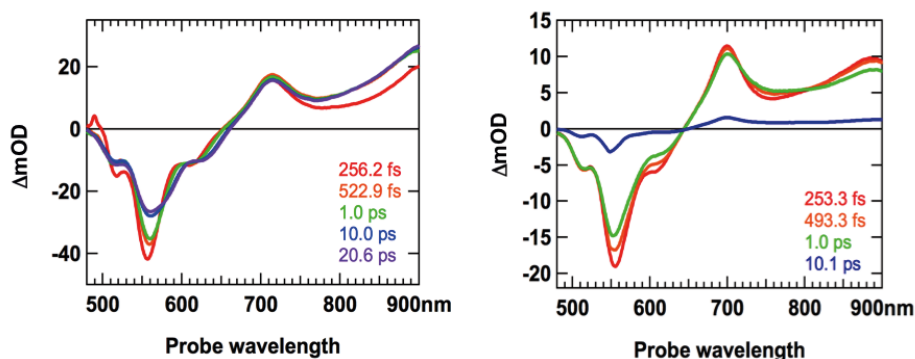


Figure A. 9 Transient absorption spectra of **3a** (left) and **3b** (right) in benzonitrile with respect to different time delays between pump and probe light.

A.4 References

- (1) Sengupta, S.; Dubey, R. K.; Hoek, R. W. M.; van Eeden, S. P. P.; Gunbaş, D. D.; Grozema, F. C.; Sudhölter, E. J. R.; Jager, W. F., Synthesis of Regioisomerically Pure 1,7-Dibromoperylene-3,4,9,10-tetracarboxylic Acid Derivatives. *The Journal of Organic Chemistry* **2014**, 79 (14), 6655-6662.
- (2) Dubey, R. K.; Inan, D.; Sengupta, S.; Sudholter, E. J. R.; Grozema, F. C.; Jager, W. F., Tunable and highly efficient light-harvesting antenna systems based on 1,7-perylene-3,4,9,10-tetracarboxylic acid derivatives. *Chemical Science* **2016**, 7 (6), 3517-3532.
- (3) Dubey, R. K.; Efimov, A.; Lemmetyinen, H., 1,7- And 1,6-Regioisomers of Diphenoxy and Dipyrroliidynyl Substituted Perylene Diimides: Synthesis, Separation, Characterization, and Comparison of Electrochemical and Optical Properties. *Chemistry of Materials* **2011**, 23 (3), 778-788.
- (4) Yuan, Z.; Xiao, Y.; Li, Z.; Qian, X., Efficient Synthesis of Regioisomerically Pure Bis(trifluoromethyl)-Substituted 3,4,9,10-Perylene Tetracarboxylic Bis(benzimidazole). *Organic Letters* **2009**, 11 (13), 2808-2811.
- (5) Perrin, L.; Hudhomme, P., Synthesis, Electrochemical and Optical Absorption Properties of New Perylene-3,4:9,10-bis(dicarboximide) and Perylene-3,4:9,10-bis(benzimidazole) Derivatives. *European Journal of Organic Chemistry* **2011**, 2011 (28), 5427-5440.
- (6) Dubey, R. K.; Westerveld, N.; Sudholter, E. J. R.; Grozema, F. C.; Jager, W. F., Novel derivatives of 1,6,7,12-tetrachloroperylene-3,4,9,10-tetracarboxylic acid: synthesis, electrochemical and optical properties. *Organic Chemistry Frontiers* **2016**, 3 (11), 1481-1492.

B • Appendix for Chapter 3

B.1 Synthesis and characterization

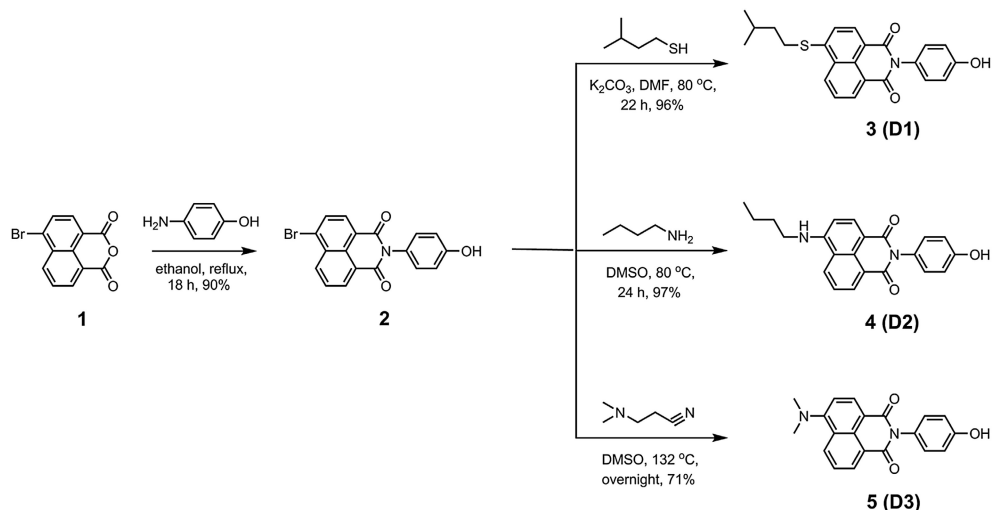
The energy donor naphthalimide derivatives (**3–5**), outlined in **Scheme B.1**, were obtained from commercially available 4-bromo- 1,8-naphthalic anhydride **1**. The compounds were synthesized in two steps in high yields. First, imidization of **1** with 4-aminophenol yielded *N*-(4'-hydroxyphenyl)-4-bromonaphthalene monoimide **2**.¹ Subsequently, the bromine was substituted by isopentylthio, *n*-butylamino, and dimethylamino groups to obtain compounds **3**, **4**, and **5**, respectively.²

The synthesis of light-harvesting antenna systems was carried out from the regioisomerically pure 1,7-dibromoperylene- 3,4,9,10-tetracarboxylic acid derivatives 1,7-dibromoperylene monoimide dibutylester **6**, 1,7-dibromoperylene bisimide **9**, and 1,7-dibromoperylene monoanhydride diester **12**. These perylene derivatives were obtained according to a previously reported procedure.³ For the synthesis of antenna systems **D1A2** and **D2A2** (**Scheme B.2**), the naphthalene derivatives **3** and **4** were separately reacted with regioisomerically pure 1,7-dibromoperylene monoimide diester **6**, (**A2**). This phenoxy substitution reaction was carried out in dry toluene in the presence of K₂CO₃ and 18-crown-6 at 95 and 105 °C to obtain **D1A2** and **D2A2**, respectively, in good yields. The same procedure was followed to synthesize antenna systems **D2A3** and **D3A3** using the naphthalene derivatives **4** and **5**, respectively, and 1,7-dibromoperylene bisimide **9** (**A3**) as shown in **Scheme B.3**.

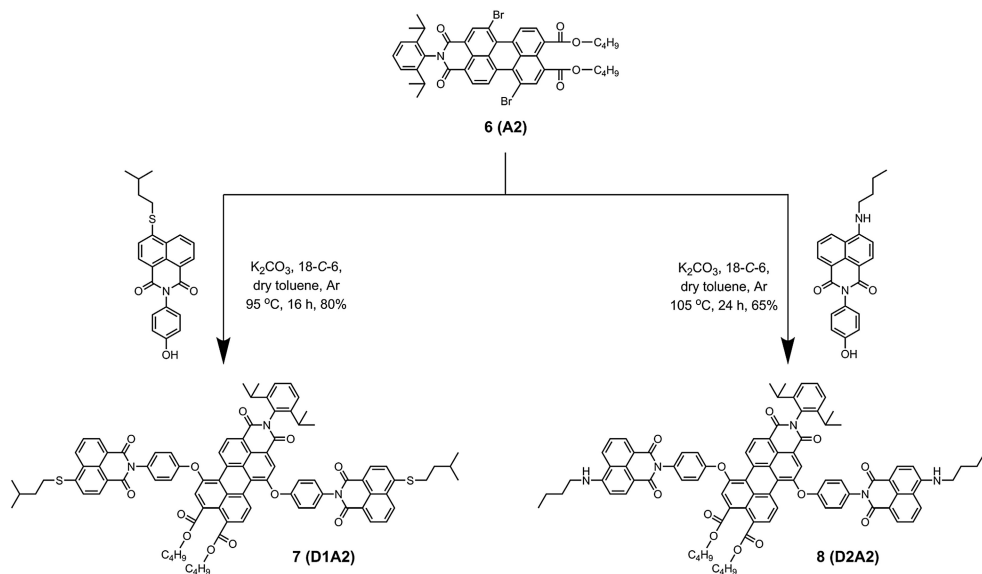
The synthesis of the antenna system **D1A1** was found to be more challenging (**Scheme B.4**). The coupling reaction was first attempted by reacting 1,7-dibromoperylene tetrabutylester **15**, (**A1**) with naphthalene derivative **3**. However, compound **D1A1** was not obtained, not even after employing the harshest possible reaction conditions; refluxing DMF in the presence of Cs₂CO₃. This result can be rationalized based on the fact that perylene tetrabutylester **15** is significantly less electron deficient compared to perylene monoimides and bisimides, due to the absence of strong electron withdrawing imide groups.³ This decreased electron deficiency of the perylene core in **15** reduces its reactivity towards the nucleophilic substitution reaction. Therefore, the synthesis of **D1A1** was carried out using the perylene derivative **12**, which is more reactive than **15** owing to the presence of an electron withdrawing anhydride group. Following this approach, **D1A1** was obtained in two steps. The first step involved the substitution of bromines with **3** in anhydrous NMP at 120 °C to obtain compound **13** in 39% yield. Subsequently, the esterification of the anhydride group yielded the antenna system **D1A1** in 76% yield. The low yield in the first step of this reaction was most likely due to the reaction of the nucleophilic phenol with the anhydride group.

For spectroscopic and electrochemical characterization, reference energy-donor compounds **ref-D1**, **ref-D2**, and **ref-D3**, and reference acceptor compounds **ref-A1**, **ref-A2**, and **ref-A3**, were synthesized (**Figure B.1**). The reference energy-donors were prepared

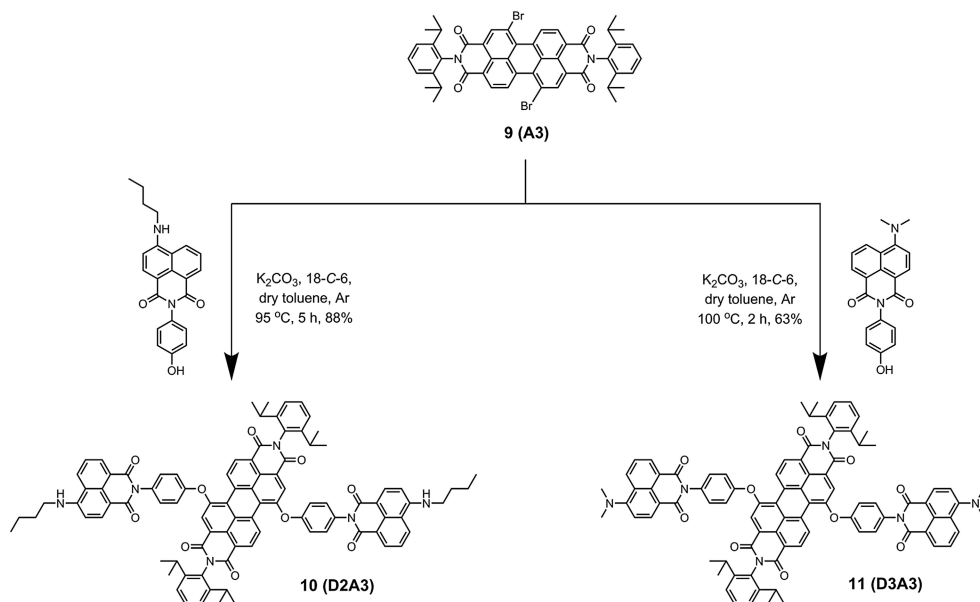
according to the similar procedure as followed for **D1**, **D2**, and **D3**. (In **ref-D1**, a phenyl group instead of a methoxyphenyl group was attached to the naphthylimide. This is the case because the electron-rich methoxyphenyl group strongly quenches the excited state of the 4-isopentylthionaphthalene monoimide.) The synthesis of the reference perylene compounds was achieved according to previously reported procedures.^{3,4}



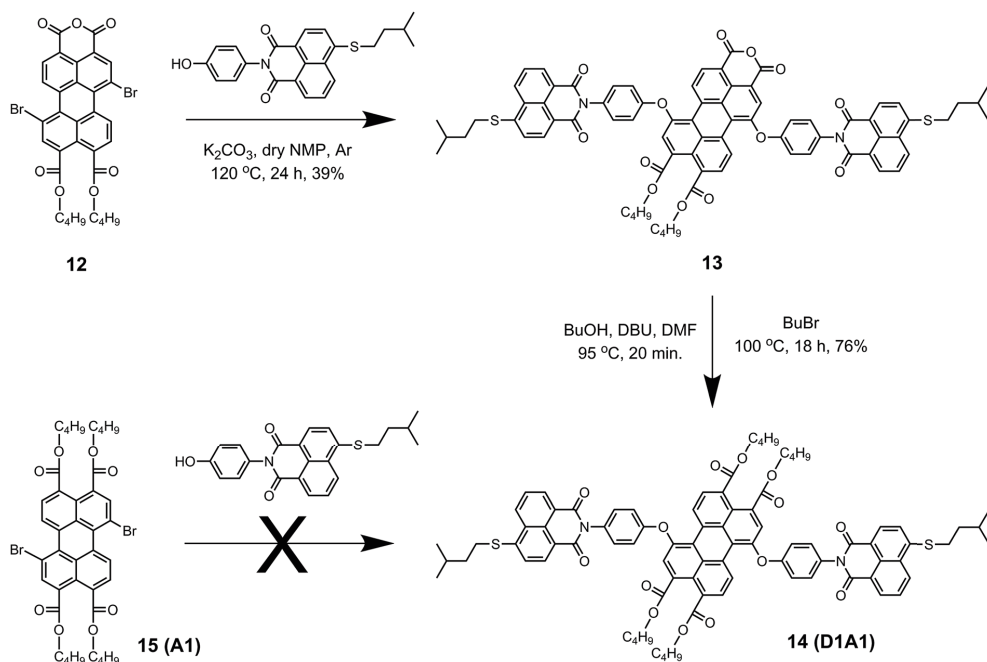
Scheme B. 1 Synthesis of 4-substituted naphthalene monoimide derivatives **D1**, **D2**, and **D3** (3–5).



Scheme B. 2 Synthesis of the antenna systems **D1A2** (7) and **D2A2** (8) from the perylene derivative **6** (**A2**).



Scheme B. 3 Synthesis of antenna systems **D2A3** (10) and **D3A3** (11) from 1,7-dibromoperylene bisimide **9 (A3)**.



Scheme B. 4 Synthesis of the antenna **D1A1**.

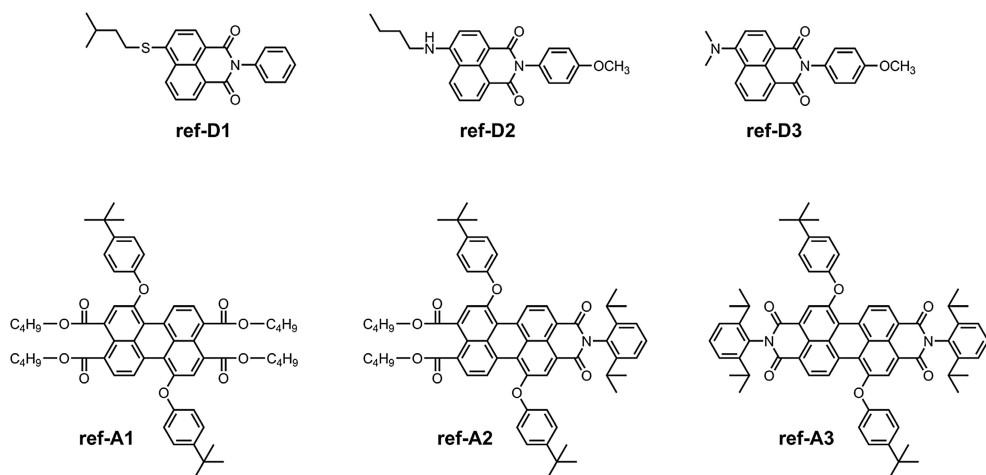


Figure B. 1 Structure of model energy-donors and acceptors used in the spectroscopic and electrochemical studies.

B.2 ^1H NMR analysis of antenna system D2A2

The aromatic region of the ^1H NMR spectrum of **D2A2** was compared with the spectrum of **ref-D2** to obtain information regarding the mutual orientation of the two moieties in the antenna systems (**Figure B.1**). The assignment of the various signals to the naphthalene ring protons was performed with the help of ^1H - ^1H COSY measurements (**Figure B.2**). The perylene core protons are indicated by asterisks. In case of the close-proximity of the two chromophores, the aromatic ring current generated from the perylene moiety will affect the chemical shifts of the proton signals of the naphthalene rings and vice versa.^{5,6} In the antenna system **D2A2**, however, all the naphthalene core protons (H^2 , H^3 , H^5 , H^6 , and H^7) have retained their chemical shift values compared to **ref-D2**. This observation leads to the conclusion that the two chromophores are oriented away from each other and do not experience any through-space interaction. This observation is also indicative of the absence of ground-state interactions between the two chromophores, i.e. the absence of conjugation between them. The same phenomenon was observed for all other antenna systems that we synthesized. Another noteworthy aspect of the NMR spectrum of **D2A2** is the small ~ 0.07 ppm difference in the chemical shift that is observed for all the naphthalene proton resonances. This chemical shift difference reveals that both naphthalene units in compound **D2A2** are inequivalent. For all antenna molecules based on the *centrosymmetric* acceptors **A1** and **A3**, the proton resonances of both naphthalene units are identical and chemical shift differences have not been observed. Finally, it should be noted that the absence of additional resonances in the ^1H NMR spectrum of **D2A2** reflects the high purity of this compound.

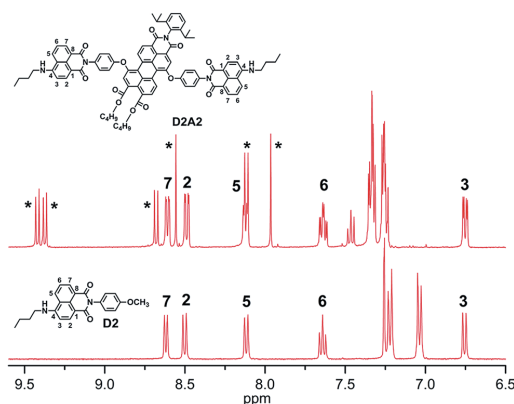


Figure B. 2 Comparison of the ^1H NMR spectra (aromatic regions) of compounds **D2A2** and **ref-D2** in CDCl_3 . The perylene core protons are indicated by asterisks.

B.3 Synthesis Details

Synthesis of N-(4'-hydroxyphenyl)-4-bromonaphthalene-1,8-dicarboxy monoimide (**2**)

A mixture of 4-bromo-1,8-naphthalic anhydride **1** (4.00 g, 14.44 mmol) and 4-aminophenol (1.89 g, 17.24 mmol), in ethanol (120 mL), was refluxed for 18 h. The reaction mixture was filtered after being cooled to room temperature. Thereafter, the residue was washed with ethanol and dried to obtain compound **2** (4.79 g, 13.00 mmol, 90%) as a white solid. ^1H NMR (400 MHz, DMSO-d_6): δ = 9.68 (s, 1H), 8.55 (d, J = 6.4 Hz, 2H), 8.31 (d, J = 7.6 Hz, 1H), 8.22 (d, J = 7.6 Hz, 1H), 8.00 (t, J = 7.6 Hz, 1H), 7.14 (d, J = 8.0 Hz, 2H), 6.87 ppm (d, J = 8.0 Hz, 2H). ^{13}C NMR (100 MHz, DMSO-d_6): δ = 163.8, 163.7, 157.7, 133.0, 132.0, 131.8, 131.3, 130.3, 130.2, 129.5, 129.2, 129.0, 127.0, 123.8, 123.0, 115.9 ppm.

Synthesis of N-(4'-hydroxyphenyl)-4-(isopentylthio) naphthalene-1,8-dicarboxy monoimide (**3**)

N-(4'-Hydroxyphenyl)-4-bromonaphthalene-1,8-dicarboxy monoimide **2** (1.20 g, 3.26 mmol), 3-methyl-1-butanethiol (1.22 mL, 9.78 mmol), and K_2CO_3 (2.03 g, 14.67 mmol) were taken in DMF (40 mL). The reaction mixture was stirred at 80 $^\circ\text{C}$ for 22 h. Afterwards, it was poured into water (200 mL) to precipitate the crude product overnight. The precipitate was filtered off, washed with several portions of water to remove all the residual DMF and 3-methyl-1-butanethiol, and dried in a vacuum oven. Subsequently, it was dissolved in MeOH and filtered to remove insoluble impurities. MeOH was evaporated to afford compound **3** (1.22 g, 3.12 mmol, 96%). ^1H NMR (400 MHz, DMSO-d_6): δ = 9.68 (br. s, 1H), 8.55–8.42 (m, 2H), 8.31 (d, J = 7.6 Hz, 1H), 7.84 (t, J = 7.6 Hz, 1H), 7.71 (d, J = 8.0 Hz, 1H), 7.10 (d, J = 8.4 Hz, 2H), 6.84 (d, J = 8.4 Hz, 2H), 3.23 (t, J = 7.2 Hz, 2H), 1.85–1.73 (m, 1H), 1.60 (q, J = 7.2 Hz, 2H), 0.94 ppm (d, 6.5 Hz, 6H). ^{13}C NMR (100 MHz, DMSO-d_6): δ = 164.1, 164.0, 157.6, 145.1, 131.4, 130.9, 130.3, 130.0, 129.2, 128.3, 127.6, 127.2, 123.7, 123.4, 119.3, 115.8, 37.1, 29.7, 27.6, 22.6 ppm.

Synthesis of N-(4'-hydroxyphenyl)-4-(*n*-butylamino) naphthalene-1,8-dicarboxy monoimide (**4**)

A 50 mL round-bottomed flask was charged with N-(4'-hydroxyphenyl)- 4-

bromonaphthalene-1,8-dicarboxy monoimide **2** (1.00 g, 2.72 mmol), *n*-butylamine (4.02 mL, 40.80 mmol), and DMSO (30 mL). The reaction mixture was stirred at 80°C for 24h and the resultant solution was poured in water (200 mL) to precipitate the crude product. The precipitate was filtered off, washed with several portions of water, and dried in a vacuum oven to afford compound **4** (0.95 g, 2.64 mmol, 97%) as a yellow solid. ¹H NMR (400 MHz, DMSO-*d*₆): δ = 9.60 (s, 1H), 8.75 (d, *J* = 8.4 Hz, 1H), 8.41 (d, *J* = 7.2 Hz, 1H), 8.24 (d, *J* = 8.4 Hz, 1H), 7.79 (t, *J* = 5.2 Hz, 1H), 7.69 (t, *J* = 7.8 Hz, 1H), 7.05 (d, *J* = 8.8 Hz, 2H), 6.84 (d, *J* = 8.8 Hz, 2H), 6.80 (d, *J* = 8.4 Hz, 1H), 3.39 (q, *J* = 6.8 Hz, 2H), 1.75–1.66 (m, 2H), 1.49–1.39 (m, 2H), 0.96 ppm (t, *J* = 7.6 Hz, 3H). ¹³C NMR (100 MHz, DMSO-*d*₆): δ = 163.9, 163.1, 156.6, 150.4, 134.0, 130.4, 129.7, 129.6, 128.5, 127.1, 123.9, 122.1, 120.0, 115.1, 115.0, 107.5, 103.4, 42.3, 29.7, 19.6, 13.5 ppm.

Synthesis of N-(4'-hydroxyphenyl)-4-(dimethylamino) naphthalene-1,8-dicarboxy monoimide (5)

A mixture of N-(4'-methoxyphenyl)-4-bromonaphthalene-1,8-dicarboxy monoimide **2** (0.50 g, 1.36 mmol), 3-(dimethylamino) propionitrile (0.62 mL, 5.43 mmol), and DMSO (15 mL) was stirred at 132 °C overnight. After cooling down to room temperature, the resultant mixture was poured in water (200 mL) to precipitate the crude product. The precipitate was filtered off, washed with several portions of water, and dried. Subsequently, it was refluxed in MeOH (50 mL), filtered off after cooling, and dried to get compound **5** (0.32 g, 0.96 mmol, 71%) as a dark yellow solid. ¹H NMR (400 MHz, DMSO-*d*₆): δ = 9.59 (br. s, 1H), 8.50 (d, *J* = 8.4 Hz, 1H), 8.40 (d, *J* = 7.2 Hz, 1H), 8.28 (d, *J* = 8.4 Hz, 1H), 7.72 (t, *J* = 7.6 Hz, 1H), 7.16 (d, *J* = 8.4 Hz, 1H), 7.01 (d, *J* = 8.4 Hz, 2H), 6.83 (d, *J* = 8.4 Hz, 2H), 3.39 ppm (s, 6H). ¹³C NMR spectrum could not be measured because of the low solubility of the compound.

Synthesis of N-(2',6'-diisopropylphenyl)-1,7-bis[N'-(*p*-phenyloxy)-(4''-isopentylthio-*r*'',8''-dicarboxy naphthalene monoimide)]perylene-3,4,9,10-tetracarboxy monoimide dibutylester (7**, D1A2)**

A mixture of compound **3** (70 mg, 0.18 mmol), K₂CO₃ (50 mg, 0.36 mmol), and 18-crown-6 (95 mg, 0.36 mmol), in dry toluene (30 mL), was stirred for 45 minutes at room temperature under an argon atmosphere. Subsequently, 1,7-dibromoperylene monoimide dibutylester (**6**, A2) (50 mg, 0.06 mmol) was added. Thereafter, the reaction mixture was stirred for 16 h at 95 °C under an argon atmosphere. After being cooled to room temperature, the solvent was removed by rotary evaporation. The residue was washed with ethanol and water, and dried. The crude product was purified using column chromatography (silica-60/CHCl₃) to afford the antenna system **D1A2** (70 mg, 0.05 mmol, 80%). ¹H NMR (400 MHz, CDCl₃): δ = 9.41 (d, *J* = 8.0 Hz, 1H), 9.37 (d, *J* = 8.0 Hz, 1H), 8.68 (d, *J* = 8.0 Hz, 1H), 8.67–8.60 (m, 4H), 8.56 (s, 1H), 8.51 (dd, *J* = 8.0 and 1.2 Hz, 2H), 8.12 (d, *J* = 8.0 Hz, 1H), 7.97 (s, 1H), 7.80–7.75 (m, 2H), 7.56 (dd, *J* = 8.0 and 2.4 Hz, 2H), 7.50–7.44 (m, 1H), 7.37–7.31 (m, 6H), 7.29–7.24 (m, 4H), 4.38–4.31 (m, 4H), 3.22–3.14 (m, 4H), 2.80–2.72 (m, 2H), 1.89–1.76 (m, 6H), 1.75–1.67 (m, 4H), 1.54–1.41 (m, 4H), 1.20–1.14 (m, 12H), 1.06–0.85 ppm (m, 18H). ¹³C NMR (100 MHz, CDCl₃): δ = 168.26, 167.45, 164.21, 163.54, 162.82, 155.78, 155.69, 152.49, 152.31, 146.37, 146.29, 145.73, 133.99, 133.19, 131.99, 131.24, 131.07, 130.65, 130.58, 129.71, 129.61, 128.63, 128.57, 128.14, 126.75, 126.69, 126.63, 126.44, 125.59, 125.33, 123.99, 123.27, 123.10, 122.49, 121.59, 118.80, 118.65, 118.56, 65.88, 65.55, 37.09, 30.64, 30.48,

30.29, 29.13, 27.69, 24.06, 22.25, 19.29, 19.21, 13.82 ppm. MS (ESI-TOF): [M]⁺ calculated for C₉₀H₈₁N₃O₁₂S₂, 1459.52616; found, 1459.53383.

Synthesis of N-(2',6'-diisopropylphenyl)-1,7-bis[N'-(*p*-phenyloxy)-(4''-butylamino-*r''*,8''-dicarboxy naphthalene monoimide)]perylene-3,4,9,10-tetracarboxy monoimide dibutylester (8, D2A2)

Compound 4 (70 mg, 0.19 mmol), K₂CO₃ (50 mg, 0.36 mmol), and 18-crown-6 (126 mg, 0.48 mmol) were taken in dry toluene (85 mL). The resultant mixture was stirred at room temperature for 20 minutes and subsequently at 50 °C for another 20 minutes under an argon atmosphere. Afterwards, 1,7-dibromoperylene monoimide dibutylester (**6**, **A2**) (50 mg, 0.06 mmol) was added and the reaction mixture was stirred for 24 h at 105 °C under an argon atmosphere. After being cooled to room temperature, the solvent was removed by rotary evaporation. The residue was washed with methanol and water. The dried residue was refluxed in MeOH (100 mL) and filtered off after cooling down to room temperature. Finally, the crude product was purified using column chromatography (silica-60/DCM, CHCl₃) to afford the antenna system **D2A2** (55 mg, 0.04 mmol, 65%). ¹H NMR (400 MHz, CDCl₃): δ = 9.42 (d, J = 8.4 Hz, 1H), 9.37 (d, J = 8.0 Hz, 1H), 8.68 (d, J = 8.0 Hz, 1H), 8.61 (d, J = 7.2 Hz, 2H), 8.56 (s, 1H), 8.48 (d, J = 8.8 Hz, 2H), 8.15–8.09 (m, 3H), 7.97 (s, 1H), 7.67–7.60 (m, 2H), 7.46 (t, J = 8.0 Hz, 1H), 7.38–7.24 (m, 7H), 6.75 (dd, J = 8.4 and 2.8 Hz, 2H), 5.35–5.28 (m, 2H), 4.38–4.30 (m, 4H), 3.46–3.38 (m, 4H), 2.80–2.71 (m, 2H), 1.86–1.74 (m, 8H), 1.58–1.40 (m, 8H), 1.20–1.15 (m, 12H), 1.09–0.80 ppm (m, 12H). ¹³C NMR (100 MHz, CDCl₃): δ = 168.31, 167.49, 164.85, 164.19, 163.61, 162.91, 155.52, 155.39, 152.66, 152.49, 149.91, 145.78, 134.99, 133.14, 132.04, 131.78, 131.56, 131.26, 131.15, 130.78, 130.72, 130.56, 130.26, 129.69, 129.48, 129.40, 128.57, 128.12, 126.69, 126.60, 126.40, 126.36, 125.50, 125.26, 124.66, 123.98, 123.17, 123.09, 122.66, 121.51, 120.25, 118.64, 118.53, 109.76, 104.40, 65.90, 65.56, 43.42, 30.93, 30.64, 30.48, 29.13, 24.07, 20.33, 19.30, 19.21, 13.86, 13.83 ppm. MS (ESITOF): [M]⁺ calculated for C₈₈H₇₉N₅O₁₂, 1397.63271; found, 1397.61057.

Synthesis of N,N'-bis(2',6'-diisopropylphenyl)-1,7-bis[N'-(*p*-phenyloxy)-(4''-butylamino-*r''*,8''-dicarboxy naphthalene monoimide)]perylene-3,4,9,10-tetracarboxy bisimide (10, D2A3)

In a dry 100 mL round-bottom flask, weighed amounts of compound 4 (58 mg, 0.16 mmol), K₂CO₃ (38 mg, 0.28 mmol), and 18-crown-6 (74 mg, 0.28 mmol) were taken. Subsequently, anhydrous toluene (50 mL) was added. The reaction mixture was stirred for 15 min at room temperature and subsequently at 50 °C for another 15 min under an argon atmosphere. Thereafter 1,7-dibromoperylene bisimide (**9**, **A3**) (40 mg, 0.05 mmol) was added and the reaction mixture was stirred at 95 °C for 5 h. After being cooled to room temperature, the solvent was removed by rotary evaporation and the residue was washed with MeOH and water. The dried residue was refluxed in ethanol (200 mL) and filtered off to remove any unreacted compound 4. Finally, column chromatography (silica-60/1 : 1 DCM–CHCl₃) was performed to afford the desired antenna system **D2A3** (58 mg, 0.04 mmol, 88%). ¹H NMR (400 MHz, CDCl₃): δ = 9.65 (d, J = 8.4 Hz, 2H), 8.75 (d, J = 8.0 Hz, 2H), 8.63 (s, 2H), 8.60 (d, J = 7.2 Hz, 2H), 8.48 (d, J = 8.4 Hz, 2H), 8.11 (d, J = 8.4 Hz, 2H), 7.63 (t, J = 7.6 Hz, 2H),

7.48 (t, $J=7.6$ Hz, 2H), 7.35 (t, $J=8.8$ Hz, 7H), 7.28 (m, 5H), 6.74 (d, $J=8.4$ Hz, 2H), 5.33 (s, 2H), 3.46–3.37 (m, 4H), 2.82–2.71 (m, 4H), 1.85–1.75 (m, 4H), 1.55–1.49 (m, 4H), 1.23–1.16 (m, 24H), 1.02 ppm (t, $J=7.2$ Hz, 6H). ^{13}C NMR (100 MHz, CDCl_3): δ = 164.83, 164.16, 163.34, 162.65, 155.25, 153.82, 149.83, 145.72, 135.03, 133.47, 132.00, 131.61, 131.32, 130.87, 130.44, 130.25, 129.70, 129.61, 129.22, 126.71, 126.56, 126.26, 125.87, 124.72, 124.42, 124.05, 123.12, 122.66, 120.23, 118.45, 109.84, 104.45, 43.43, 30.98, 29.18, 24.08, 20.33, 13.85 ppm. MS (ESI-TOF): $[\text{M}]^+$ calculated for $\text{C}_{92}\text{H}_{78}\text{N}_6\text{O}_{10}$, 1426.57794; found, 1426.58144.

Synthesis of N,N'-bis(2',6'-diisopropylphenyl)-1,7-bis[N'-(*p*-phenyloxy)-(4''-dimethylamino-*r''*,8''-dicarboxy naphthalene monoimide)]perylene-3,4,9,10-tetracarboxy bisimide (II, D3A3)

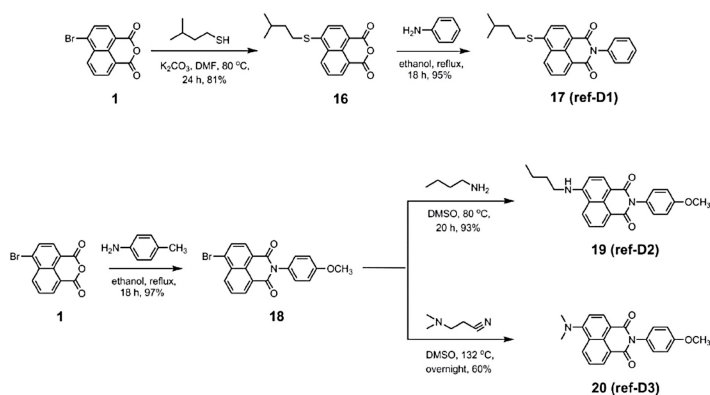
Weighed amounts of compound **5** (52 mg, 0.16 mmol), K_2CO_3 (40 mg, 0.29 mmol), and 18-crown-6 (77 mg, 0.29 mmol) were taken in anhydrous toluene (50 mL). The mixture was stirred for 20 min at room temperature and, thereafter, 1,7-dibromoperylene bisimide (**9**, A3) (40 mg, 0.05 mmol) was added. The reaction mixture was stirred at 100 °C for 2 h. After being cooled to room temperature, the solvent was removed by rotary evaporation and the residue was washed with MeOH and water. The dried residue was refluxed in methanol (150 mL) and filtered off to remove any unreacted compound **5** and other soluble impurities. Finally, column chromatography (silica-60/ CHCl_3) was performed to afford the desired antenna system **D3A3** (40 mg, 0.03 mmol, 63%). ^1H NMR (400 MHz, CDCl_3): δ = 9.65 (d, J = 8.0 Hz, 2H), 8.75 (d, J = 8.4 Hz, 2H), 8.63 (s, 2H), 8.59 (d, J = 7.2 Hz, 2H), 8.49 (t, J = 7.6 Hz, 4H), 7.68 (t, J = 7.6 Hz, 2H), 7.48 (t, J = 8.0 Hz, 2H), 7.40–7.26 (m, 12H), 7.13 (d, J = 8.0 Hz, 2H), 3.13 (s, 12H), 2.82–2.70 (m, 4H), 1.25–1.14 ppm (m, 24H). ^{13}C NMR (100 MHz, CDCl_3): δ = 164.75, 164.14, 163.31, 162.61, 157.32, 155.37, 153.73, 145.70, 133.43, 133.16, 131.71, 131.67, 131.53, 131.33, 130.82, 130.66, 130.42, 129.70, 129.61, 129.21, 126.76, 126.59, 125.91, 125.28, 124.92, 124.46, 124.05, 123.04, 122.70, 118.48, 114.65, 113.31, 44.76, 29.18, 24.07 ppm. MS (ESITOF): $[\text{M}]^+$ calculated for $\text{C}_{88}\text{H}_{70}\text{N}_6\text{O}_{10}$, 1370.51534; found, 1370.51784.

Synthesis of 1,7-bis[N'-(*p*-phenyloxy)-(4''-isopentylthio-*r''*,8''-dicarboxy naphthalene monoimide)]perylene-3,4,9,10-tetracarboxy tetrabutylester (14, D1A1)

The antenna system **D1A1** was synthesized in the following two steps: (i) a mixture of 1,7-dibromoperylene monoanhydride dibutylester **12** (100 mg, 0.15 mmol), compound **3** (200 mg, 0.51 mmol), and K_2CO_3 (100 mg, 0.72 mmol), in anhydrous NMP (20 mL), was stirred at 120 °C for 24 h under an argon atmosphere. The resultant mixture was poured into water (200 mL) to precipitate the crude product. The precipitate was filtered off and washed with several portions of water. The dried residue was refluxed in ethanol (150 mL) and filtered off to remove any unreacted compound **3** and other soluble impurities. Product **13** (75 mg, 39%) was used as such in the next step without NMR characterization due to its low solubility. (ii) Compound **13** (75 mg, 0.06 mmol), butanol (200 μL , 2.19 mmol), and DBU (200 μL , 1.34 mmol) were stirred in DMF (20 mL) for 20 min at 95 °C. Thereafter, butylbromide (200 μL , 1.85 mmol) was added and the reaction mixture was stirred at 100 °C for 18 h. The resultant mixture was poured into water (200 mL) to precipitate the crude product. The precipitate was filtered off, and washed with several portions of water. The dried residue was refluxed in

methanol (100 mL) and filtered off (after cooling) to remove the soluble impurities. The process was repeated two times. Finally, silica gel column chromatography was performed on the crude product. Impurities were removed by eluting with DCM and the pure antenna system **D1A1** (63 mg, 0.044 mmol, 76%) was achieved. ^1H NMR (400 MHz, CDCl_3): δ = 9.07 (d, J = 8.4 Hz, 2H), 8.65 (d, J = 7.2 Hz, 2H), 8.61 (d, J = 8.8 Hz, 2H), 8.50 (d, J = 7.6 Hz, 2H), 8.05 (d, J = 8.4 Hz, 2H), 7.89 (s, 2H), 7.77 (t, J = 8.4 Hz, 2H), 7.56 (d, J = 8.0 Hz, 2H), 7.31 (d, J = 8.8 Hz, 4H), 7.22 (d, J = 8.8 Hz, 4H), 4.37–4.26 (m, 8H), 3.18 (t, J = 7.6 Hz, 4H), 1.87–1.66 (m, 14H), 1.55–1.39 (m, 8H), 1.05–0.94 ppm (m, 24H). ^{13}C NMR (100 MHz, CDCl_3): δ = 168.4, 167.6, 164.2, 164.1, 156.0, 150.9, 146.2, 131.9, 131.8, 131.2, 130.9, 130.8, 130.5, 129.9, 129.6, 129.5, 128.6, 127.4, 126.6, 125.3, 125.2, 123.5, 123.2, 122.5, 118.9, 118.6, 65.6, 65.3, 37.1, 30.6, 30.5, 30.3, 27.7, 22.2, 19.3, 19.2, 13.8 ppm. MS (ESI-TOF): $[\text{M}]^+$ calculated for $\text{C}_{86}\text{H}_{82}\text{N}_2\text{O}_{14}\text{S}_2$, 1430.52074; found, 1430.53751.

Syntheses and Characterization of Model Donors:



Scheme B. 5 Synthesis of naphthalene monoimide derivatives used as model-donors in the spectroscopic and electrochemical studies (**ref-D1**, **ref-D2**, and **ref-D3**).

(i) Synthesis of 4-(isopentylthio)naphthalene-1,8-dicarboxy Monoanhydride (**16**):

Synthesized from 4-bromo-1,8-naphthalic anhydride **1** (1.00 g, 3.61 mmol) and 3-methyl-1-butanethiol (1.35 mL, 10.83 mmol), K_2CO_3 (2.25 g, 16.25 mmol), and DMF (12 mL). The reaction mixture was stirred at 80 °C for 24 h. Afterwards, it was poured into the water (200 mL) to precipitate the crude product overnight. The precipitate was filtered off, washed with several portions of water to remove all the residual DMF and 3-methyl-1-butanethiol, and dried in vacuum oven. Subsequently, it was dissolved in chloroform and filtered to remove insoluble impurities. Chloroform was evaporated to afford the product **16** (0.88 g, 81%). ^1H NMR (400 MHz, CDCl_3): δ = 8.59 (t, J = 8.0 Hz, 2H), 8.44 (d, J = 7.6 Hz, 1H), 7.76 (t, J = 7.6 Hz, 1H), 7.51 (d, J = 8.0 Hz, 1H), 3.18 (t, J = 7.6 Hz, 2H), 1.89–1.78 (m, 1H), 1.76–1.68 (m, 2H), 1.00 ppm (d, J = 6.8 Hz, 6H).

(ii) Synthesis of N-phenyl-4-(isopentylthio)naphthalene-1,8-dicarboxy Monoimide (**17**):

Synthesized in a similar manner as compound **2** from 4-(isopentylthio)naphthalene-1,8-

dicarboxy Monoanhydride **16** (0.50 g, 1.66 mmol), aniline (0.19 g, 1.99 mmol), and ethanol (15 mL). The crude product was purified by column chromatography (silica-60/CHCl₃) to afford the compound **17** (0.59 g, 95%). ¹H NMR (400 MHz, CDCl₃): δ = 8.65 (d, J = 7.20 Hz, 1H), 8.61 (d, J = 8.4 Hz, 1H), 8.51 (d, J = 7.6 Hz, 1H), 7.77 (t, J = 8.4 Hz, 1H), 7.55 (m, 3H), 7.48 (d, J = 7.2 Hz, 1H), 7.31 (d, J = 6.8 Hz, 2H), 3.18 (t, J = 7.6 Hz, 2H), 1.82 (septet, 1H), 1.72 (q, J = 7.2 Hz, 2H), 1.00 (d, J = 6.4 Hz, 6H). ¹³C NMR (100 MHz, CDCl₃): δ = 164.2, 146.1, 135.4, 131.9, 131.1, 130.4, 129.6, 129.3, 128.7, 128.6, 126.6, 123.2, 122.6, 119.0, 37.1, 30.3, 27.7, 22.2 ppm.

(iii) Synthesis of N-(4'-Methoxyphenyl)-4-bromonaphthalene-1,8-dicarboxy Monoimide (18):

Synthesized in a similar manner as compound **2** from 4-bromo-1,8-naphthalic anhydride **1** (2.00 g, 7.22 mmol) and 4-methoxyaniline (1.07 g, 8.69 mmol) to afford compound **18** (2.68 g, 97%) as a white solid. ¹H NMR (400 MHz, DMSO-d₆): δ = 8.60 (t, J = 8.8 Hz, 2H), 8.34 (d, J = 8.0 Hz, 1H), 8.26 (d, J = 8.0 Hz, 1H), 8.04 (t, J = 8.0 Hz, 1H), 7.29 (d, J = 8.8 Hz, 2H), 7.06 (d, J = 8.8 Hz, 2H), 3.83 ppm (s, 3H). ¹³C NMR (100 MHz, DMSO-d₆): δ = 163.8, 163.7, 159.4, 133.1, 132.0, 131.8, 131.4, 130.4, 129.5, 129.3, 129.2, 128.6, 123.9, 123.2, 114.6, 55.8 ppm.

(iv) Synthesis of N-(4'-Methoxyphenyl)-4-(n-butylamino)naphthalene-1,8-dicarboxy Monoimide (19):

Synthesized as per the procedure followed for compound **4** from N-(4'-methoxyphenyl)-4-bromonaphthalene-1,8-dicarboxy Monoimide **18** (0.30 g, 0.79 mmol), n-butylamine (1.17 mL, 11.80 mmol), and DMSO (24 mL). The crude product was purified by column chromatography (silica-60/1:1 CHCl₃-EtOAc) to obtain compound **19** (0.27 g, 93%) as yellow solid. ¹H NMR (400 MHz, DMSO-d₆): δ = 8.72 (d, J = 8.4 Hz, 1H), 8.40 (d, J = 7.6 Hz, 1H), 8.23 (d, J = 8.4 Hz, 1H), 7.75 (t, J = 5.2 Hz, 1H), 7.67 (t, J = 7.6 Hz, 1H), 7.18 (d, J = 8.8 Hz, 2H), 7.01 (d, J = 8.8 Hz, 2H), 6.77 (d, J = 8.4 Hz, 1H), 3.80 (s, 3H), 3.36 (q, J = 6.4 Hz, 2H), 1.69 (m, 2H), 1.42 (m, 2H), 0.94 ppm (t, J = 7.6 Hz, 3H). ¹³C NMR (100 MHz, DMSO-d₆): δ = 164.6, 163.8, 159.1, 151.2, 134.7, 131.2, 130.6, 129.5, 129.1, 124.6, 122.8, 120.7, 114.4, 108.3, 104.2, 55.8, 43.1, 30.4, 20.3, 14.2 ppm.

(v) Synthesis of N-(4'-Methoxyphenyl)-4-(dimethylamino)naphthalene-1,8-dicarboxy Monoimide (20):

Synthesized as per the procedure followed for compound **5** from N-(4'-methoxyphenyl)-4-bromonaphthalene-1,8-dicarboxy monoimide **18** (0.30 g, 0.79 mmol), 3-(dimethylamino)propionitrile (0.35 mL, 3.14 mmol), and DMSO (25 mL). The crude product was purified by column chromatography (silica-60/CHCl₃) to obtain compound **20** (0.16 g, 60%). ¹H NMR (400 MHz, CDCl₃): δ = 8.61 (d, J = 7.2 Hz, 1H), 8.50 (t, J = 8.4 Hz, 2H), 7.69 (t, J = 7.2 Hz, 1H), 7.22 (d, J = 7.6 Hz, 2H), 7.14 (d, J = 8.0 Hz, 1H), 7.05 (d, J = 7.6 Hz, 2H), 3.87 (s, 3H), 3.13 ppm (s, 6H). ¹³C NMR (100 MHz, CDCl₃): δ = 164.9, 164.4, 159.4, 157.1, 132.9, 131.4, 131.3, 129.6, 128.3, 125.4, 124.9, 123.3, 115.1, 114.6, 113.3, 55.5, 44.8 ppm.

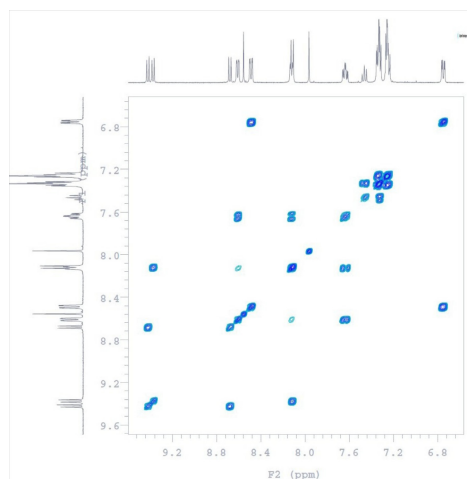


Figure B. 3 ^1H – ^1H COSY spectrum of antenna **D2A2** in CDCl_3 .

B.4 Cyclic Voltammetry

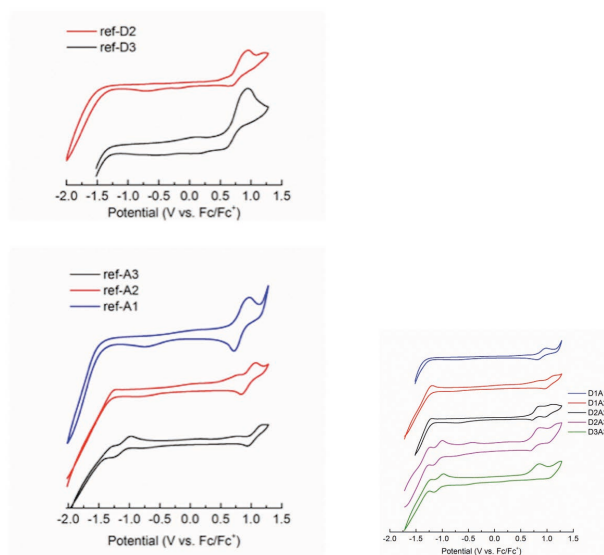


Figure B. 4 Cyclic voltammograms of the model compounds and antenna systems.

Note: No redox activity was observed for **ref-D1** in the measured potential window. **ref-D2** and **ref-D3** did not exhibit any reduction peak. For **ref-A2**, a very small irreversible reduction peak was obtained at ca. -1.30 V. No reduction peak was observed for **ref-A1**.

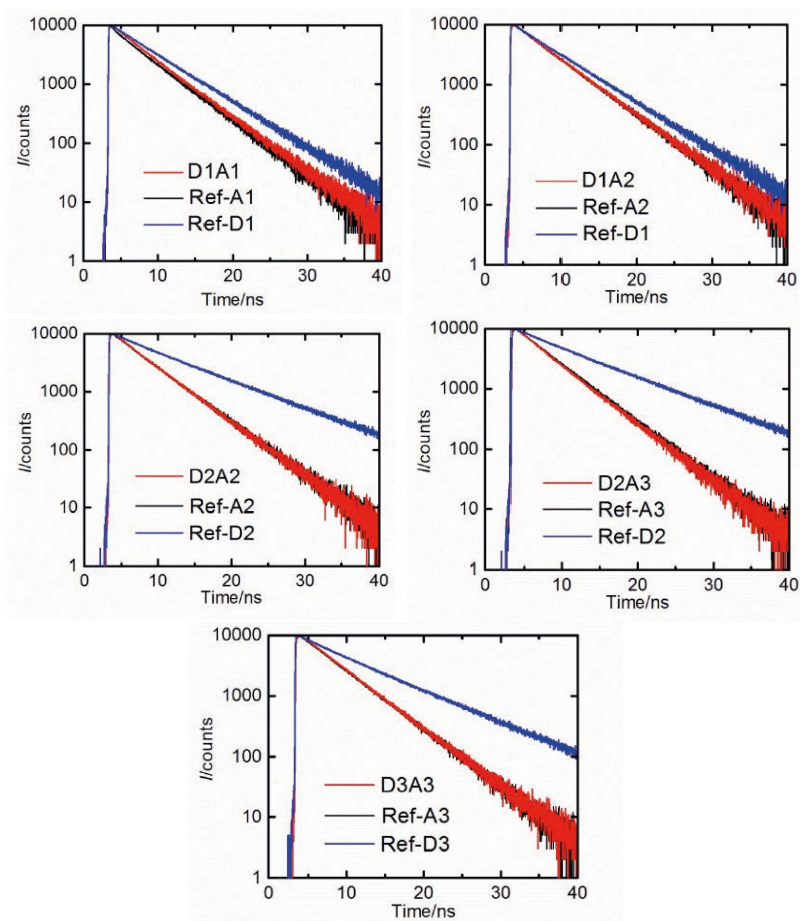
B.5 Extra Experimental Data

Figure B. 5 Fluorescence decay curves of antenna systems and respective reference compounds in toluene after excitation at 400 nm.

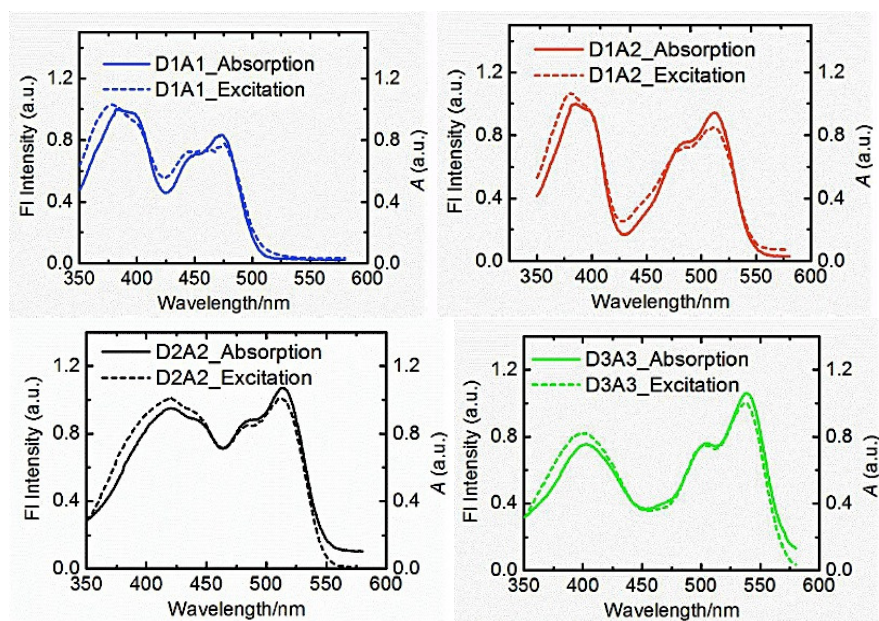
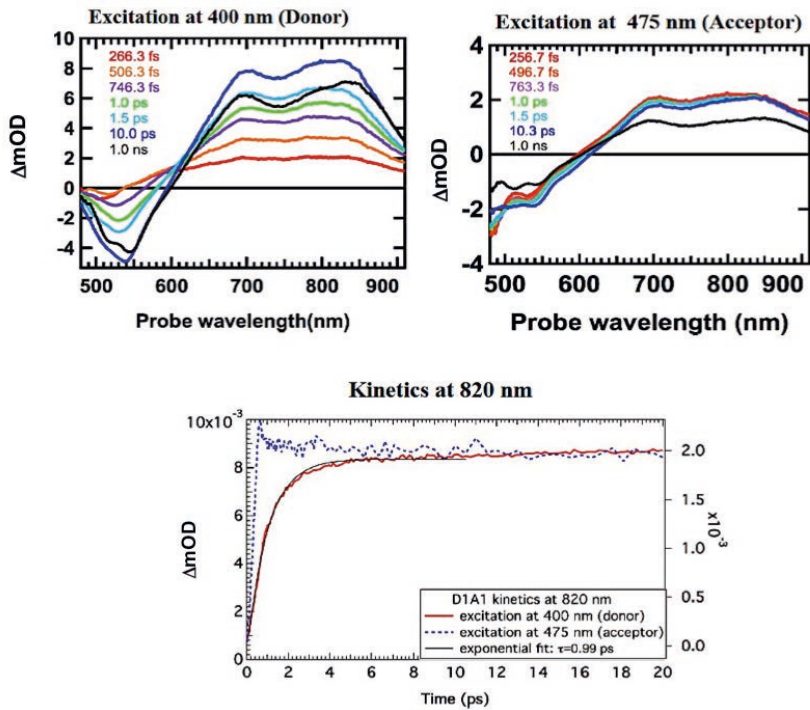


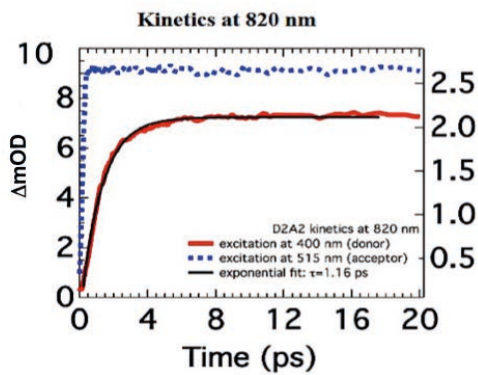
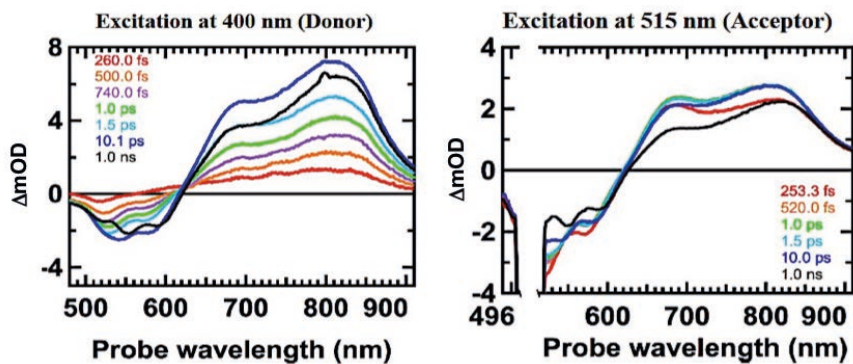
Figure B. 6 Comparison of absorption and emission spectra of antenna systems in toluene.

Figure B. 7 Transient absorption spectra of antenna systems in toluene and their decay kinetics at 820 nm.

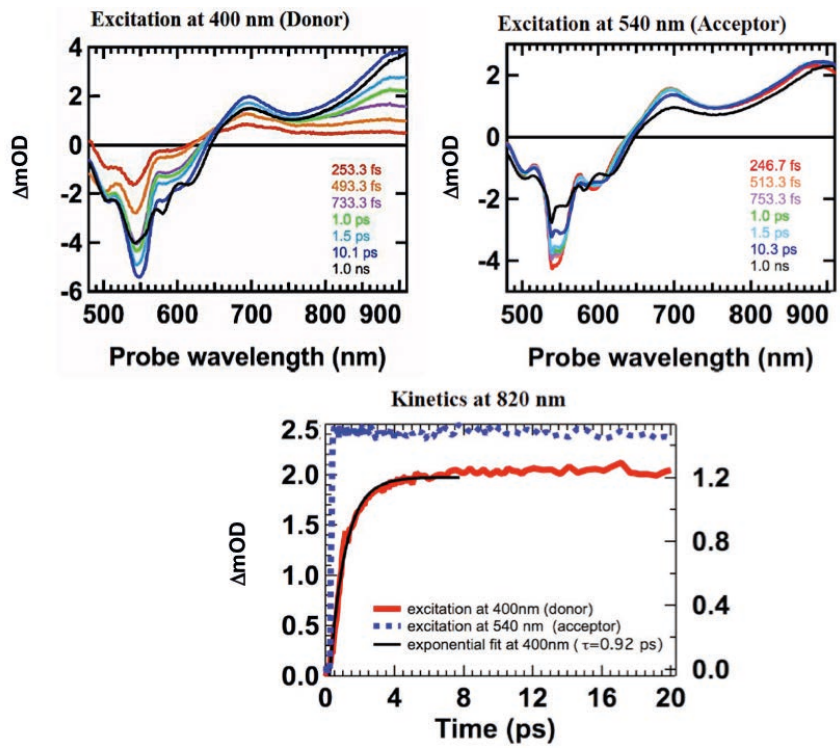
(i) D1A1



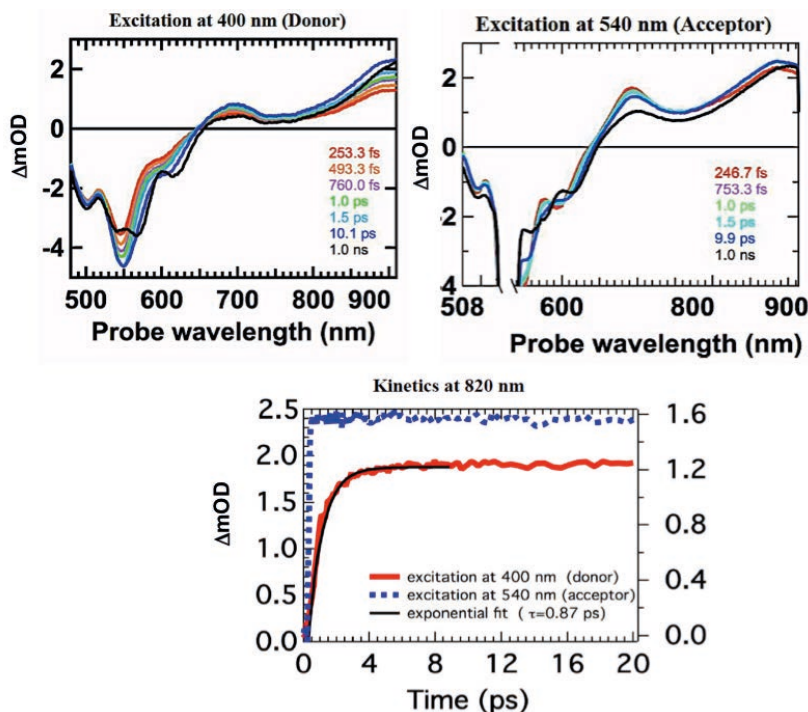
(ii) D2A2



(iii) D2A3



(iv) D3A3

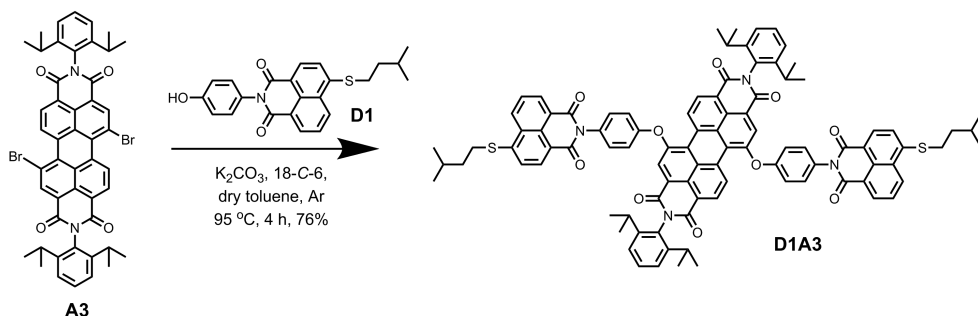


B.6 References

- (1) Bamesberger, A.; Schwartz, C.; Song, Q.; Han, W.; Wang, Z.; Cao, H., Rational design of a rapid fluorescent approach for detection of inorganic fluoride in MeCN-H₂O: a new fluorescence switch based on N-aryl-1,8-naphthalimide. *New Journal of Chemistry* **2014**, *38* (3), 884-888.
- (2) Kollár, J.; Hrdlovič, P.; Chmela, Š.; Sarakha, M.; Guyot, G., Synthesis and transient absorption spectra of derivatives of 1,8-naphthalic anhydrides and naphthalimides containing 2,2,6,6-tetramethylpiperidine; triplet route of deactivation. *Journal of Photochemistry and Photobiology A: Chemistry* **2005**, *170* (2), 151-159.
- (3) Sengupta, S.; Dubey, R. K.; Hoek, R. W. M.; van Eeden, S. P. P.; Gunbaş, D. D.; Grozema, F. C.; Sudhölter, E. J. R.; Jager, W. F., Synthesis of Regioisomerically Pure 1,7-Dibromoperylene-3,4,9,10-tetracarboxylic Acid Derivatives. *The Journal of Organic Chemistry* **2014**, *79* (14), 6655-6662.
- (4) Dubey, R. K.; Efimov, A.; Lemmetyinen, H., 1,7- And 1,6-Regioisomers of Diphenoxo and Dipyrrolidinyl Substituted Perylene Diimides: Synthesis, Separation, Characterization, and Comparison of Electrochemical and Optical Properties. *Chemistry of Materials* **2011**, *23* (3), 778-788.
- (5) Dubey Rajeev, K.; Niemi, M.; Kaunisto, K.; Efimov, A.; Tkachenko Nikolai, V.; Lemmetyinen, H., Direct Evidence of Significantly Different Chemical Behavior and Excited-State Dynamics of 1,7- and 1,6-Regioisomers of Pyrrolidinyl-Substituted Perylene Diimide. *Chemistry A European Journal* **2013**, *19* (21), 6791-6806.
- (6) Dubey Rajeev, K.; Kumpulainen, T.; Efimov, A.; Tkachenko Nikolai, V.; Lemmetyinen, H., Close Proximity Dibenzo[a,c]phenazine-Fullerene Dyad: Synthesis and Photoinduced Singlet Energy Transfer. *European Journal of Organic Chemistry* **2010**, *2010* (18), 3428-3436.

C ● Appendix for Chapter 4

C.1 Synthesis and Characterization D1A3



N-(4'-Hydroxyphenyl)-4-(isopentylthio)naphthalene-1,8-dicarboxy Monoimide (**D1**) (55 mg, 0.14 mmol), K_2CO_3 (38 mg, 0.28 mmol), and 18-Crown-6 (73 mg, 0.28 mmol) were taken in anhydrous toluene (50 mL). The resultant mixture was stirred at room temperature for 20 minutes under argon atmosphere. Subsequently, 1-7-dibromoperylene bisimide (**A3**) (40 mg, 0.05 mmol) was added and the reaction mixture was stirred for 4 h at 95 °C. The progress of the reaction was monitored by TLC analysis. After being cooled to room temperature, the solution was washed with water. Organic phase was collected and toluene was removed by rotary evaporation. Finally, the crude product was purified by silica gel column chromatography (first with 1:1 DCM- $CHCl_3$ and then with $CHCl_3$) to afford the antenna system **D1A3** (52 mg, 76%). 1H NMR (400 MHz, $CDCl_3$): δ = 9.64 (d, J = 8.0 Hz, 2H), 8.75 (d, J = 8.0 Hz, 2H), 8.66–8.58 (m, 6H), 8.49 (d, J = 8.0 Hz, 2H), 7.76 (t, J = 8.4 Hz, 2H), 7.55 (d, J = 8.0 Hz, 2H), 7.48 (t, J = 8.0 Hz, 2H), 7.38–7.32 (m, 8H), 7.28 (d, J = 8.8 Hz, 4H), 3.17 (t, J = 7.6 Hz, 4H), 2.80–2.71 (m, 4H), 1.88–1.77 (m, 2H), 1.70 (q, J = 8.0 Hz, 4H), 1.20–1.14 (m, 24H), 0.98 ppm (d, J = 6.8 Hz, 12H). ^{13}C NMR (100 MHz, $CDCl_3$): δ = 164.187, 163.290, 162.605, 155.473, 153.688, 146.408, 145.679, 133.400, 131.996, 131.355, 131.327, 131.255, 130.772, 130.513, 130.392, 129.694, 129.620, 129.587, 129.206, 128.617, 126.681, 126.628, 126.582, 125.875, 124.466, 124.045, 123.051, 122.712, 122.481, 118.746, 118.549, 37.078, 30.285, 29.174, 27.671, 24.058, 22.230.

C.2 Structure of Model Compounds

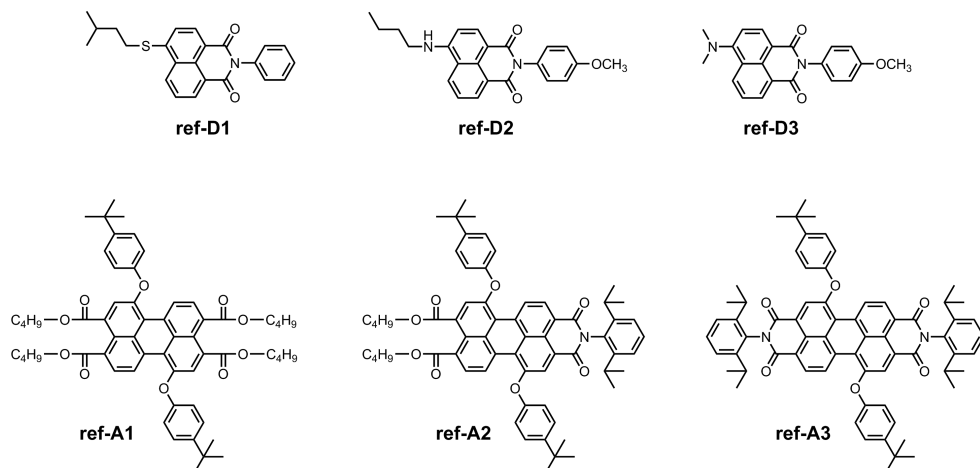


Figure C. 1 Structure of model naphthalene and model perylene compounds used in the spectroscopic studies.

C.3 Energies of Charge Separation from Excited Donor

Table C. 1 Energies of charge separation from the excited donor, calculated using **Equation C.1**.

Comp	Naphthalimide		Perylene		$\Delta G^{\circ}_{CS^c}$ In DCM (eV)
	$E_{1/2\text{ ox}}^a$	E_{SI}^b (eV)	$E_{1/2\text{ red}}^a$	E_{SI}^c (eV)	
D1A1	+1.20 ^d	2.80	−1.55 ^e	2.41	0.09
D1A2	+1.20 ^d	2.80	−1.34	2.37	−0.08
D1A3	+1.20 ^d	2.80	−1.08	2.15	−0.12
D2A2	+0.80	2.60	−1.33	2.35	−0.48
D2A3	+0.79	2.58	−1.09	2.15	−0.52
D3A3	+0.74	2.58	−1.07	2.15	−0.57

^a Scan rate 0.10 V/s. ^b Energy of the first singlet excited-state from absorption and emission measurements. ^c Driving force for charge separation with respect to perylene singlet excited-state, according to Equation 4.1. ^d Calculated oxidation potential. No oxidation signal was detected in the measured potential window. ^e Value taken from compound A1.

C.4 Equations for Fluorescence Quenching

$$k_F = \frac{\phi_F}{\tau_F} \quad k_{nr} = \frac{k_F}{\phi_F} - k_F \quad (\text{C.1})$$

C.5 Steady State Absorption and Emission in Chloroform

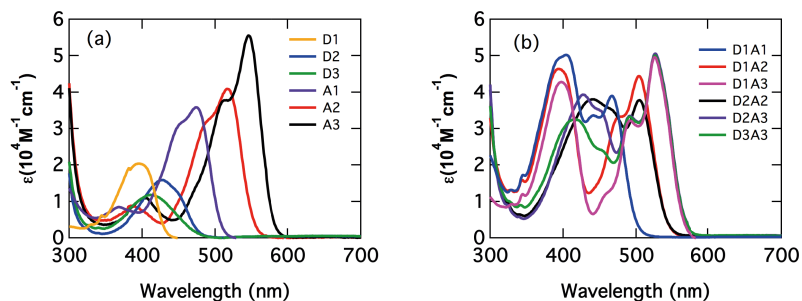


Figure C. 2 UV/Vis absorption spectra in chloroform (a) reference donor and acceptor compounds (b) antenna systems.

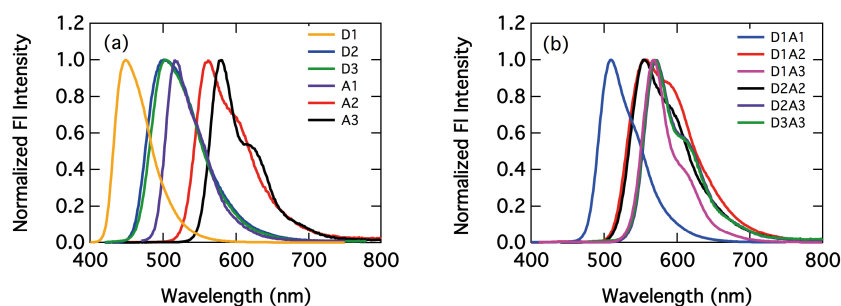


Figure C. 3 Normalized steady state emission spectra in chloroform (a) reference donor and acceptor compounds (b) antenna systems.

C.6 Comparison of Absorption and Excitation Spectra in Chloroform

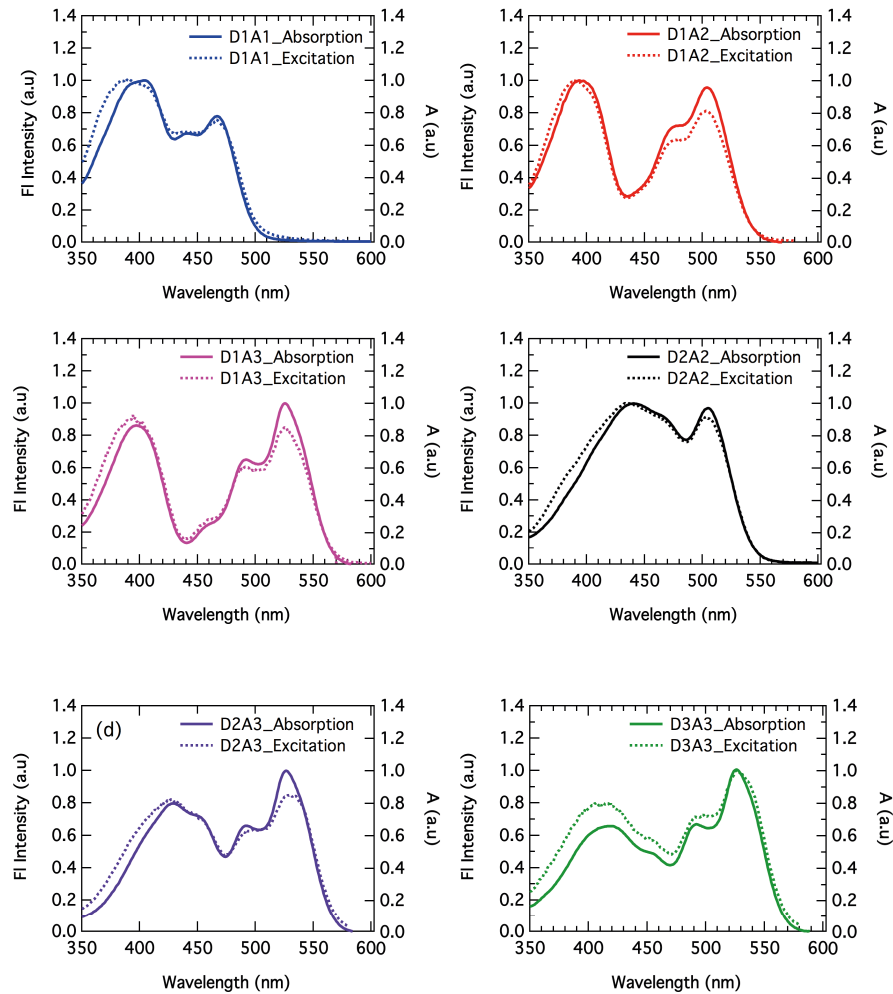


Figure C. 4 Excitation spectra (dashed-line) of the antenna systems measured at $\lambda_{\text{em}}=650$ nm along with absorption spectra (solid-line) in chloroform.

C.7 Comparison of Absorption and Excitation Spectra in Benzonitrile

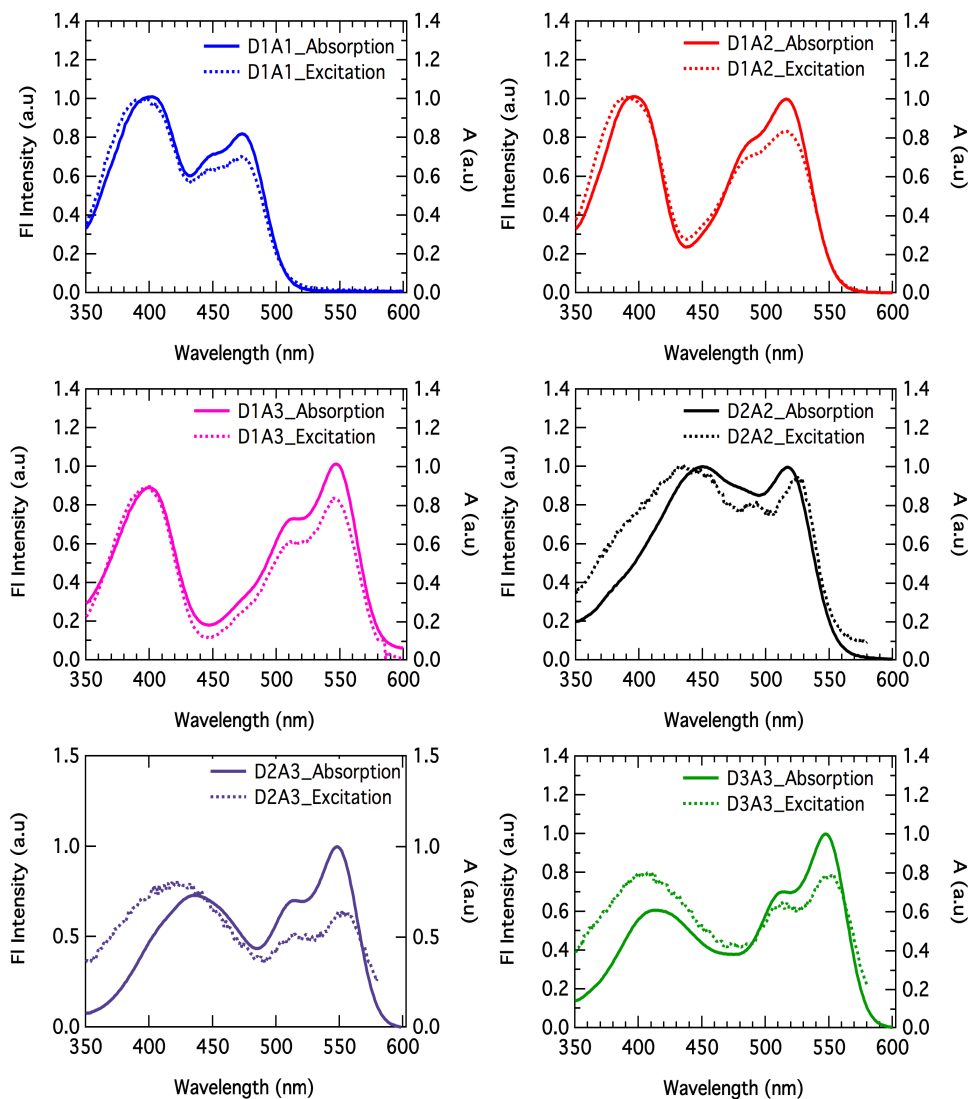


Figure C. 5 Excitation spectra (dashed-line) of the antenna systems measured at $\lambda_{\text{em}}=650$ nm along with absorption spectra (solid-line) in benzonitrile.

C.8 Fluorescence Decay Curves in Chloroform

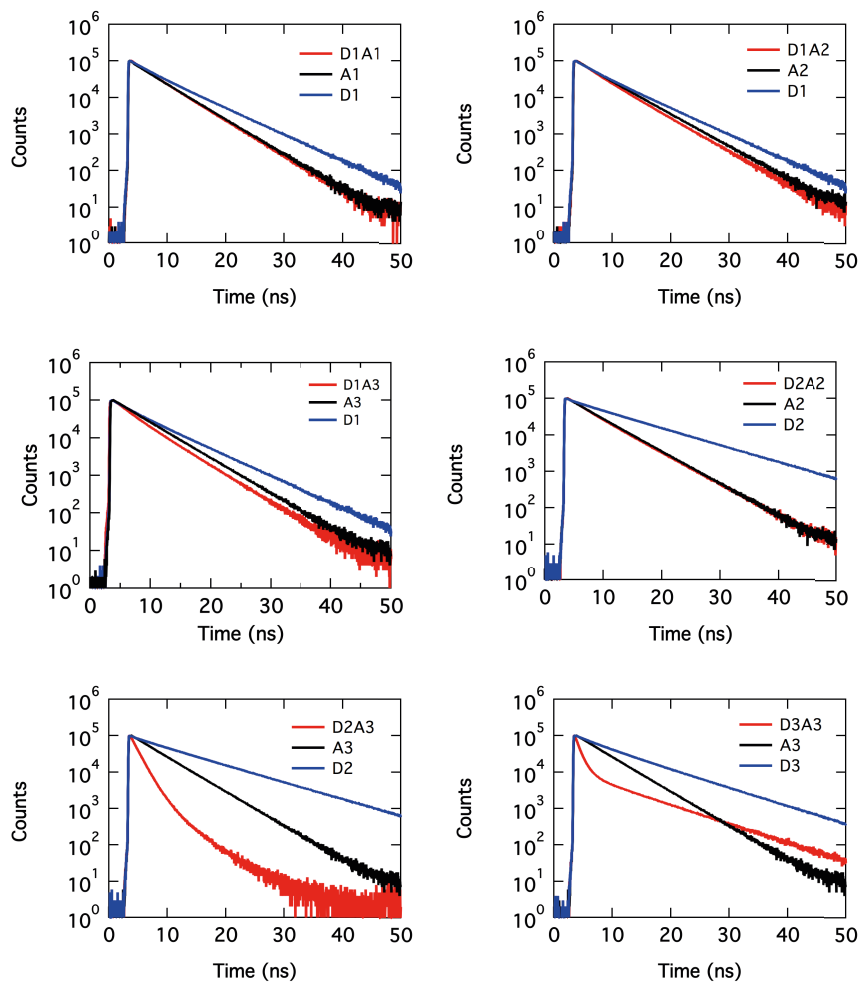


Figure C. 6 Fluorescence decay curves of antenna systems and their reference compounds in chloroform after excitation at 400 nm.

C.9 Fluorescence Decay Curves in Benzonitrile

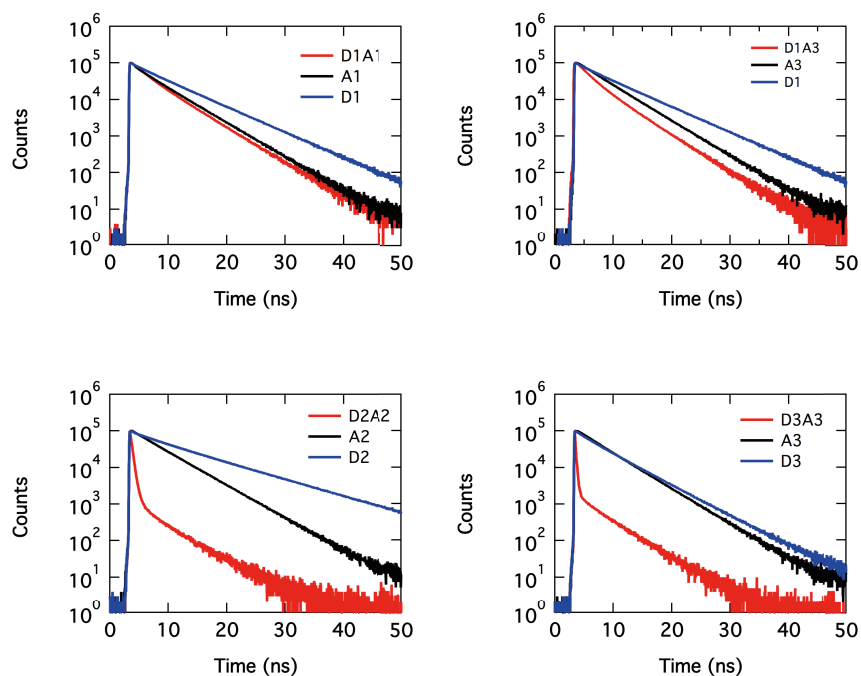


Figure C. 7 Fluorescence decay curves of antenna systems and their reference compounds in benzonitrile after excitation at 400 nm.

C.10 Transient Absorption Spectra of A1, A2, and A3

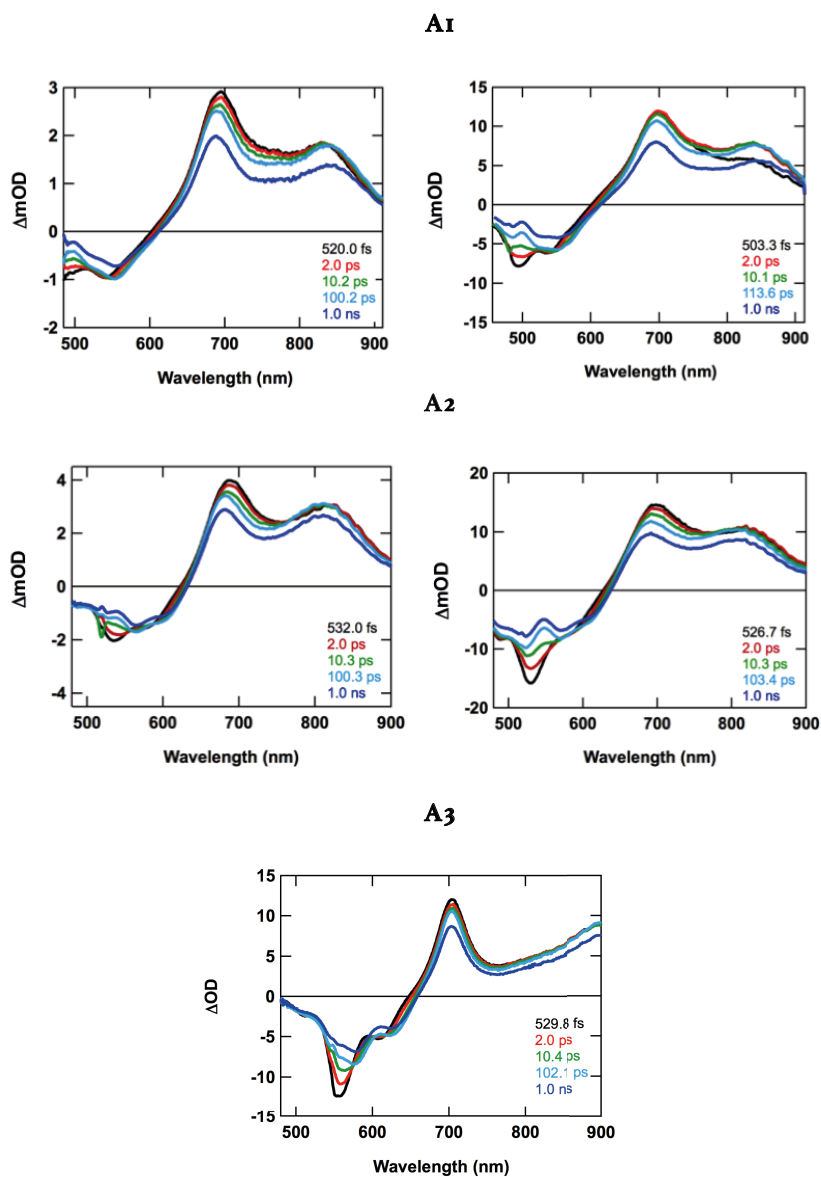


Figure C. 8 Transient absorption spectra of (a) A1 ($\lambda_{\text{ex}} = 480$ nm) in chloroform (left) and benzonitrile (right); (b) A2 ($\lambda_{\text{ex}} = 520$ nm) in chloroform (left) and benzonitrile (right); (c) A3 in chloroform.

C.II Transient Absorption Spectra of D1A1

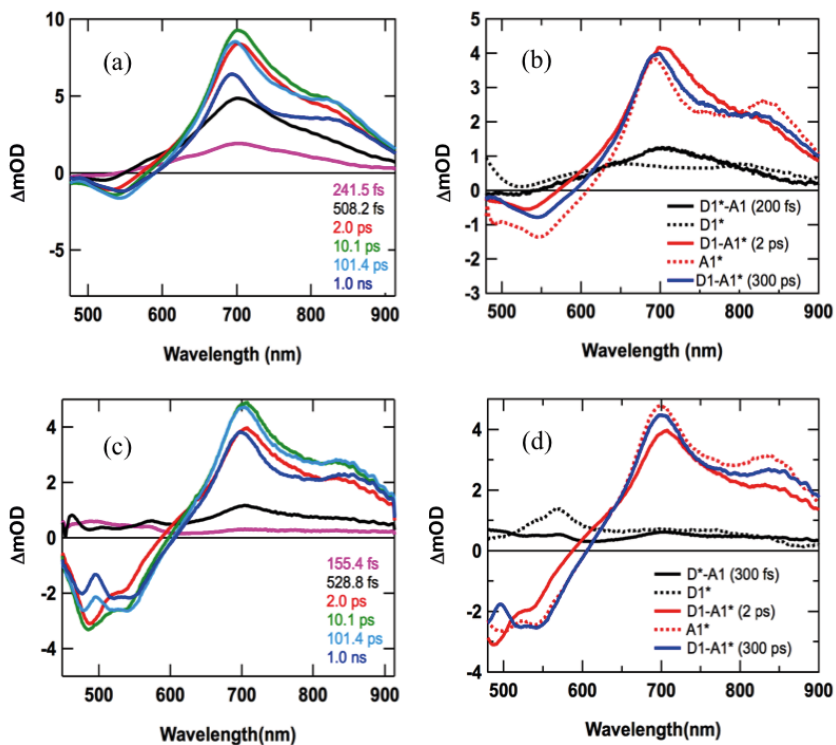


Figure C. 9 Transient absorption spectra of **D1A1** in (a) chloroform after selective excitation of naphthalene chromophore (b) **D1A1** spectra along with that of **D1** and **A1** (c) benzonitrile after selective excitation of naphthalene chromophore (d) **D1A1** spectra along with that of **D1** and **A1**.

C.12 Transient Absorption Spectra of D1A2

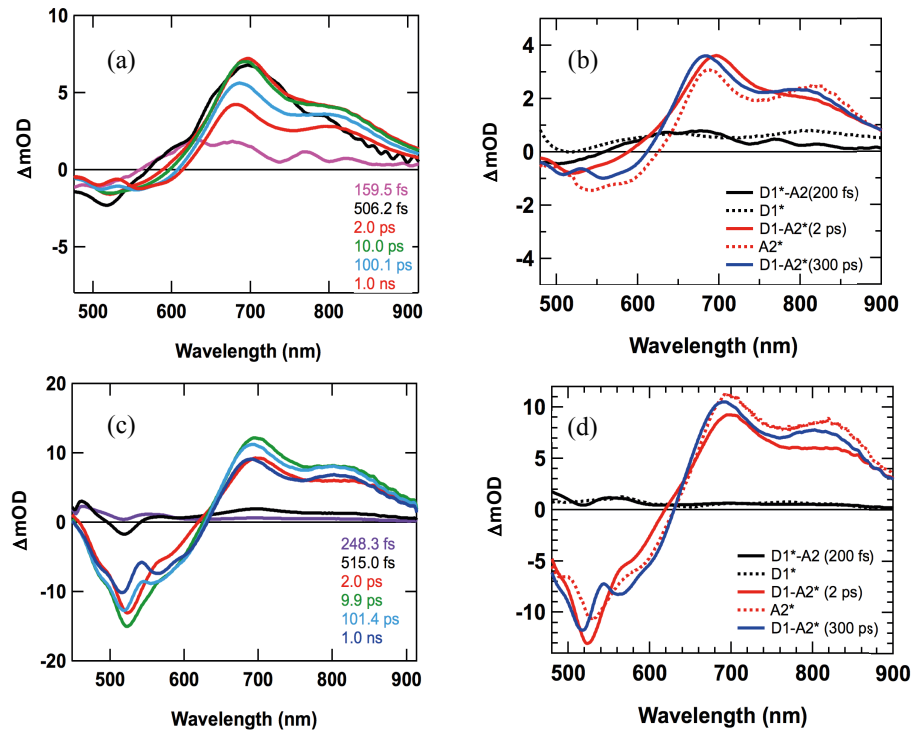


Figure C. 10 Transient absorption spectra of **D1A2** in (a) chloroform after selective excitation of naphthalene chromophore (b) **D1A2** spectra along with that of **D1** and **A2** (c) benzonitrile after selective excitation of naphthalene chromophore (d) **D1A2** spectra along with that of **D1** and **A2**.

C.13 Transient Absorption Spectra of D2A2

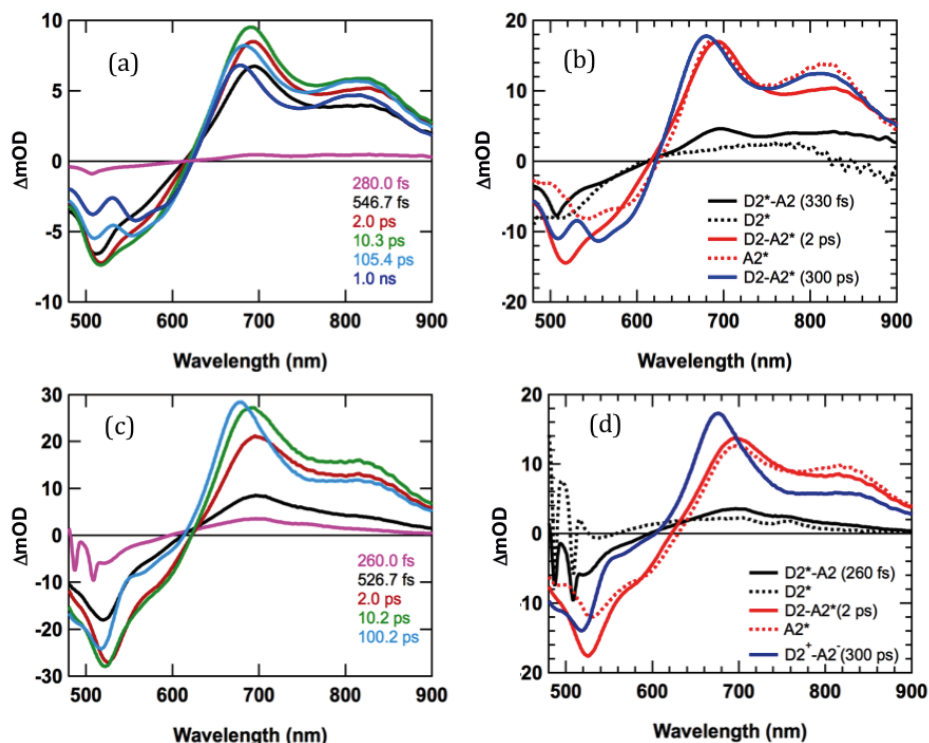


Figure C. 11 Transient absorption spectra of **D2A2** in (a) chloroform after selective excitation of naphthalene chromophore (b) **D2A2** spectra along with that of **D2** and **A2** (c) benzonitrile after selective excitation of naphthalene chromophore (d) **D2A2** spectra along with that of **D2** and **A2**.

C.14 Transient Absorption Spectra of D₃A₃

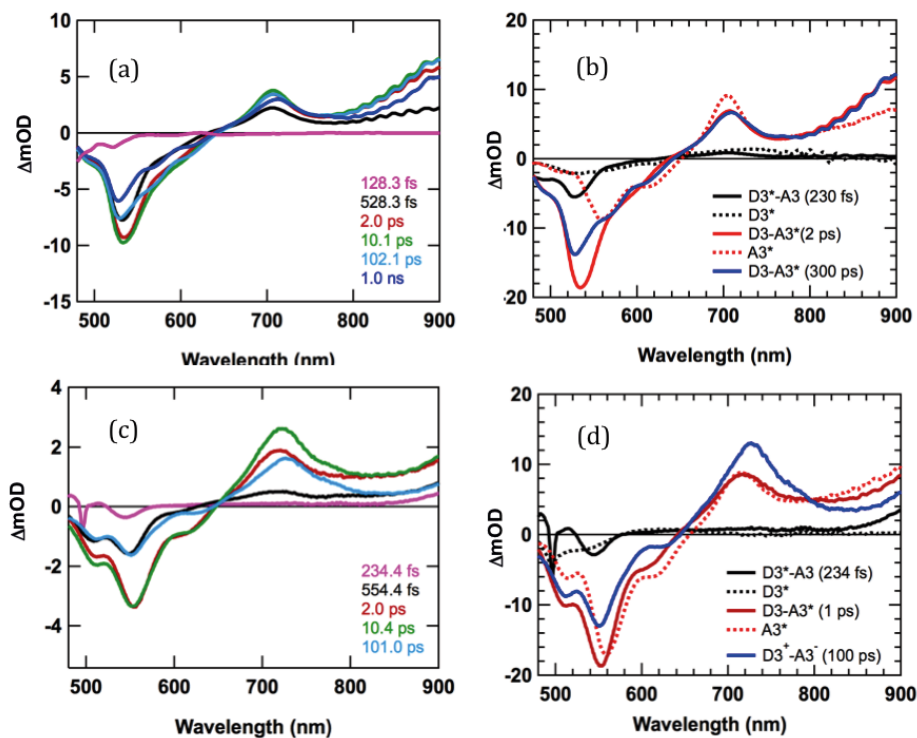


Figure C. 12 Transient absorption spectra of **D₃A₃** in (a) chloroform after selective excitation of naphthalene chromophore (b) **D₃A₃** spectra along with that of **D₃** and **A₃** (c) benzonitrile after selective excitation of naphthalene chromophore (d) **D₃A₃** spectra along with that of **D₃** and **A₃**.

C.15 Details of Global and Target Analysis

To model the pre-assumed kinetic profiles after the excitation of donor, target analysis is applied to transient absorption spectra. By using the scheme suggested in the paper, transient absorption (ΔOD) spectra of excited or radical ion states involved (what we called as species) with their population profiles. The obtained spectra of possible species involved in photo physical processes were compared with all excited state of model donors (**ref-D1***, **ref-D2***, **ref-D3***) and acceptors (**ref-A1***, **ref-A2***, **ref-A3***) as well as the radical ions. The quality of the fit is given in Figure S15-20.

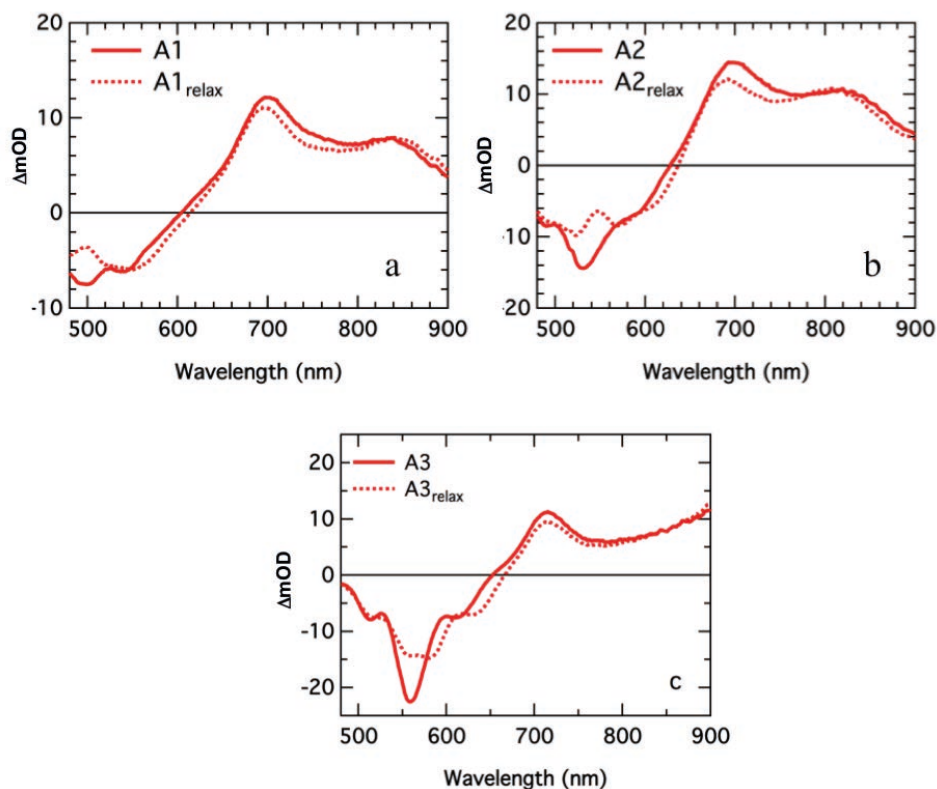


Figure C. 13 Species spectra obtained after global analysis for (a) **A1**, (b) **A2**, (c) **A3** in benzonitrile

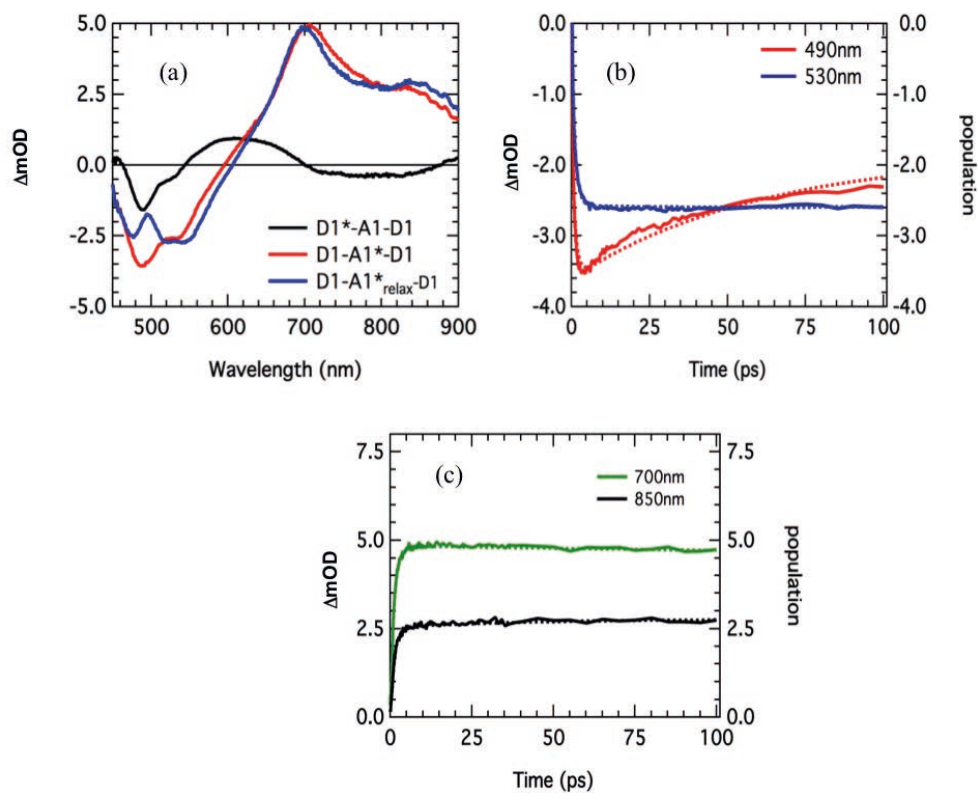


Figure C. 14 (a) The species obtained after the target analysis for **D1A1** (b) and (c) Kinetic traces (solid) and the population profiles (dashed) for **D1A1** in benzonitrile

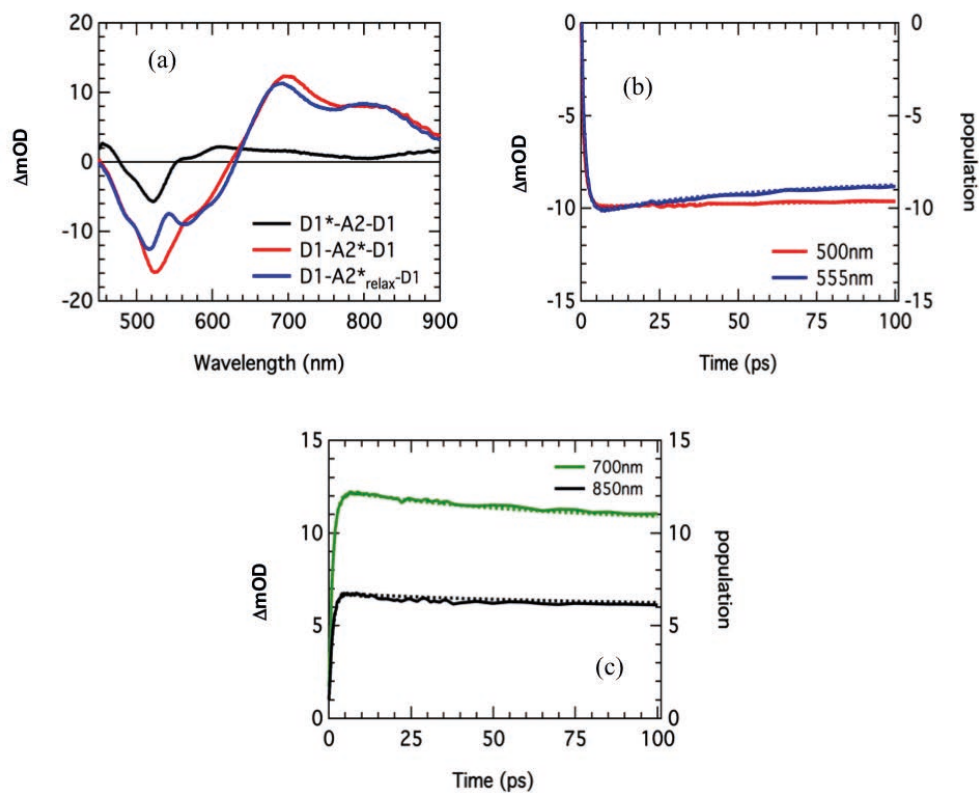


Figure C. 15 (a) The species obtained after the target analysis for **D1A2** (b) and (c) Kinetic traces (solid) and the population profiles (dashed) for **D1A2** in benzonitrile.

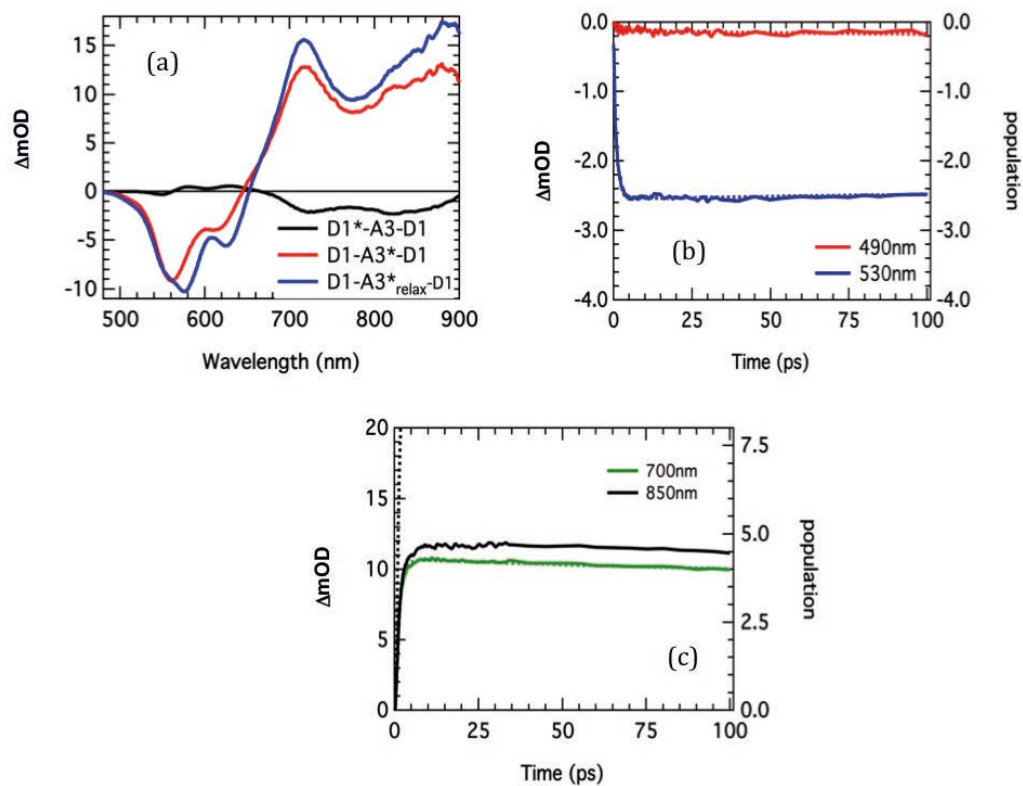


Figure C. 16 (a) The species obtained after the target analysis for **D1A3** (b) and (c) Kinetic traces (solid) and the population profiles (dashed) for **D1A3** in benzonitrile.

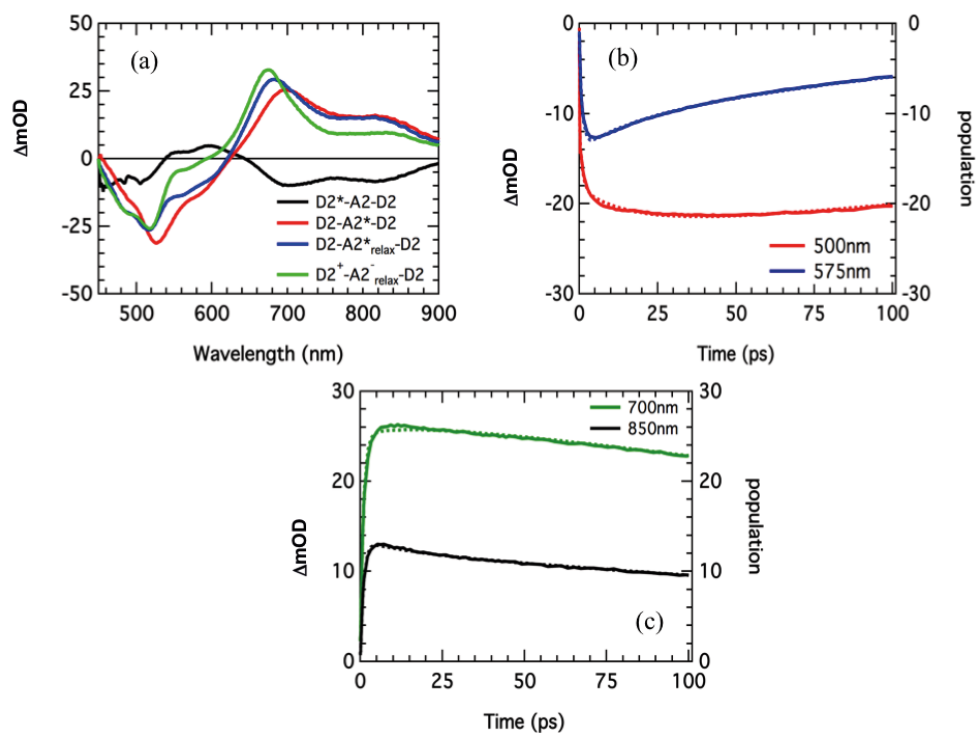


Figure C. 17 (a) The species obtained after the target analysis for **D2A2** (b) and (c) Kinetic traces (solid) and the population profiles (dashed) for **D2A2** in benzonitrile

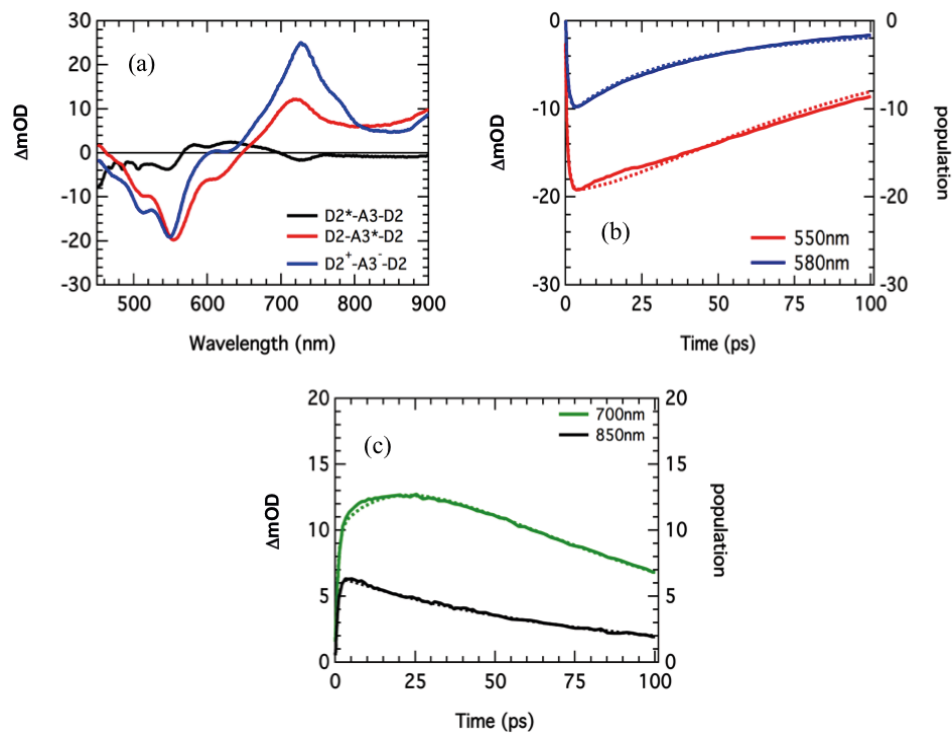


Figure C. 18 (a) The species obtained after the target analysis for **D2A3** (b) and (c) Kinetic traces (solid) and the population profiles (dashed) for **D2A3** in benzonitrile

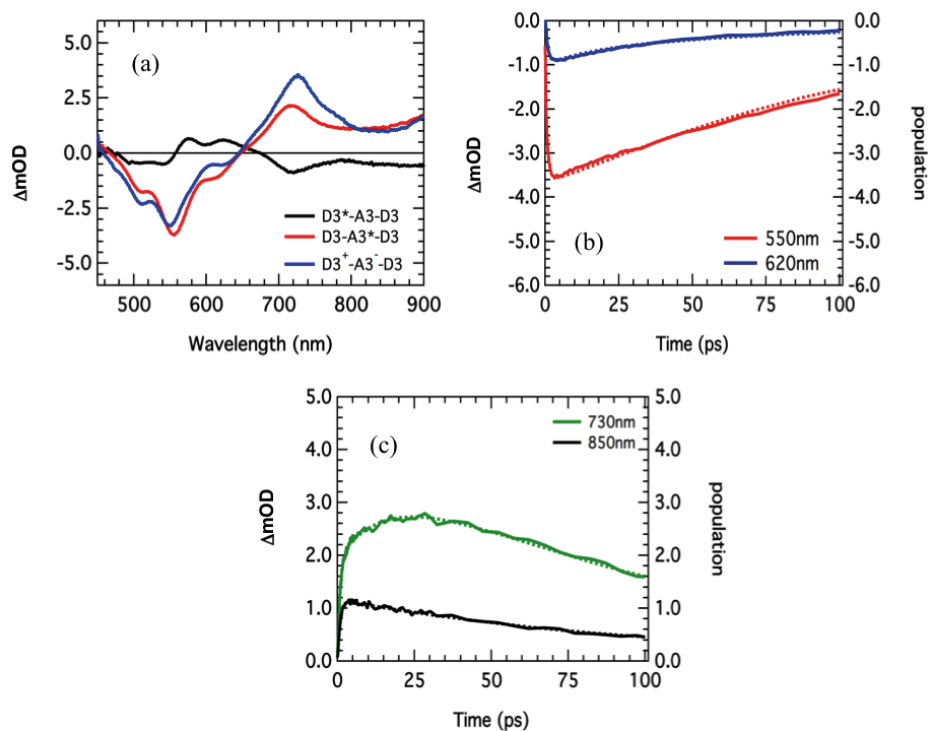


Figure C. 19 (a) The species obtained after the target analysis for **D3A3** (b) and (c) Kinetic traces (solid) and the population profiles (dashed) for **D3A3** in benzonitrile

D ● Appendix for Chapter 5

D.1 Synthesis and Characterization

Synthesis of *N*-[(4'-Boc-amino)phenyl]-4-bromonaphthalene-1,8-dicarboxy

Monoimide (2): A mixture of 4-bromo-1,8-naphthalic anhydride **1** (1.00 g, 3.61 mmol) and 4-(*N*-Boc-amino)aniline (0.90 g, 4.33 mmol), in ethanol (60 mL), was refluxed for 18 h. The reaction mixture was cooled to room temperature and the precipitate was collected by filtration. Thereafter, the precipitate was washed with ethanol and dried to obtain the compound **2** (1.27 g, 75%) as a white solid. ¹H NMR (400 MHz, DMSO-*d*₆): δ = 9.49 (s, 1H), 8.61–8.55 (m, 2H), 8.33 (d, *J* = 8.0 Hz, 1H), 8.24 (d, *J* = 8.0 Hz, 1H), 8.02 (t, *J* = 8.0 Hz, 1H), 7.54 (d, *J* = 8.0 Hz, 2H), 7.22 (d, *J* = 8.0 Hz, 2H), 1.48 ppm (s, 9H).

Synthesis of *N*-[(4'-Boc-amino)phenyl]-4-(*n*-butylamino)naphthalene-1,8-dicarboxy

Monoimide (3): A 50 mL round-bottomed flask was charged with compound **2** (0.80 g, 1.71 mmol), *n*-butylamine (2.6 mL, 1.90 g, 25.68 mmol), and DMSO (24 mL). The reaction mixture was stirred at 80 °C for 24 h and the resultant solution was poured in water (500 mL) to precipitate the crude product. The precipitate was filtered off and washed with several portions of water. Afterwards, washed with a small amount of methanol and dried in vacuum oven to afford the compound **3** (0.76 g, 97%) as yellow solid. ¹H NMR (400 MHz, CDCl₃): δ = 8.59 (d, *J* = 7.2 Hz, 1H), 8.48 (d, *J* = 8.4 Hz, 1H), 8.10 (d, *J* = 8.4 Hz, 1H), 7.62 (t, *J* = 8.0 Hz, 1H), 7.49 (d, *J* = 7.6 Hz, 2H), 7.20 (d, *J* = 7.6 Hz, 2H), 6.73 (d, *J* = 8.4 Hz, 1H), 6.58 (s, 1H), 5.28 (s, 1H), 3.45–3.36 (m, 2H), 1.84–1.74 (m, 2H), 1.55–1.45 (m, 11H), 1.02 ppm (t, *J* = 7.2 Hz, 3H).

Synthesis of *N*-(4'-aminophenyl)-4-(*n*-butylamino)naphthalene-1,8-dicarboxy

Monoimide (4): Compound **3** (1.21 g, 2.63 mmol) was stirred for 2 h in a mixture of chloroform (45 mL) and CF₃COOH (10 mL) at room temperature. Afterwards, the solvents were evaporated under vacuum. The resultant residue was stirred in an aqueous solution of K₂CO₃ (pH = 9) and then filtered, washed with water, and dried to afford the compound **4** (0.91 g, 96%). ¹H NMR (400 MHz, DMSO-*d*₆): δ = 8.70 (d, *J* = 8.4 Hz, 1H), 8.38 (d, *J* = 7.2 Hz, 1H), 8.21 (d, *J* = 8.8 Hz, 1H), 7.72 (s, 1H), 7.66 (t, *J* = 8.0 Hz, 1H), 6.88 (d, *J* = 8.4 Hz, 2H), 6.76 (d, *J* = 8.8 Hz, 1H), 6.66 (d, *J* = 8.4 Hz, 2H), 3.45–3.36 (m, 2H), 1.73–1.62 (m, 2H), 1.45–1.36 (m, 2H), 0.93 ppm (t, *J* = 7.2 Hz, 3H).

Synthesis of compound 6: A 50 mL round-bottom flask was charged with regioisomerically pure 1,7-dibromoperylene monoanhydride diester **5** (0.10 g, 0.15 mmol), compound **4** (0.16 g, 0.45 mmol), acetic acid (0.09 mL, 1.48 mmol), and anhydrous NMP (20 mL). The reaction mixture was stirred at 110 °C for 18 h under Ar atmosphere. After being

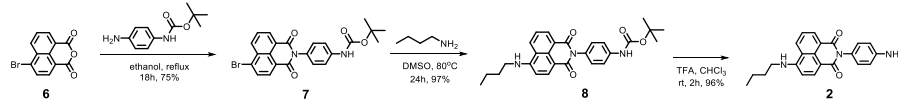
cooled to room temperature, toluene (100 mL) was added to the reaction mixture and the resultant solution was washed with slightly acidic water (3 x 200 mL). Organic layer was collected and evaporated by rotary evaporation. The solid residue was chromatographed on silica (DCM to chloroform) to afford the desired product **6** (0.83 g, 55%). ¹H NMR (400 MHz, CDCl₃): δ = 9.27 (d, J = 8.0 Hz, 1H), 9.24 (d, J = 8.0 Hz, 1H), 8.93 (s, 1H), 8.72 (d, J = 8.0 Hz, 1H), 8.65 (d, J = 7.2 Hz, 1H), 8.52 (d, J = 8.0 Hz, 1H), 8.34 (s, 1H), 8.16 (t, J = 8.4 Hz, 2H), 7.66 (t, J = 8.0 Hz, 1H), 7.54–7.46 (m, 4H), 6.76 (d, J = 8.4 Hz, 1H), 4.39–4.30 (m, 4H), 3.47–3.40 (m, 2H), 1.88–1.72 (m, 6H), 1.56–1.42 (m, 6H), 1.07–0.95 ppm (m, 9H).

Synthesis of compound 7 (Imido-D₂A₂): A mixture of 4-*tert*-butylphenol (44 mg, 0.29 mmol), anhydrous potassium carbonate (80 mg, 0.58 mmol), 18-crown-6 (160 mg, 0.60 mmol) in anhydrous toluene (100 mL) was stirred for 20 minutes at room temperature under argon atmosphere. Subsequently, compound **6** (100 mg, 0.10 mmol) was added. The reaction was continued for 18 h at 90 °C and then allowed to cool down to room temperature. The reaction mixture was extracted with water (3 x 100 mL). The organic phase was collected, and toluene was evaporated. The solid residue was chromatographed on silica, eluting with chloroform, to afford the desired product **7** (69 mg, 61%). ¹H NMR (400 MHz, CDCl₃): δ = 9.41 (d, J = 8.0 Hz, 1H), 9.39 (d, J = 8.0 Hz, 1H), 8.62 (d, J = 7.2 Hz, 1H), 8.60 (d, J = 8.4 Hz, 1H), 8.50 (d, J = 8.4 Hz, 1H), 8.38 (s, 1H), 8.11 (d, J = 8.4 Hz, 1H), 8.04 (d, J = 8.0 Hz, 1H), 7.77 (s, 1H), 7.62 (t, J = 8.0 Hz, 1H), 7.48–7.40 (m, 8H), 7.08 (d, J = 8.8 Hz, 2H), 7.05 (d, J = 8.8 Hz, 2H), 6.74 (d, J = 8.4 Hz, 1H), 5.29 (s, 1H), 4.30 (t, J = 6.4 Hz, 2H), 4.24 (t, J = 6.4 Hz, 2H), 3.45–3.37 (m, 2H), 1.84–1.72 (m, 4H), 1.70–1.56 (m, 4H), 1.54–1.42 (m, 4H), 1.35 (s, 9H), 1.33 (s, 9H), 1.03 (t, J = 7.6 Hz, 3H), 0.97 (t, J = 7.6 Hz, 3H), 0.89 ppm (t, J = 7.2 Hz, 3H). MS (ESI-TOF): [M]⁺ Calculated for C₇₄H₇₀N₃O₁₀, 1160.49673; found, 1160.49972.

Synthesis of compound 9: A 50 mL round-bottom flask was charged with 1,6,7,12-tetrachloroperylene bisanhydride monoanhydride diester **8** (130 mg, 0.25 mmol), compound **4** (330 mg, 0.92 mmol), acetic acid (0.40 mL), and anhydrous NMP (14 mL). The reaction mixture was stirred at 90 °C for 18 h under Ar atmosphere. After being cooled to room temperature, toluene (100 mL) was added to the reaction mixture and the resultant solution was washed with slightly acidic water (3 x 200 mL). Organic layer was collected and evaporated by rotary evaporation. The solid residue was chromatographed on silica using chloroform as eluent to afford the desired product **9** (131 mg, 44%). ¹H NMR (400 MHz, CDCl₃): δ = 8.82–8.76 (m, 6H), 8.65 (d, J = 8.4 Hz, 2H), 8.35 (d, J = 8.4 Hz, 2H), 7.87 (t, J = 8.0 Hz, 2H), 7.58–7.50 (m, 8H), 7.20 (d, J = 8.4 Hz, 2H), 3.58 (t, J = 7.6 Hz, 4H), 1.90–1.82 (m, 4H), 1.58–1.50 (m, 4H), 1.03 ppm (t, J = 7.2 Hz, 6H).

Synthesis of compound 10 (Imido-D₂A₄): A mixture of compound **9** (60 mg, 0.05 mmol), 4-*tert*-butylphenol (52 mg, 0.35 mmol) and anhydrous potassium carbonate (48 mg, 0.35 mmol) was stirred for 6 h at 90 °C in anhydrous NMP (12 mL) under an inert atmosphere. After being cooled to room temperature, toluene (100 mL) was added and the reaction mixture was extracted with slightly acidic water (3 x 200 mL). The organic phase was collected, and toluene was evaporated. The solid residue was chromatographed on silica,

eluting with chloroform, to afford the desired product **10** (48 mg, 58%). ^1H NMR (400 MHz, CDCl_3): δ = 8.61 (d, J = 7.6 Hz, 2H), 8.50 (d, J = 7.6 Hz, 2H), 8.28 (s, 4H), 8.10 (d, J = 8.4 Hz, 2H), 7.64 (t, J = 7.2 Hz, 2H), 7.46–7.40 (m, 8H), 7.23 (d, J = 7.6 Hz, 8H), 6.84 (d, J = 7.6 Hz, 8H), 6.75 (d, J = 8.4 Hz, 2H), 5.25 (s, 2H), 3.45–3.37 (m, 4H), 1.84–1.76 (m, 4H), 1.27 (s, 36H), 1.03 ppm (t, J = 7.2 Hz, 6H). MS (ESI-TOF): $[\text{M}]^+$ Calculated for $\text{C}_{108}\text{H}_{94}\text{N}_6\text{O}_{12}$, 1666.67637; found, 1666.68261.



Scheme D. 1 Synthesis of 4-butylamino substituted naphthalene monoimide precursor **2**.

D.2 Structure of Model Compounds

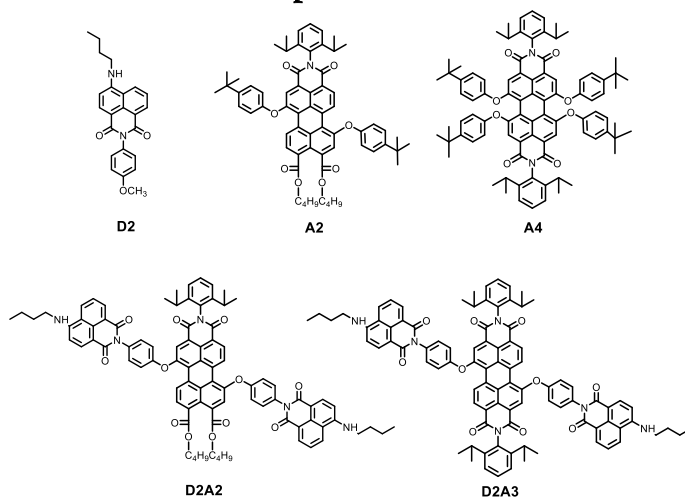


Figure D. 1 Model compounds **D2**, **A2** and **A4** and bay antenna molecule **D2A2**

D.3 Rehm-Weller Equation

$$\Delta G_{CS}^0 = [E_{ox}(D) - E_{red}(A)] - E_{00}(A) - \frac{e^2}{r_{DA}\epsilon_s} + e^2 \left(\frac{1}{2r_D} + \frac{1}{2r_A} \right) \left(\frac{1}{\epsilon_s} - \frac{1}{\epsilon_{ref}} \right) \quad (\text{D.1})$$

D.4 Photophysical Properties in Toluene

Table D. 1 Photo-physical properties of the reference compounds and donor-acceptor systems in toluene ^a Fluorescence Quantum Yield ^b Fluorescence lifetime (λ_{exc} = 400 nm)

Compounds	ϕ_{FL}^a	$\tau_{FL}(\text{ns})^b$
A2	0.95	4.67
Im-D2A2	0.85	1.4(34%)/4.0 (66%)
A4	0.98	5.50
Im-D2A4	0.90	1.3(13%)/5.2 (87%)

D.5 Excitation Spectrum of Im-D2A2

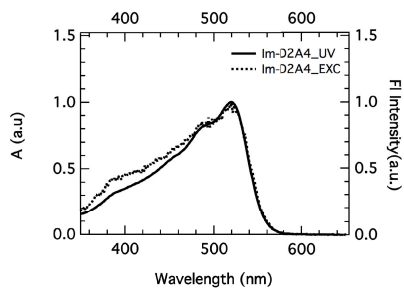


Figure D. 2 Excitation spectrum of **Im-D2A2** (dashed-line) measured at $\lambda_{em} = 650$ nm along with the absorption spectrum (solid-line) in benzonitrile

D.6 Time Resolved Florescence Data

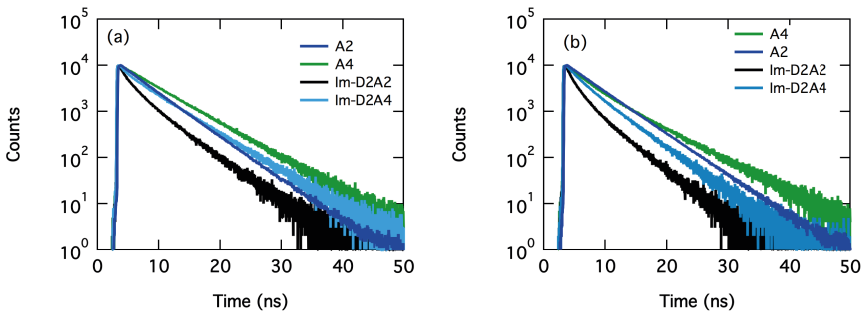


Figure D. 3 Time resolved fluorescence data of **Im-D2A2**, **Im-D2A4** and reference acceptors **A2**, **A4** (a) in toluene (b) in benzonitrile

D.7 Transient Absorption Spectra of Im-D2A4

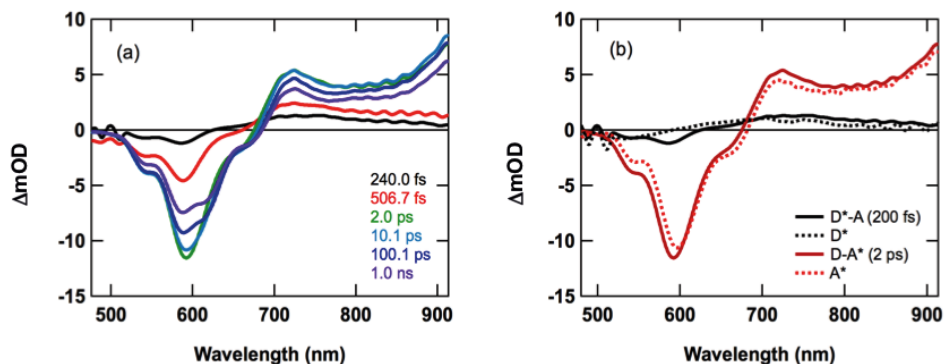


Figure D. 4 (a) Time evolution of the femtosecond transient absorption spectra of **Im-D2A4** excitation at 430 nm in benzonitrile (b) The spectra of **Im-D2A4** with the dissociation of species after different time delays along with reference donor and reference acceptor

D.8 Transient Absorption Spectra of Reference Compounds

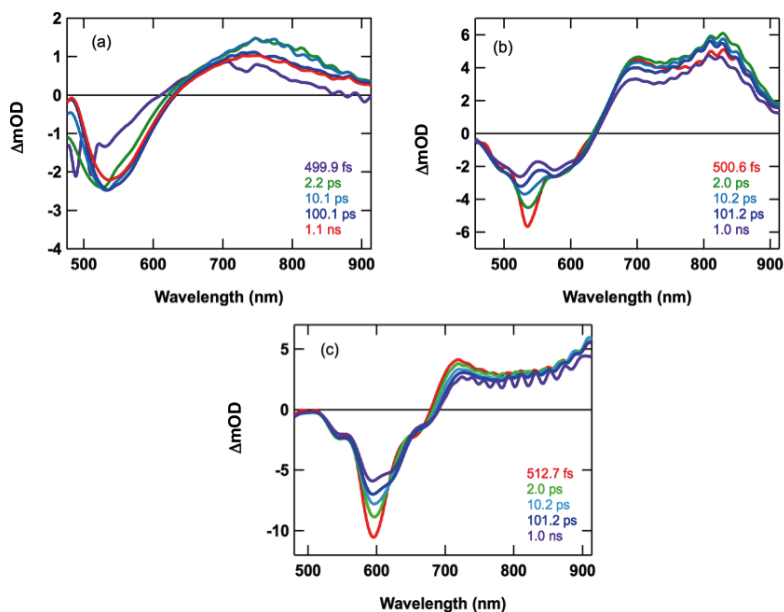


Figure D. 5 Time evolution of the femtosecond transient absorption spectra in benzonitrile of (a) **D2** excitation at 430 nm (b) **A2** excitation at 530 nm (c) **A4** excitation at 580 nm

S

ummary

In nature, solar energy conversion occurs with a process called photosynthesis. Although the overall energy efficiency of the storage of the energy of sunlight into biomass is low, the individual photophysical processes that occur have a high quantum yield. In the latter sense, natural photosynthesis can serve as a valuable inspiration for the design of artificial light harvesting systems with the final goal of achieving efficient energy conversion. In this thesis, different approaches are explored to construct new artificial light harvesting systems with a special focus on the systematic study of the individual photophysical processes that take place.

In **Chapter 2**, we report on the synthesis and the photophysical properties of a series of donor-acceptor molecules where the strength of the acceptor is varied systematically. In these molecules, electron donating 4-methoxyphenyl groups are attached to 1,7 bay positions of four different perylene tetracarboxylic acid derivatives. Additionally, two more molecules were synthesized where a 4-methoxyphenyl group is attached at imide position. Photophysical characterization, both by steady state and time-resolved spectroscopy, showed that, charge transfer from donor to acceptor in these compounds depends on three variables: solvent polarity, the electronic nature of perylene core (acceptor strength) and the position of donor. The electronic nature of perylene core affects charge transfer such that perylene tetra esters, which constitute the least electron deficient core in the series, show charge transfer only in polar acetonitrile. By changing the core to a perylene monoimide, the electron deficiency of the perylene core is increased, leading to charge transfer being observable in chloroform already. The most electron deficient perylene core, perylene bisimide, shows charge transfer in both polar and nonpolar solvents. Using transient absorption spectroscopy and density function theory calculations, we show that the initial excited state is localized on the acceptor, but that charge transfer occurs almost instantaneously. The position of the donor (bay-area vs. imide position) was found to have a deciding effect on the rate and efficiency of charge transfer. Changing the donor position from bay to imide results in disappearance of charge transfer. This study indicates approaches to influence charge transfer that occurs in donor-substituted perylene dyes that will be valuable in later chapters.

In **Chapter 3**, we used the information from Chapter 2 to develop new light harvesting systems. Two naphthalene chromophores that act as energy donors were attached to the 1,7-bay positions of perylene-3,4,9,10-tetracarboxy derivatives. As a rule, artificial light harvesting systems should have a good spectral coverage to harvest as much of the solar spectrum as possible. All antenna systems described in Chapter 3 have absorption features between 350 and 580 nm. In addition, the absorption of the model acceptors and the emission of the model donor have a sufficient spectral overlap, which is a requirement for an efficient excited energy transfer (EET) by the Förster mechanism. Energy transfer in these compounds was studied by steady state and time-resolved spectroscopy using the non-polar solvent toluene. We observed that after selective excitation of the naphthalene donor-moiety the

excited state energy is transferred to the perylene acceptor within a picosecond. The excited perylene acceptor decays back to the ground state by fluorescence on a nanosecond time-scale. This time-scale is comparable to the fluorescence lifetime of the unsubstituted acceptor. No photoinduced charge transfer was observed although it is possible thermodynamically. It is concluded that this might be due to rigid phenol linker in between donor and acceptor.

In **Chapter 4**, we used the same antenna systems as in Chapter 3 and a new compound called D1A3 and studied the effect of solvent polarity on the excited state dynamics. As noted above, all compounds absorb in the visible and they all show energy transfer on a picosecond timescale. This energy transfer was found to be independent of solvent polarity and only slightly affected by the molecular structure. On the other hand, charge transfer can be expected to depend on both solvent polarity and molecular structure. For the donor-acceptor molecules with a strong electron donor and electron acceptor, we observed the occurrence of charge transfer in chloroform (D2A3 and D3A3), after the initial very fast energy transfer. The charge transfer in chloroform is slow $\tau_{CT} \sim 1.7\text{-}2$ ns, and comparable with the fluorescence rate of the acceptor. In benzonitrile, the same two antenna systems and also D2A2 exhibit much faster charge transfer on a 120 ps timescale. In the remaining antenna system only energy transfer is observed even in the highly polar benzonitrile, which is due to the reduced driving force for charge separation.

In **Chapter 5**, based on the knowledge from the previous chapters, we turn our attention to the properties of donor-acceptor model systems where the energy donor is attached to the imide position. Two new antenna molecules were synthesized and their photophysical properties were studied in benzonitrile. This study reveals that the undesired charge transfer that was observed when introducing the donor moieties in the bay area can be controlled in an effective manner by placing the energy donors at the imide positions. For both perylene monoimide and bisimide acceptors the charge transfer that was observed for the bay area analogues was completely absent, even in benzonitrile solvent. This strongly reduced tendency to give charge transfer is due to a combination of a large charge separation distance, thus reducing the driving force for charge separation, combined with a small electronic coupling for charge transfer through the imide nitrogen. At the same time, the energy transfer is largely maintained, as the energetics are not influenced by the transfer distance, as they are for charge separation.

To conclude, in this thesis a detailed overview is presented on the photophysics of perylene-based donor acceptor systems. It is shown that the dynamics of energy transfer, the spectral coverage of the artificial antennas and the extent to which (unwanted) charge transfer occur can be influenced by altering the architecture of the antenna systems and the solvent surroundings. This offers new insights that can eventually lead to efficient light-harvesting antennas that can be applied in devices for artificial photosynthesis.

Samenvatting

In de natuur vindt de conversie van zonne-energie plaats in het zogenoemde fotosynthese proces. Hoewel de totale efficiëntie van de opslag van de energie van het zonlicht in de vorm van biomassa laag is, is de kwantum-efficiëntie van de individuele fotofysische processen erg hoog. Gezien dit laatste feit kan natuurlijke fotosynthese dienen als een waardevolle inspiratiebron voor het ontwerpen van kunstmatige systemen om licht te oogsten. Het uiteindelijke doel hiervan is het efficiënt omzetten van energie. In dit proefschrift worden verschillende aanpakken bestudeerd om nieuwe licht-oogstende systemen te maken, met speciale aandacht voor het systematisch bestuderen van de individuele fotofysische processen die plaatsvinden.

In **Hoofdstuk 2** worden de synthese en de fotofysische eigenschappen van een series donor-acceptor moleculen beschreven. In deze moleculen wordt het elektron-stuwende of zuigende karakter systematisch gevarieerd. In de moleculen die zijn bestudeerd zijn elektron-stuwende 4-methoxyfenyl groepen gebonden aan de 1,7 (bay) posities van vier verschillende peryleen-tetracarbonzuur verbindingen. Hiernaast zijn er nog twee extra moleculen gesynthetiseerd waarin de 4-methoxyfenyl gebonden is op de imide-positie. Fotofysische karakterisatie van deze moleculen, zowel met steady-state als tijdsopgeloste spectroscopie laat zien dat ladingsoverdracht in deze verbindingen afhankelijk is van drie variabelen: de polariteit van het oplosmiddel, de elektronenstructuur van de peryleen-kern (het elektron zuigende karakter) en de positie van de elektron stuwende groep. Als de peryleen kern bestaat uit een peryleen-tetra-ester, de minst elektron deficiënte acceptor in de serie, treedt alleen ladingsoverdracht op in het polaire oplosmiddel acetonitril. Wanneer de kern wordt veranderd in een peryleen-monoimide wordt het elektron deficiënte karakter verhoogd waardoor er in dit geval al in chloroform landingsscheiding optreedt. De meest elektron deficiënte kern laat elektronoverdracht zien in zowel polaire als apolaire oplosmiddelen. Met behulp van transient-absorptie spectroscopie en dichtheids-functioneel theorie berekeningen demonstreren we dat de initiële aangeslagen toestand gelokaliseerd is op de acceptor, maar dat ladingsoverdracht vrijwel instantaan optreedt. De positie van de donor (bay-positie tegenover de imide positie) heeft een doorslaggevend effect op snelheid en efficiëntie van ladingsoverdracht. Door het veranderen van de donor van de bay- naar de imide positie verdwijnt de ladingoverdracht volledig. Deze studie geeft inzicht in benaderingen om ladingsoverdracht in donor-gesubstitueerde peryleen te beïnvloeden en is van belang voor volgende hoofdstukken.

In **Hoofdstuk 3** gebruiken we de informatie uit hoofdstuk 2 voor het ontwerpen van nieuwe licht-oogstende moleculen. Twee naftaleen chromoforen die zich gedragen als energie-donoren zijn vastgemaakt aan peryleen-3,4,9,10-tetracarbonzuur verbindingen op de 1, 7-bay posities. Als regel moeten kunstmatige licht-oogstende moleculen een zo groot mogelijk deel van het licht van de zon absorberen. Alle antennesystemen die beschreven worden in hoofdstuk 3 absorberen licht met golflengtes tussen 350 nm en 580 nm. Hiernaast

is de spectrale overlap van de absorptie van de acceptor en de emissie van de donor voldoende groot. Dit laatste is een vereiste voor efficiënte aangeslagen-toestandsenergie overdracht volgens het Förster mechanisme. We hebben energieoverdracht in deze systemen bestudeerd met behulp steady-state en tijdsopgeloste spectroscopie in het apolaire oplosmiddel toluen. Na selectieve absorptie van licht in de naftaleen energie-donor wordt de aangeslagen-toestandsenergie binnen een picoseconde overgedragen naar de peryleen-acceptor. De aangeslagen toestand van de peryleen-acceptor vervalt terug naar de grondtoestand door fluorescentie op een nanoseconde tijdschaal. Deze tijdschaal komt overeen met de fluorescentielevensduur van de ongesubstitueerde acceptor. Voor deze verbindingen wordt in toluen geen foto-geïnduceerde ladingsoverdracht gezien, hoewel dit thermodynamisch gezien in eerste benadering wel mogelijk zou moeten zijn. Dit zou kunnen komen door de rigide phenol-linker tussen de donor en de acceptor.

In **Hoofdstuk 4** gebruiken we dezelfde antennesystemen als in hoofdstuk 3 en een nieuwe verbinding genaamd D1A3 om het effect van de polariteit van het oplosmiddel op de aangeslagentoestandsdynamica te bestuderen. Zoals hierboven beschreven absorberen alle verbindingen in het zichtbare gebied en laten ze allemaal energieoverdracht zien op een picoseconde tijdschaal. In dit hoofdstuk laten we zien de snelheid van ladingsoverdracht onafhankelijk is van de polariteit van het oplosmiddel, en slechts zwak afhankelijk van de moleculaire structuur. In tegenstelling tot energieoverdracht wordt voor ladingsoverdracht wel een sterke afhankelijkheid verwacht van de polariteit van het oplosmiddel en van de elektronenstructuur van het molecuul. Voor de donor-acceptor moleculen met een sterke elektron donor en acceptor (D2A3 en D3A3) zien we ladingsoverdracht in chloroform, volgend op initiële energieoverdracht. De ladingsoverdracht in chloroform is langzaam, $t_{CT} \sim 1.7\text{-}2$ ns, en vergelijkbaar met de fluorescentie levensduur van de acceptor. In benzonitril laten dezelfde twee antenne systemen, alsmede D2A2 veel snellere ladingsoverdracht zien op een tijdschaal van ~ 120 ps. In de overige antenne systemen werd alleen energyoverdracht gezien, zelfs in de sterk polaire oplosmiddelen. Dit laatste komt door de gereduceerde drijvende kracht voor ladingsscheiding.

In **Hoofdstuk 5**, verleggen we de aandacht naar donor-acceptor modelsystemen waar de energiedonor is gekoppeld via de imide positie. Hiervoor zijn twee nieuwe antenne systemen gesynthetiseerd en hun fotofysische eigenschappen zijn bestudeerd in benzonitril. Deze studie laat zien dat de ongewenste ladingsoverdracht die werd gezien wanneer de donorgroepen op de bay posities geplaatst werden volledig afwezig is, zelfs als benzonitril als oplosmiddel wordt gebruikt. Deze sterk gereduceerde tendens om ladingsoverdracht te vertonen is het gevolg van een combinatie van de grotere afstand voor ladingsscheiding en de kleine elektronische koppeling door de imide-binding. Tegelijkertijd blijft het vermogen om energieoverdracht te geven vrijwel volledig behouden omdat hiervoor de drijvende kracht niet word beïnvloed door de overdrachtsafstand, wat voor ladingsoverdracht wel het geval is.

In **Hoofdstuk 6** wordt een verder studie van energieoverdracht vanaf de imide positie beschreven, waarbij gebruik gemaakt word van drie nieuwe antenne systemen. In deze systemen is de naftaleen-donor aan de peryleen-bisimide acceptor gekoppeld op de imide positie, maar hiervan gescheiden door een fenyl-brug van toenemende lengte. Alle antenne systemen absorberen licht tussen 350-550 nm. Na initiële excitatie van de donor vind energieoverdracht plaats naar de acceptor. De snelheid van energieoverdracht neemt sterk af

met toenemende afstand tussen de donor en acceptor, zoals verwacht voor de afstandsafhankelijkheid van Förster energieoverdracht die afneemt met $1/r^6$. Er vindt voor geen enkel geval fotogeïnduceerde ladingsoverdracht plaats, wat consistent is met de observaties in Hoofdstuk 5.

Ter conclusie, in dit geeft een gedetailleerd overzicht van de fotofysica van peryleen-gebaseerde donor-acceptor systemen. Er wordt gedemonstreerd dat de dynamica van energieoverdracht, het spectrale bereik van de kunstmatige antenne systemen en de mate waarin (ongewenste) ladingsoverdracht plaatsvind beïnvloed kan worden door het veranderen van de architectuur van de antenne systemen en hun oplosmiddel omgeving. Dit geeft nieuwe inzichten die uiteindelijk kunnen leiden tot efficiënte licht-oogstende antennes die kunnen worden toegepast in apparaten voor kunstmatige fotosynthese.

Acknowledgements

As any accomplishment, this thesis could not be done without the help of others. I would like to take time and thank all the people who are involved in any point of these four years. First of all, I would like to acknowledge my promotor Dr. Ferdinand Grozema. Ferdinand, I would like to thank you for giving me opportunity to do my PhD research in your group. You helped me throughout every point in my PhD both research and personal development. Bedankt voor uw voortdurende steun! Second, I would like to thank my copromotor Dr. Wolter Jager. I would like to thank you for your continuous support on my manuscripts and conversations on our projects. Bedankt! I would like to express my gratitude to other faculty members of optoelectronic materials group. Dr. Tom Savanije, Dr. Arjan Houtepen and Prof. dr. Laurens Siebbeles, thank you all for your help on my projects. I would like to thank Prof. dr. Angela Sastre-Santos for her collaboration in my work.

I would like to thank to Dr. Natalie Gorczak-Vos. Natalie, you were there in any moment of my PhD even the times you are not in the group anymore. Thank you for teaching me how to use instruments and how to be critical on results. I would not able to solve some of my problems without you. Thank you for giving me opportunity to be a paronymph in your defense. I would like to thank your friendship as well in any moment of these four years. Another big thanks goes to Dr. Rajeev Dubey. Rajeev, I cannot express my gratitude for your all support during my PhD. Thank you for your synthesis of our antenna molecules, your continuous support on the discussion of results and helping me on manuscripts. I had so much fun to work with you.

I would like to thank Wil Stolk, Heleen van Rooijen and Cecilia Quick-Verdier for helping me any administrative problem. Another thanks go to Ruben Abellon and Jos Thieme for their technical support. Another thanks to my student, Jorrit Bleeker, for his hard work.

I would like to thank my funding agency NWO for their support in my research as well as my personal development. I would like to thank my committee member and my paronymphs.

I would like to thank Aditya Kulkarni, Prashant Bhaskar, Silke Diedenhofen and Hamit Eren for their friendship. Thank you guys for listening me and giving your support! I would like to express my thanks to Kevin Felter. Kevin, we could not finish the project on metaloxides. Nevertheless, PhDI group will remain eventhough we don't work on that. Another thanks to my all office mates: Francesca Pietra, Yu Bi, Dengyang Gao, Davide Bartesaghi, Sudeep Maheswari and Valentina Casseli. We had so much fun in our office, talk about different stuff in everyday and make a lot of fun activities! I would like to thank rest of OM group members for all their support and friendship.

I would like to thank all my friends in Delft for their amazing friendship. A special thanks to Fahimeh Nafezarafi for her friendship. Thank you Reyhan Aydogan, Taygun Kekec, Melika Gul, Paula Perez-Rodriguez, Tugce Akkaya for your friendship. I would like to express my thanks to my lifelong friend Meltem Ayguler.

I would like to thank special people in my life. Joshua Carey Julian, I cannot tell how much your love and support helped me during the hardest time in my PhD. Thank you loving me, believing me and encouraging me in any moment. I cannot wait the next chapters in our lives. I am sure it will be hella good! ☺

To my special ones, my mother Mukaddes Inan and my father Ali Ilhan Inan, I would like to thank you. Benim her zaman yanımda olup, bana sonsuz destek sagladiginiz icin cok teşekkür ederim. Sizin gibi bir aileye sahip olmak bana hayattaki en büyük hediye. Sizin bana olan güveniniz ve gururunuz sayesinde pek çok zorun ustesinden geldim. Sizi çok seviyorum ve bu tezi size ithaf ediyorum.

This thesis is dedicated to Mukaddes Inan and Ali Ilhan Inan



Curriculum Vitae

Damla Inan

Damla Inan was born on 26 November 1989 in Eskisehir, Turkey. She moved to Izmir at the age of 10 where she completed her secondary school in 2007. The same year, she received a full scholarship from Bilkent University, Turkey. She studied chemistry and worked one year on the thesis project of thin film fabrication and characterization. In 2012, she was selected for Erasmus Mundus program Surface, Electro, Radio and Photo Chemistry, SERP Chem from Universite Paris Sud, France. She received a full scholarship from the European Union. For one and half years, she studied in three different universities in three countries: Università di Genova-Italy, Universidade do Porto-Portugal and Universite Paris-Sud-France. She moved for the last semester to Porto to research on sol-gel film coating on optical sensors for her graduation project. She graduated from masters in the summer of 2014. Subsequently, from September 2014 to September 2018, she was a PhD student at the Optoelectronic Materials Section at Delft University of Technology. She carried out experimental and computational research on energy and charge transfer on organic molecules under supervision of Dr. F.C Grozema and Dr. W.F. Jager. From 1st of September, she is working as an application engineer in ASML, Veldhoven.

List of Publications

1. **D. Inan**, R.K. Dubey, W.F. Jager and F.C. Grozema *Tailoring Photophysical Processes of Perylene-Based Light Harvesting Antenna Systems with Molecular Structure and Solvent Polarity*, submitted to The Journal of Physical Chemistry C (**2018**)
2. **D. Inan**, D. D. Gunbas, J.M. Madern, W.F. Jager and F.C. Grozema *Efficient and Long Range Förster Resonance Energy Transfer in Perylene-3,4,9,10-Tetracarboxylic Derivatives*, in preparation (**2018**)
3. **D. Inan**, R. K. Dubey, W. F. Jager, and F. C. Grozema *Inhibition of Intramolecular Charge Transfer in Perylene Imide Light-Harvesting Antenna Molecules by Topological Modifications*, in preparation (**2018**)
4. **D. Inan**, R. K Dubey, N. Westerveld, J. Bleeker, W.F Jager, F.C Grozema, *Substitution Effects on the Photoinduced Charge-Transfer Properties of Novel Perylene-3,4,9,10-tetracarboxylic Acid Derivatives*. The Journal of Physical Chemistry A, 121 (24), 4633-4644. (**2017**)
5. R. K Dubey, **D. Inan**, S. Sengupta, E. J. R Sudholter, F. C. Grozema, W. F. Jager, *Tunable and highly efficient light-harvesting antenna systems based on 1,7-perylene-3,4,9,10-tetracarboxylic acid derivatives*. Chemical Science, 7 (6), 3517-3532. (**2016**)
6. J. Follana-Berná, **D. Inan**, V. M. Blas-Ferrando, N. Gorczak, J. Ortiz, F. Manjón, F.Fernández-Lázaro, F. C. Grozema, and Á. Sastre-Santos *Synthesis and Photophysical Properties of Conjugated and Nonconjugated Phthalocyanine–Perylenediimide Systems* The Journal of Physical Chemistry C 120 (46), 26508-26513 (**2016**)

List of Presentations

The results described in this thesis were presented at the following meetings:

Oral Contributions

- I. Physics at Veldhoven 2016, Veldhoven, The Netherlands
- II. Chemical Engineering Department Colloquium, 2017, Delft, The Netherlands

Discussion Leadership

- III. Gordon Research Seminar Photochemistry, 2017 Bates College-Maine, The United States of America
- IV. Gordon Research Seminar Solar Fuels, 2018 Ventura, The United States of America

Poster Contributions

- V. CHAINS 2015, Veldhoven, The Netherlands (Poster Pitch as well)
- VI. FRET 2016, Göttingen, Germany
- VII. Computational Sciences For Future Energy 2016 Utrecht, The Netherlands
- VIII. Gordon Research Seminar / Gordon Research Conference Photochemistry 2017 Maine, The United States of America
- IX. Gordon Research Seminar / Gordon Research Conference Photochemistry 2018 Ventura, The United States of America
- X. CHAINS 2017, Veldhoven, The Netherlands

